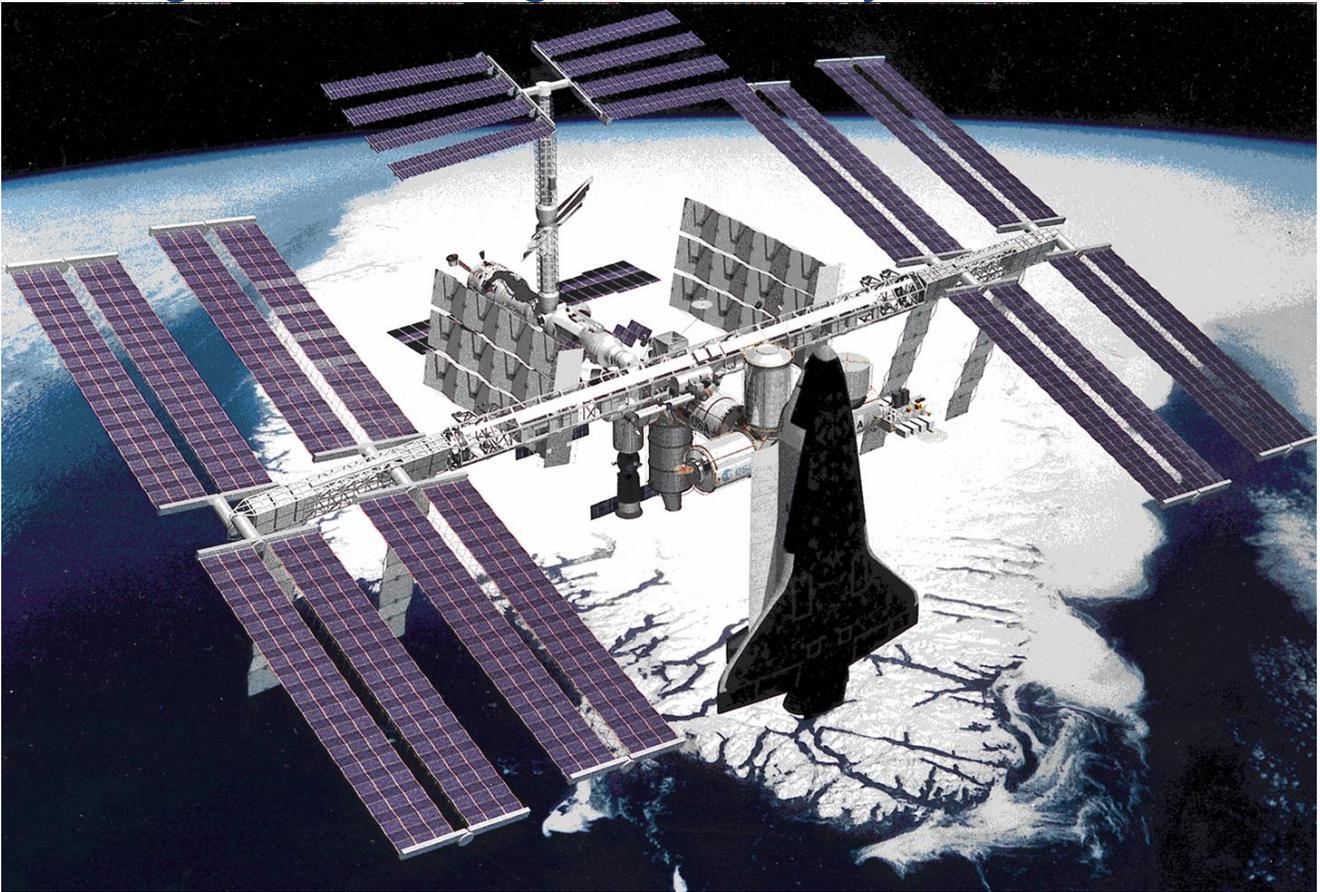# Space Station Attitude Control and Momentum Management Design and Analysis

In this example we will design and analyze the control system of a large and flexible Space Station in orbit around the earth. The attitude control system (ACS) stabilizes the spacecraft attitude by using reaction control jets (RCS) and control moment gyros (CMG). We will design a control system, not only to control the Station attitude, but also to manage the CMG momentum and will analyze the system's stability and performance using simulations and classical frequency response analysis methods. The Space Station configuration is one of the original dual keel concepts similar to the picture in Figure 1b. It consists of a truss structure with some attached modules for the crew, equipment, experiments, etc. which are located near the center of the structure. The Space Station orbit is circular and its attitude is almost constant relative to the Local Vertical Local Horizontal (LVLH) frame. The LVLH x-axis is in the direction of the velocity vector, the z-axis is pointing towards the earth center and the y-axis towards the right solar array.

The Attitude Control System has different modes of operation that use both: RCS jets and CMGs, either independently or simultaneously. They are used for: maneuvering, attitude hold, momentum management using RCS or using CMG control, Shuttle docking, etc. One of the control modes is the TEA seeking mode where the spacecraft attitude converges to the Torque Equilibrium Attitudes (TEA). The CMGs are considered as a cluster located near the center and not modeled individually with steering logic. They are momentum exchange devices that have limited torque and momentum. Momentum is the integral of torque, that is, they can only supply torque for a limited time before they

saturate and when they do they require momentum desaturation. Momentum dump is achieved either by firing RCS jets or by applying gravity gradient torque. The Station has a horizontal boom with two rotating solar arrays which are always pointing towards the sun, completing, therefore, one rotation per orbit relative to the spacecraft. The aerodynamic disturbances cause the CMG momentum to cycle but the control system prevents it from reaching saturation. They consist of steady torques and also cyclic components that excite the spacecraft attitude to oscillations. There are two frequency components associated with the cyclic disturbance torques: one is at orbital rate ω_o due to the difference in atmospheric density between the sunny and the dark sides of the earth, and the second component is at twice the orbital rate $2\omega_o$ caused by drag variation due to the solar arrays rotation. In this mode of operation the function of the CMG control system is not to maneuver the Space Station attitude but to stabilize it at the TEA and to attenuate the attitude oscillations which are caused by cyclic aerodynamic disturbances.
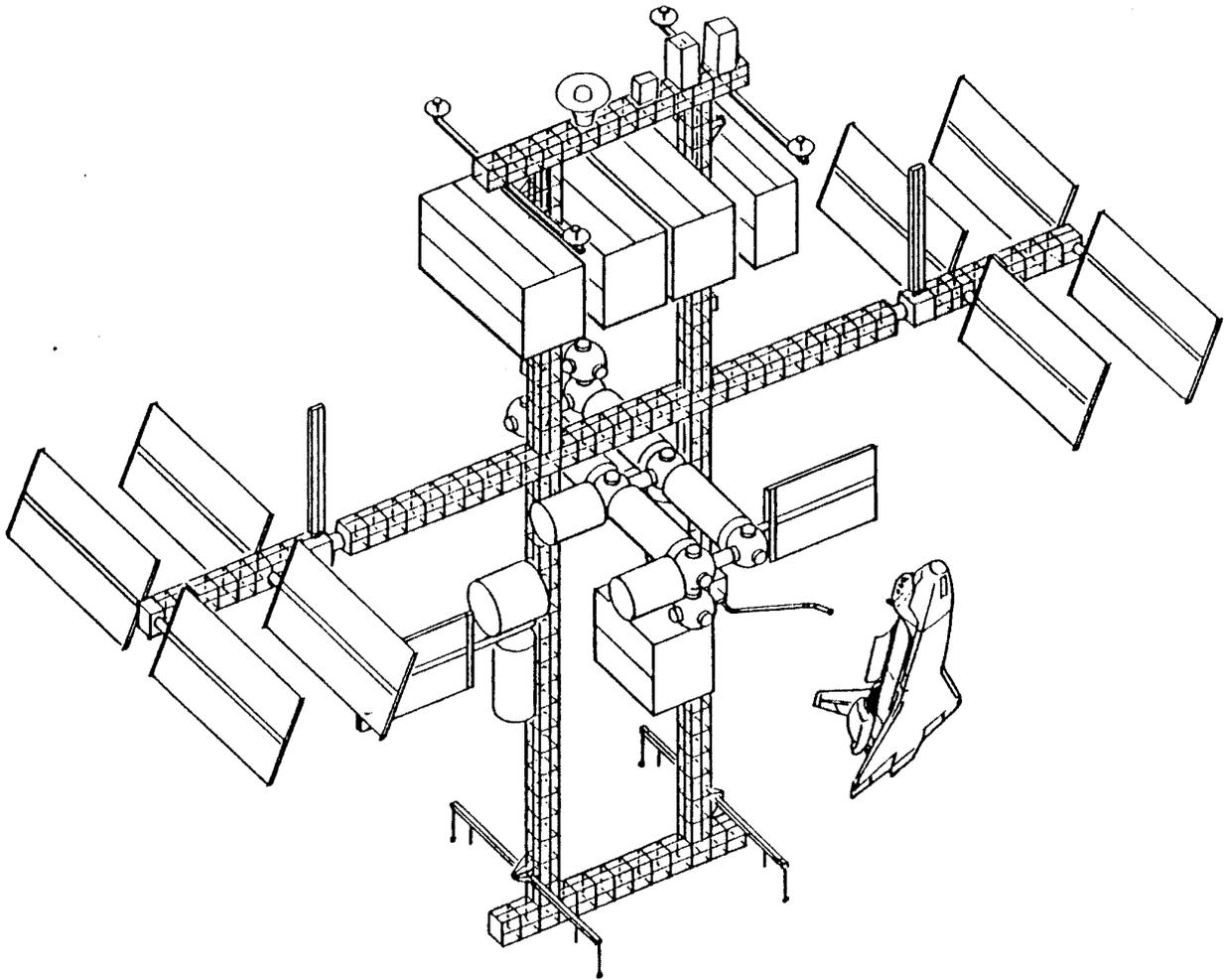

Figure 1b Dual-Keel Space Station Configuration

2

The purpose of this example is to familiarize the analyst with the Flixan program, create rigid and flexible spacecraft models and use them for control design and simulations. We will develop linear and non-linear rigid and flexible spacecraft models, and design LQR state-feedback gains for attitude control and momentum management. Since the spacecraft is stabilized in the LVLH frame the dynamic model attitude and rates are calculated in the LVLH frame. We will also analyze the system's stability and performance by using simulations and frequency response analysis. The analysis is separated into four main sections.

- In Section 1 we demonstrate how to use the flexible structure modeling program to create spacecraft state-space models from modal data (modal frequencies and shapes) that were created from a finite elements model. Rigid-body dynamic models are created by using only the first 6 rigid-body modes. We will show how to define different types of actuators and sensors and specify their locations on the flexible structure, how to compare the modal strength between actuator and sensor nodes and how to select a set of dominant modes to be included in the flex model. We will also show how to analyze the ACS stability and performance including flexibility using simple RCS and CMG controllers.

- In Section 2 we will develop linear and non-linear rigid-body dynamic models relative to the LVLH frame using Matlab/ Simulink, design LQR state-feedback controllers for attitude control and momentum management, and perform time domain simulations in different ACS modes of operation.

- In Section 3 we will combine the non-linear rigid models from Section 2 with the flexible structure models generated in Section 1 and perform simulations, stability analysis and sensitivity analysis to disturbances.

- In Section 4 we will use the flight vehicle modeling program to generate the flexible Space Station model. In addition to flexibility this model includes also the rigid-body and CMG dynamics linearized in the LVLH attitude. We will repeat the analysis of the previous sections and compare results.
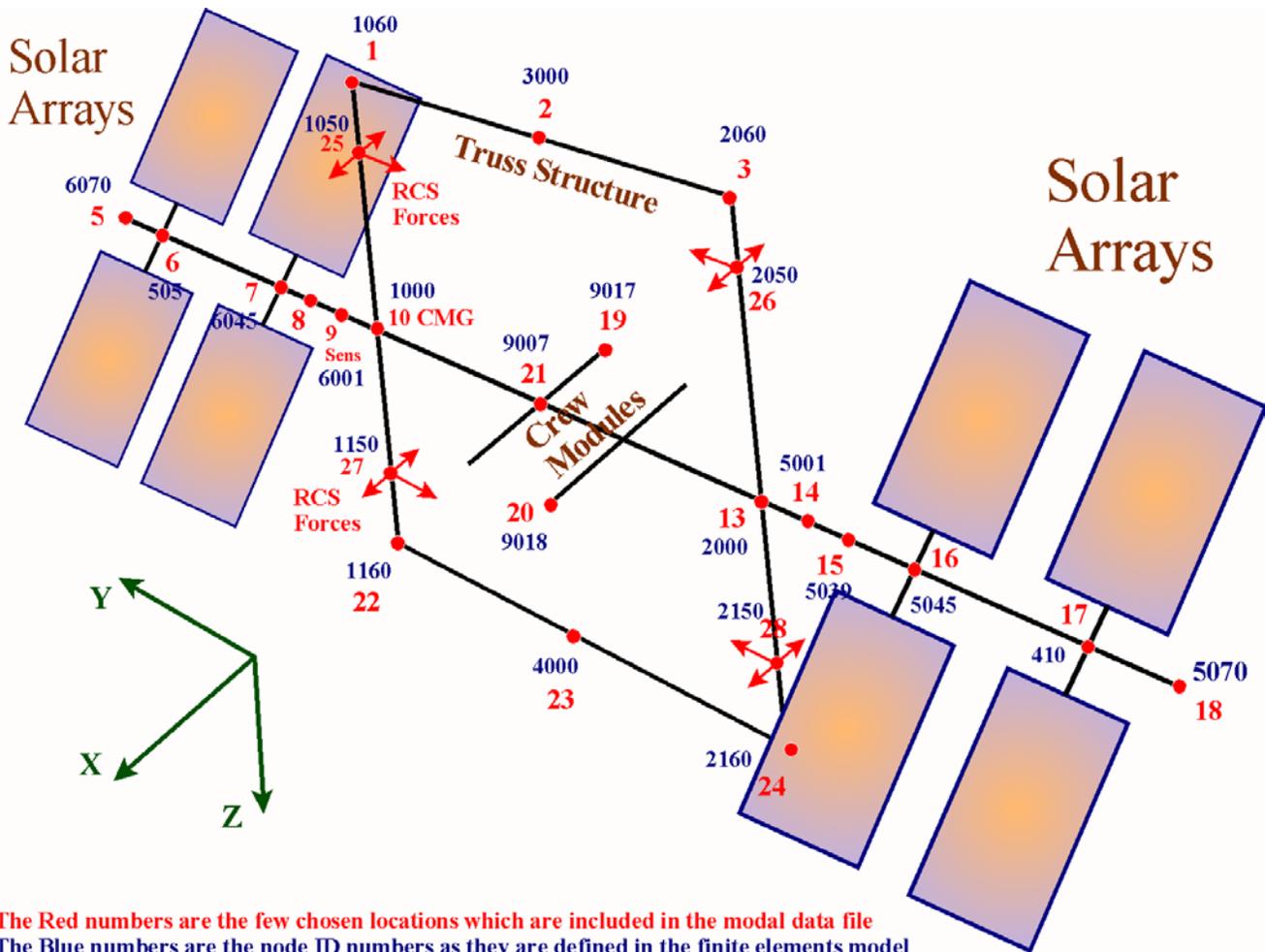
1. Linear Analysis Using Finite Element Models

In this section we will design a preliminary attitude control system for the Space Station using linear state-space systems derived from a finite element flex model (FEM). The files for this linear analysis are in folder "*Examples\ Large Space Station\ (a) Mat Flex Lin (FEM)*". The structural modal data were extracted from a Nastran FEM output, reformatted, and have already been reduced to the first 55 modes at 28 structural locations (nodes). The modal data are saved in standard format recognizable by Flixan in file "*FlexSpaceStruct.Mod*" containing the mode shapes (ϕ_{ij}) and slopes (σ_{ij}) at each node (i) and mode frequency (j). The first 6 modes are rigid body modes at zero frequency and the remaining are structural modes at incremental frequencies in (rad/sec).

The modal data units are in standard Nastran units. The modal displacements are in (inches/inch), the modal slopes are in (rad/inch), and the modal masses are in (lb-sec^2/inch). The damping coefficients for all modes are set to ζ=0.005 and the modal masses are normalized to unity. We are not going to use all the modes, but we will select 38 modes from the modal data file, scale them, and use them to create the state-space systems. We will also need a file that describes the 28 nodes in the same order as they appear in the modal data file. It is known as the nodes map "*FlexSpaceStruct.Nod*", shown in the table below. This file is used in menus to facilitate the mode selection process, as it will be discussed later. It includes is a short description for each node, and they are identified by a node number (1 to 28) and a long node ID number that is derived from the Nastran output.

```
NODE IDENTIFICATION TABLE FOR THE LARGE SPACE STATION WITH SOLAR ARRAYS AND CMG
Node Description                      Node No   FEM ID   Node Location X,Y,Z (feet)
-------------------------------------------------------------------------------------
Payload boom, (top-right)               1       1060
Payload boom, (center)                  2       3000
Payload boom, (top-left)                3       2060
Not Used                                4       3100
Right Solar Array Boom                  5       6070      0.0    232.35     18.0
Right Solar Array (Connect)             6        505
Right SA Boom, Outboard the Hinge       7       6045
Right SA Boom, Inboard the Hinge Servo  8       6039
Right Boom (Sensor Assembly)            9       6001
Right Keel/Boom Intersect, CMG Location 10      1000
CG Center of Structure                  11      7001
Left Keel/Boom Intersection             12      7010
Not Used                                13      2000
Left Boom                               14      5001
Left Boom, Inboard the Hinge Servo      15      5039
Left SA Boom, Outboard the Hinge Servo  16      5045
Left Solar Array (Connect)              17       410
Left SA Boom, Extreme end               18      5070      0.0   -224.63     16.0
Right Habitat Module                    19      9017
Module, (Front Dock)                    20      9018
Center Habitat Module                   21      9007
Bottom Payload Boom (Right)             22      1160
Bottom Payload Boom (Center)            23      4000
Bottom Payload Boom (Left) Antenna      24      2160
Top Right RCS Thruster Assembly         25      1050      0.0     73.7     -185.0
Top Left RCS Thrusters Assembly         26      2050      0.0    -65.58    -185.0
Bottom Right RCS Thruster Assembly      27      1150      0.0     73.7      144.0
Bottom Left RCS Thrusters Assembly      28      2150      0.0    -65.58     144.0
-------------------------------------------------------------------------------------
```

The Red numbers are the few chosen locations which are included in the modal data file
The Blue numbers are the node ID numbers as they are defined in the finite elements model

Figure 1.1 Node Numbers, Nastran IDs, and their Locations in the Structural Model

Figure 1.1 shows the locations of the various nodes which are included in the map file. The station is controlled by a cluster of double gimbal CMGs which are mounted together at node #10. The attitude sensors are in node #9. There are four RCS jet pods located in nodes (25, 26, 27, and 28). Each RCS pod has three jets of 20 (lb) each firing in three directions. All four RCS pods can fire in the ±x directions. The two jets on the left side generate forces in the +y direction and the two jets on the right side generate forces in the –y direction, as shown in Figure 1.1. Our spacecraft model will not use all the structure nodes available in the files. It is, however, a good practice to include sufficient nodes in the modal data file in case they may become useful in future models at a later time.

In Section 1.1 we describe how to create the data file "*FlexSpaceStruct.Inp*" that contains the input datasets for three Space Station models. The datasets contain locations and directions of input forces and torques, sensor locations and directions, sensor types, selected modal data, etc for 3 spacecraft models:

a. a flexible spacecraft with rigid-body modes,
b. a flexible spacecraft without rigid-body modes, and
c. a spacecraft with only 6 rigid body modes

The datasets are processed by the flexible spacecraft modeling program to create the flexible Station systems. The state-space systems are saved in systems file "*FlexSpaceStruct.Qdr*". In the following sections we will also design a jet selection logic that determines an optimal combination of jets to fire in order to rotate the vehicle in a direction demanded by the ACS. The jets in the Space Station models are represented as throttling devices with zero nominal thrust.

## 1.1 Creating Flexible Space Station State-Space Models

In this section we will describe how to create Space Station models by defining the spacecraft configuration in terms of actuator and sensor locations, types of, and directions. How to select a set of dominant structural modes from the modal data file, and how to use the "*Flexible Spacecraft Modeling*" option of the Flixan program to generate state-space systems for simulations and control analysis. In order to create a new flexible spacecraft system one has to specify its configuration in an input data file (.inp). The dataset that specifies the flex spacecraft is either created interactively or by modifying a previously created dataset. In the following example we will describe how to use the Flixan program to create the flexible Space Station input dataset interactively from scratch by means of window dialogs. When the flexible spacecraft dataset is complete, it is a lot easier to modify it using an editor and rerun it in order to create a different state-space model. The dataset can also be processed in batch mode.

Start the Flixan program and select the folder "*Examples\ Large Space Station*". From the Flixan main menu select "*Program Functions*", then "*Flight Vehicle/ Spacecraft Modeling Tools*", and "*Flex Spacecraft (from Modal Data)*". From the filenames selection menu select the input data and the system filenames "*FlexSpaceStruct.Inp*" and "*FlexSpaceStruct.Qdr*". At the bottom of the filenames selection menu click on "*Create a New Input Set*" to enter the spacecraft data interactively since at this point we assume that the input dataset does not exist in file yet.
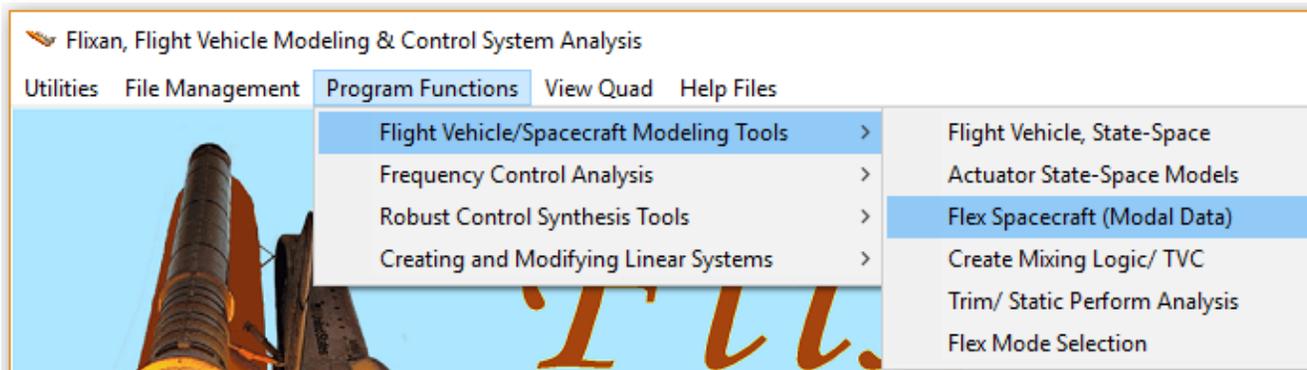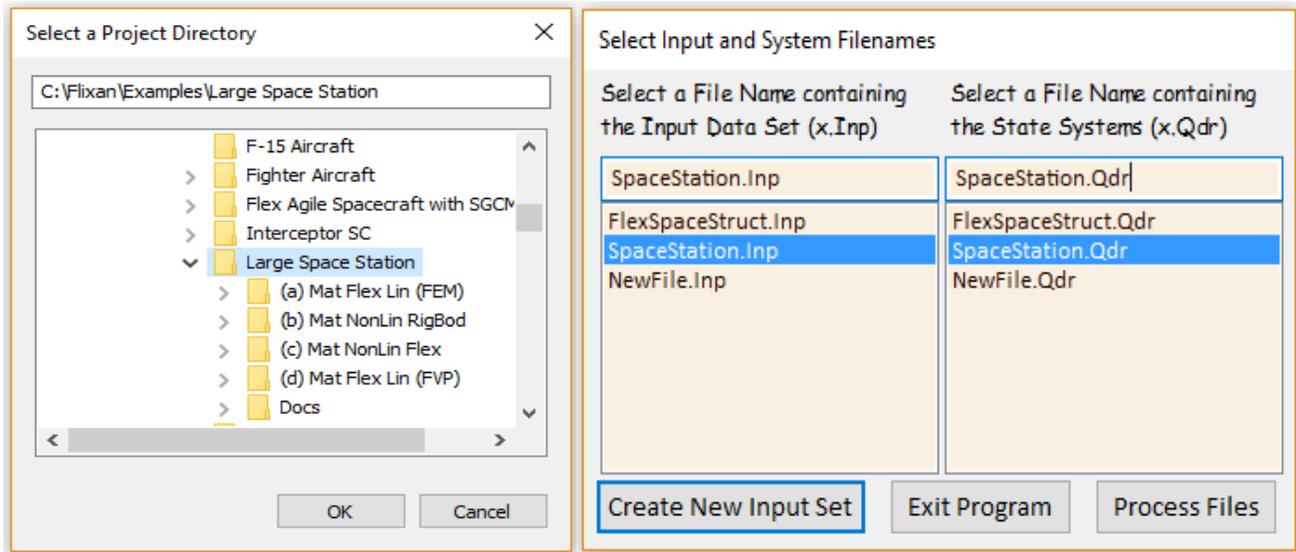
The following menu lists the titles of the flexible spacecraft data sets which are already saved in the input data file "*FlexSpaceStruct.Inp*". There are already three datasets included, but since we are creating a new dataset we are not going to select them, but instead click on "*Create New*" button to create a new flex spacecraft dataset in this file.
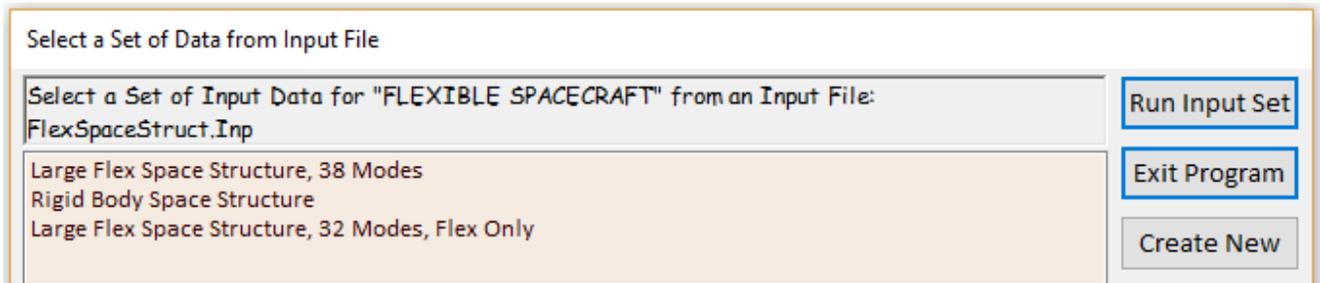
In the following dialog the user must enter the title of the new flexible spacecraft dataset to be created "*Large Flexible Structure, 38 Modes*". Also, the number of force excitation points (11) and the number of torque excitation points (6) which are inputs to the spacecraft structure. You must also define the outputs. That is, enter the number of sensors that measure linear translation, velocity, or acceleration (7), and the number of sensors that measure rotation, rotation rate, or rotational acceleration (8).

The dialog also has three filename menus for selecting 3 files, (a) the modal data filename (.Mod), (b) the nodes map filename (.Nod), and (c) the H-parameters file (.Hpr). The H-parameters are additional data that couple bending mode excitation to hinge torques created by rotating bodies, such as gimbaling payloads, cameras, antennas, etc. In this example we do not have an H-parameters file because this vehicle does not have any rotating appendages. The solar array joints are locked in the finite elements model (FEM). The user must select the modal data and the nodes map filenames which are the only ones appearing in the menus. The yellow field at the bottom of the dialog is for entering some text comments by the user that describes the spacecraft. This text is for documentation purposes and it appears in comment lines in the data files, below the system title. Click on "Continue" to proceed.

In the blue menus that follow the user must select locations in the finite elements model that correspond to the excitation and measurement points that were defined in the spacecraft input data dialog above. The menus display the node descriptions and numbers from the map file (.Nod), and the user must select a node and a direction for each actuator or sensor.

For example, we must associate the 11 force excitation points previously defined with their corresponding nodes in the FEM. We must also define the force directions. In this case, force #1 is applied at node #25 in the x direction (1,0,0), force #2 is applied at node #25 in the -y direction (0,-1,0), force #3 is applied at node #26 in the x direction, force #4 is applied at node #26 in the y direction, and so on.

Forces number 9, 10, and 11 represent crew disturbances and they are applied at central habitat module in node #21 in the x, y, and z directions respectively. Some of the inputs are shown below. Click "OK" after entering each force input to continue.

Define Locations and Directions of the System Inputs

Define a Direction Vector for Force Excitation : 1 along x,y,z   1.00   0.00   0.00

Select a Location (Node) for Force Excitation : 1

OK   Cancel

#	Location	Node
1	Payload boom, (top-right)	1060
2	Payload boom, (center)	3000
3	Payload boom, (top-left)	2060
4	Unknown	3100
5	Right Solar Array Boom	6070
6	Right Solar Array (Connect)	505
7	Right SA Boom, Outboard the Hinge	6045
8	Right SA Boom, Inboard the Hinge Servo	6039
9	Right Boom (Sensor Assembly)	6001
10	Right Keel/Boom Intrsect, CMG Location	1000
11	CG Center of Structure	7001
12	Left Keel/Boom Intersection	7010
13	Unknown	2000
14	Left Boom	5001
15	Left Boom, Inboard the Hinge Servo	5039
16	Left SA Boom, Outboard the Hinge Servo	5045
17	Left Solar Array (Connect)	410
18	Left SA Boom, Extreme End	5070
19	Right Habitat Module	9017
20	Module, (Front Dock)	9018
21	Center Habitat Module	9007
22	Bottom Payload Boom (Right)	1160
23	Bottom Payload Boom (Center)	4000
24	Bottom Payload Boom (Left) Antena	2160
25	Top Right RCS Thruster Assembly	1050
26	Top Left RCS Thrusters Assembly	2050
27	Bottom Right RCS Thruster Assembly	1150
28	Bottom Left RCS Thrusters Assembly	2150

Similarly, we must define 6 nodes and the corresponding directions for the 6 torques applied. There are three control torques about x, y, and z axes, generated by the CMGs cluster at node #10. The menu/dialog below defines the first control torque about the x-axis. There are also three disturbance torques that must be defined at node #1, about x, y, and z axes, due to a gimbaling payload that creates reaction disturbances. Click "OK" after defining each torque input to continue.

Define Locations and Directions of the System Inputs

Define a Direction Vector for Torque Excitation: 1 along x,y,z

| | 1.00 | 0.00 | 0.00 | OK |

Select a Location (Node) for Torque Excitation: 1

Cancel

Payload boom, (top-right)	1	1060
Payload boom, (center)	2	3000
Payload boom, (top-left)	3	2060
Unknown	4	3100
Right Solar Array Boom	5	6070
Right Solar Array (Connect)	6	505
Right SA Boom, Outboard the Hinge	7	6045
Right SA Boom, Inboard the Hinge Servo	8	6039
Right Boom (Sensor Assembly)	9	6001
Right Keel/Boom Intrsect, CMG Location	10	1000
CG Center of Structure	11	7001
Left Keel/Boom Intersection	12	7010
Unknown	13	2000
Left Boom	14	5001
Left Boom, Inboard the Hinge Servo	15	5039
Left SA Boom, Outboard the Hinge Servo	16	5045
Left Solar Array (Connect)	17	410
Left SA Boom, Extreeme End	18	5070
Right Habitat Module	19	9017
Module, (Front Dock)	20	9018
Center Habitat Module	21	9007
Bottom Payload Boom (Right)	22	1160
Bottom Payload Boom (Center)	23	4000
Bottom Payload Boom (Left) Antena	24	2160
Top Right RCS Thruster Assembly	25	1050
Top Left RCS Thrusters Assembly	26	2050
Bottom Right RCS Thruster Assembly	27	1150
Bottom Left RCS Thrusters Assembly	28	2150

The next step is to define the 7 accelerometer measurements. There are three accelerometers at the attitude control sensors node #9 measuring about x, y, and z, two accelerometers at the right end of the solar array boom (node #5), and another two at the left end of the solar array boom (node #18). The menu below shows how translational acceleration sensor #1 is defined by selecting the node title, the measurement direction from the direction menu, and the acceleration option from the sensor type: (position, velocity, acceleration) menu. Click the "Select" button to continue. Sensors #2 and #3 are also located at node #9 measuring in the y and z directions respectively.

Define Locations and Directions of the System Outputs

Select a Location (Node) for Translation Sensor 1

Location	Node	Value
Payload boom, (top-right)	1	1060
Payload boom, (center)	2	3000
Payload boom, (top-left)	3	2060
Unknown	4	3100
Right Solar Array Boom	5	6070
Right Solar Array (Connect)	6	505
Right SA Boom, Outboard the Hinge	7	6045
Right SA Boom, Inboard the Hinge Servo	8	6039
Right Boom (Sensor Assembly)	9	6001
Right Keel/Boom Intrsect, CMG Location	10	1000
CG Center of Structure	11	7001
Left Keel/Boom Intersection	12	7010
Unknown	13	2000
Left Boom	14	5001
Left Boom, Inboard the Hinge Servo	15	5039
Left SA Boom, Outboard the Hinge Servo	16	5045
Left Solar Array (Connect)	17	410
Left SA Boom, Extreeme End	18	5070
Right Habitat Module	19	9017
Module, (Front Dock)	20	9018
Center Habitat Module	21	9007
Bottom Payload Boom (Right)	22	1160
Bottom Payload Boom (Center)	23	4000
Bottom Payload Boom (Left) Antena	24	2160
Top Right RCS Thruster Assembly	25	1050
Top Left RCS Thrusters Assembly	26	2050
Bottom Right RCS Thruster Assembly	27	1150
Bottom Left RCS Thrusters Assembly	28	2150

Define a Direction Vector for Translation Sensor 1 and also what type of measurement

Sensor Direction

Along-X
Along-Y
Along-Z

Sensor Type

Position
Velocity
Acceleration

Select

Cancel

11

The selection of sensor #4 is similar. It is located at the extreme right end of the solar array boom (node #5) and it is measuring acceleration in the x direction. Sensor #5 is also located at node #5 and it is measuring acceleration in the z direction. Click "Select" to continue.

We must finally define the 8 rotational measurements. There are three rate gyros at the ACS sensors (node #9) measuring about x, y, z axes. That is, three rate gyros at an antenna location (node #24) about x, y, z, and two pitch rotational acceleration sensors outboard the solar array hinges (nodes #7 and #16). The selection of sensor #1 and sensor #7 are shown in the next two dialogs. Using the two menus at the bottom of the menu we can select the measurement direction (roll, pitch, yaw), and the sensor type (position, velocity, acceleration). In this case, rotational sensor #1 is located at node #9 and it is measuring roll rate. Similarly, rotational sensor #7 is located at node #7, which is the right SA boom and it is measuring pitch acceleration.

Define Locations and Directions of the System Outputs

Select a Location (Node) for Rotational Sensor: 1

#	Location	Node
1	Payload boom, (top-right)	1060
2	Payload boom, (center)	3000
3	Payload boom, (top-left)	2060
4	Unknown	3100
5	Right Solar Array Boom	6070
6	Right Solar Array (Connect)	505
7	Right SA Boom, Outboard the Hinge	6045
8	Right SA Boom, Inboard the Hinge Servo	6039
9	Right Boom (Sensor Assembly)	6001
10	Right Keel/Boom Intrsect, CMG Location	1000
11	CG Center of Structure	7001
12	Left Keel/Boom Intersection	7010
13	Unknown	2000
14	Left Boom	5001
15	Left Boom, Inboard the Hinge Servo	5039
16	Left SA Boom, Outboard the Hinge Servo	5045
17	Left Solar Array (Connect)	410
18	Left SA Boom, Extreme End	5070
19	Right Habitat Module	9017
20	Module, (Front Dock)	9018
21	Center Habitat Module	9007
22	Bottom Payload Boom (Right)	1160
23	Bottom Payload Boom (Center)	4000
24	Bottom Payload Boom (Left) Antena	2160
25	Top Right RCS Thruster Assembly	1050
26	Top Left RCS Thrusters Assembly	2050
27	Bottom Right RCS Thruster Assembly	1150
28	Bottom Left RCS Thrusters Assembly	2150

Define a Direction Vector for Rotational Sensor: 1 and also what type of measurement

Sensor Direction: Roll | Pitch | Yaw

Sensor Type: Position | Velocity | Acceleration

Select   Cancel

Define Locations and Directions of the System Outputs

Select a Location (Node) for Rotational Sensor: 7

#	Location	Node
1	Payload boom, (top-right)	1060
2	Payload boom, (center)	3000
3	Payload boom, (top-left)	2060
4	Unknown	3100
5	Right Solar Array Boom	6070
6	Right Solar Array (Connect)	505
7	Right SA Boom, Outboard the Hinge	6045
8	Right SA Boom, Inboard the Hinge Servo	6039
9	Right Boom (Sensor Assembly)	6001
10	Right Keel/Boom Intrsect, CMG Location	1000
11	CG Center of Structure	7001
12	Left Keel/Boom Intersection	7010
13	Unknown	2000
14	Left Boom	5001
15	Left Boom, Inboard the Hinge Servo	5039
16	Left SA Boom, Outboard the Hinge Servo	5045
17	Left Solar Array (Connect)	410
18	Left SA Boom, Extreme End	5070
19	Right Habitat Module	9017
20	Module, (Front Dock)	9018
21	Center Habitat Module	9007
22	Bottom Payload Boom (Right)	1160
23	Bottom Payload Boom (Center)	4000
24	Bottom Payload Boom (Left) Antena	2160
25	Top Right RCS Thruster Assembly	1050
26	Top Left RCS Thrusters Assembly	2050
27	Bottom Right RCS Thruster Assembly	1150
28	Bottom Left RCS Thrusters Assembly	2150

Define a Direction Vector for Rotational Sensor: 7 and also what type of measurement

Sensor Direction: Roll | Pitch | Yaw

Sensor Type: Position | Velocity | Acceleration

Select   Cancel

So far we have defined the actuator and sensor points on the structure, their directions, and type of measurements. This information will be saved in the input data file "*FlexSpaceStruct.Inp*". We are not defining the actuator and sensor dynamics now. They will be defined later in the simulation block diagram by transfer function blocks. At this point the program activates the mode selection process requesting the user to select a number of flex modes from the modal data file "*FlexSpaceStruct.Mod*". We usually do not include all of the available flex modes in the spacecraft state-space model but only the strongest ones. The structural modes are processed by a mode selection program and the strongest modes are included in the flexible spacecraft dataset together with the actuator and sensors definitions. This mode-selection program is different but similar to the mode selection program used in the flight vehicle program.

At this point the program opens the following dialog where the user specifies how the modes will be compared. In this case we are comparing all modes from #1 to #55. We will use only one excitation force point and measure the structure excitation using only one rotational sensor. Note that, this is only for mode comparison purposes and not for defining the simulation model inputs and outputs. We have already defined the spacecraft inputs and outputs. Use the default graphics option for manually selecting the modes and ignore the number of modes to be selected field.
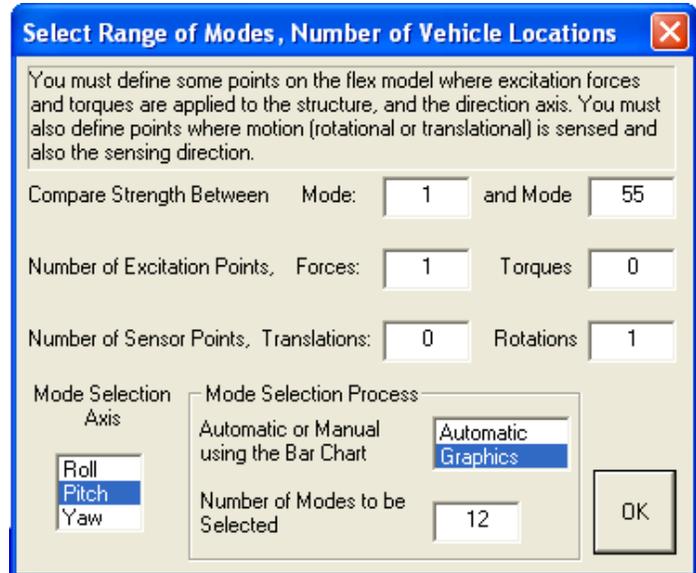
The following dialog is used for scaling the selected modal data in order to convert them from units of (inches) to units of (feet). The modal mass is scaled up by a factor of (12) to be converted from (lb-sec^2/inch) to (lb-sec^2/ft). The modal displacements do not change because they go from (inches/inch) to (feet/ft). The modal slopes are also scaled up by a factor of (12) to be converted from (radians /inch) to (radians/feet). The signs for the coordinate axes transform do not change because the directions of (X, Y, Z) axes are the same in both FEM and Flixan models.
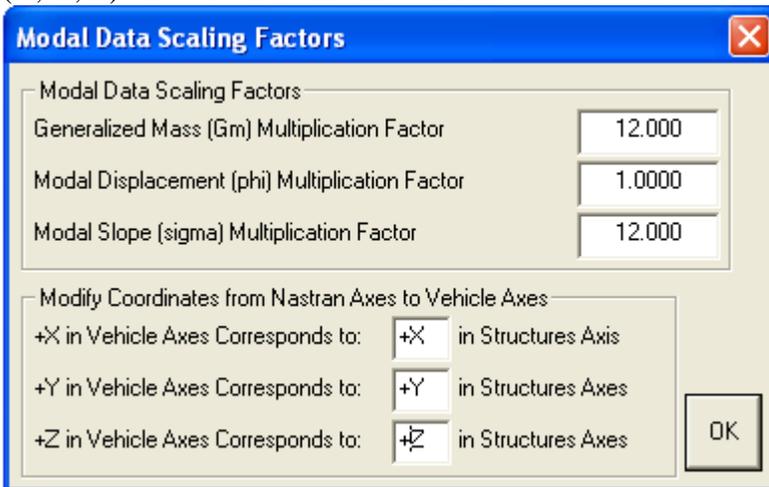
The next step is for defining force excitation points used for mode selection purposes only and not for defining the system inputs. The dialogs are similar to the ones used for defining the spacecraft input and output nodes, but now they are used to define the excitation and measurement locations and directions for mode strength comparison. The background color of these menus is different from the previous menus in order to avoid confusion. In this case we have defined only one force excitation point to excite the structure at node #25 in the +z direction. Click "OK" to continue.

Table of Vehicle Structure FEM Nodes

In mode selection, in order to calculate the relative mode strength of a number of modes in a specified direction you must define some node points in the Nastran model where the excitation forces or torques will be applied and also the forcing directions.

Similarly, you must also define the sensor points (translations or rotations) and the sensing directions.

OK   **Cancel**

Select a Location (Node) for Force Excitation : 1

Axis

Node Description	Node Number	Nastran Node ID
Payload boom, (top-right)	1	1060
Payload boom, (center)	2	3000
Payload boom, (top-left)	3	2060
Unknown	4	3100
Right Solar Array Boom	5	6070
Right Solar Array (Connect)	6	505
Right SA Boom, Outboard the Hinge	7	6045
Right SA Boom, Inboard the Hinge Servo	8	6039
Right Boom (Sensor Assembly)	9	6001
Right Keel/Boom Intrsect, CMG Location	10	1000
CG Center of Structure	11	7001
Left Keel/Boom Intersection	12	7010
Unknown	13	2000
Left Boom	14	5001
Left Boom, Inboard the Hinge Servo	15	5039
Left SA Boom, Outboard the Hinge Servo	16	5045
Left Solar Array (Connect)	17	410
Left SA Boom, Extreeme End	18	5070
Right Habitat Module	19	9017
Module, (Front Dock)	20	9018
Center Habitat Module	21	9007
Bottom Payload Boom (Right)	22	1160
Bottom Payload Boom (Center)	23	4000
Bottom Payload Boom (Left) Antena	24	2160
Top Right RCS Thruster Assembly	25	1050
Top Left RCS Thrusters Assembly	26	2050
Bottom Right RCS Thruster Assembly	27	1150
Bottom Left RCS Thrusters Assembly	28	2150

Axis:
Along-X
Along-Y
Along-Z

Direction
+ (positive)
- (negative)

Node Description, Node Number, Nastran Node ID Number, Location Coordinates (X, Y, Z)

Similarly, we have also defined one rotational sensor at node #9 for modal comparison purposes. It is measuring in the positive pitch direction. Click "OK" to continue.

Table of Vehicle Structure FEM Nodes

In mode selection, in order to calculate the relative mode strength of a number of modes in a specified direction you must define some node points in the Nastran model where the excitation forces or torques will be applied and also the forcing directions.

Similarly, you must also define the sensor points (translations or rotations) and the sensing directions.

OK

Cancel

Select a Location (Node) for Rotational Sensor: 1

Axis

Roll
Pitch
Yaw

| Node Description	Node Number	Nastran Node ID
Payload boom, (top-right)	1	1060
Payload boom, (center)	2	3000
Payload boom, (top-left)	3	2060
Unknown	4	3100
Right Solar Array Boom	5	6070
Right Solar Array (Connect)	6	505
Right SA Boom, Outboard the Hinge	7	6045
Right SA Boom, Inboard the Hinge Servo	8	6039
Right Boom (Sensor Assembly)	9	6001
Right Keel/Boom Intrsect, CMG Location	10	1000
CG Center of Structure	11	7001
Left Keel/Boom Intersection	12	7010
Unknown	13	2000
Left Boom	14	5001
Left Boom, Inboard the Hinge Servo	15	5039
Left SA Boom, Outboard the Hinge Servo	16	5045
Left Solar Array (Connect)	17	410
Left SA Boom, Extreeme End	18	5070
Right Habitat Module	19	9017
Module, (Front Dock)	20	9018
Center Habitat Module	21	9007
Bottom Payload Boom (Right)	22	1160
Bottom Payload Boom (Center)	23	4000
Bottom Payload Boom (Left) Antena	24	2160
Top Right RCS Thruster Assembly	25	1050
Top Left RCS Thrusters Assembly	26	2050
Bottom Right RCS Thruster Assembly	27	1150
Bottom Left RCS Thrusters Assembly	28	2150

Direction

+ (positive)
- (negative)

Node Description, Node Number, Nastran Node ID Number, Location Coordinates (X, Y, Z)

The program calculates the modal strength for all modes, calculates the modal strength, and plots its magnitude in the bar log-chart below. Each vertical bar represents the strength of the corresponding mode and the height is proportional to its strength. Initially, before selection all bars are red. A mode is selected when you click on it with the mouse cursor and it changes color to green. In this case we are selecting 38 modes including the first six rigid body modes. It is a good practice to repeat the mode comparison using different excitation and sensor combination points and different directions. In the final selection the strongest modes are included after considering several combination runs.
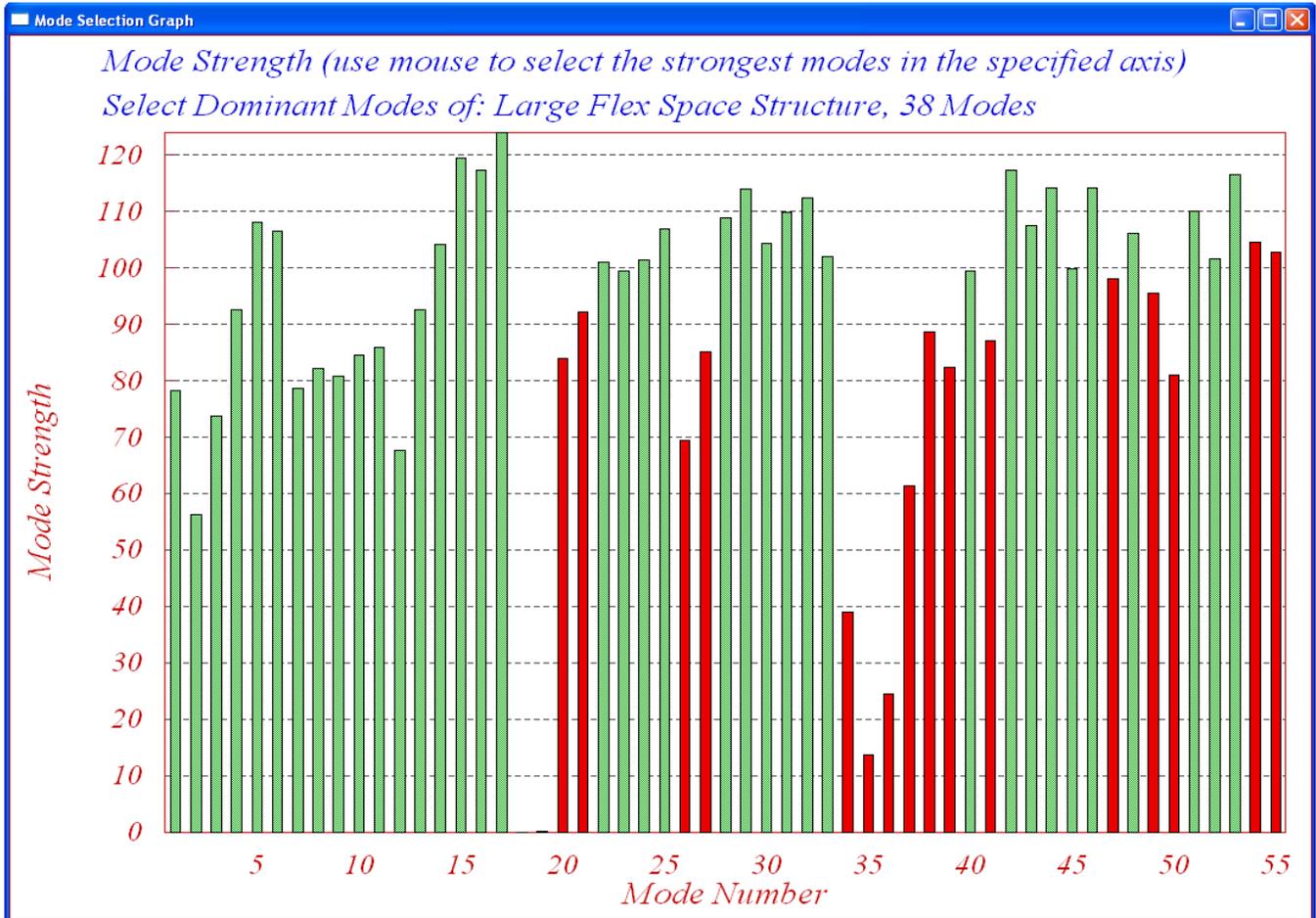

After selecting a number of modes interactively, press "Enter" on the keyboard and the program will create the flexible spacecraft input dataset in file: "*FlexSpaceStruct.Inp*", under the title: "*Large Flex Space Structure, 38 Modes*". It will also process the data using the flexible spacecraft modeling program and it will save the state-space model in file: "*FlexSpaceStruct.Qdr*" under the same title "*Large Flex Space Structure, 38 Modes*". This system must also be exported to the Matlab folder "*Large Space Station\Mat Flex Lin*" for further control analysis.

Exporting the Flexible Space Station System to the Matlab Folder

The Space Station systems must also be reformatted to Matlab m-file in subdirectory "*(a) Mat Flex Lin (FEM)*" for further analysis, using the Flixan "Export to Matlab" utility. Start Flixan and select the project directory: "*Examples\Large Space Station*". Then go to "*Utilities*" and select "*Matlab Conversions*", and then "*Export to Matlab*". From the systems menu select the systems file "*FlexSpaceStruct.Qdr*" that contains three Space Station systems and click OK. You must also select the destination directory "*\Large Space Station\(a) Mat Flex Lin (FEM)*" where the m-file will be placed for Matlab analysis.
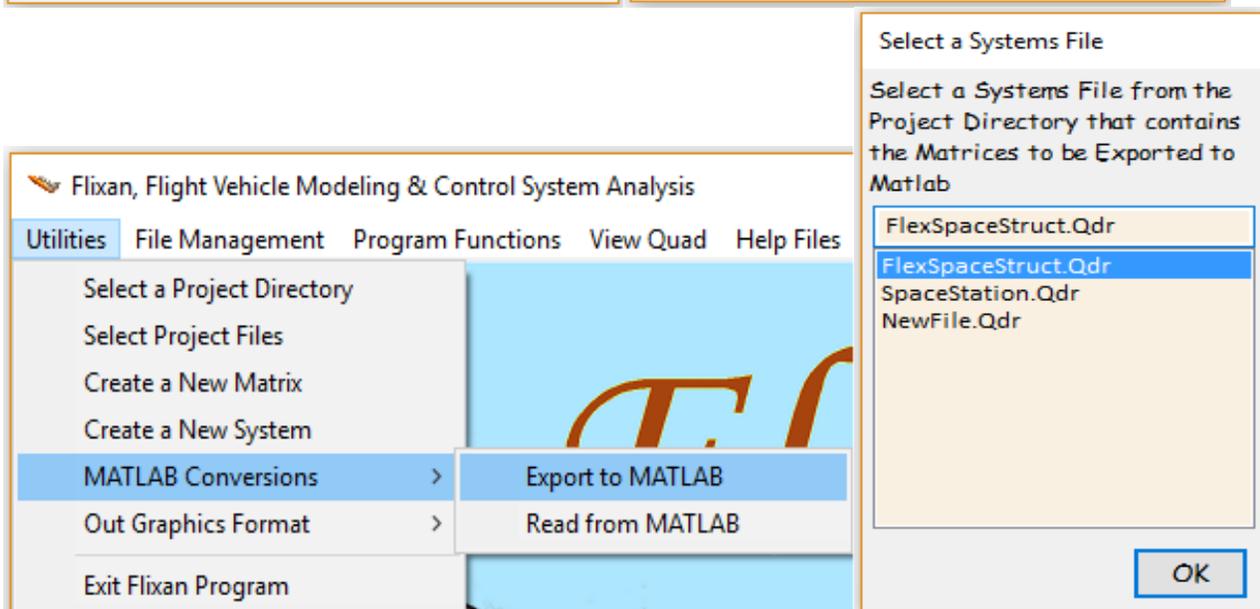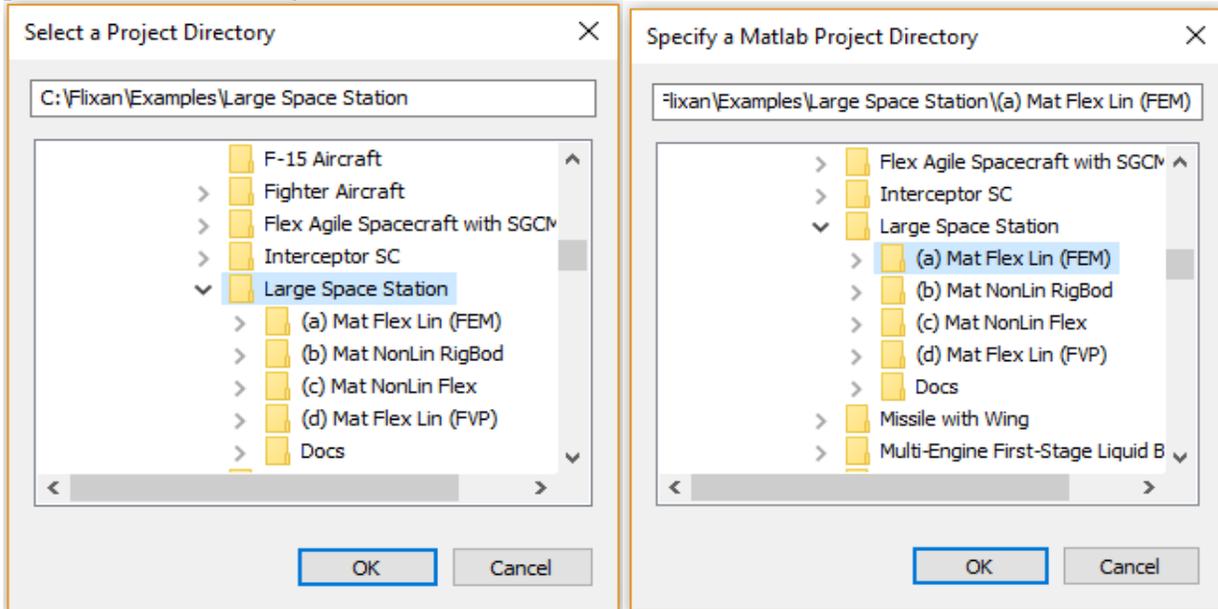
Use the next dialog to specify that the system will be saved as an m-file function of 4 matrices (A, B, C, D). The next menu shows the titles of systems in file "*FlexSpaceStruct.Qdr*". Select the first title: "*Large Flex Space Structure, 38 Modes*" and click on "Select". Finally enter the name of the m-file to save the system (without the extension .m), and click OK. The name of the m-file is "lfss_38m.m". It contains the four state-space matrices of the flexible spacecraft system and it will be loaded into Matlab for control analysis. The Matlab conversion process can be repeated for the other two Space Station systems.
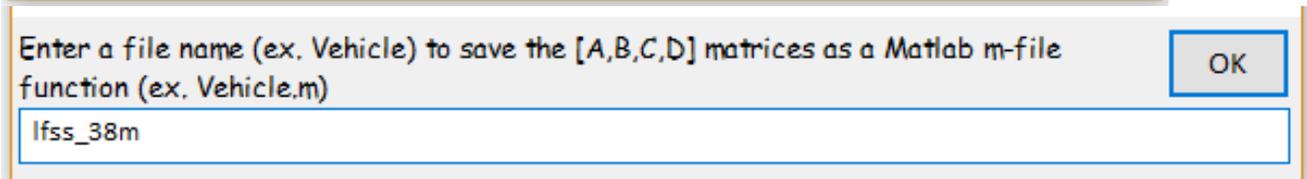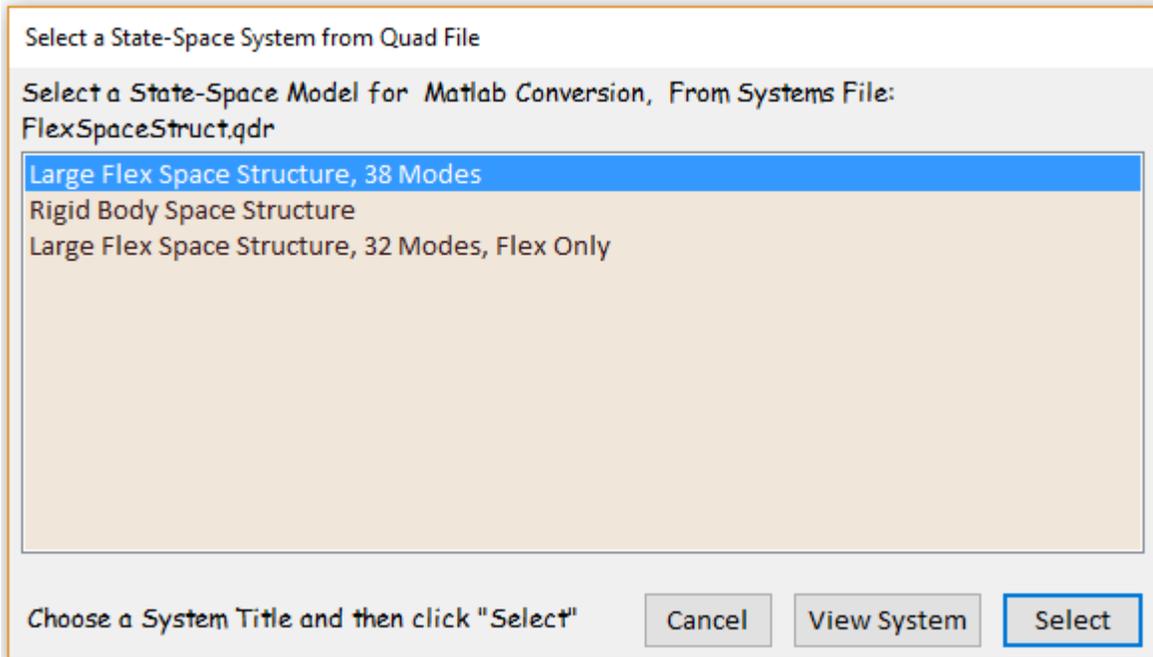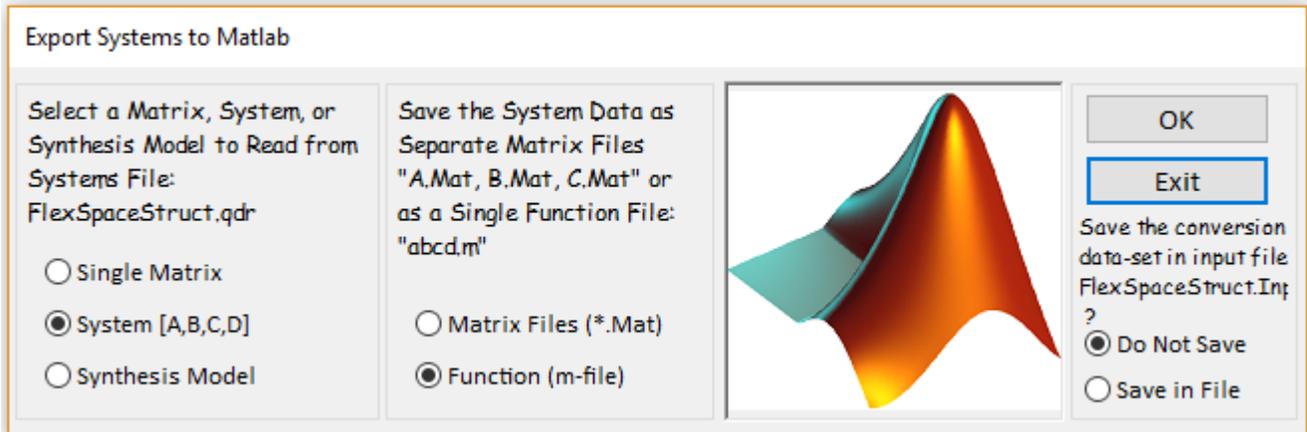
Processing the Input Data in Batch Mode

The interactive process described for generating the Space Station models is slow and it is only used when we begin a new project. It is not necessary to rerun the spacecraft program interactively and the Matlab conversions every time but after we have created the spacecraft datasets we can modify and reprocess them much faster in batch mode, as we shall see. In order to process the datasets in batch, the user must create a batch set that is usually located at the top of the input file. The batch will process the datasets very fast by calling their corresponding programs and saving the data in the systems file and in m-files for further analysis using Matlab. The batch set will process almost instantaneously all datasets created for a particular project which are saved in the same input file.

In this example we have included a batch set in file "*FlexSpaceStruct.Inp*" that will process the three spacecraft datasets by calling the flex spacecraft program, 3 times. It will also convert the state-space systems to Matlab m-files. To run the batch and process the datasets, go to the Flixan main menu and select "*File Management*", "*Manage Input Files*", and then "*Edit/ Process Input Data*".
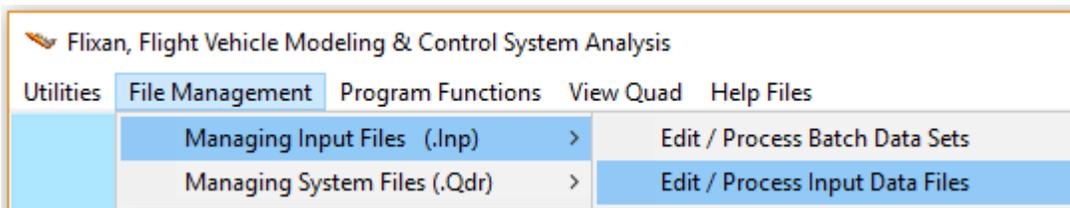
The input file manager dialog comes up. It can be used to process each individual dataset using the corresponding Flixan program. It has two menus. From the left menu select the input data file "*FlexSpaceStruct.Inp*" and then click on "*Select Input File*". The menu on the right shows all input datasets which are in this file and the corresponding programs that will process them. In this case select the top dataset which is the batch with title "*Batch for preparing flexible Space Station models*" and click on "*Process Input Data*" to process the batch. The batch will process the three spacecraft models, convert them to Matlab format, and save the state-space systems in directory "*Examples\ Large Space Station*".
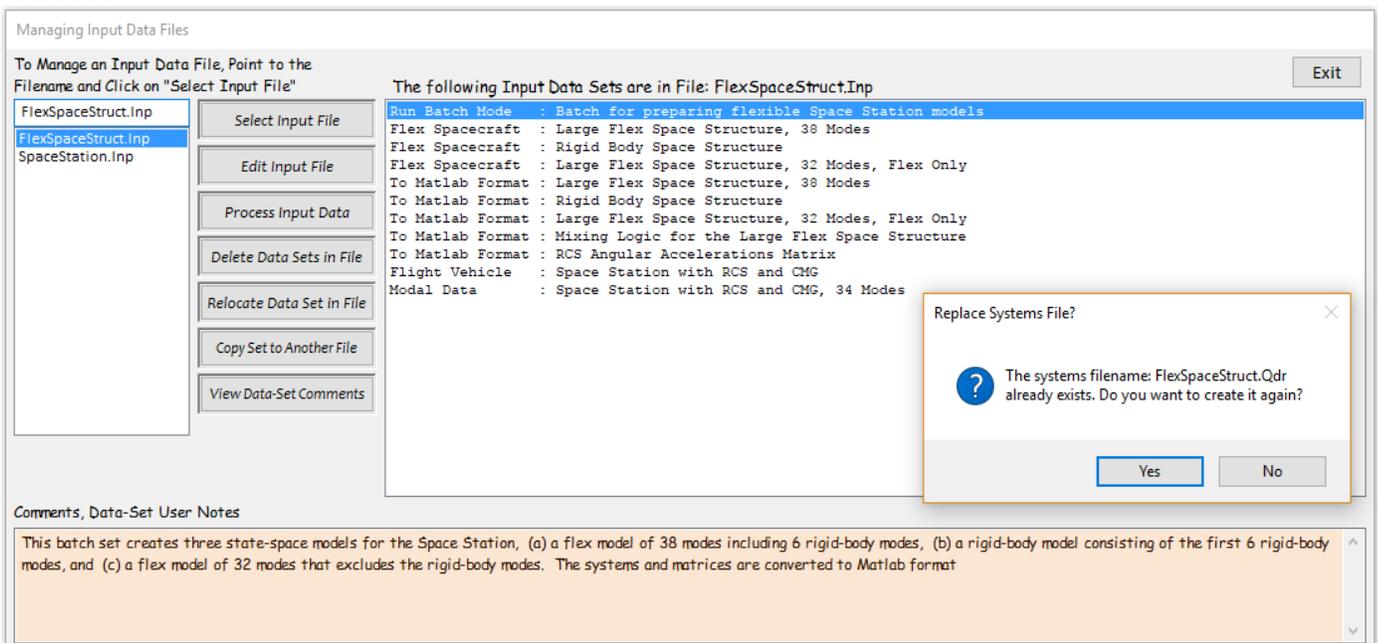
1.2 Designing a Preliminary CMG Attitude Control System

Figure 1.2.1 shows a closed-loop simulation model consisting of a simple CMG attitude control system with a PD controller that supplies torque to the linear spacecraft system. It is implemented in Simulink model "*Lin_CMG_Sim.mdl*" located in folder "*Large Space Station\ (a) Mat Flex Lin (FEM)*". The attitude control system bandwidth is set to 20 times the orbital frequency. The gains are scaled by the moments of inertia matrix (J) to provide the same bandwidth in all 3 axes.
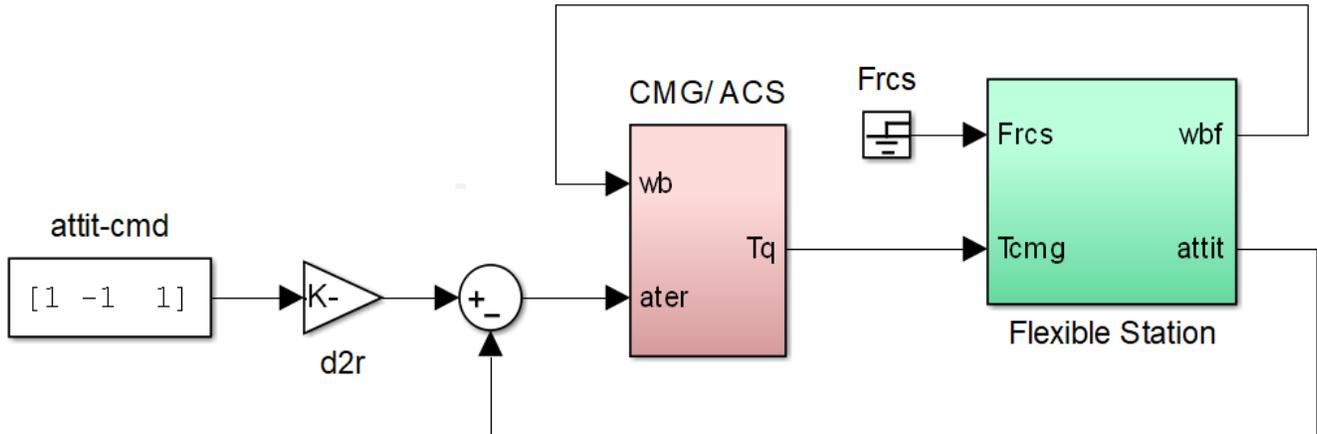

Figure 1.2.1 Flex Space Station Simulation Model "*Lin_CMG_Sim.Mdl*" for CMG/ PD Attitude Control

The control system is shown expanded in Figure 1.1.2. The yellow block is the CMG gimbal dynamics represented by 2nd order transfer functions of bandwidth 2 (rad/sec). The output is a 3-dimensional torque that drives the flex vehicle model in roll, pitch, and yaw directions.
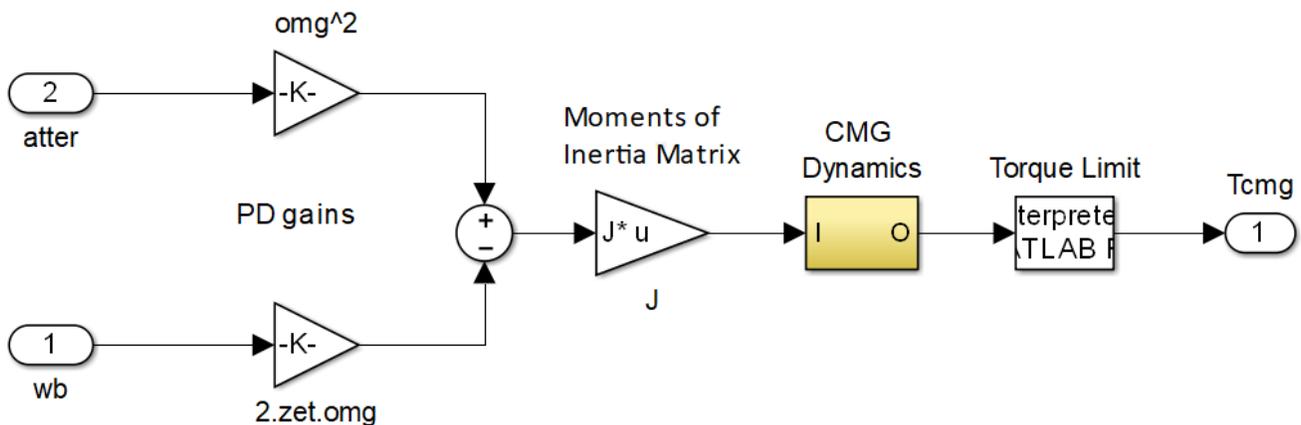
Figure 1.2.2 PD Controller for the CMG Attitude Control System

The Space Station dynamics (green block) is shown expanded in Figure 1.2.3. It consists of the continuous state-space system "*lfss_38m.m*", title: "*Large Flex Space Structure, 38 Modes*" that was created by the Flixan flexible spacecraft modeling program. This system includes 32 flexible modes plus the first 6 rigid-body modes. It is loaded into Matlab workspace by running the file "start.m" which also initializes the simulation parameters. The state-space system "*lfss_38m.m*" is included in the Simulink model "*Lin_CMG_Sim.Mdl*", as shown in Figure 1.2.3.

Figure 1.2.3 Flexible Space Station Model

Large Flexible Space Station Structure with 38 Modes

Inputs = 17
1   Fx RCS No 1 Applied at Node # 25 (lbf)
2   Fy RCS No 2 Applied at Node # 25 (lbf)
3   Fx RCS No 3 Applied at Node # 26 (lbf)
4   Fy RCS No 4 Applied at Node # 26 (lbf)
5   Fx RCS No 5 Applied at Node # 27 (lbf)
6   Fy RCS No 6 Applied at Node # 27 (lbf)
7   Fx RCS No 7 Applied at Node # 28 (lbf)
8   Fy RCS No 8 Applied at Node # 28 (lbf)

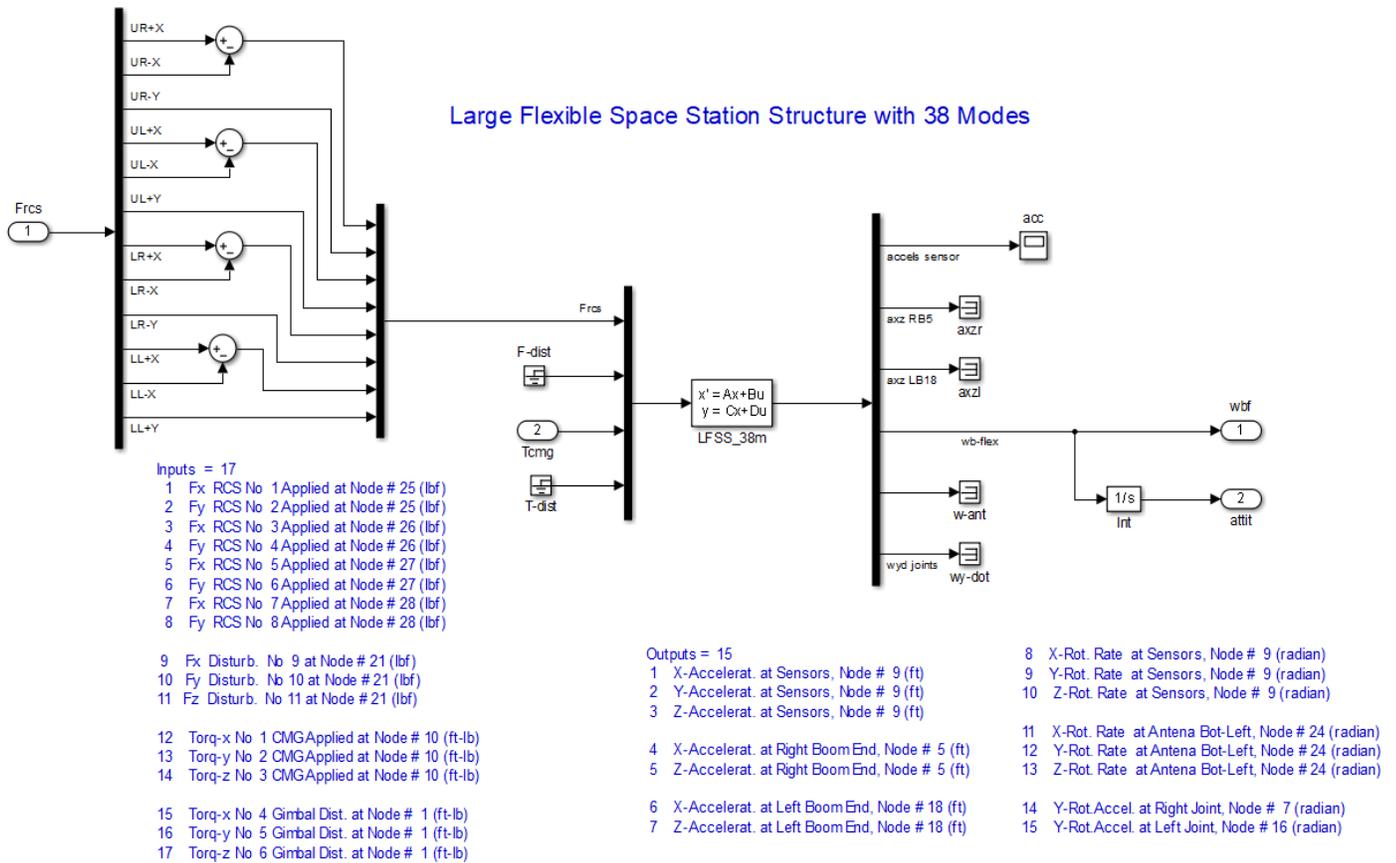9   Fx Disturb. No 9 at Node # 21 (lbf)
10 Fy Disturb. No 10 at Node # 21 (lbf)
11 Fz Disturb. No 11 at Node # 21 (lbf)

12 Torq-x No 1 CMG Applied at Node # 10 (ft-lb)
13 Torq-y No 2 CMG Applied at Node # 10 (ft-lb)
14 Torq-z No 3 CMG Applied at Node # 10 (ft-lb)

15 Torq-x No 4 Gimbal Dist. at Node # 1 (ft-lb)
16 Torq-y No 5 Gimbal Dist. at Node # 1 (ft-lb)
17 Torq-z No 6 Gimbal Dist. at Node # 1 (ft-lb)

Outputs = 15
1   X-Accelerat. at Sensors, Node # 9 (ft)
2   Y-Accelerat. at Sensors, Node # 9 (ft)
3   Z-Accelerat. at Sensors, Node # 9 (ft)

4   X-Accelerat. at Right Boom End, Node # 5 (ft)
5   Z-Accelerat. at Right Boom End, Node # 5 (ft)

6   X-Accelerat. at Left Boom End, Node # 18 (ft)
7   Z-Accelerat. at Left Boom End, Node # 18 (ft)

8   X-Rot. Rate at Sensors, Node # 9 (radian)
9   Y-Rot. Rate at Sensors, Node # 9 (radian)
10 Z-Rot. Rate at Sensors, Node # 9 (radian)

11 X-Rot. Rate at Antena Bot-Left, Node # 24 (radian)
12 Y-Rot. Rate at Antena Bot-Left, Node # 24 (radian)
13 Z-Rot. Rate at Antena Bot-Left, Node # 24 (radian)

14 Y-Rot.Accel. at Right Joint, Node # 7 (radian)
15 Y-Rot.Accel. at Left Joint, Node # 16 (radian)

1.2.1 CMG System Response to Attitude Commands

Figure 1.2.4 shows the closed-loop system's response to a simultaneous 1° Command in all 3 axes. Notice that the CMG torque saturates at 150 (ft-lb). The system bandwidth is the same in all 3 axes.
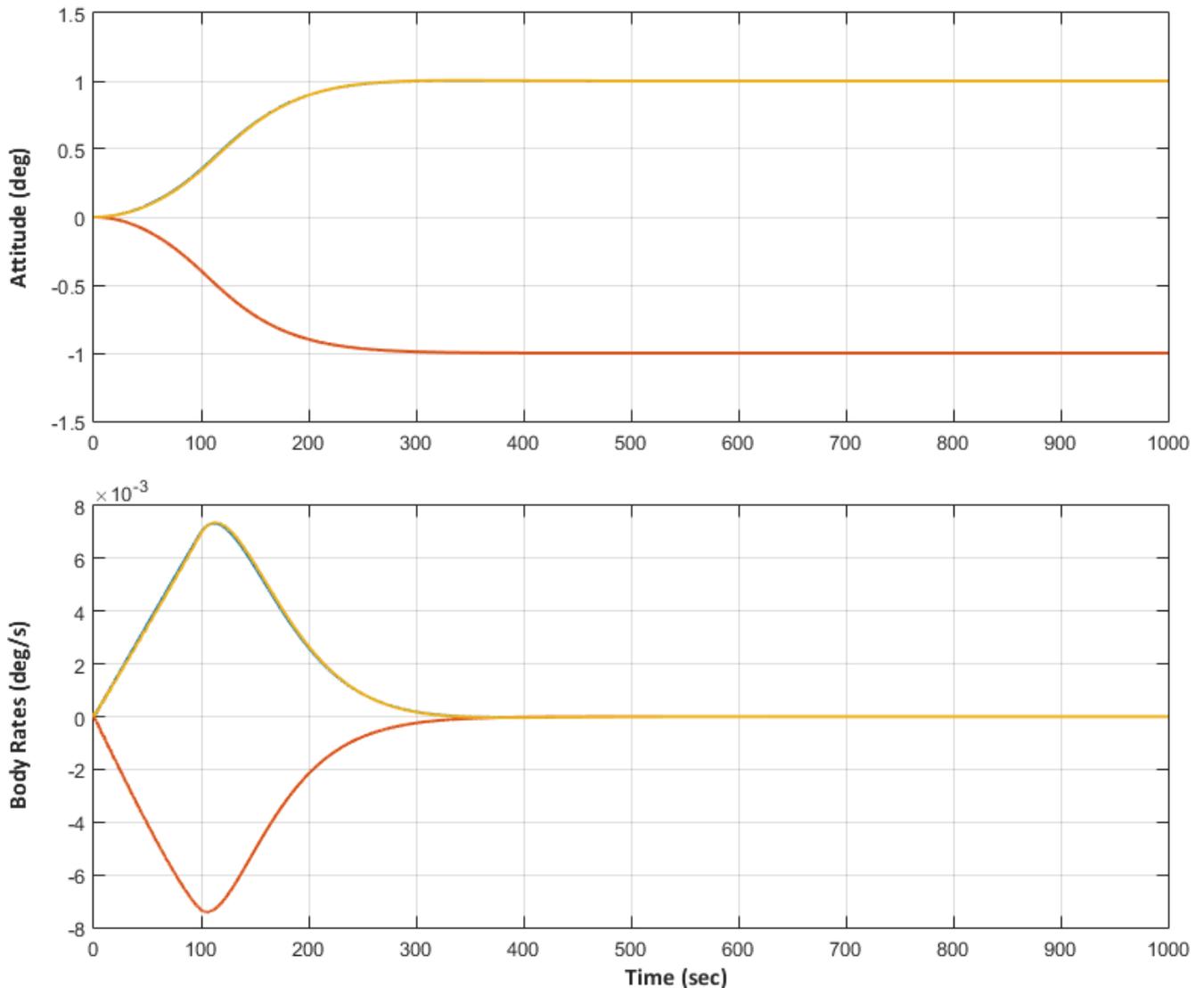

Space Station Linear Simulation, cmd=[1, -1, 1]
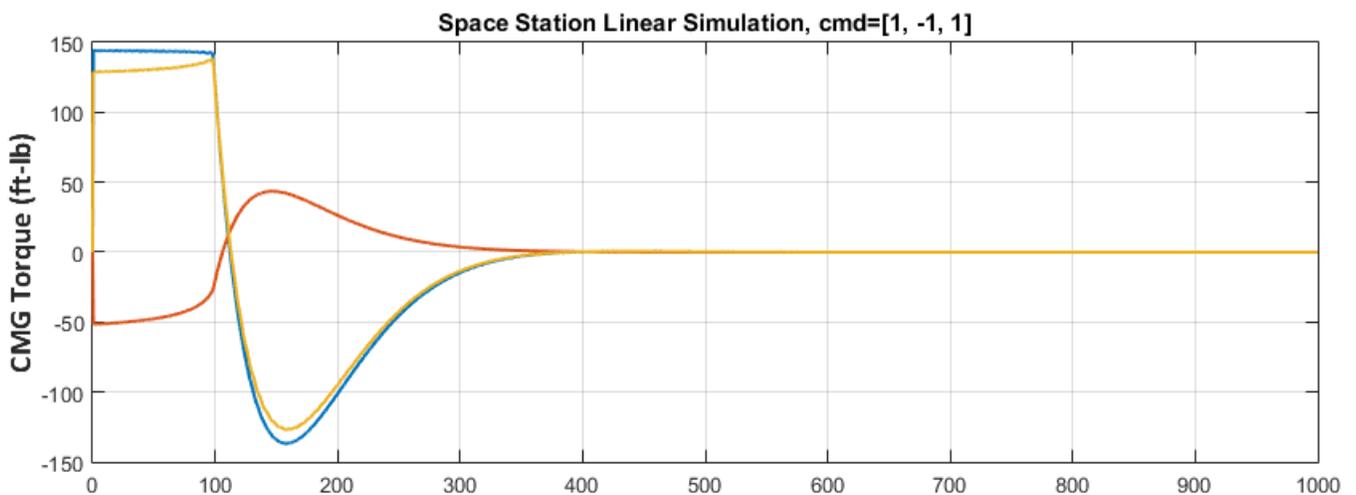
Figure 1.2.4 CMG Simulation System Response to 1º Attitude Commands

1.2.2 Open-Loop Model for Frequency Response Analysis

The Simulink model "*Open_Loop_CMG.mdl*", shown in Figure 1.2.5 below, is used for open-loop frequency response analysis. It consists of the same vehicle and controller subsystems, and it is located in the same folder "*Large Space Station\ (a) Mat Flex Lin (FEM)*". The control loops must be opened, one at a time, to perform linear stability analysis. The m-file "*start.m*" initializes the mass properties and control parameters for the simulations.

The Matlab function (linmod) is used to calculate the state-space system of the open-loop model with the other 2 loops closed. For roll analysis, for example, the roll loop is opened and the pitch and yaw loops are closed, as shown in Fig 1.2.5. The file "freq.m" calculates the frequency response across the two open ends. Figures 1.2.6 and 1.2.7 show the Bode and Nichols plots for the roll and yaw axes respectively.

```
% Initialization File: start.m
global J JI wo Th nt r2d d2r Accel Ts Tmax Kr
global ang_acc deadband kledge ratlim_up ratlim_lo
r2d=180/pi; d2r=pi/180;
Th=20; nt=12; Ts=0.02;                          % Thrusters
wo= 0.0011;                                      % Orbital Rate
omg=20*wo; zeb=0.85;                             % ACS bandwidth, damping
Tmax=200;                                        % Max Torque
J= [0.1187e9, -0.476e7, -0.1216e7; ...
   -0.476e7,  0.3863e8, -0.4303e6; ...
   -0.1216e7, -0.4303e6, 0.1101e9];
JI= inv(J);
[Ave, Bve, Cve, Dve]= rbsc;                      % Load Flixan Rigid-Body Vehicle Model
[Ave, Bve, Cve, Dve]= lfss_38m;                  % Load Vehicle Model from Flixan
load Krcs.mat -ascii                             % Jet Select Matrix (roll,ptch,yaw)
load Accel.mat -ascii                            % Thrusters Acceleration Matrix
Ainv=Pinv(Accel);

% Phase Plane Logic in (deg)
ang_acc=Th*[2*160/J(1,1), 4*160/J(2,2), 4*70/J(3,3)]*15;
deadband = [1.0,  1.0,  1.0]*0.5;                % RCS dead-band
kledge   = [1.2,  1.2,  1.2];
ratlim_up= [0.14, 0.08, 0.13]*0.2;               % Upper rate Limit
ratlim_lo= [0.14, 0.08, 0.13]*0.34*0.2;          % Lower rate Limit
Na_max=0.636/(deadband(1)*d2r);                  % Max Describing Function
Kr(1)= ratlim_up(1) /(2*ang_acc(1));             % attit + rate mixing gain
Kr(2)= ratlim_up(2) /(2*ang_acc(2));
Kr(3)= ratlim_up(3) /(2*ang_acc(3));
```
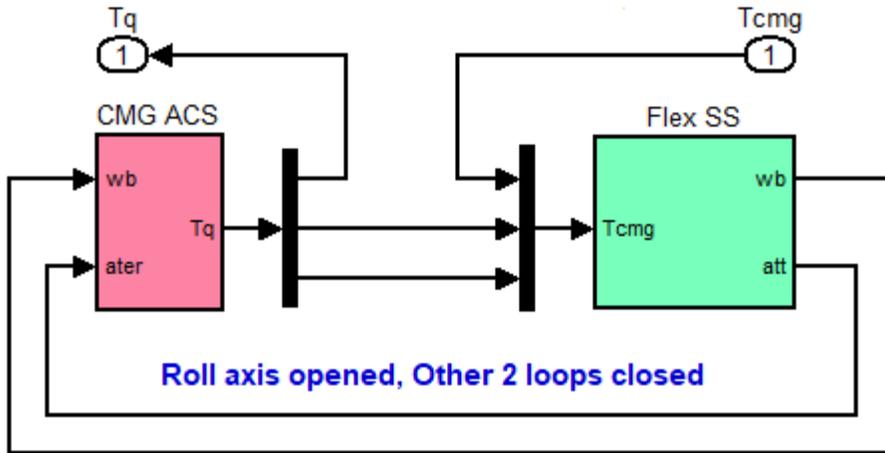

Figure 1.2.5 Block Diagram used for Open-Loop Frequency Response Analysis
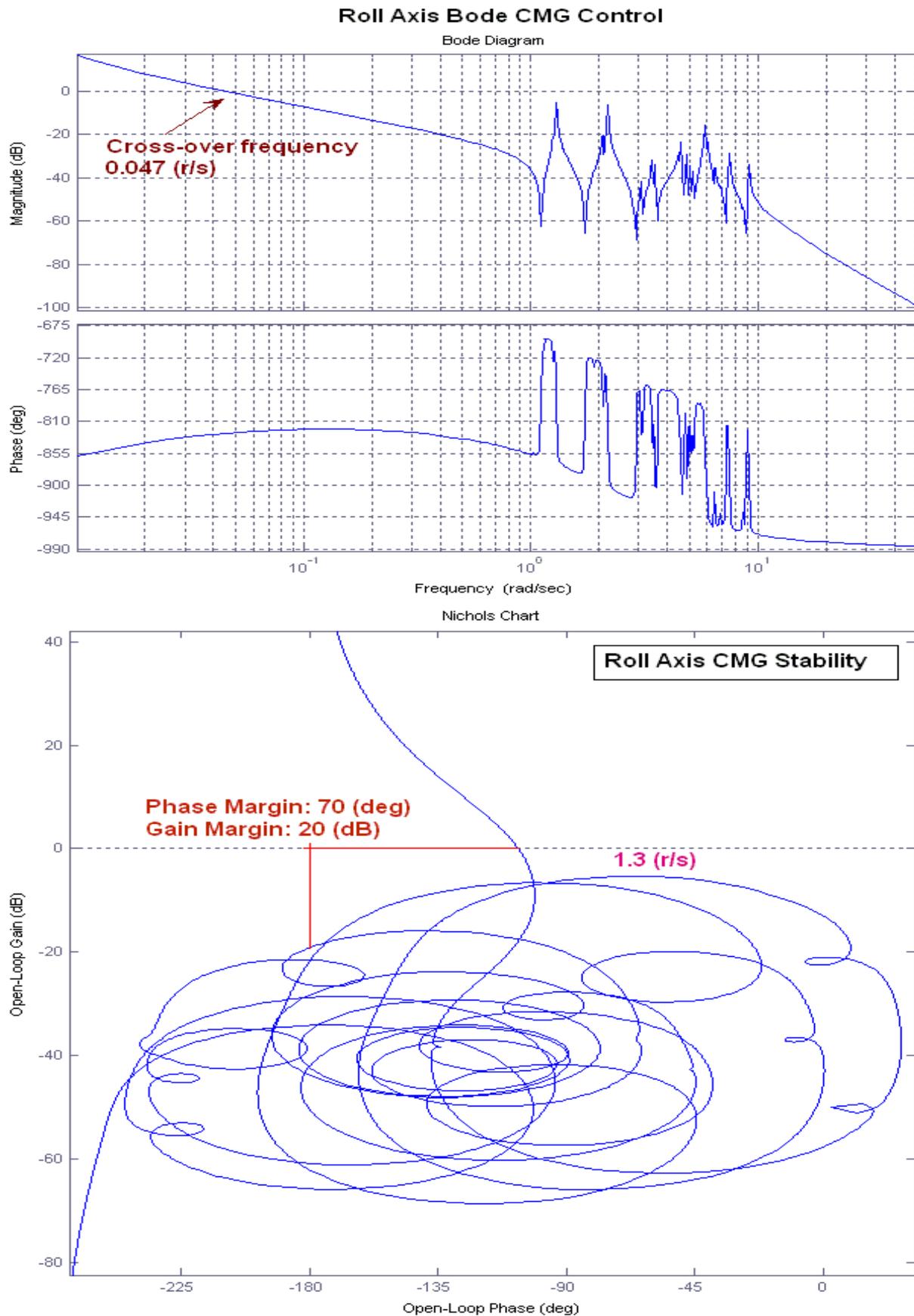
Figure 1.2.6 Roll Axis Stability Analysis Showing the Gain and Phase Margins
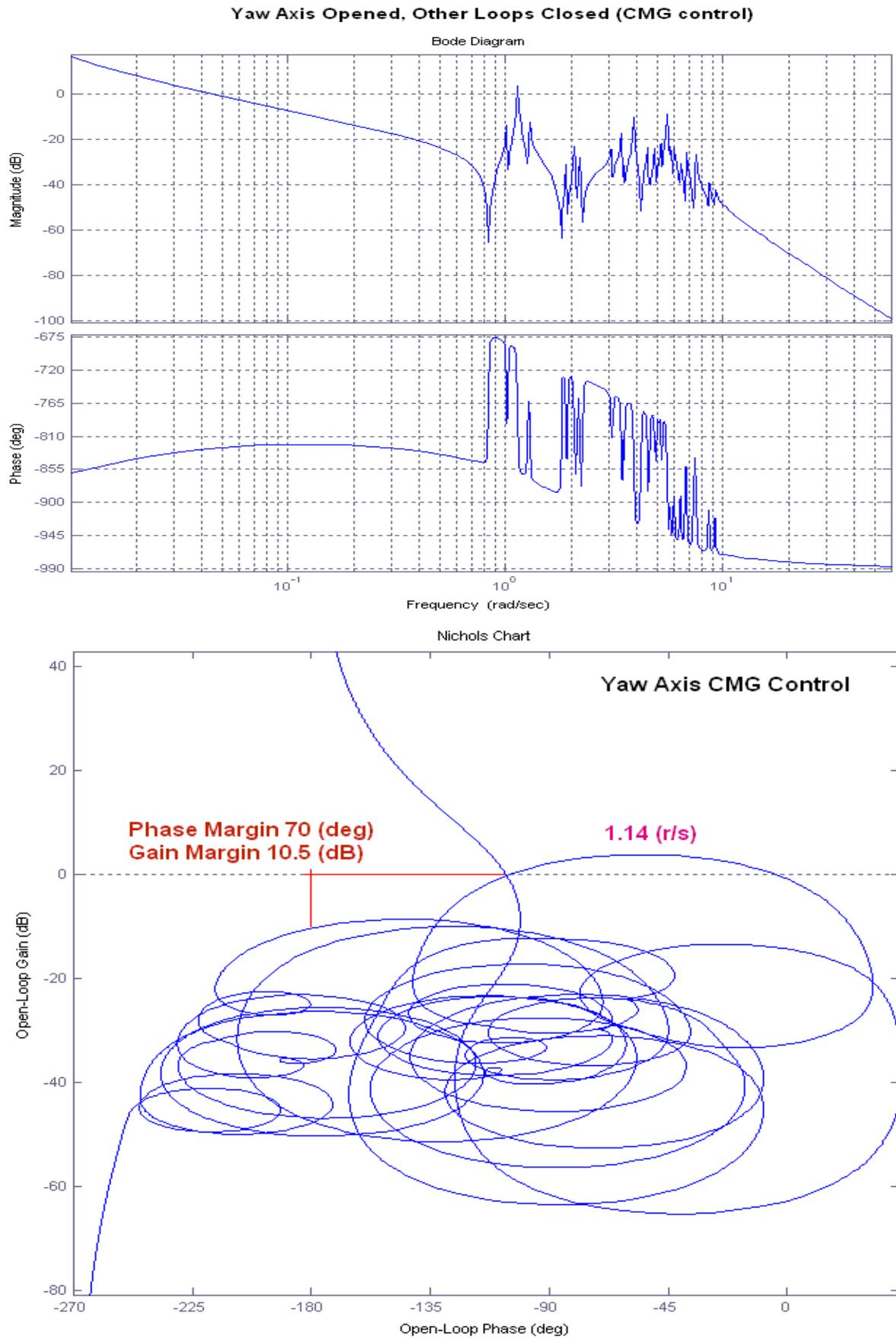
Yaw Axis Opened, Other Loops Closed (CMG control)

Bode Diagram

Nichols Chart

Figure 1.2.7 Yaw Axis Stability Analysis Showing the Gain and Phase Margins

1.2.3 Sensitivity Analysis to Disturbances

Sensitivity analysis of the CMG control system to disturbances is used to analyze the spacecraft response to external excitations. When the Space Station operates under CMG control it must provide a disturbance free environment for micro-gravity experiments. Sensitivity analysis in the frequency domain using singular value plots is a good indication of the amount of disturbance isolation achieved between excitation and sensor locations. This is the reason why we have included additional inputs and outputs in our analysis models than those necessary for attitude control feedback. The dynamic model includes disturbance inputs coming from the crew compartment and from a noisy instrument at the top boom. We have also included outputs for sensitivity analysis such as an earth pointing antenna at the bottom boom and a couple of optical instruments located at the extreme ends of the solar array boom.

The next two examples calculate the sensitivity responses between two separate groups of inputs and two separate groups of outputs. The Simulink model "*Lin_CMG_Sensitiv.Mdl*" in Figure 1.2.8 is used for analyzing sensitivity to disturbances and it has the CMG/ ACS loop closed. In the first sensitivity analysis case the input is a (3x1) disturbance torque at node #1 which is at the top boom and the output is a (3x1) angular rate at an antenna located at the bottom boom. The Simulink model "*Lin-CMG-Sensitiv.mdl*" in Figure 1.2.8 is modified to select the proper inputs and outputs and the function "linmod" calculates the state-space system for the corresponding inputs and outputs. The sigma plots are obtained by running the file "freq.m" and the function "sigma" calculates the SV frequency response between the selected input and output vectors. Figure 1.2.9 shows the frequencies where the antenna is most sensitive from the disturbances exciting node #1.

The second sensitivity analysis case is similar. The Simulink model "*Lin_CMG_Sensitiv.Mdl*" was modified using different sets of inputs and outputs, as shown in Figure 1.2.10. The inputs now are 3 forces (x, y, z) representing excitations from the crew compartment and the output is two accelerometers in the (x, z) directions located at the extreme left side of the solar array boom. The SV sensitivity response is shown in figure 1.2.11.

```
% Frequency Response Analysis File: freq.m
start
[Ao,Bo,Co,Do]=linmod('Lin_CMG_Sensitiv');    % Sensitivity Transfer Funct.
sys=ss(Ao,Bo,Co,Do);                          % frequency response analysis
figure(4); sigma(sys,w)
```
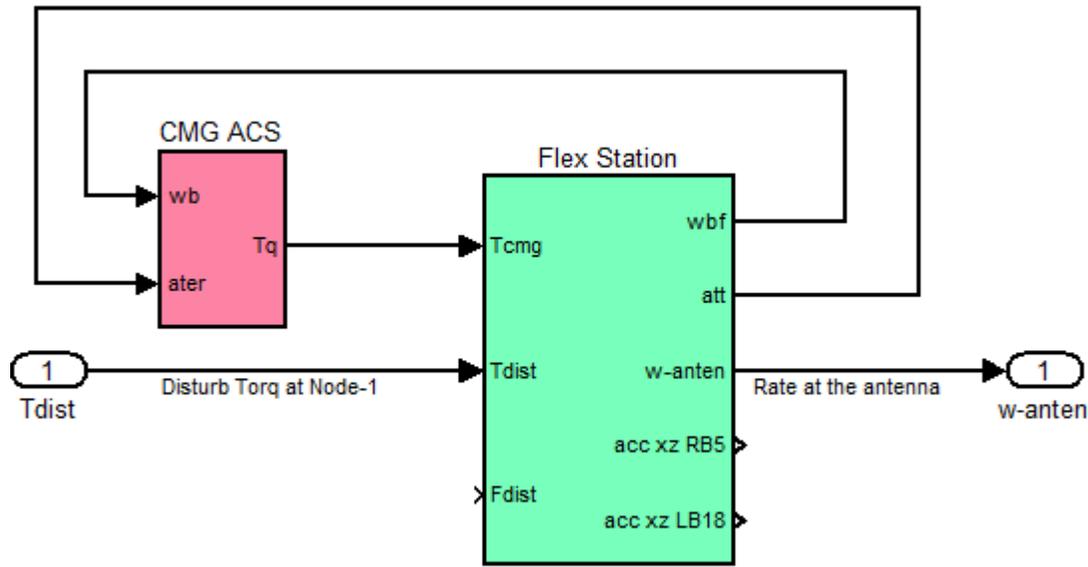
Figure 1.2.8 Simulink model "Lin_CMG_Sensitiv.mdl" used for Analyzing Sensitivity between Node #1 and Node #24
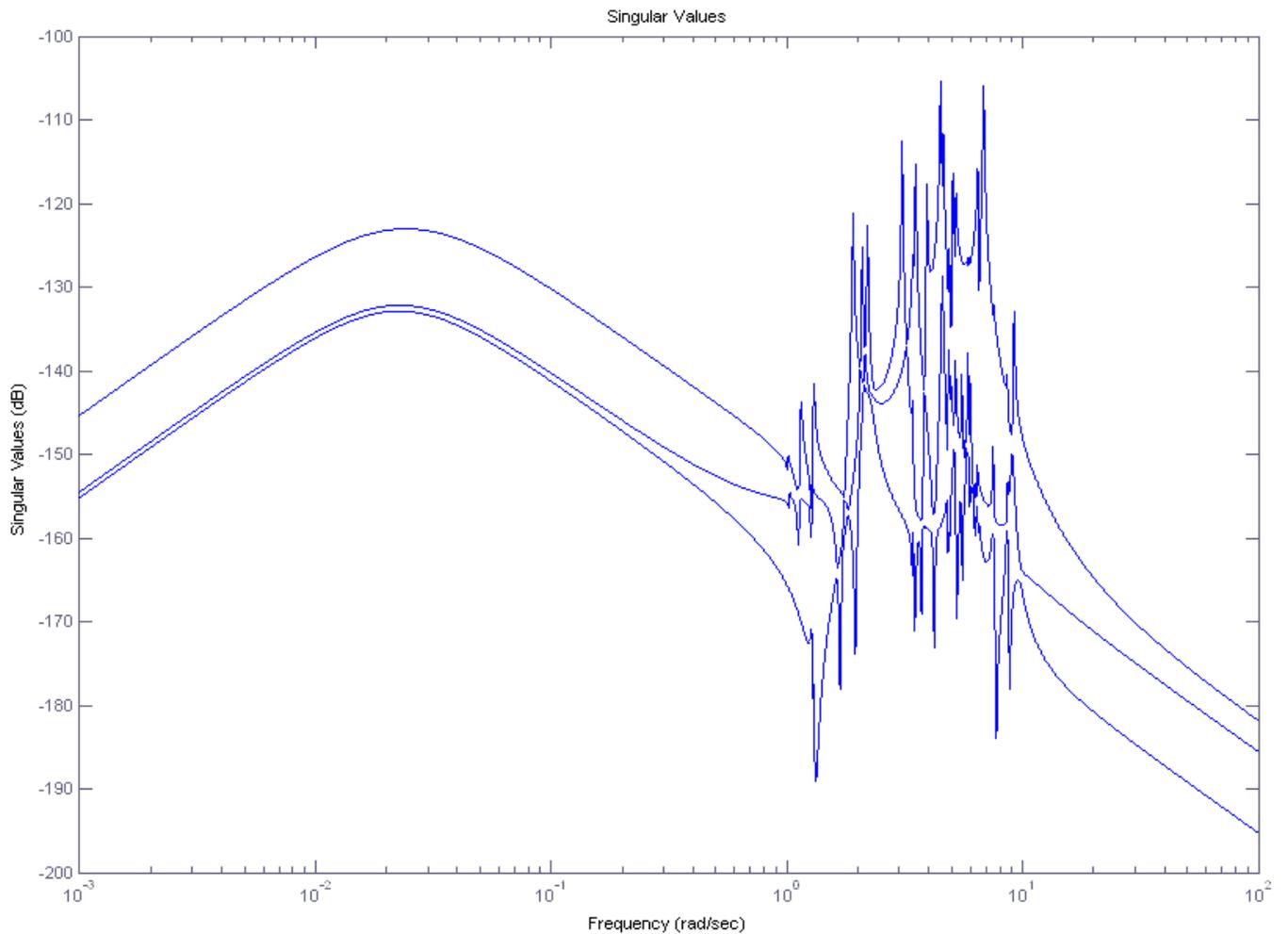

Figure 1.2.9 Sensitivity Response between Torques at Node #1 (top) to Rates at the bottom Antenna at Node #24
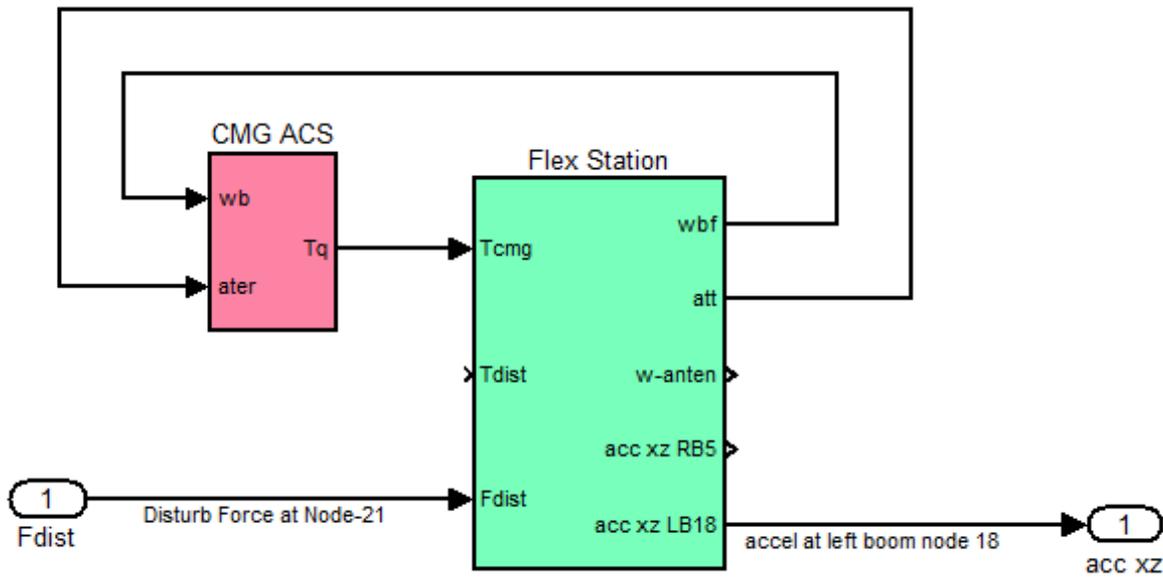
Figure 1.2.10 Simulink model "Lin_CMG_Sensitiv.mdl" used for Analyzing Sensitivity between Node #21 and Node #18
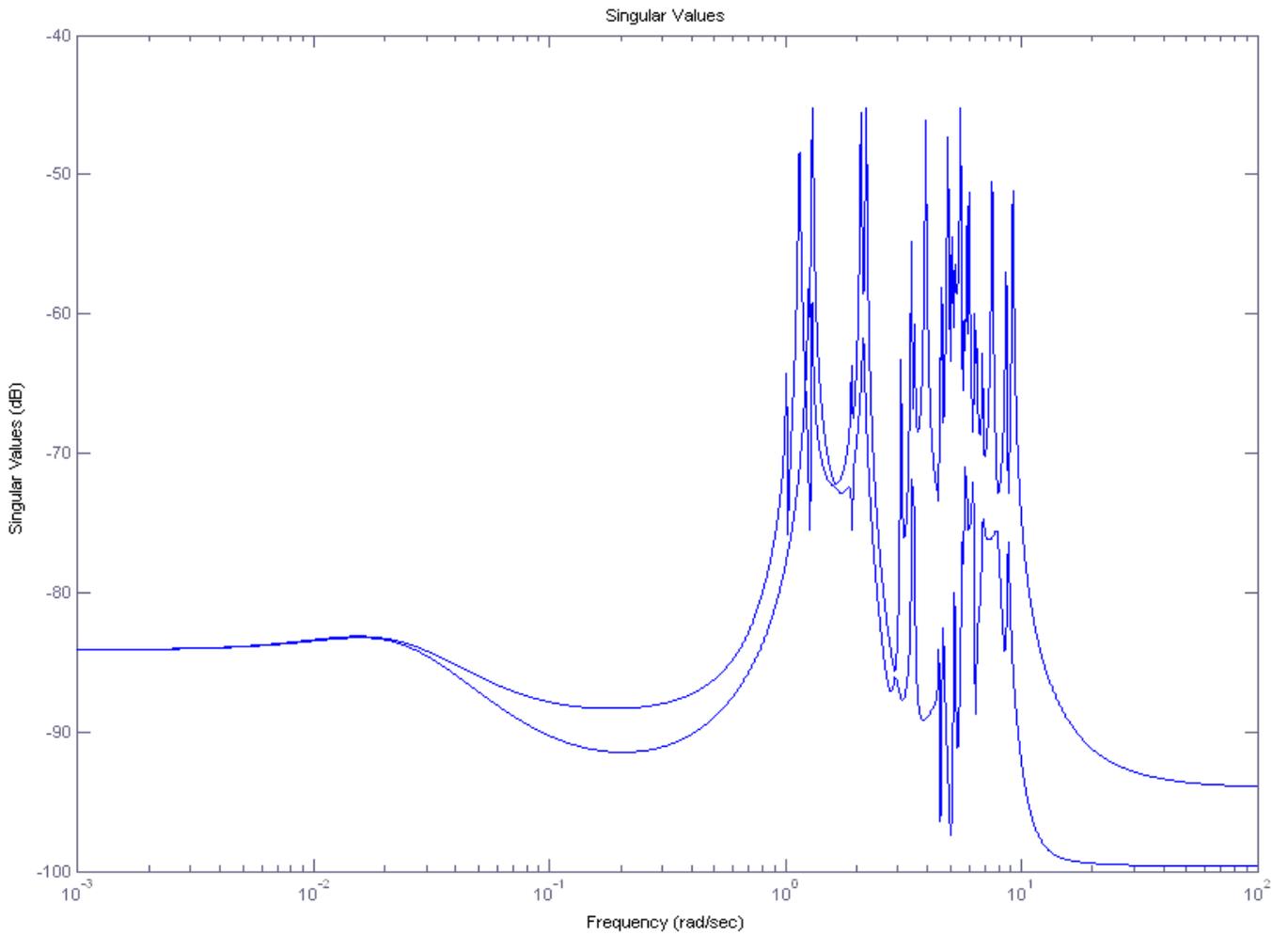

Figure 1.2.11 Sensitivity Response between Torques at the Crew Compartment Node #21 to the Accelerometers at the extreme end of the SA boom Node #18

1.3 Designing a Preliminary RCS Attitude Control System

The Simulink model "*Lin_RCS_Sim.mdl*" in folder *"Large Space Station\(a) Mat Flex Lin (FEM)"*, shown in Figure 1.3.1, is a simple simulation of the RCS Attitude Control System. The linear spacecraft model (green block) was described earlier and shown in detail in Figure 1.2.3. It includes the Flixan generated spacecraft m-file "*lfss_38m.m*" consisting of 6 rigid-body modes and 32 flex modes.
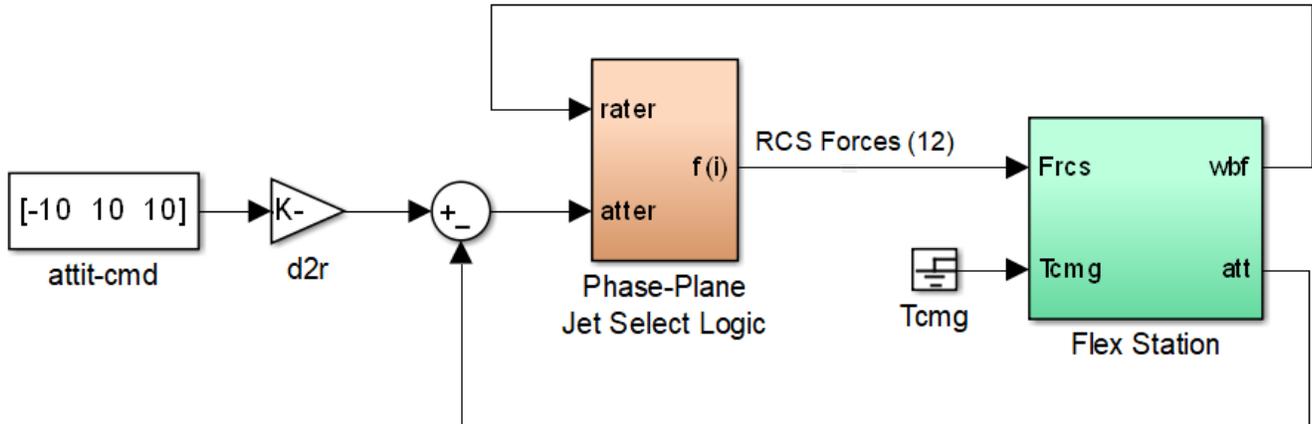

Figure 1.3.1 Space Station RCS Simulation Model "*Lin_RCS_Sim.mdl*" using a Linear Flex Model

The orange block includes the phase-plane and jet-selection logic. The inputs to the phase-plane logic are attitude errors and the vehicle rate. It calculates the rotation vector about which the vehicle must rotate in order to reposition from the initial orientation to the commanded attitude. The jet selection logic uses dot-product to calculate the torque contributions from all 12 jets in the required direction and selects a few jets that will contribute the biggest moment in the rotational direction.
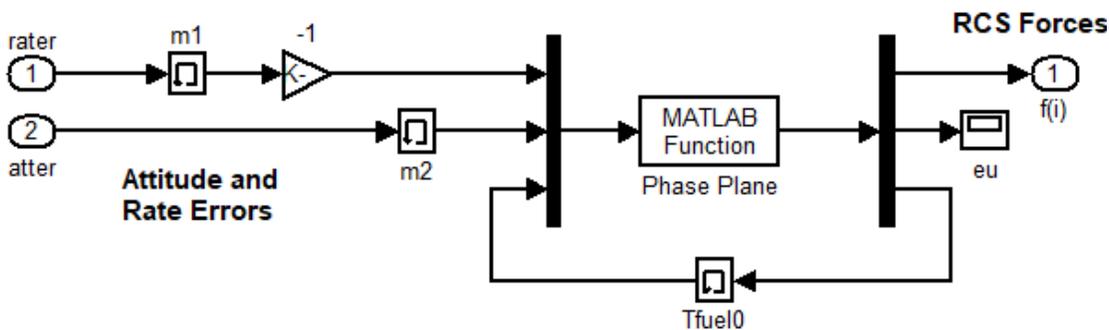
The jet selection output is a vector of 12 jet forces and the logic fires up to 3 jets at a time. The remaining jet thrusts are zero. The phase plane and the jet selection logic block are shown in more detail below. It is implemented in Simulink using the Matlab functions "*Phase_Plane.m*" and "*Jet_Select_dot.m*". The phase-pane function also calculates the fuel usage. The phase-plane parameters such as the dead-band and rate limits are loaded into Matlab by the initialization file "start.m". Additional parameters, such as, number of jets, thrust, jet locations, and thrust directions are also loaded into Matlab workspace and they are used by the jet selection logic to determine which jets must be fired to provide rotation in the direction commanded by the phase-plane logic. Notice that the jet selection logic output is 12 jet forces but the RCS force inputs to the flex spacecraft model are 8 RCS jet forces. They are actually throttles (not forces) that vary from zero to ±1. This is because in the logic there are four jets firing in the +x direction and four jets firing in the -x direction, obviously with a positive thrust. In the spacecraft model, however, each ±x jet pair can be represented with a single thruster that receives either +1 or -1 throttle that corresponds to either positive or negative 20 (lb) of thrust. Figure 1.2.3 shows the conversion of the ±x RCS jet forces from the jet-select logic to match the throttle inputs in the spacecraft model.

Figure 1.3.2 shows the phase-plane logic that determines the jet firing direction as a function of the rate and attitude errors. It consists of three regions: a region of zero firing, a region of positive jet firing, and a region of negative jet firing. The logic uses three phase planes, one for each axis. The firing decision is made based on the rate and attitude error combination in the rotation direction to reduce error.
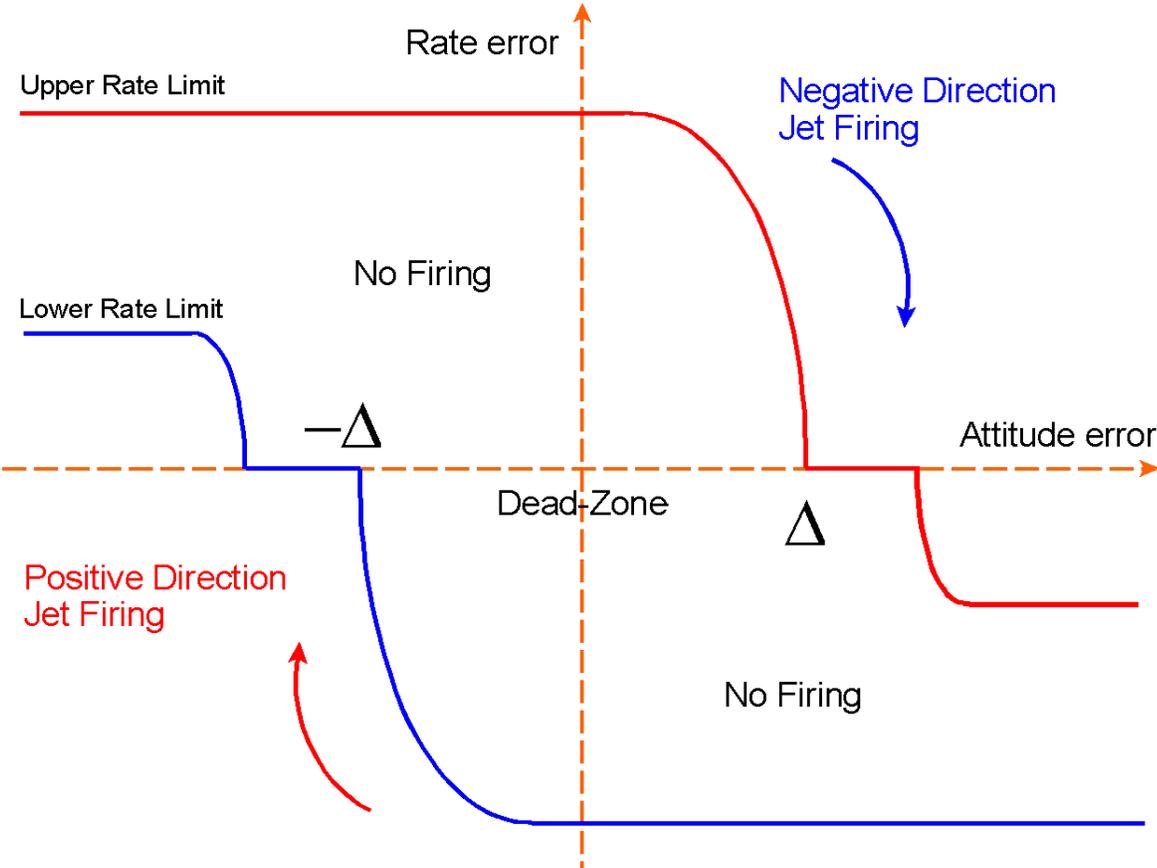

Figure 1.3.2 Phase-Plane Shows Conditions for Jet Firing

1.3.1 Frequency Domain Analysis Using Describing Function

The Describing Function (DF) analysis method will be used in this section to analyze stability of this spacecraft and to design bending filters for its highly flexible structure. The filters are notches and low-pass and they are needed to attenuate the modes and to prevent the jet firings from exciting the flex modes into limit cycles. It is impossible to prevent the structure from getting excited when the jets are firing but it is possible prevent the flex modes from being driven into limit-cycling. The DF is a single-input-single-output method that requires the non-linearity to be contained in a single SISO block. It is not easy to apply the DF method in this case using the exact phase-plane non-linearity because the phase-plane logic has two inputs (attitude error and rate). We will, therefore, try to approximate it with a SISO non-linearity that operates in a similar fashion but it is much easier to analyze.

The DF method allows us to analyze sensitivity of the flex modes to instability or measure how close they are to limit-cycling. It helps us determine at what frequencies it is necessary to design filters that will prevent flex modes from limit-cycling. When the system is limit-cycling at a certain frequency, the rate and attitude error trajectory inside the phase-plane in figure 1.3.2 will be very similar to the trajectory produced by a much simpler phase-plane shown in Figure 1.3.3. The switching lines of the simple phase-plane are chosen so the limit-cycle trajectory resembles the non-linear trajectory. In this approximation the non-linearity can be modeled as a dead-zone whose input is a combination of attitude plus rate error as shown in figure 1.3.4.

$$slope \approx \frac{1}{K_r} \approx -\frac{\omega_{\lim}}{\dfrac{\omega_{\lim}^2}{2\,a_{\lim}} + 0.1\Delta}$$

Rate error

Negative Direction Jet Firing

$\theta_e + K_r\omega_e > 1.1\Delta$

No Firing

-1.1 Δ

Dead-Zone   1.1 Δ Attitude error

Positive Direction Jet Firing

$\theta_e + K_r\omega_e < -1.1\Delta$
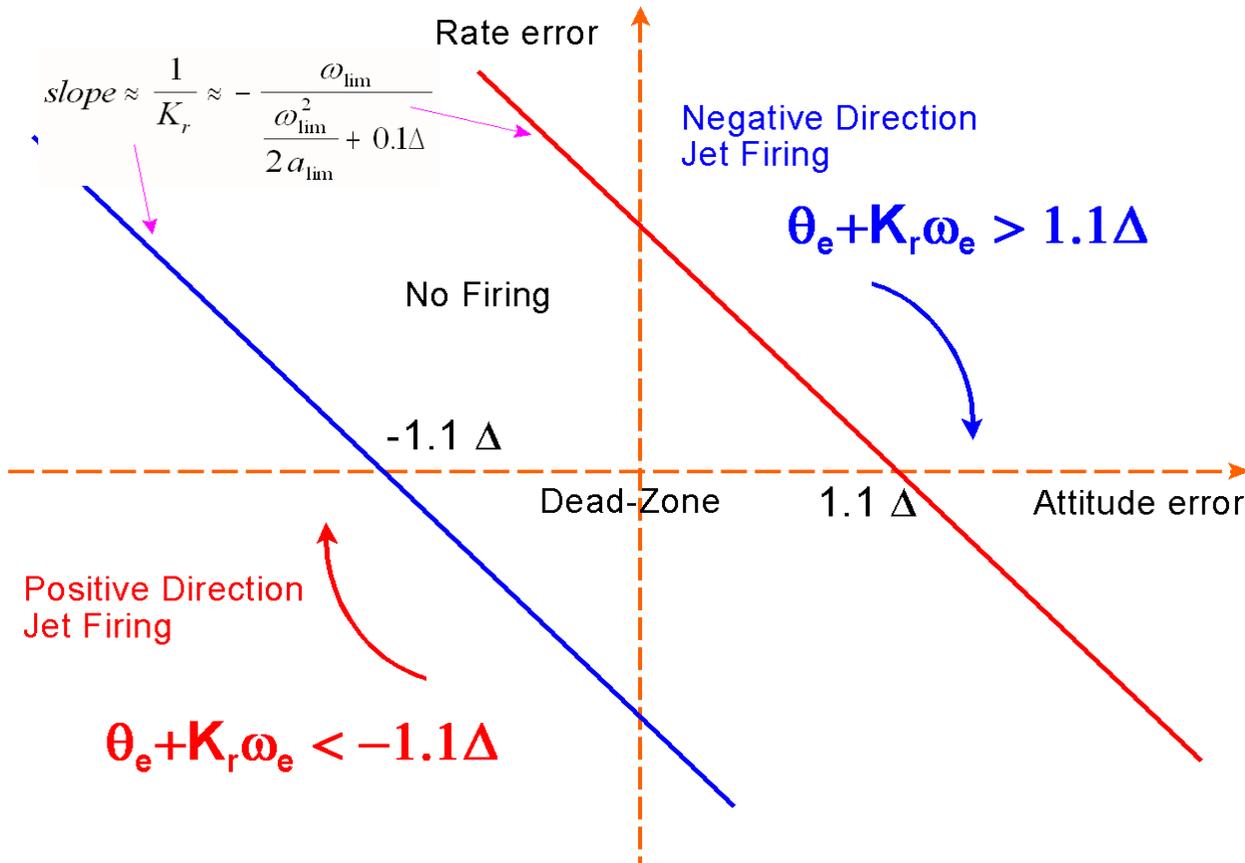
Figure 1.3.3 Phase-Plane Approximation for DF Analysis

$$K_r = \dfrac{\dfrac{\omega_{lim}^2}{2\, a_{lim}} + 0.1\Delta}{\omega_{lim}}$$
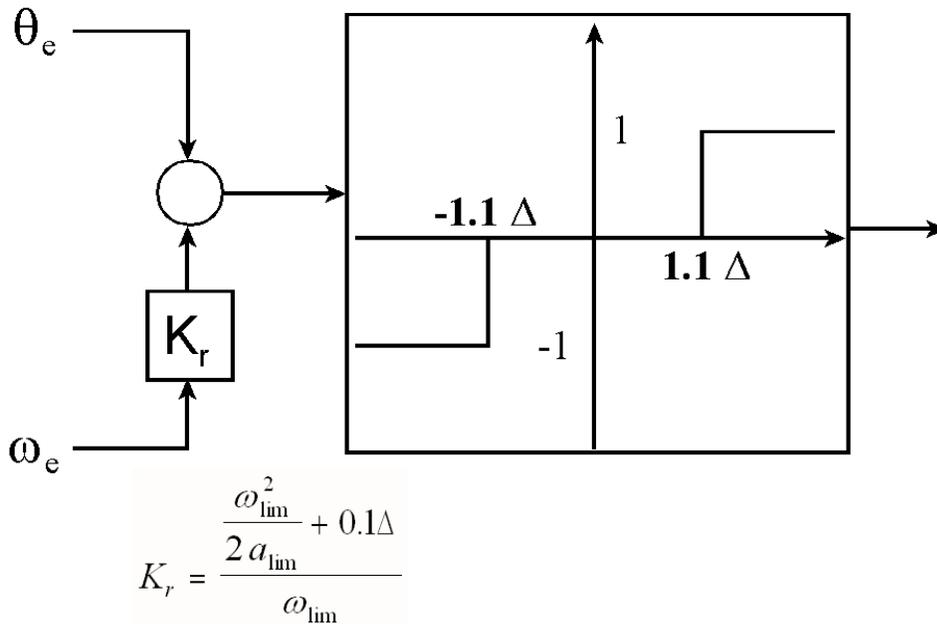
Figure 1.3.4 The Phase-Plane Non-Linearity can be approximated by a Dead-Band Non-Linearity for DF Analysis

When a sinusoid of amplitude (a) and a frequency (ω) is applied to a memory-less type of non-linearity such as the dead-band, the output will be a periodic function of the same frequency. If we decompose the output signal, ignore the harmonics, and keep only the fundamental frequency which is at the same frequency as the input signal, the Describing Function (DF) is defined to be the ratio of the fundamental signal amplitude divided by the input signal amplitude. The DF of this non-linearity is a function of amplitude (a) and not frequency. It represents the gain N(a) of the non-linearity at different amplitudes. For a dead-band non-linearity with a dead zone (Δ) radians, the DF N(a) is given by equation 1.3.5. Its maximum value is of importance because it represents the minimum point of the 1/N(a) locus which is important for stability analysis.

$$N(a) = \frac{4}{\pi a}\sqrt{1 - \frac{\Delta^2}{a^2}}$$

$$N(a)_{max} = \frac{0.636}{\Delta} \qquad when \quad a = \frac{\Delta}{0.7}$$

Equation 1.3.5 Describing Function of the Dead-Band Non-Linearity and its Maximum Value

According to the DF theory a limit cycle will occur when $G(j\omega) = -1/N(a)$, which means that in order to avoid limit cycling the two loci should not intersect when we plot them together either on a Nichols or a Nyquist diagram. The intersection points on the G(jω) locus will predict the frequencies of the oscillations and on the 1/N(a) locus will predict the amplitudes of the limit-cycles, since there may be more than one limit-cycle. The Simulink model "*Open_Loop_RCS.mdl*" in Figure 1.3.6, is used for calculating the normalized frequency response G(jω) of the Space Station in order to apply the Describing Function method. It approximates the open-loop linear dynamics of the attitude control system G(s) excluding the non-linearity. The attitude and rate errors in the specified direction combine together as in Fig. 1.3.4 to create a SISO system whose input and output would normally connect across the dead-zone non-linearity closing the feedback loop. Since it is a SISO system we can only analyze DF stability in one rotational direction at a time and the rotational axis is defined as a constant unit vector input that affects two subsystems in Fig. 1.3.6. This implementation allows us to analyze stability not only in roll, pitch and yaw, but also in other skewed directions since each rotational direction corresponds to a unique set of jets that excite the structure differently. For DF analysis, the -1/N(a) locus is drawn on the same Nichols chart where intersections between the two loci may indicate possible limit-cycles.
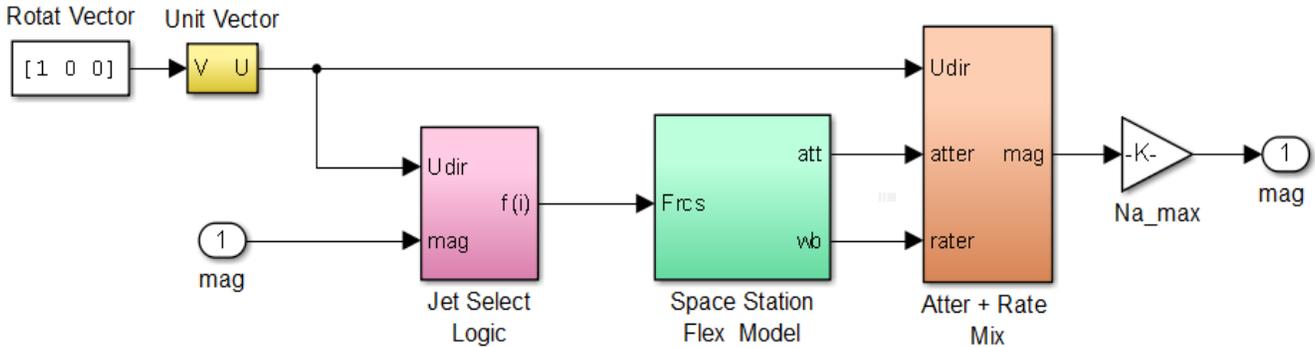

Figure 1.3.6 Simulink Model "Open_Loop_RCS.Mdl" used for Calculating the G(jω)N(a)$_{max}$ Frequency Response for Describing Function Analysis. The Rotational Axis Direction is defined as Input Vector

The linear system model G(s) includes flexibility and its excitation is constrained to a single rotational axis, the direction of the input vector. It includes a linearized version of the jet select logic, implemented in function "JSel_ln.m", which averages the positive and negative jets affecting the specified direction. The logic selects the jets contributing positive accelerations in the selected direction. It selects also the jets contributing in the opposite direction and applies negative thrusts in the jets contributing in the reverse direction. Positive and negative thrusts are averaged in this linear model to produce the same average acceleration as if only positive jets were firing. This creates a more symmetrical system for linear analysis. The output of G(s) is also measured along the specified direction. It is a vector combination of attitude error plus rate multiplied by gain Kr. This output vector is resolved (dotted) in the specified direction using function Mix.m to produce a scalar output which is the vehicle response in the specified direction. G(s) is therefore excited in the specified direction and its response is only measured in the same direction, which may be roll, pitch, yaw, or any other skewed directions. The G(s) plant is also scaled by multiplying it with the maximum value N(e)$_{max}$ of the DF. This is for convenience because in Matlab the (+) sign in Nichols and Nyquist plots now represent the minimum point of the scaled -1/N(e) locus and makes it easier to measure the relative margin between the two loci.

After specifying the rotational axis you must run the file "freq.m" which uses the Matlab function "linmod" to compute the system G(s), calculates the frequency response and plots it on a Nichol's chart. On the same Nichols chart we overlay the inverse DF locus -1/N(a), as shown in Figures 1.3.7 for roll, pitch, and yaw. The DF locus repeats itself every 360° and it appears as vertical red lines along the -180° lines with their minimum points (+) approaching the G(s) locus. Filtering is necessary in order to avoid intersections between G(s) and -1/N(a) loci and to prevent limit-cycles whose frequency and amplitude are determined by the intersection points. Prior to filtering we discovered that there were several intersections between the red and blue loci and we designed notch filters to prevent intersections and limit-cycles. The bending filters are included in the rate gyro outputs in the Space Station dynamics block in figure 1.3.6. Note that the system does not oscillate at all intersection frequencies. Different types of disturbances excite different limit-cycle frequencies.

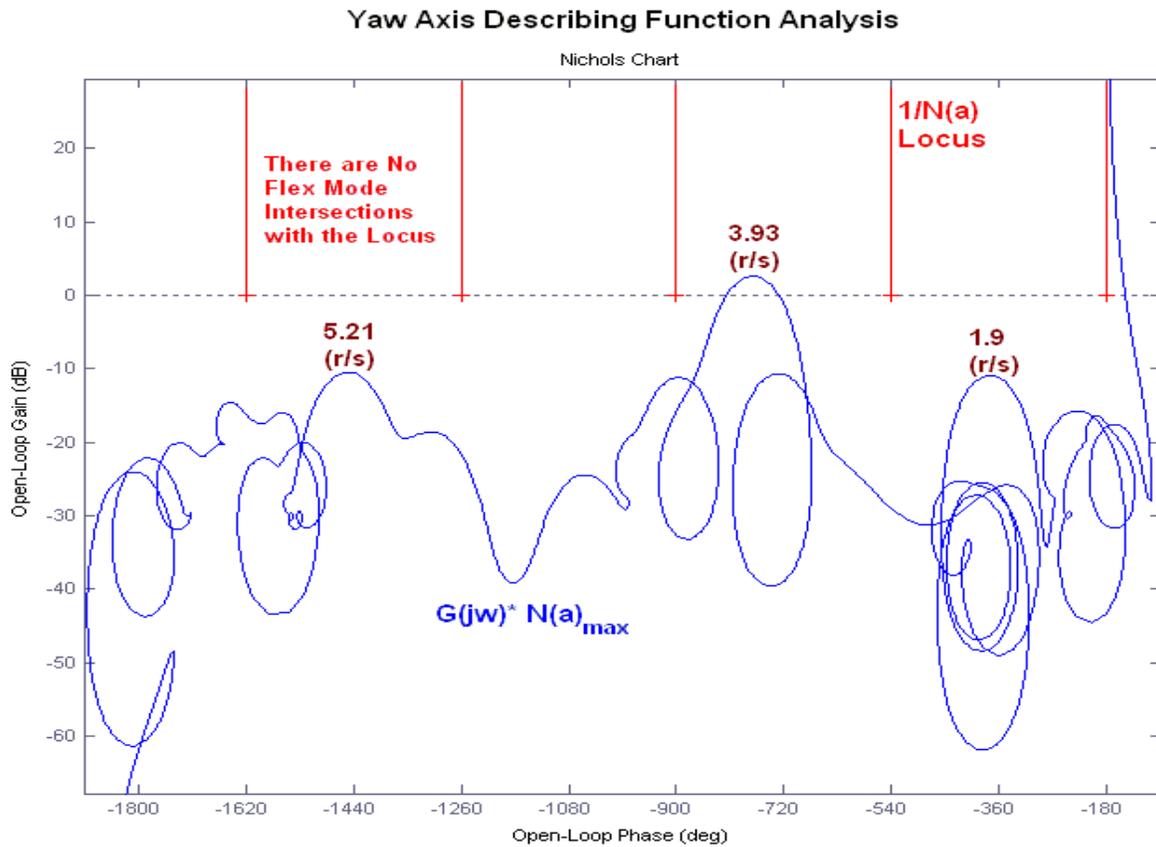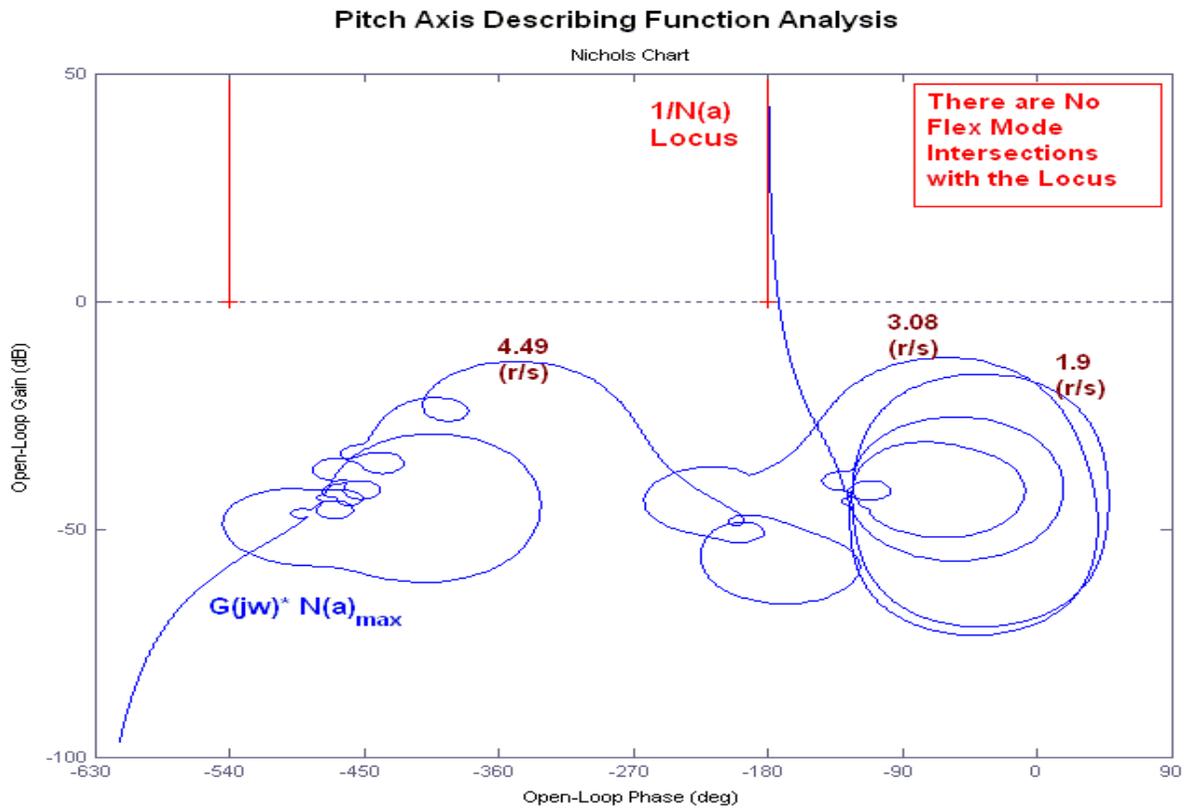

Roll Axis Describing Function Analysis
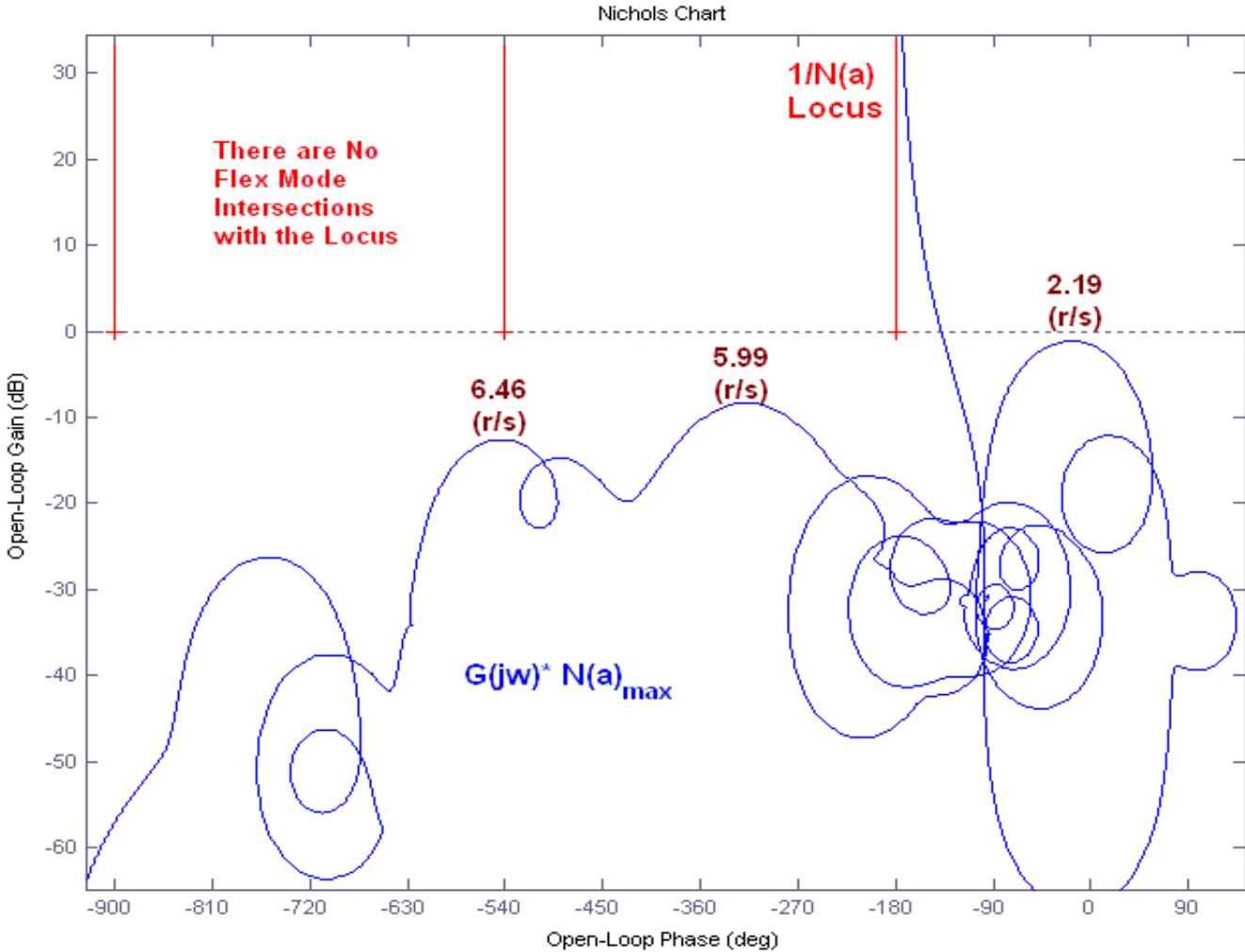
Figure 1.3.7 Describing Function analysis shows no Intersections between the Loci indicating that there are No Limit-Cycles. Most of the Flex Modes are Gain Stable except for one which is Phase Stable.

1.3.2 RCS Closed-Loop Simulation

We will now demonstrate the stability of the RCS attitude control system using a simulation. Figure 1.3.1 shows the Simulink model "*Lin_RCS_Sim.mdl*" that is used for closed-loop simulations. It includes the same phase-plane and spacecraft dynamics models as those used in frequency domain analysis. The system is commanded to perform an arbitrary (-10°, 10°, 10°) 3-axes attitude maneuver and its response is shown in Figure 1.3.8. There is a strong structural mode excitation by the RCS firing. The flex oscillations, however, decay without any limit-cycling, as predicted by the DF analysis.
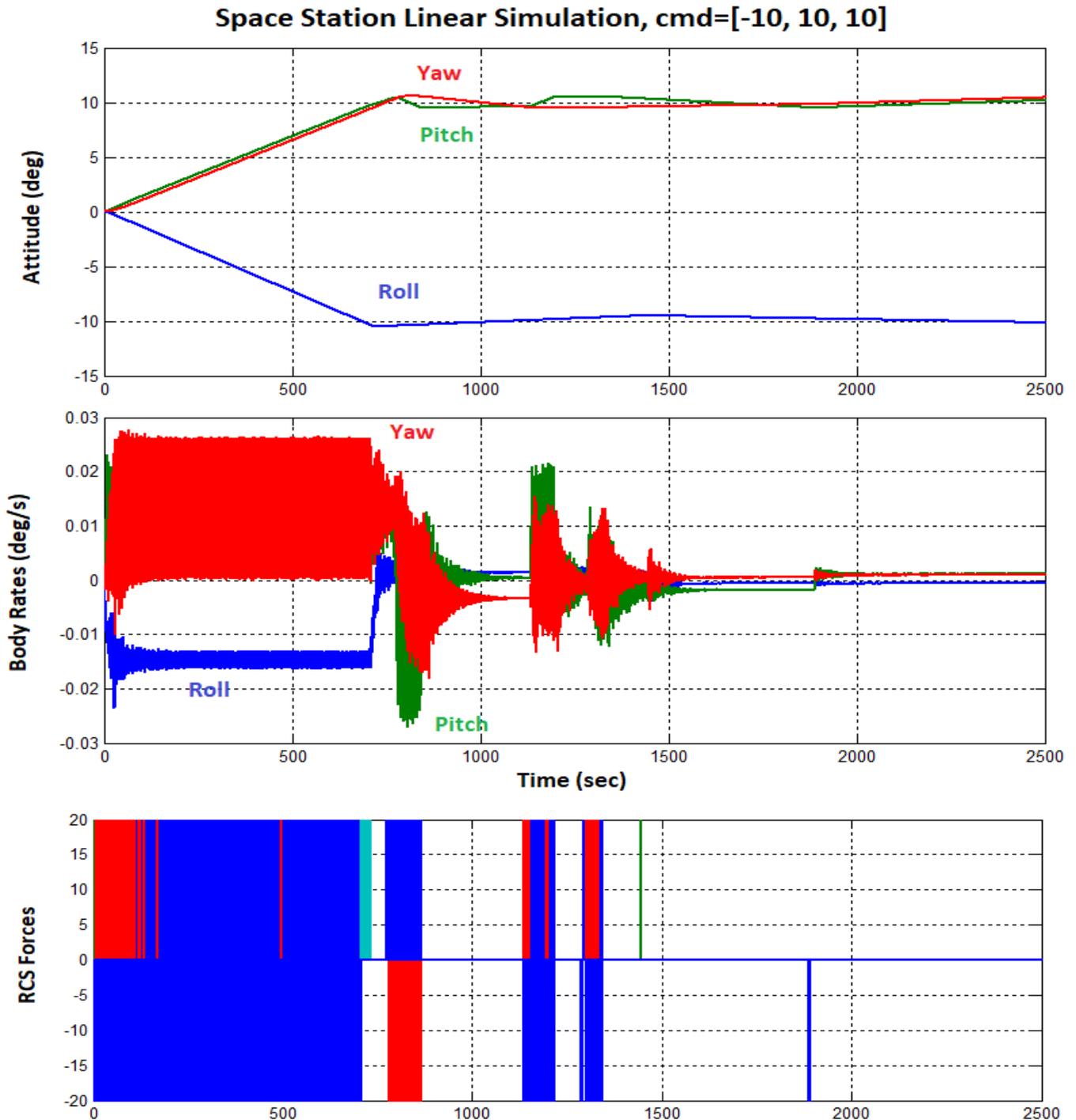

Figure 1.3.9 Closed-Loop System Response to an Attitude Maneuver Command, Shows no Limit-Cycling

2. Non-Linear Rigid Body Modeling and Control Design

In the previous section we developed a preliminary attitude control system for the Space Station using CMGs and reaction control jets for a linear spacecraft model that is inertially fixed and it is derived from a finite elements model. In this section we will focus and analyze the non-linear spacecraft dynamics and we will improve our dynamic models and control design by taking into consideration that the Space Station is rotating at constant orbital rate ω_o since its z-axis is pointing towards the earth. Rigid-body models will be developed and control systems to stabilize the Station with respect to the local vertical local horizontal frame, and the analysis will be performed in Matlab. The LVLH frame rotates at orbital rate and the spacecraft ACS attempts to keep the spacecraft at constant attitude relative to the LVLH. The LVLH x axis is in the velocity direction, the z axis is pointing towards the center of the earth, and the y axis is perpendicular to the x-z plane pointing towards the right solar array. The following equations describe the Space Station rigid body non-linear dynamics relative to the LVLH frame.

$$I\underline{\dot{\omega}} = -(\underline{\omega} \times I\underline{\omega}) + 3\omega_o^2(\underline{c} \times I\underline{c}) + \underline{T}_d + \underline{T}_c$$

$$I = \begin{bmatrix} I_{XX} & I_{XY} & I_{XZ} \\ I_{XY} & I_{YY} & I_{YZ} \\ I_{XZ} & I_{YZ} & I_{ZZ} \end{bmatrix}; \quad c = \begin{bmatrix} -\sin\theta\cos\psi \\ \cos\phi\sin\theta\sin\psi + \sin\phi\cos\theta \\ -\sin\phi\sin\theta\sin\psi + \cos\phi\cos\theta \end{bmatrix}$$

$$\begin{pmatrix} \dot{\phi} \\ \dot{\theta} \\ \dot{\psi} \end{pmatrix}_{LVLH} = \frac{1}{\cos\psi} \begin{bmatrix} \cos\psi & -\cos\phi\sin\psi & \sin\phi\sin\psi \\ 0 & \cos\phi & -\sin\phi \\ 0 & \sin\phi\cos\psi & \cos\phi\cos\psi \end{bmatrix} \omega + \begin{pmatrix} 0 \\ \omega_o \\ 0 \end{pmatrix}$$

$$\dot{h}_{CMG} = -(\omega \times h_{CMG}) - T_c$$

Equation 2.1 Non-Linear Equations of Motion of a Spacecraft in the Rotating LVLH frame

Where: $\underline{\omega}$ is the spacecraft body rate, ω_o is the Space Station orbital rate (0.0011 rad/sec). The first two non-liner terms on the RHS of the top moment equation are the gyroscopic and gravity gradient torques. The torques T_c and T_d represent the CMG control and external disturbance torques applied to the spacecraft. The spacecraft attitude is initialized relative to the LVLH frame with an initial pitch rate equal to $-\omega_o$ (rad/sec). The attitude kinematics equation calculates the vehicle Euler angles (ϕ, θ, ψ) with respect to the LVLH frame from the body rates. The bottom part of Equation 2.1 calculates the rate of change of the CMG momentum as a function of the torque T_c applied to the spacecraft by the CMG array.

The internal CMG steering dynamics and the steering logic are not included in this simple model. A more detailed CMG model would include the relationship between the CMG gimbal rates and the output torques. It would also include the steering logic which translates the torque demands coming from the ACS to gimbal rate commands that drive the gimbal servos. The steering logic calculation is obtained by solving a pseudo-inverse of the gimbal dynamics and requires the exact geometry of the CMG configuration, the gimbal angles, and the CMG momentum. The steering design is not simple because of singularities or "gimbal locks" that may occur when the CMG array cannot provide torques in some directions which are demanded by the ACS. There are singularity avoidance algorithms that attempt to bypass gimbal lock situations and they are presented in other examples. They produce, however, small disturbances on the spacecraft. The simplified models used in this analysis do not include the CMG steering details but treat the CMG array as an integrated momentum control unit and approximate the CMG servo system with second order transfer functions of 2 (rad/sec) bandwidth that provide torque in roll, pitch, and yaw directions. The detailed wheel precession dynamics and the steering logic can be included later in the dynamic models as separate CMG dynamics block.

The Matlab analysis files for Section 2 are located in folder: *"Large Space Station\ (b) Mat NonLin RigBod"*. The non-linear Equations 2.1 are coded as a Matlab function *"Rigbod-Dynam-LVLH.m"* which is running as a subsystem block, shown in Figure 2.1, in the simulation models. The inputs to the spacecraft subsystem are: CMG control torques (T_c), disturbance torques (T_d), and the 12 RCS forces. There are 15 outputs: the body rates (3), the vehicle attitude relative to the LVLH frame (3), the CMG momentum in body axes (3), the total spacecraft and CMG system momentum (3), and the vehicle rates in the LVLH frame (3). The gravity gradient dynamics are calculated internally as a function of the Euler angles. This vehicle dynamics function also calculates the transformation matrix CB2L used to transform the vehicle attitude and rate from body to LVLH frame. It calculates the derivative of the 9-state-vector which is updated by an integrator loop around the function.
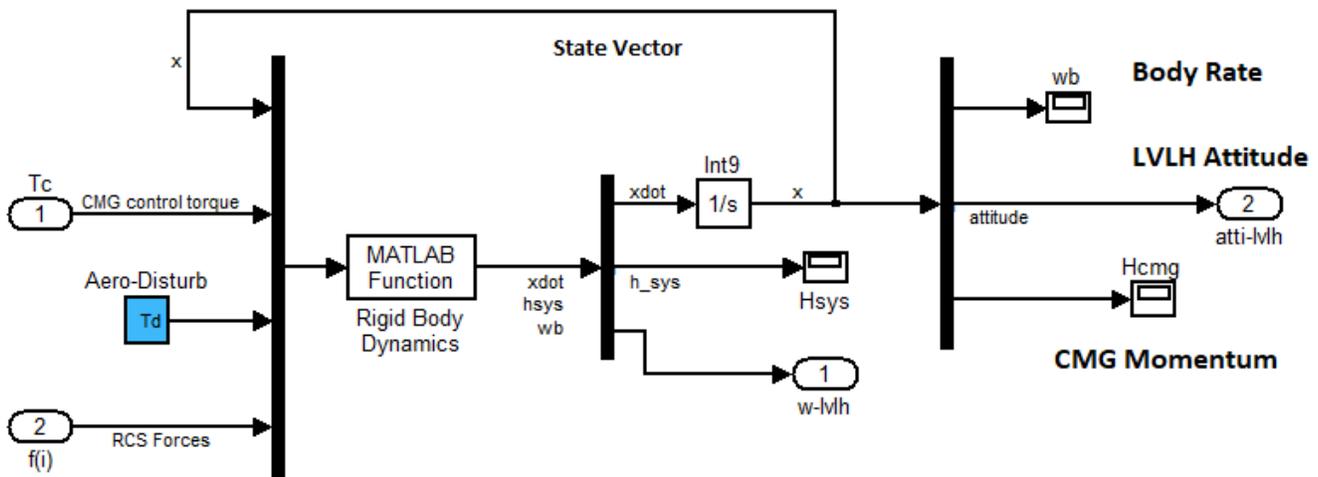

Figure 2.1 Non-Linear Space Station Dynamics Containing Function: Rigbod-Dynam-LVLH.m

The aerodynamic disturbance torque T_d consists of steady torques and also cyclic components that excite the spacecraft attitude to oscillations. The cyclic components are mainly caused by the rotation of the solar arrays at orbital rate ω_o since they are always pointing towards the sun, completing one rotation per orbit relative to the spacecraft. There are two frequency components associated with the cyclic disturbance torques: one is at orbital rate ω_o due to the difference in atmospheric density between the sunny and the dark sides of the earth, and the second component is at twice the orbital rate $2\omega_o$ caused by drag variation due to the solar arrays rotation. There is less drag when the arrays are

horizontal and more drag when they are vertical. The aero disturbance is stronger in pitch direction because the moment-arm distance between the vehicle CG and the center of pressure is longer. The roll, pitch, and yaw disturbance torque (T_d) used in the simulations is:

$$T_d = \begin{bmatrix} 1 + \sin \omega_o t + 0.5 \sin 2\omega_o t \\ 8 + 3 \sin \omega_o t + 0.5 \sin 2\omega_o t \\ 1 + \sin \omega_o t + 0.5 \sin 2\omega_o t \end{bmatrix}$$

The Space Station operates in four different control modes and we shall analyze some of these modes. We have the CMG attitude control mode, the parallel RCS/CMG maneuvering mode, the CMG momentum desaturation mode using RCS, and the CMG gravity gradient desaturation mode that uses only CMGs and converges to the TEA. The CMGs are operating mainly in this Momentum Management/ TEA converging mode that orients the spacecraft at the torque equilibrium attitude and prevents the momentum from diverging. In this mode of operation the function of the CMG control system is not to maneuver the Space Station attitude but to stabilize it at the TEA and to attenuate the attitude oscillations which are caused by cyclic aerodynamic disturbances. The aerodynamic disturbances cause the CMG momentum to cycle but the control system prevents it from reaching saturation. The Momentum Management/ TEA mode is described in detail in Section 2.4.

2.1 CMG Attitude Control Mode

The closed-loop Attitude Control System using CMGs is implemented in the Simulink file "*Sim_NonLin_CMG.mdl*", shown in Figure 2.1.1. The CMG torque capability is not as strong as the RCS, and any attitude change maneuvers in this mode are performed at slower rate than RCS. The CMG advantage over RCS is that it controls the vehicle attitude steady without exciting jitter but not for very long. The CMG momentum will eventually saturate due to the effect of external disturbances and thrusters must be fired to desaturate the CMGs. In this mode the CMG/ ACS is a simple PD controller with its bandwidth set to 20 times the orbital rate.
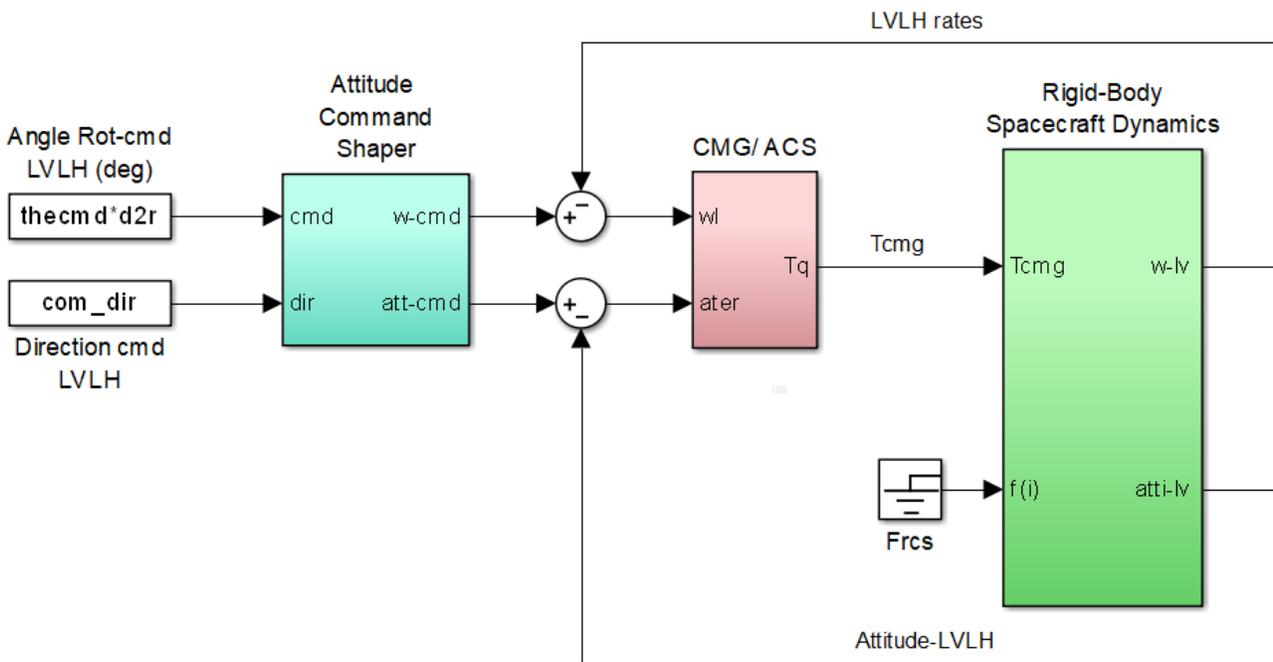

Figure 2.1.1 CMG Attitude Control System "*Sim_NonLin_CMG.mdl*"

The attitude command shaper (cyan block) is used to produce smooth attitude and rate command signals to the ACS by limiting the maneuver rate and acceleration. It is shown in detail in Figure 2.1.1b. The command shaper inputs are rotation command (thecmd) in (deg) and the rotational direction unit vector (com_dir). The command shaper parameters and limits are defined in the initialization file "start.m". The attitude command output (att-cmd) is a 3-dimensional vector: roll, pitch, yaw in (radians). The rate command output (w-cmd) is also a vector. The green vehicle dynamics block includes the non-linear rigid-body Equations 2.1, shown in Figure 2.1, which is coded in Matlab function "*Rigbod-Dynam_LVLH.m*".
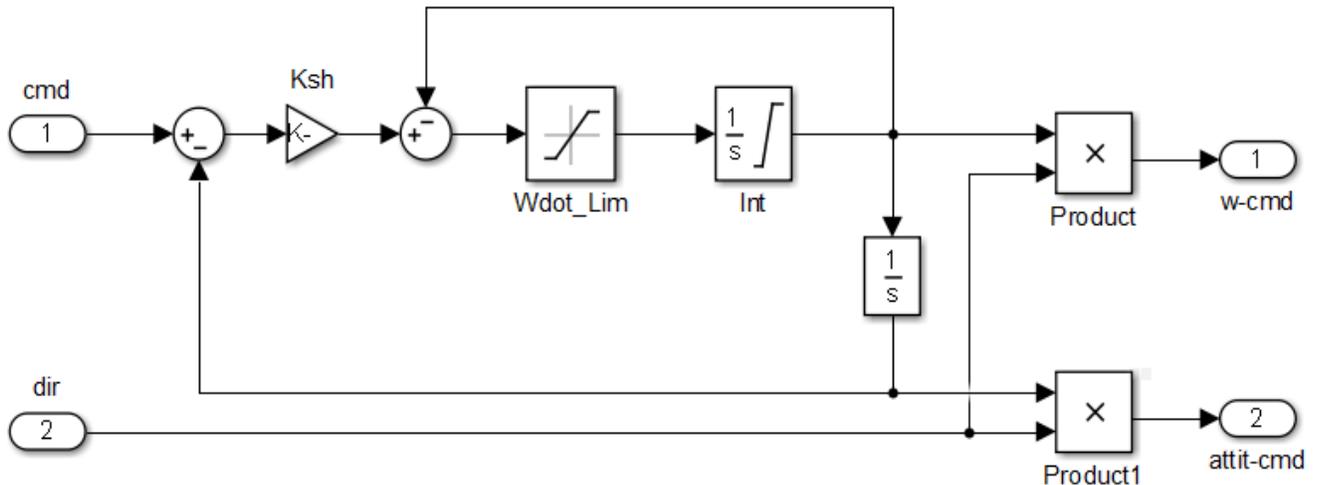

Figure 2.1.1b Command Shaper Block produces Attitude and Rate Commands that Limit Rate and Acceleration

The closed-loop Simulink model "*Sim_NonLin_CMG.mdl*" in Figure 2.1.1 will be used to perform two attitude maneuver simulations. It is initialized by running the m-file "start.m". The vector (ini) initializes the spacecraft state vector. The spacecraft LVLH attitude is initialized at zero and the pitch rate is set to $-\omega_o$.

In the first simulation we are commanding the spacecraft to rotate 3 (deg) about an arbitrary vector (1, -1, 1), and the system response is shown in Figure 2.1.2. The attitude and rate responses are good but the CMG momentum eventually builds up to very high values. In the second simulation we are commanding the Station attitude to the TEA.
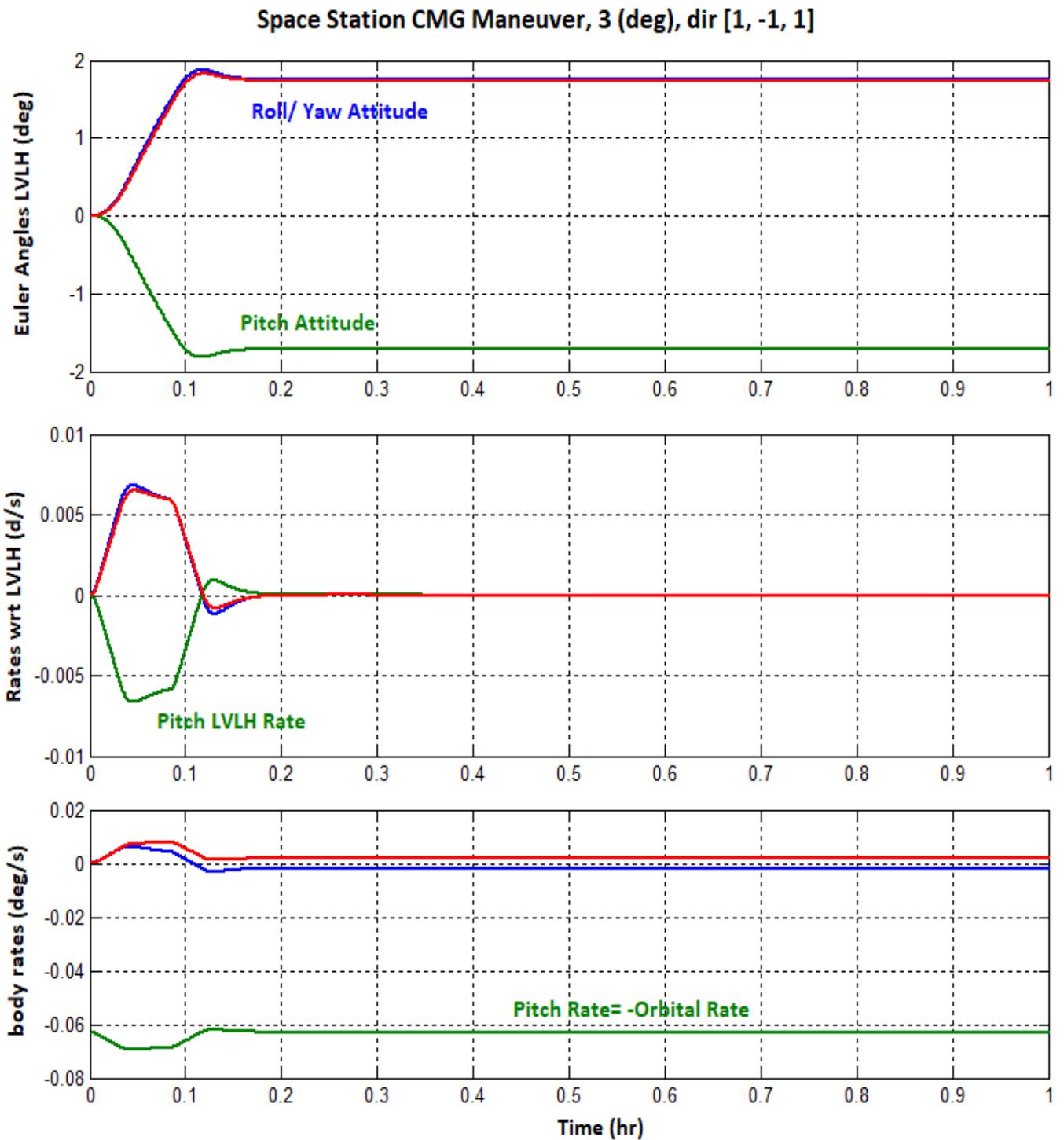
Figure 2.1.2a The CMG Attitude Control System performs 3⁰ Maneuver in 0.2 hours. The body rate is mostly negative pitch due to spacecraft rotation at orbital rate. It couples slightly in the roll and yaw directions. The LVLH rate is zero at the completion of the maneuver.

Figure 2.1.2b The ACS maintains the commanded attitude, but the CMG momentum is increasing to near saturation levels because a constant CMG torque is required to counteract the external torque which is biased. The CMG saturation is not included in the Simulink model.

The second simulation demonstrates that at the TEA the CMG momentum is not diverging because the average external torques balance at zero. It is only cycling since it is counteracting the cyclic aero disturbances. The Space Station i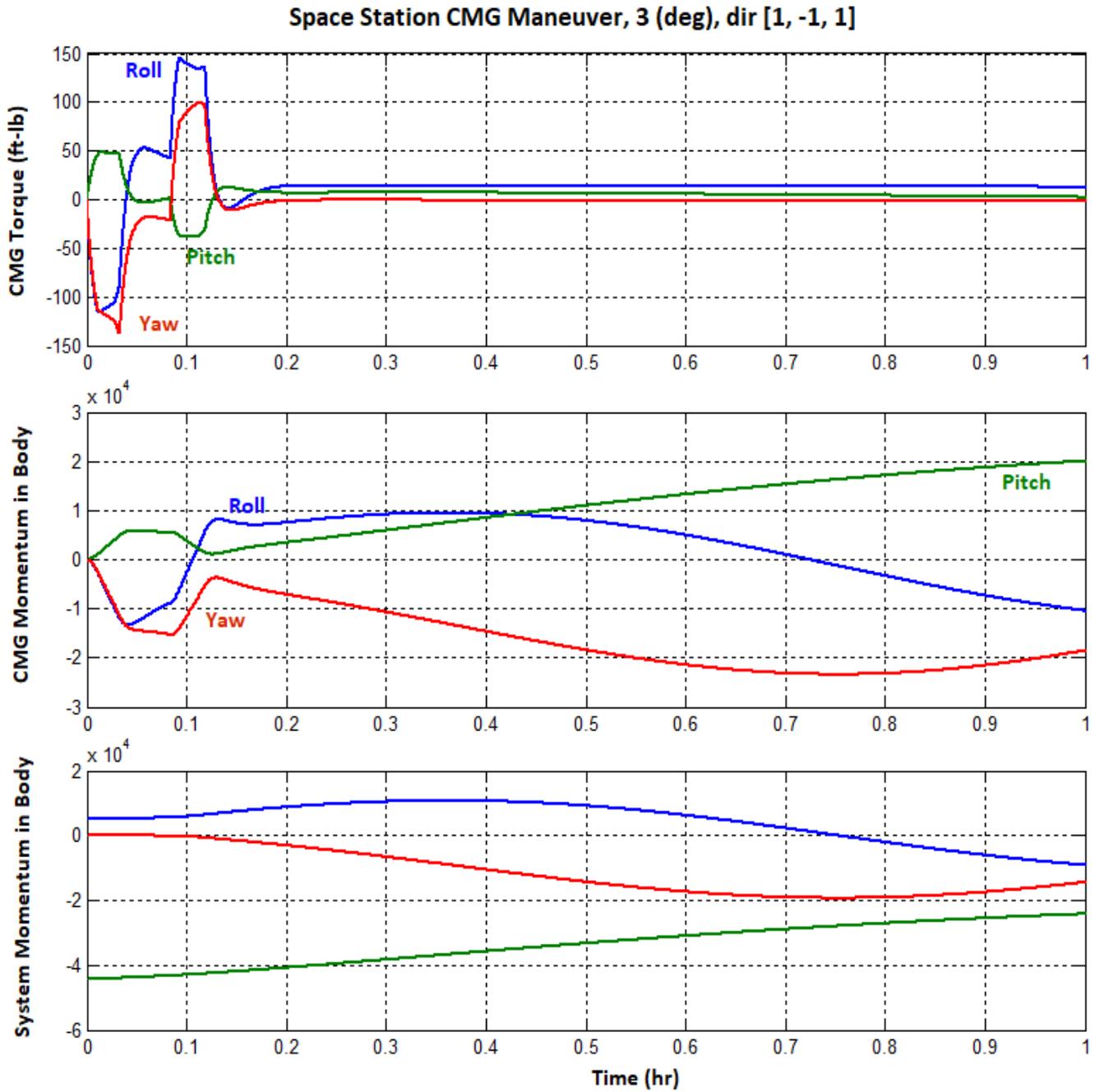s command to go to the TEA attitude, which is at (-0.5, 6.4, 3) degrees. Figure 2.1.3b shows the cycling CMG momentum which is not diverging at this attitude. This example serves as an introduction to the TEA converging CMG control mode that will be described in Section 2.4.
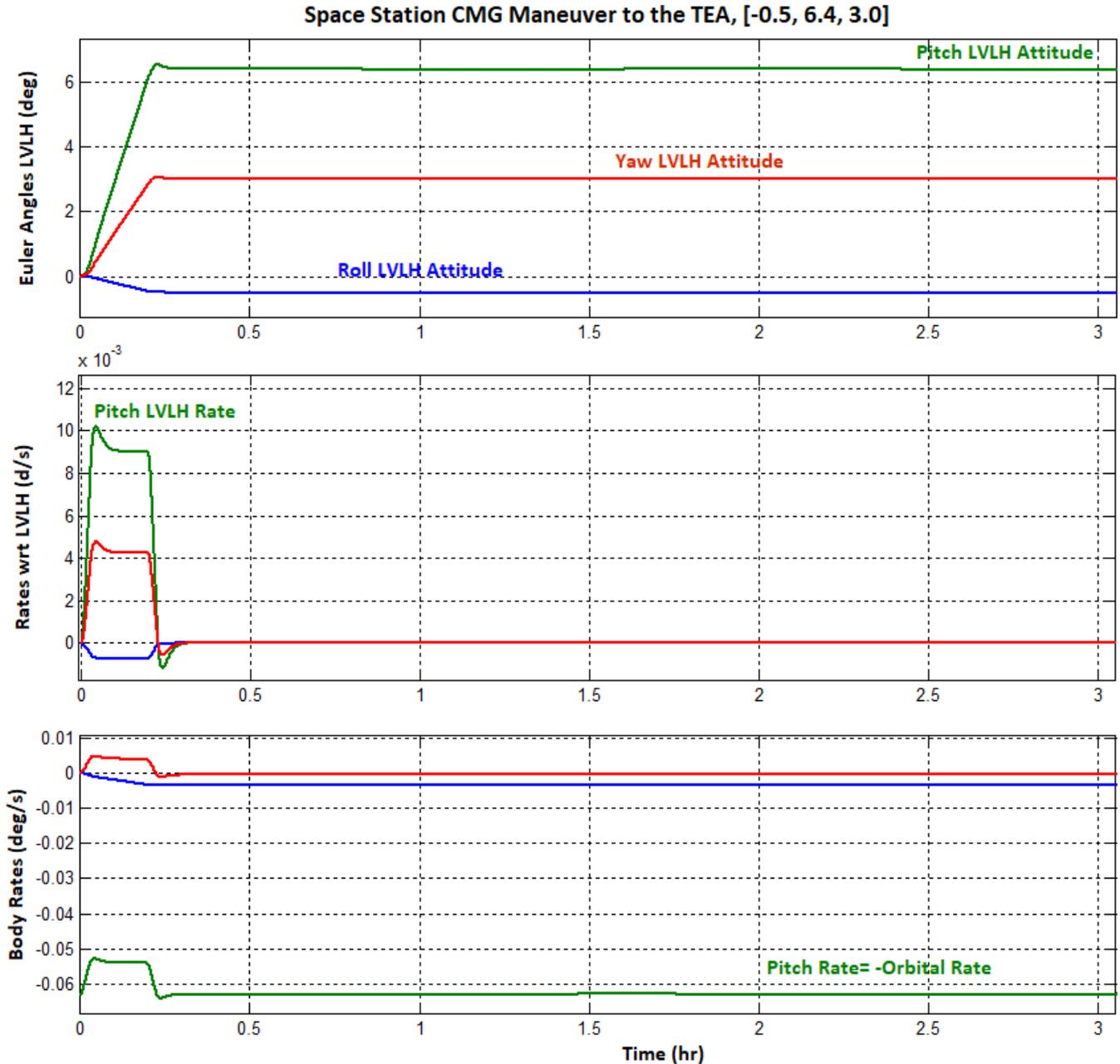
Figure 2.1.3a The vehicle attitude is commanded to TEA (-0.5º, 6.4º, 3º). The body rate is mainly negative pitch due to the orbital rate. It couples slightly in the negative roll direction (blue) because the Station has a +3º yaw LVLH attitude. At the completion of the maneuver the spacecraft rate is zero relative to the rotating LVLH frame.
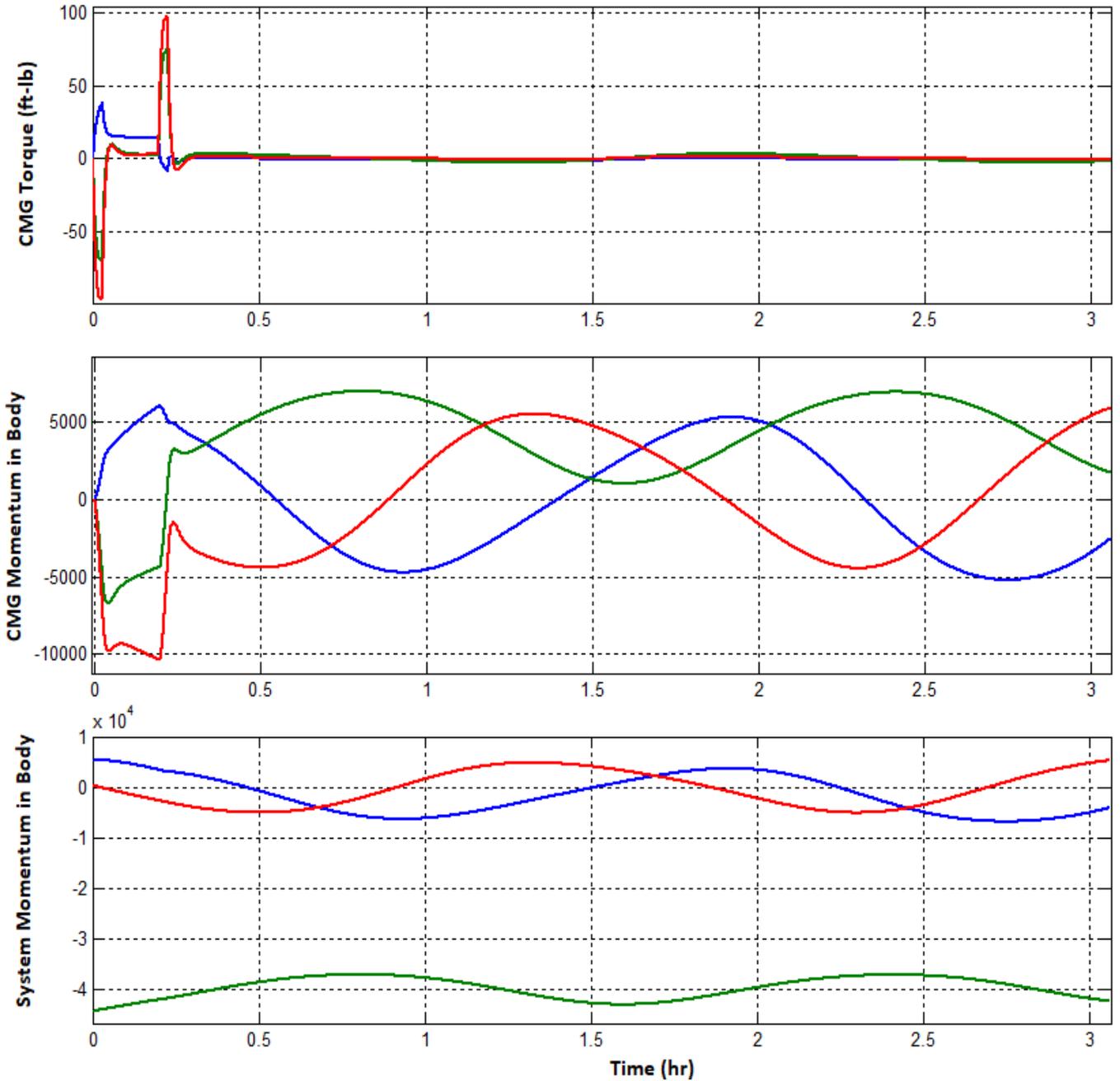
Figure 2.1.3b The CMG Momentum is cycling but its magnitude is not diverging in because the Station Attitude is at the TEA where the average aerodynamic torques are balanced with the average gravity gradient torques.

2.2 RCS Attitude Control and CMG Momentum Desaturation Using RCS

In this ACS mode the Space Station uses the RCS jets to perform attitude maneuvers, maintain a constant attitude (other than TEA during critical operations, for example, such as docking with the Space Shuttle), or to desaturate the accumulated CMG momentum. The CMG attitude control system described in Section 2.1 can also be used to point the Space Station at a constant attitude but not for a very long time. If the attitude is not at the TEA, the CMG momentum will begin to diverge and it will eventually saturate at the maximum momentum capability of the cluster. When the momentum saturates the control torque becomes zero and the Station loses attitude control. When the CMG momentum approaches saturation, the RCS is turned on to control the attitude (either at steady state or maneuvering). The CMGs are then commanded to torque in a direction that will reduce the momentum to zero while the RCS being more powerful is capable to provide the torque to react against the CMG disturbance, thus, controlling attitude and dumping momentum simultaneously. The RCS momentum dump mode is implemented in a Simulink model "*Sim_NonLin_RCS_Dump.mdl*" in subdirectory "*Examples\ Large Space Station\ (b) Mat NonLin RigBod*". The block diagram is shown in the Figure 2.2.1. The initialization script "start1.m" is used to load the simulation parameters into Matlab. This Simulink model is used to simulate two modes of operation, (a) attitude maneuvering and control using only RCS, and (b) CMG momentum desaturation using RCS.
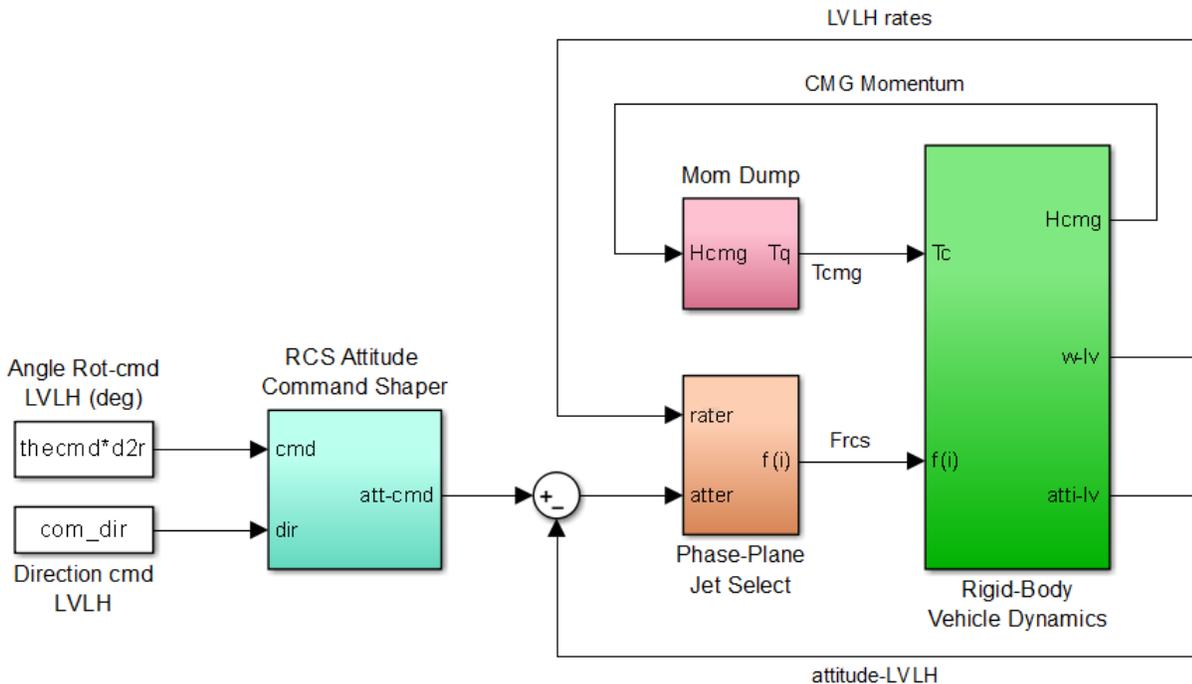
Figure 2.2.1 RCS Attitude Control with Momentum Desaturation Model "*Sim_NonLin_RCS_Dump.mdl*"

On the left side of the block diagram we have the command shaper (cyan block) that converts an attitude change command to a shaped command by limiting the command rate and acceleration. It is similar to the one used in the CMG/ ACS mode. The rate and acceleration limits the rotation angle command (thecmd) in (deg) and the rotation unit vector (com_dir) are initialized by file "start1.m". The output command (att-cmd) from the attitude command shaper is a 3-dimensional roll, pitch, yaw vector in (rad). The rate command output vector is not used here.

The RCS attitude controller uses phase-plane and jet-selection logic which is in the orange block in Fig. 2.2.1 and shown in more detail below. The inputs to the phase-plane logic are attitude errors, and spacecraft rate relative to the LVLH. The logic calculates the eigenaxis rotation vector about which it must rotate in order to reposition the spacecraft to the commanded attitude and it fires the appropriate jets that will execute the rotation as close as possible. The phase plane and the jet-selection logic are implemented in the Matlab functions "*phase_plane.m*" and "*Jet_Select_dot.m*" respectively. The phase-plane parameters such as the dead-band and rate limits are loaded into Matlab by the initialization file start1.m. The jet-select logic uses the dot-product algorithm to fire up to 3 jets at a time, that is, from the 12 available jets that will contribute the biggest moment near the maneuvering direction. The jet locations and thrust directions are also loaded in the simulation by the m-file "start1.m".
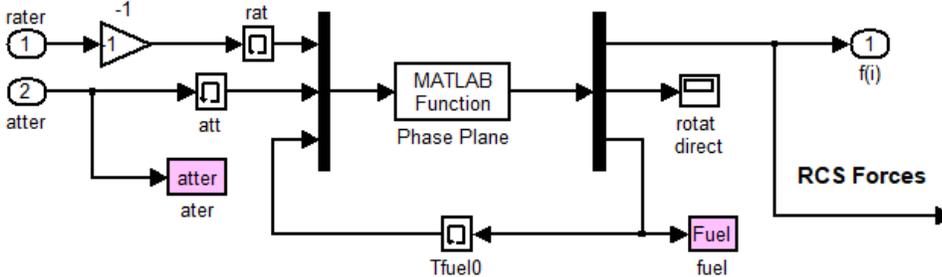
The green rigid-body vehicle block is shown in detail below. At the center of the diagram it includes the Matlab function "*Rigbod_Dynam_LVLH.m*" that contains the non-linear Space Station equations described in Section 2.
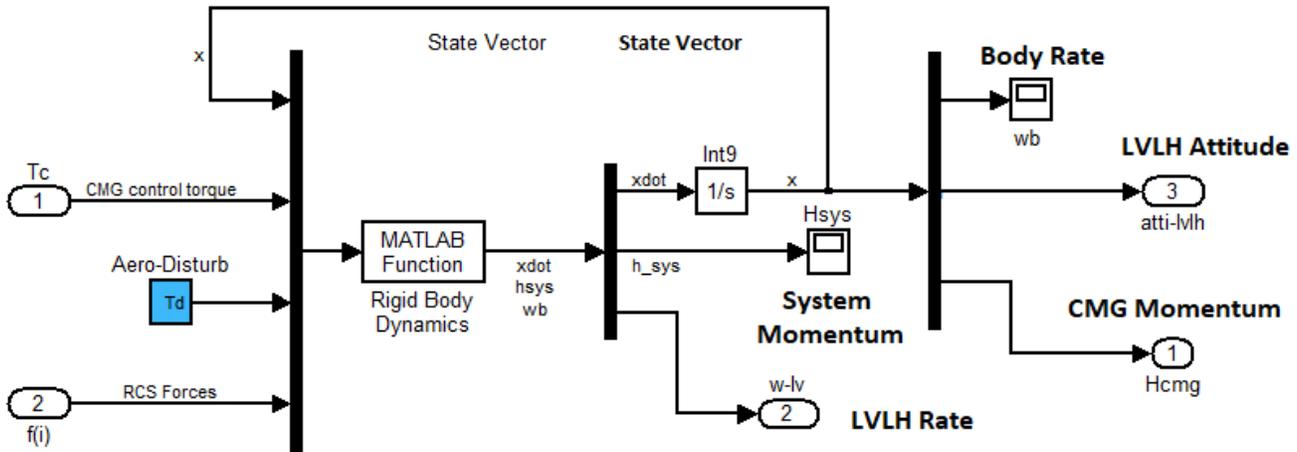
Figure 2.2.2 Space Station Dynamics Block

The purple block in Figure 2.2.1 is the momentum dump block that performs the momentum desaturation when the CMG momentum reaches a saturation level H_{max}. This block is implemented in the Matlab function "*Mom_Dump.m*". The following plots show the results from two simulations using the RCS Simulink model "*Sim_NonLin_RCS_Dump.mdl*". After running the model the file "pl.m" is used to generate the plots from the Simulink runs, as shown in Figures (2.2.3 and 2.2.4).

- The first simulation shows the spacecraft response to a 20 (deg) rotational maneuver about an arbitrary eigenaxis (1, -1, -1), using only RCS jets. The CMG torque is zero (not shown).
- The second simulation demonstrates a momentum dump. The CMG momentum is initialized at a high level in file "start.m" (a level that exceeding H_{max}) while the attitude is commanded at zero. In other words the vehicle is commanded to remain at zero LVLH attitude while the jets are firing to desaturate CMG momentum.
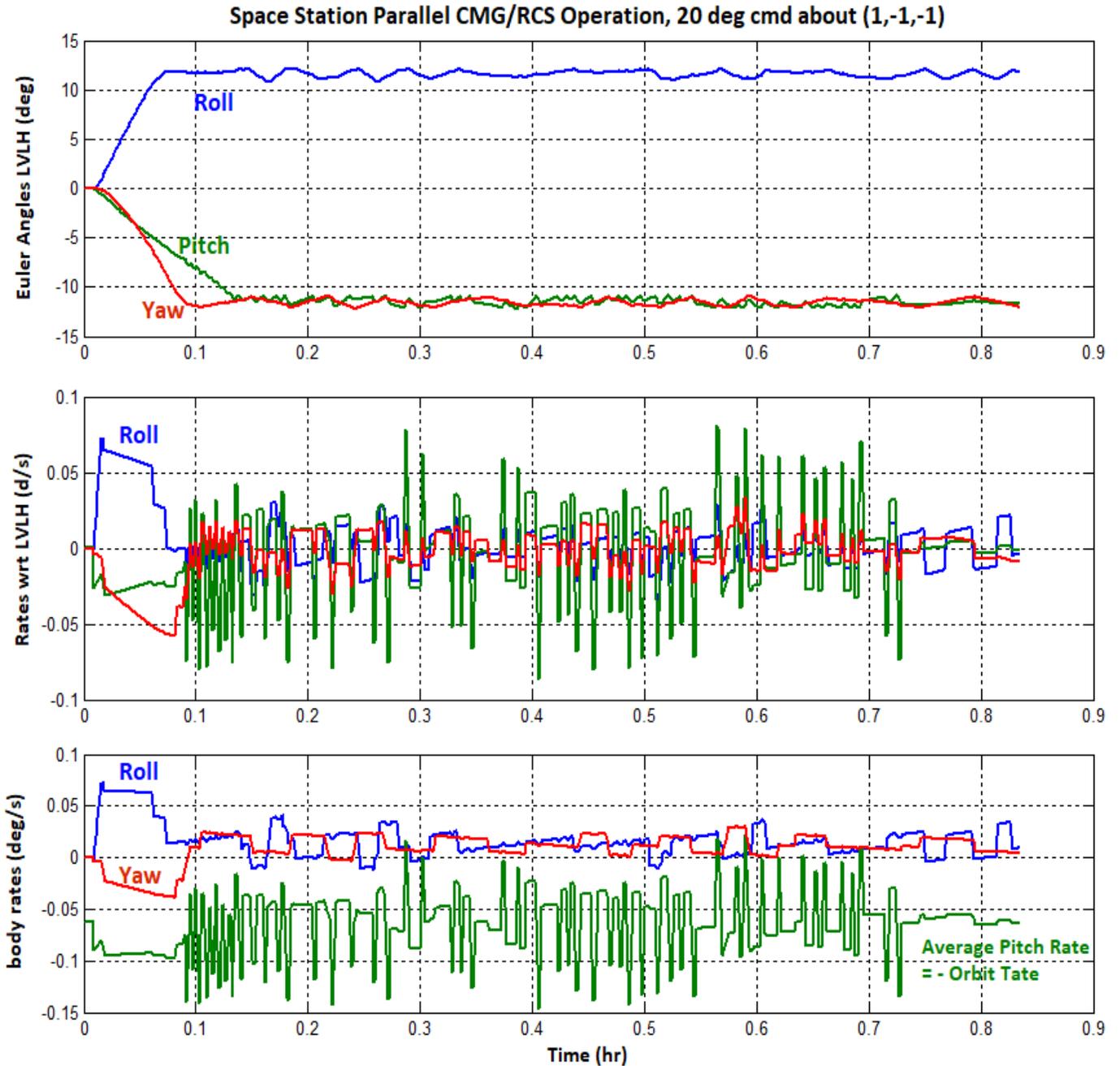
Figure 2.2.3a Spacecraft Response to 20⁰ Attitude Maneuver Command Using Only RCS. The Spacecraft Attitude reaches the Commanded Attitude and maintains it Steady against the Aero Disturbances by firing the RCS Jets
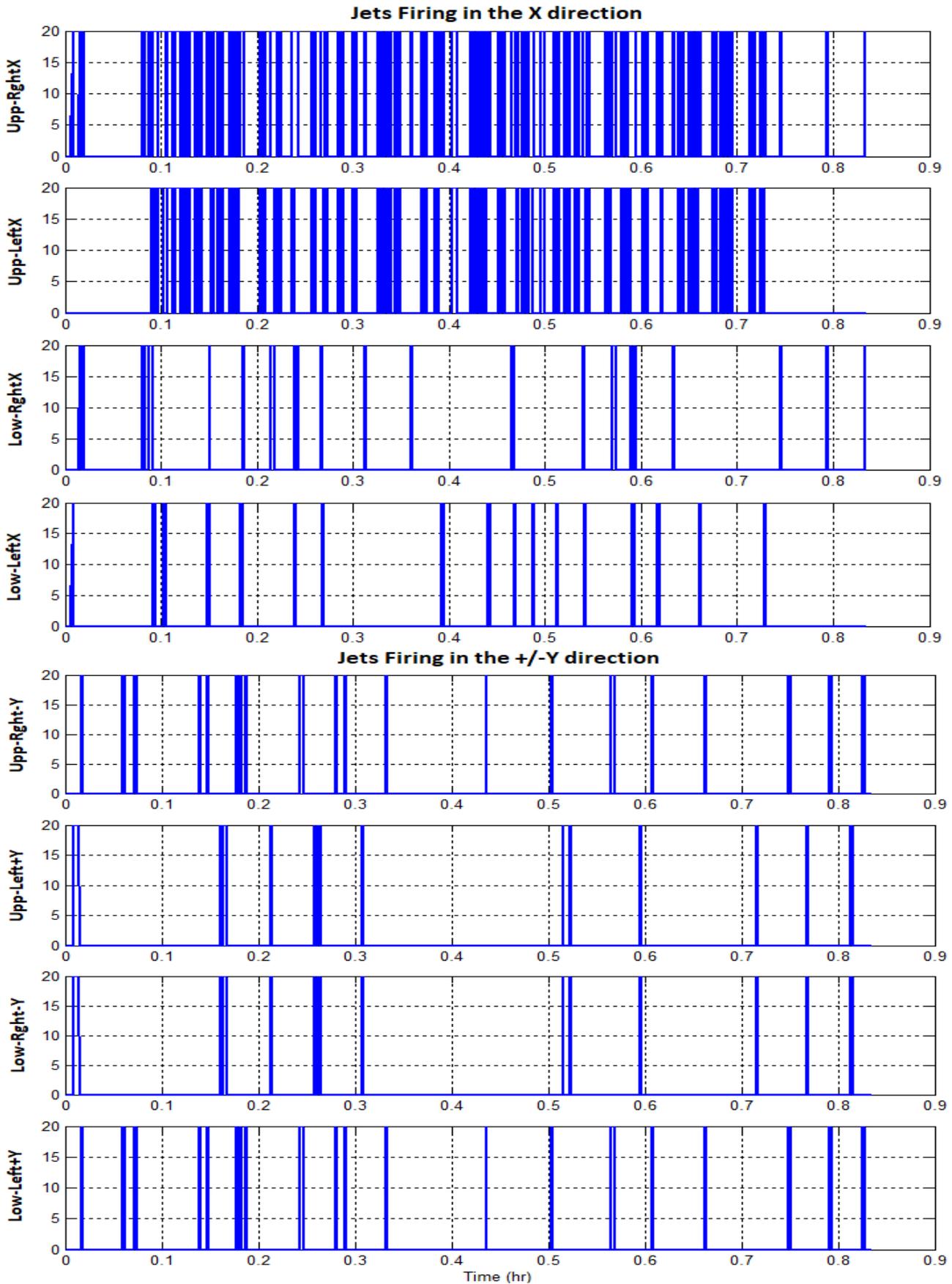
Figure 2.2.3b RCS Jets are firing to Maneuver and then Maintain the Commanded Attitude

49

The second simulation also uses the model "*Sim_NonLin_RCS_Dump.Mdl*" to demonstrate momentum desaturation. The CMG momentum is initialized at (10, 20, -10)*10^3 (ft-lb-sec), a level significantly higher than H_{max} to trigger the momentum dump operation. Maximum CMG torque is applied in a direction that desaturates the CMGs in unison, in all directions. The torque ceases to apply when the magnitude of the CMG momentum drops to a reasonably low level as specified in the momentum dump function "*Mom_Dump.m*".
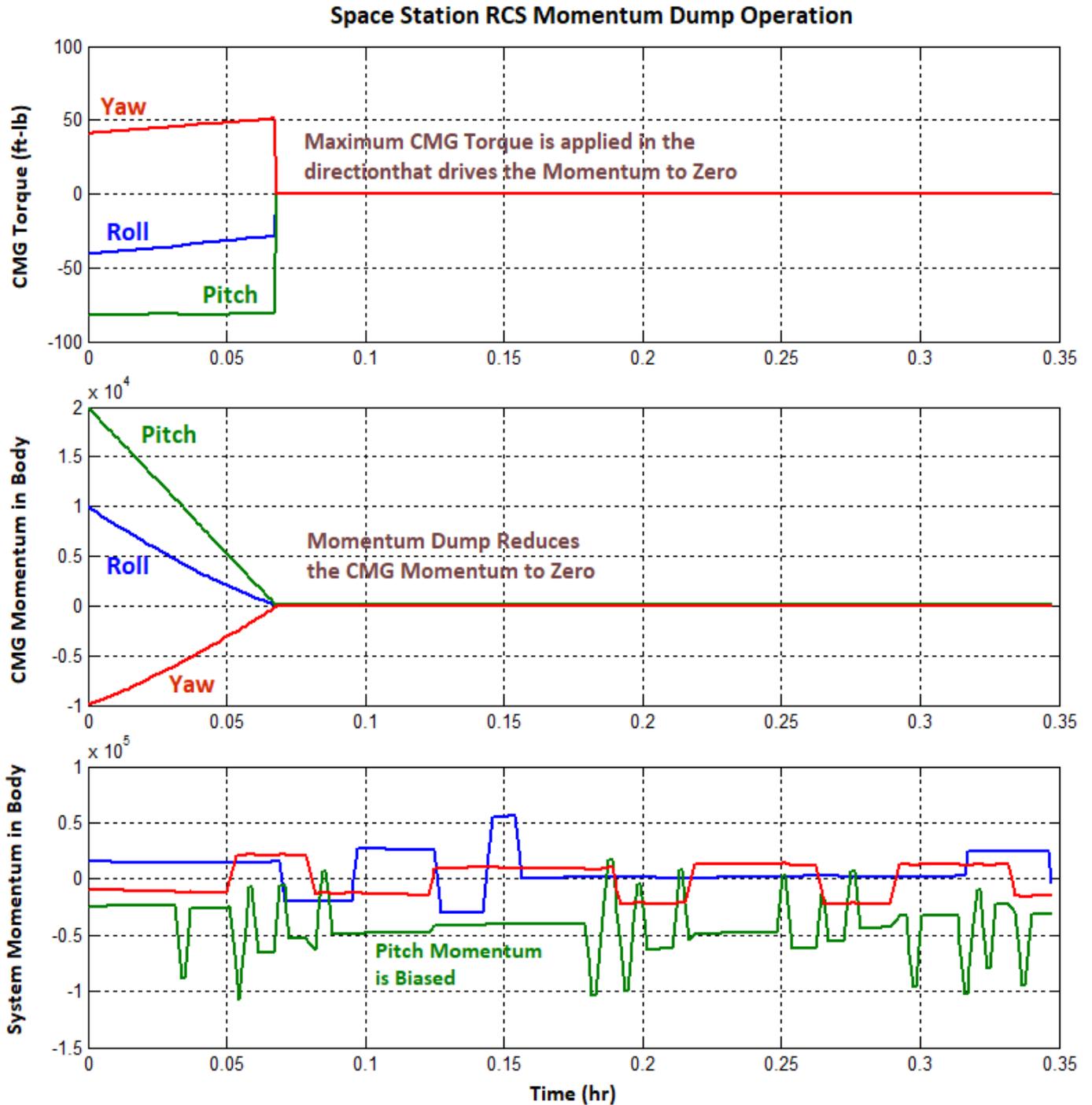
Figure 2.2.4a The CMG Torques are Commanded to Maximum in the Direction that Drives the CMG Momentum to Zero
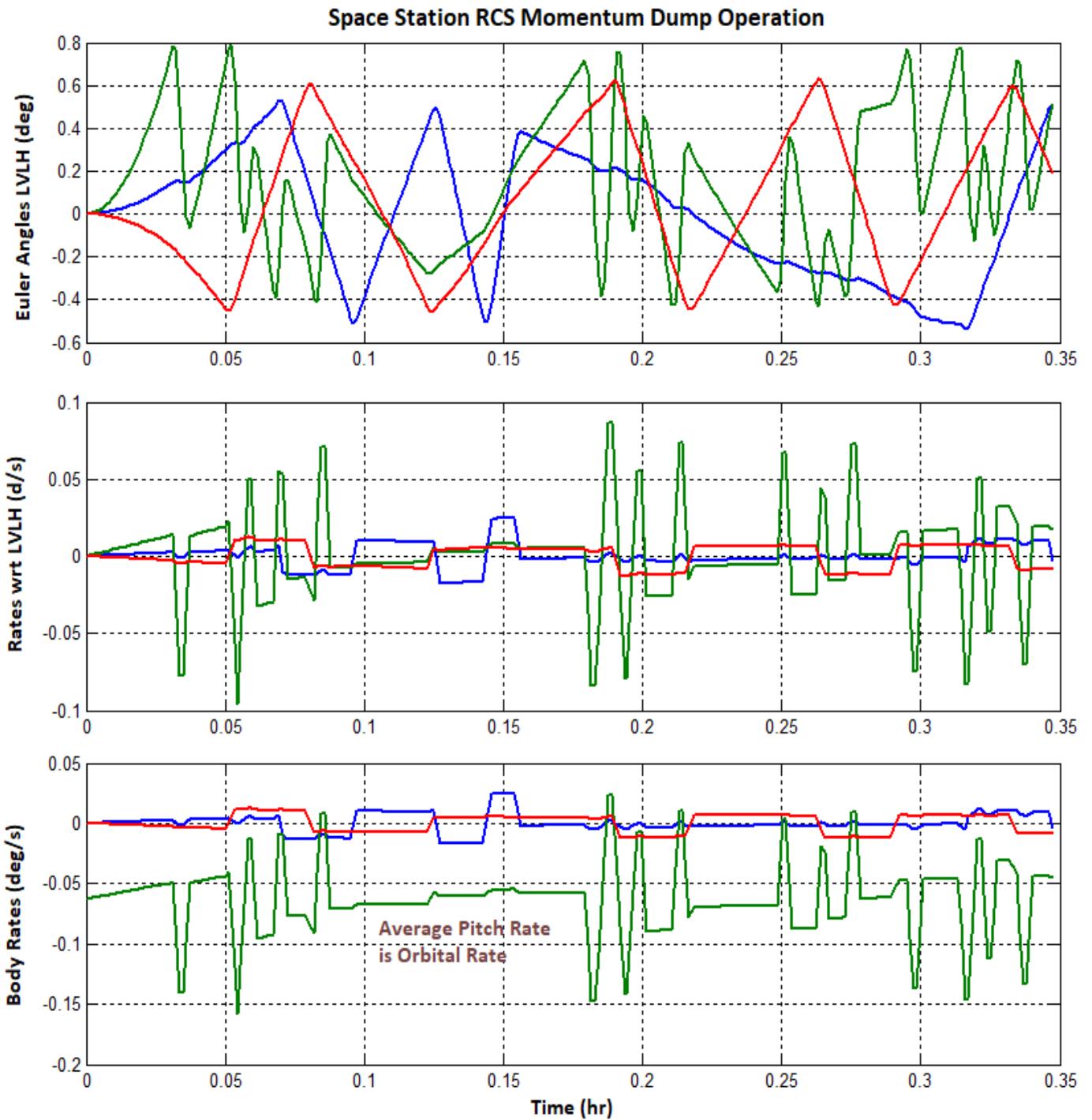
Figure 2.2.4(b) The RCS Maintains an almost Steady Attitude with Reasonably Small Errors during the CMG Desaturation. Since the Station maintains a Constant LVLH Attitude the Average Pitch Rate is equal to Negative Orbital Rate: -0.06 (rad/sec)
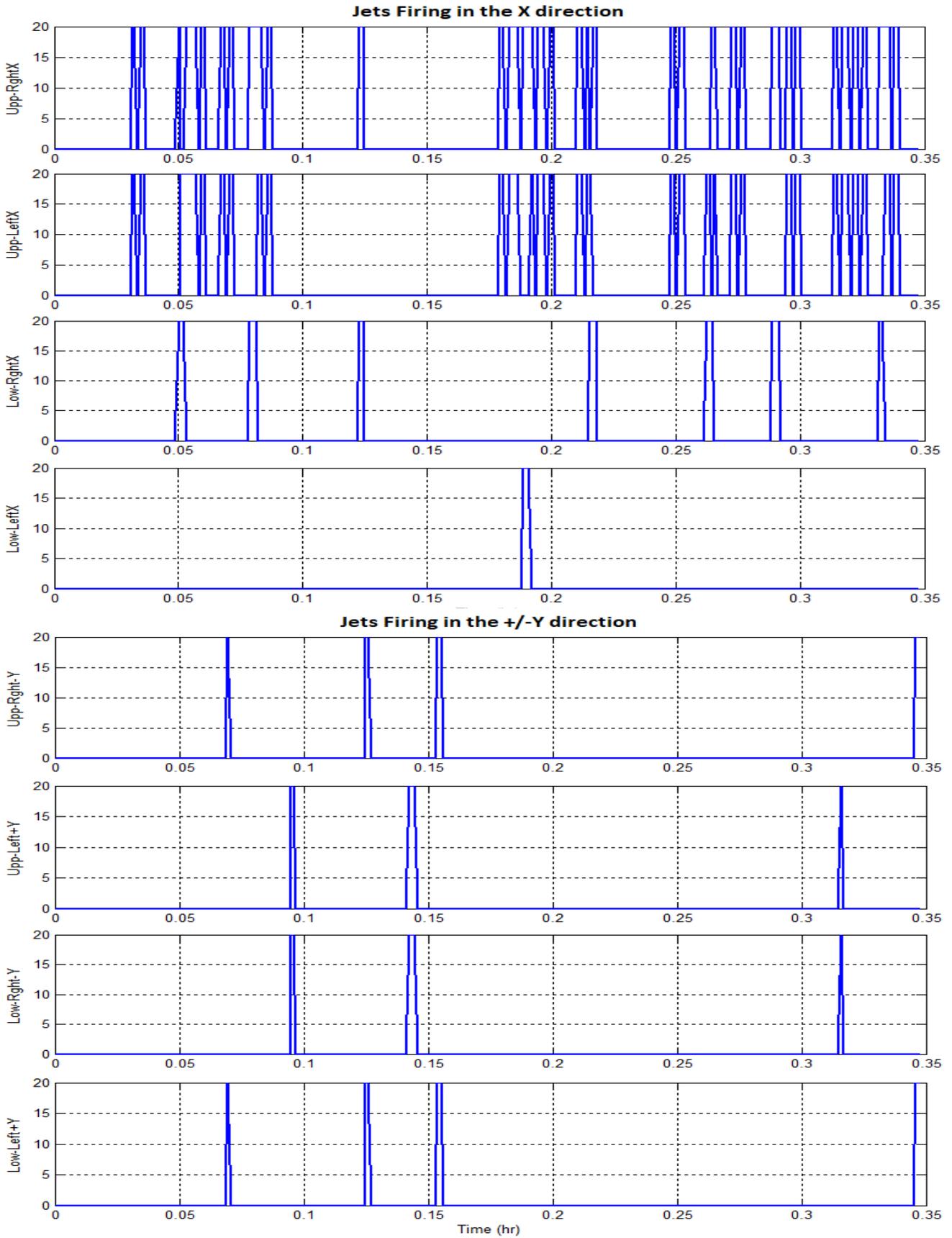
Figure 2.2.4c RCS Jet Firing During CMG Momentum Dump

2.3 Parallel CMG/ RCS Attitude Control Mode

When the Space Station performs large attitude maneuvers it initially uses the RCS jets which are more powerful for fast maneuvering and when the attitude approaches the commanded LVLH position, it switches to CMG control to maintain the commanded attitude for a while without firing jets. The CMG momentum will eventually saturate and it must be dumped with RCS. The simulation model for this attitude control mode is shown in Figure 2.3.1, and it uses both: CMG and RCS control. It is implemented in file "*Sim_NonLin_CMG_RCS.Mdl*" in folder "*Examples\ Large Space Station\ (b) Mat NonLin RigBod*".
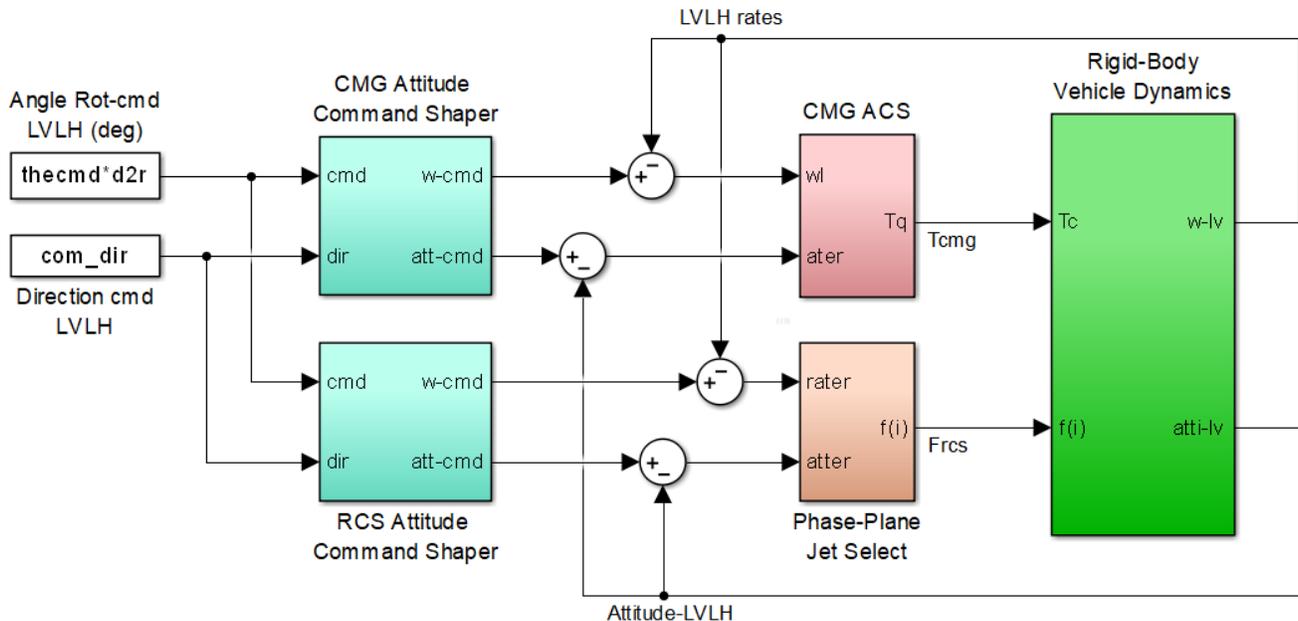
**Figure 2.3.1 Simulink Model "*Sim_NonLin_CMG_RCS.mdl*" for CMG/RCS Parallel Mode of Operation**

This Simulink model uses the same RCS phase-plane logic and CMG control system as already described. It includes two separate attitude command shapers with different rate and acceleration limits: a very smooth one for shaping the CMG commands, and a faster one for the RCS commands. A switching logic is included in the CMG/ ACS block that uses RCS only when the CMG torque demands are large and it switches to CMG control when the vehicle attitude is near the commanded position, and the torque demands become small. The green vehicle dynamics block uses the same Matlab function "*Rigbod_Dynam_LVLH.m*" that includes the non-linear Space Station Equations 2.1. It is initialized by the m-file "start2.m" and the file "Pl.m" generates the plots when the simulation is complete.

The following simulation results in Figure 2.3.2 are obtained using this model. It illustrates the transition from RCS to CMG control at the completion of a 20 degrees attitude maneuver. The RCS jets are used initially to maneuver the Station near the commanded attitude in less than 6 minutes. The pitch attitude responds faster because the Station has smaller moment of inertia in pitch. It takes a while for the attitude error to become small enough for the CMG control to be turned on and to provide a very precise attitude pointing.
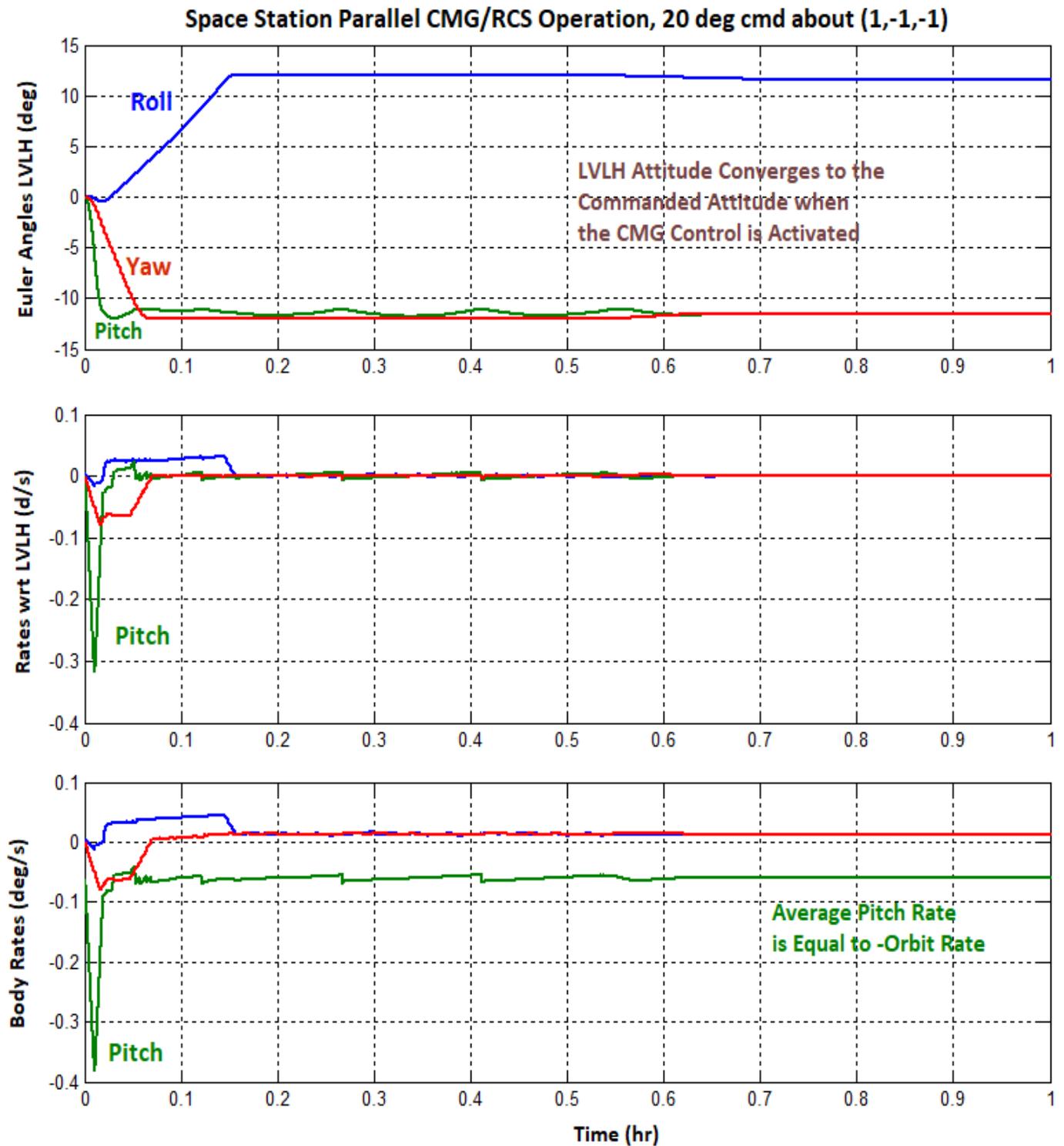
Figure 2.3.2a The Attitude Converges to the Command and the Attitude Error is Significantly Reduced to almost Zero when the ACS switches to CMGs Control

Space Station Parallel CMG/RCS Operation, 20 deg cmd about (1,-1,-1)
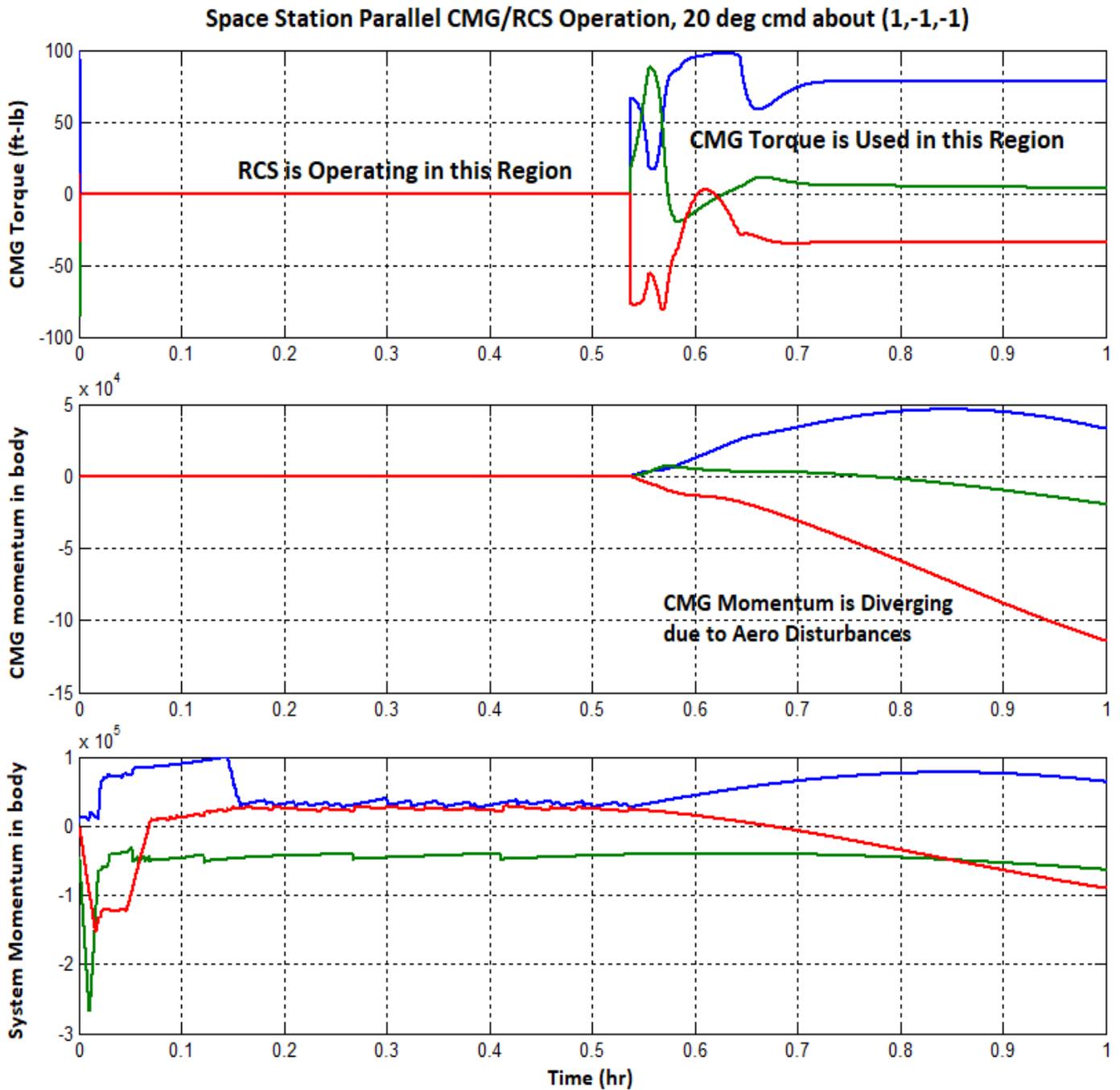
Figure 2.3.2b The CMGs are activated when the Attitude Error becomes small enough for a Smooth Transition from RCS control. The CMG Momentum, however, eventually reaches Saturation

During RCS operation the CMG system is turned off. The CMG control system is turned on at t=0.55 (hr). It requires, however, a steady CMG torque to counteract the aerodynamic and gravity gradient disturbances which leads to a secular CMG momentum build up.

55
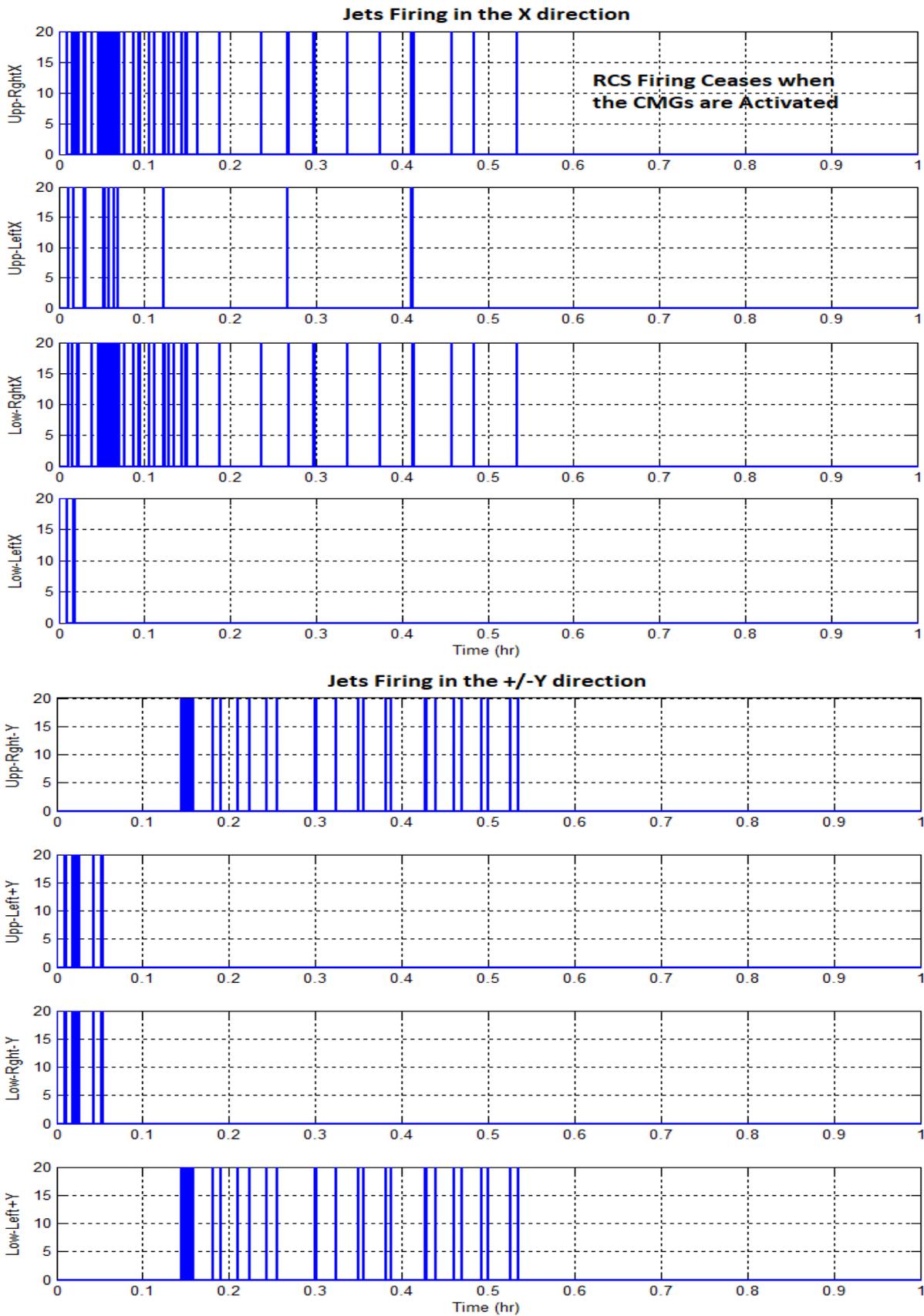
Figure 2.3.2c There is no RCS activity after t=0.55 hours because the CMGs Control the vehicle attitude

2.4 Momentum Management Mode by Using Gravity Gradient

In Section 2.1 we demonstrated that at the torque equilibrium attitude the CMG momentum is cyclic, not secular, because it does not diverge to saturation. We can, therefore, design a control mode where the Space Station attitude converges by itself (without being commanded) to the TEA where the average aerodynamic torque balances with the average gravity-gradient torque. This is accomplished by including feedback from the CMG momentum to prevent it from diverging and by this process the system attitude converges to the TEA. The momentum feedback plus additional momentum integral feedback makes this mode of operation more complex than the previous PD controller. The LQR control method will be used to design the state-feedback gain matrix that stabilizes this coupled dynamic system. It optimizes a performance index that is defined by the state and control weight matrices Qc and Rc that trade between control usage and performance. To synthesize the controller the LQR method requires a linear dynamic model linearized in the operating LVLH attitude, and the dynamic model in Equations 2.4.1 will be used for control synthesis.

$$
\begin{bmatrix} I_{XX} & I_{XY} & I_{XZ} \\ I_{XY} & I_{YY} & I_{YZ} \\ I_{XZ} & I_{YZ} & I_{ZZ} \end{bmatrix} \begin{pmatrix} \ddot{\phi} \\ \ddot{\theta} \\ \ddot{\psi} \end{pmatrix} = \omega_o \begin{bmatrix} 0 & 2I_{YZ} & I_{XX} - I_{YY} + I_{ZZ} \\ -2I_{YZ} & 0 & 2I_{XY} \\ -I_{XX} + I_{YY} - I_{ZZ} & -2I_{XY} & 0 \end{bmatrix} \begin{pmatrix} \dot{\phi} \\ \dot{\theta} \\ \dot{\psi} \end{pmatrix}
$$

$$
+ \omega_o^2 \begin{bmatrix} 4(I_{ZZ} - I_{YY}) & 3I_{XY} & -I_{XZ} \\ 4I_{XY} & 3(I_{ZZ} - I_{XX}) & I_{YZ} \\ -4I_{XZ} & -3I_{YZ} & (I_{XX} - I_{YY}) \end{bmatrix} \begin{pmatrix} \phi \\ \theta \\ \psi \end{pmatrix} + \omega_o^2 \begin{pmatrix} -4I_{YZ} \\ 3I_{XZ} \\ I_{XY} \end{pmatrix} + T_d + T_c
$$

$$
\begin{pmatrix} \dot{h}_X \\ \dot{h}_Y \\ \dot{h}_Z \end{pmatrix}_{CMG} = \omega_o \begin{pmatrix} h_Z \\ 0 \\ -h_X \end{pmatrix}_{CMG} - T_c
$$

Equation 2.4.1 Dynamic equations linearized in the LVLH frame

The state feedback control law, therefore, stabilizes not only the attitude but also the CMG momentum by keeping it oscillating around zero. It prevents it from diverging to saturation and as a result the spacecraft attitude converges to the TEA where the average aerodynamic and gravity gradient torques are balancing out. This is a continuous momentum desaturation which is very attractive because it does not require RCS propellant. It adjusts the spacecraft attitude and uses gravity gradient to prevent the CMG momentum from building up. It relies on sufficient knowledge of the vehicle mass properties for the derivation of the control gains. The resulting CMG momentum is stable and it cycles around zero as the CMGs respond to counteract the cyclic aerodynamic disturbances.

The linearized Equations 2.4.1 are derived from the non-linear equations 2.1. The body rates are replaced with the LVLH rates and the model will be used for the Space Station LQR control design. The equations include gravity gradient torque terms which are function of the spacecraft LVLH attitude. The CMG momentum integral is also included in the design model to help bound the CMG momentum. The states are: Space Station LVLH rates, attitudes, CMG momentum, and CMG momentum integral.

The design Equations 2.4.1 are included in the Matlab function "*Linear2_LVLH.m*" which is used as a subsystem block in the Simulink models "*Sim_Lin_TEA.Mdl*" and "*Vehicle_Lin.Mdl*". Their inputs are CMG torques T_c and external disturbances T_d. There are 9 outputs which are equal to the states: 3 LVLH rates, 3 LVLH attitudes, and 3 components of the CMG momentum in the body axes. It also includes the linearized gravity gradient dynamics. The Simulink model output is the rate of the state-vector $\dot{x}$ which is updated by an integrator loop around the function as shown in Figure 2.4.2.

LQR Control Design

The Simulink model "*Vehicle_Lin.Mdl*" in Figure 2.4.2 contains the augmented dynamic model that will be used in the LQR control design by the Matlab script file "*des.m*". It must first be initialized by running the m-file "*start3.m*" which also generates the design state-space matrices (A_0, B_0, C_0, D_0) by linearizing it using the Matlab function "linmod". The spacecraft 9-state vector $\underline{x}$ is obtained by integrating the output $\dot{\underline{x}}$ that comes out of function "*Linear2_LVLH.m*". In our initial design attempt we used the original unaugmented model of Equations 2.4.1 for the LQR design. The cyclic disturbance, however, occurring at orbital rate is substantial and it creates large pitch attitude oscillations at orbital frequency ω_o.

Since we know that the oscillatory disturbance is occurring at a known frequency, a more efficient approach of attenuating its effect on the pitch attitude is to introduce a resonance of the same frequency in the design system. The resonance is implemented by two additional states (α_1, α_2) which are excited by the pitch attitude oscillation θ and tuned at orbital frequency ω_o. The augmented design model now consists of 14 states and it includes the resonance states (α_1, α_2) and 3 momentum integral states which are necessary to avoid getting biased momentum. The LQR algorithm calculates the (3x14) state-feedback matrix K_{pqr}. When the design system states are properly penalized in the LQR optimization the state-feedback gain stabilizes not only the attitude but it will attenuate the pitch oscillations in θ, and keep the CMG momentum stable and oscillating around zero.
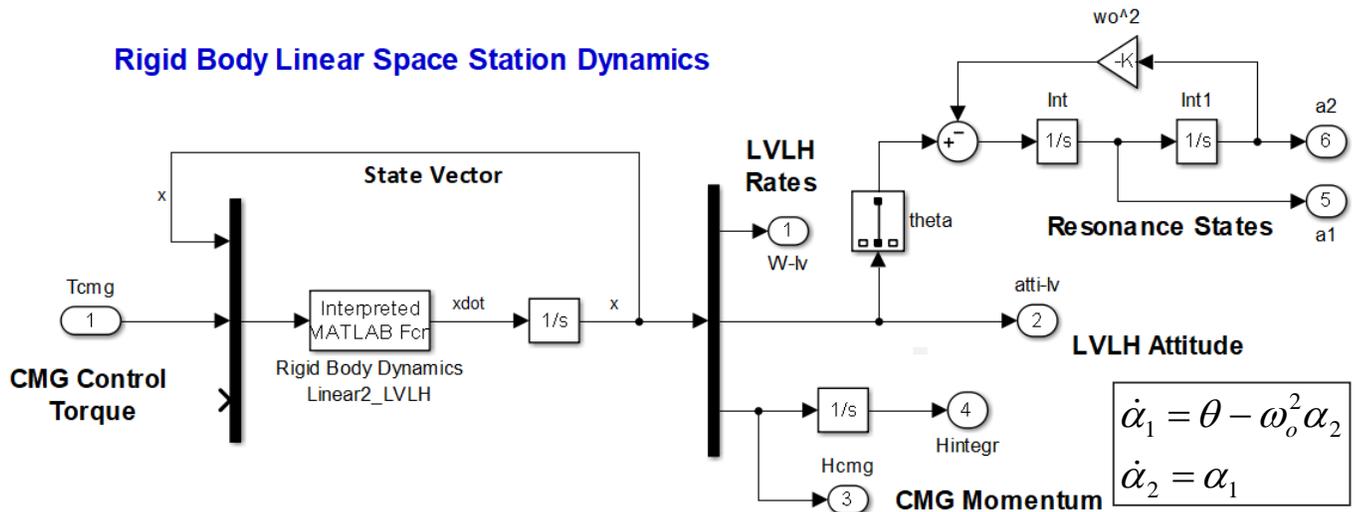
Figure 2.4.2 Augmented Design Model "Vehicle_Lin.Mdl" that Includes Equations 2.4.1, the CMG Momentum Integrals, and the Pitch Attitude Augmentation States (α_1, α_2)
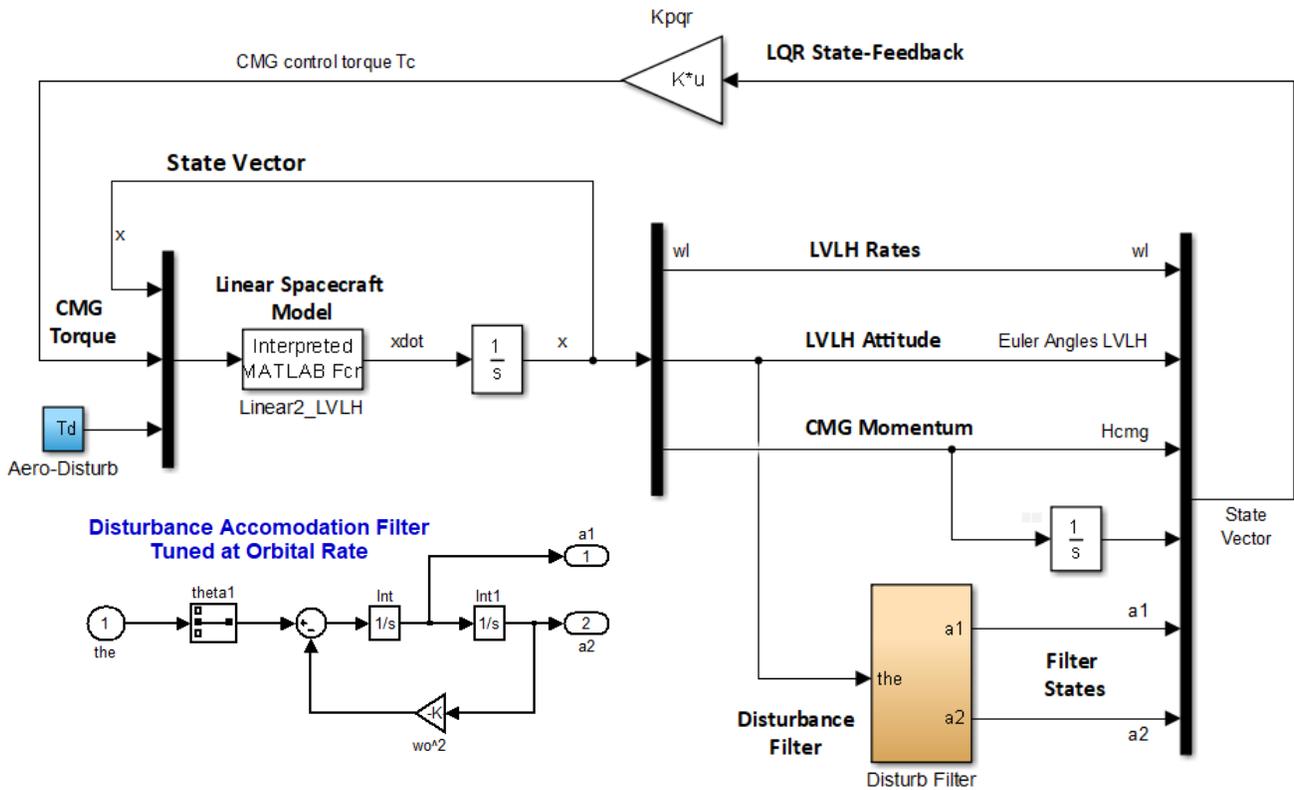
Figure 2.4.3 Linear State-Feedback Simulation Model "*Sim_Lin_TEA.Mdl*" used for testing the LQR Gains

Figure 2.4.3 shows the linear simulation model "*Sim_Lin_TEA.Mdl*" that uses the linearized Equations 2.4.1 in the Matlab function "*Linear2_LVLH.m*". It is used during the design for testing the LQR gains while adjusting the LQR optimization weighting matrices Q_c and R_c. The final control design, however, is tested in a non-linear simulation that uses the dynamic Equations 2.1. In the simulation, the two-state augmentation resonance becomes a disturbance accommodation filter and it is part of the attitude control system. The augmented state vector is fed back via the state-feedback gain K_{pqr} to produce the CMG control torque T_c.

Figure 2.4.4 shows the non-linear simulation model which is in Simulink file: "*Sim-NonLin-TEA.Mdl*". It is similar to the linear simulation but it uses the non-linear Space Station equations which are coded in the Matlab function "*Rigbod_Dynam_LVLH.m*". The model does not include any attitude commands but the inputs are aero disturbances. It is initialized by the m-file "start3.m" and "Pl3.m" plots the simulation results.

Figure 2.4.4 Non-Linear State-Feedback Simulation Model "*Sim_NonLin_TEA.Mdl*"

The simulation results in Figure 2.4.5 of the TEA converging mode show the Space Station response to the aero disturbances. The simulation demonstrates the capability of the control system to control the CMG momentum in the presence of aerodynamic disturbances and gravity gradient torques. The attitude is initialized at zero in the LVLH frame and the initial pitch body rate is equal to negative orbital rate which is $(0, -\omega_o, 0)$'. The Space Station LVLH attitude converges at the TEA where the external torques balance in all directions and at steady state the CMG momentum oscillates about zero without bias. The attitude oscillates slightly about the TEA. The pitch attitude oscillation at orbital rate has been attenuated by the disturbance filter and the only remaining oscillation in pitch is due to the aero disturbance at $(2\omega_o)$. We could have included a second disturbance filter tuned at $(2\omega_o)$ to eliminate the small pitch oscillation or a yaw oscillation filter, but we leave this as an exercise for the reader.

Figure 2.4.5 TEA Seek Mode keeps the CMG Momentum Bounded and the Attitude Converges to the TEA

The roll and yaw attitude oscillates mostly at orbital frequency ω_o. At steady-state the pitch attitude converges to 6.3° and the yaw attitude converges to 3° relative to the LVLH. The roll attitude is small at -0.5⁰. At steady-state the body rate is mainly in pitch at negative orbital rate -0.063 (rad/sec). There is a small component of rate coupling in the negative roll direction (blue), because the yaw attitude is slightly positive 3°.

Space Station Simulation TEA-Converge Mode, Response to Aero Disturb
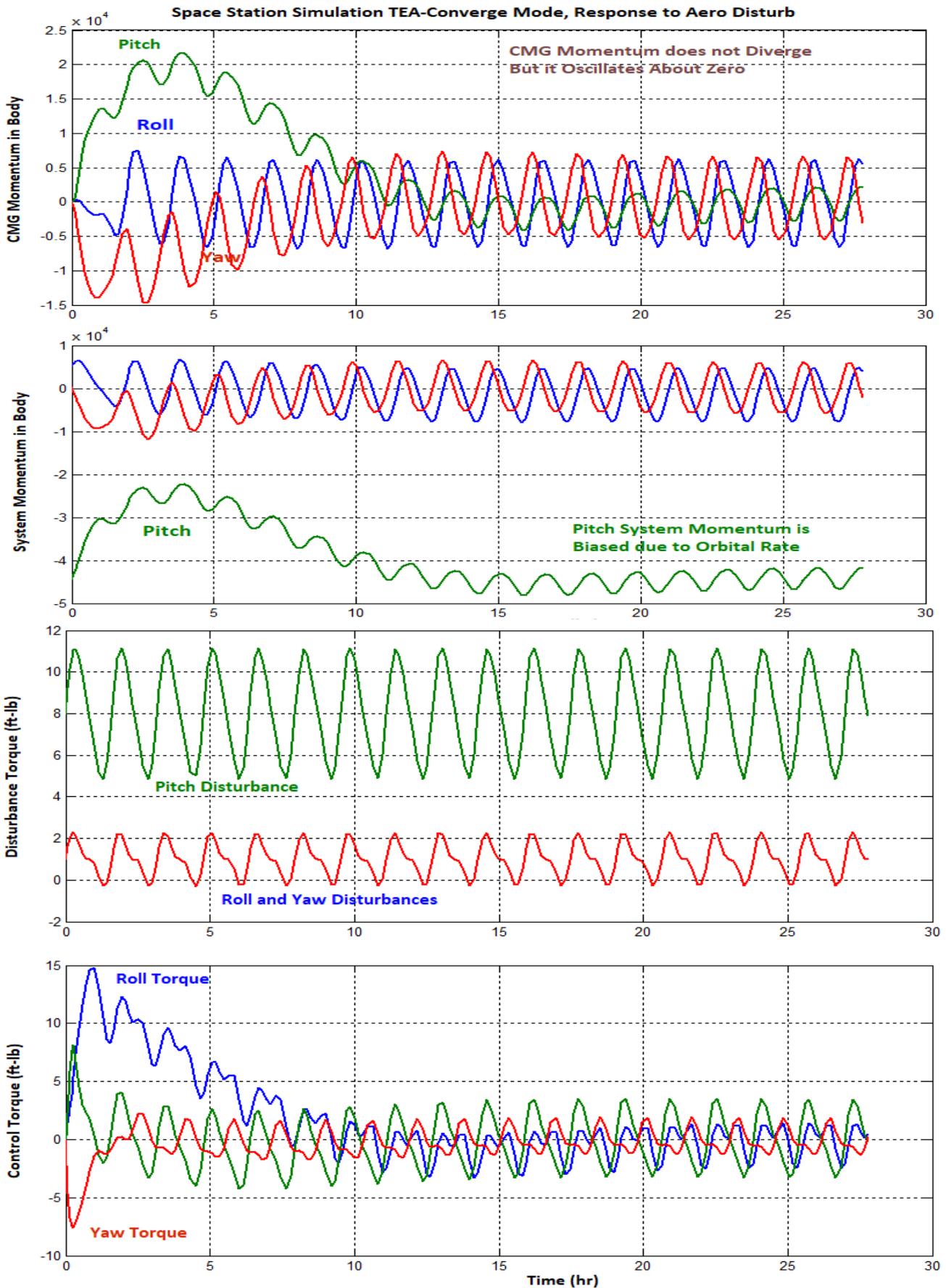
3. Non-Linear Flexible Space Station Modeling and Simulations

In this section we will include flexibility to the models developed in Section 2. We will combine the previously created non-linear rigid body model with the elastic model obtained in Section 1 to create a non-linear model with structural flexibility and will repeat the analysis and simulations using the upgraded models. The simulation models and files are in directory: *"Examples\Large Space Station\(c) Mat NonLin Flex"*. Figure 3.1 shows the spacecraft dynamics block which is included in the Simulink files. It consists of two subsystems connected in parallel: (a) the non-linear rigid-body dynamics of Equations 2.1, implemented in function "*Rigbod_Dynam_LVLH*", shown in Figure 2.1, and (b) the flexibility model that includes the flex spacecraft state-space system "*Large Flex Space Structure, 32 Modes, Flex Only*" that was created by the Flex Spacecraft Modeling program in Section 1 and was exported to Matlab function "*flex32_only.m*". The flex model obviously does not include the first six rigid-body FEM modes since the rigid dynamics is captured by the non-linear block. We will analyze the system stability as before: (a) under CMG control, and (b) under RCS control using the Describing Function method. We will also analyze stability of the TEA-Converging/ Momentum Management mode.
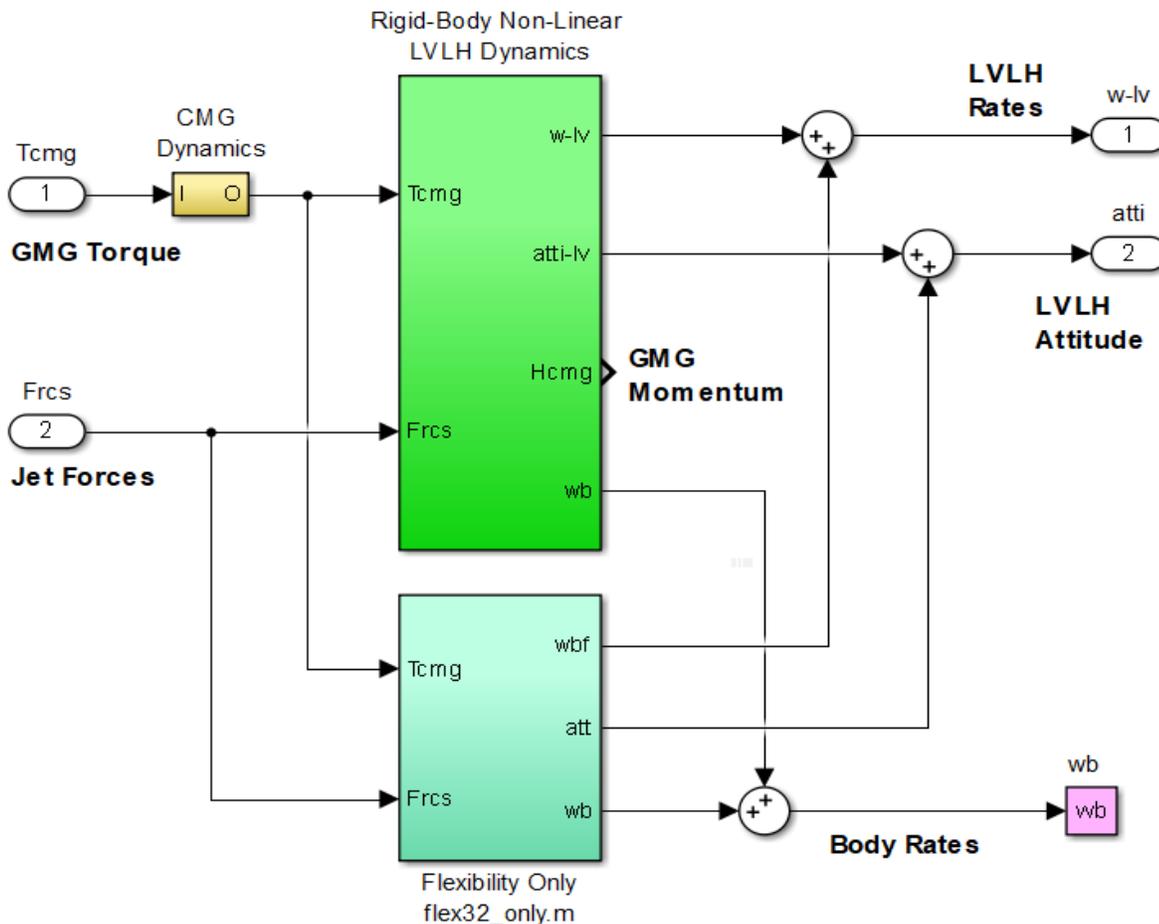

Figure 3.1 Space Station Dynamics: Includes Non-Linear and Flexibility Blocks Connected in Parallel

63
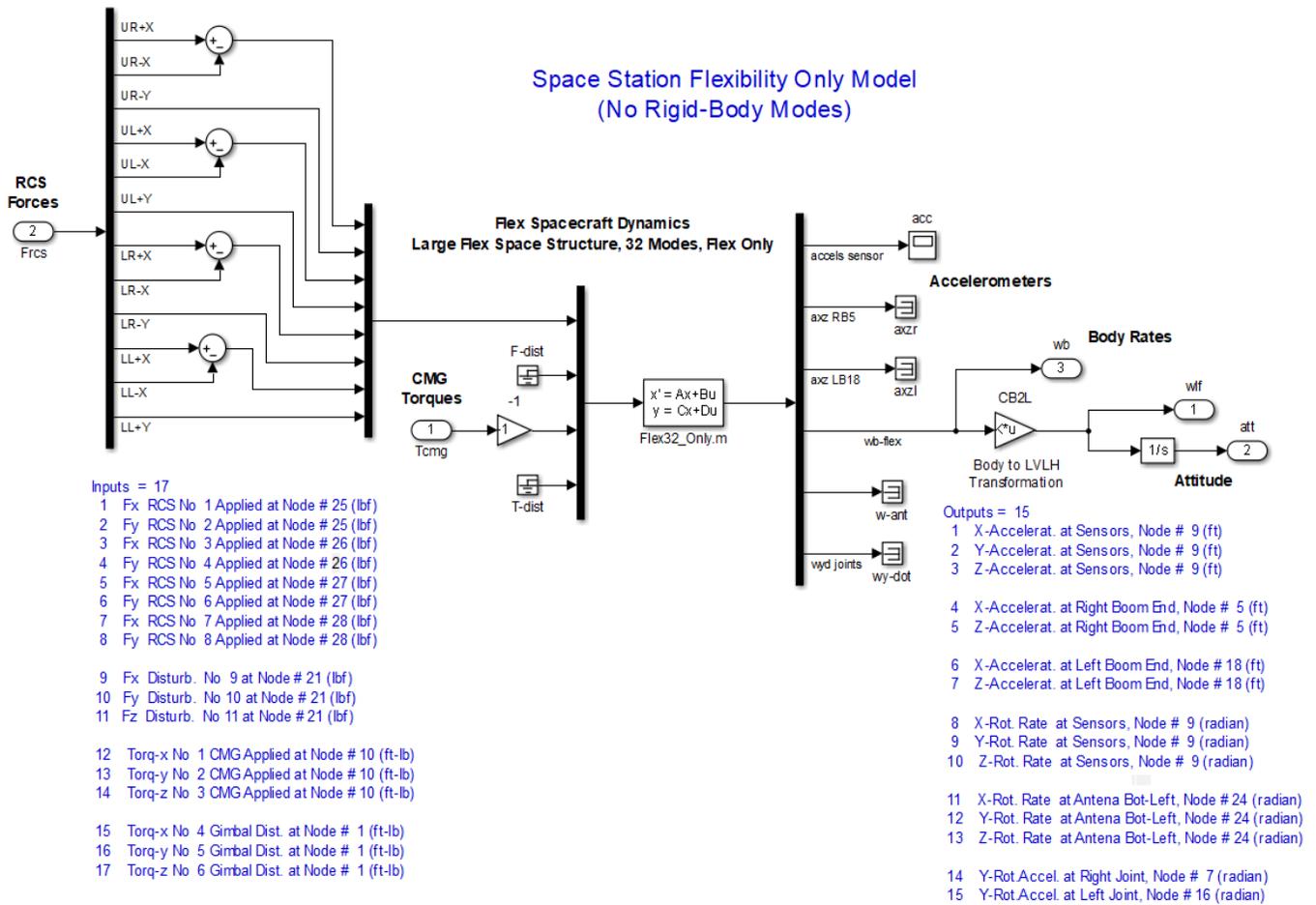
Figure 3.1b Flexible Spacecraft Dynamics Subsystem Includes 32 Flex Modes (No Rigid-Body Modes)

The CMG dynamics are included in Figure 3.1 as 2nd order transfer functions of bandwidth: 2 (rad/sec). Both rigid and flex subsystems receive the same CMG torques and RCS jet forces and their outputs are combined to capture both: the non-linear rigid-body motion and the dynamic response of the flexible structure at the sensors. The combined spacecraft outputs include: LVLH attitude measurements, LVLH rates, CMG momentum, and body rates.

We will now describe the simulation models that demonstrate the different modes of operation. They are similar to the models described in Section 2, but they include structural flexibility. System stability will be analyzed using frequency response methods. The m-file "start.m" is used to initialize parameters before running the simulations. The ACS control system gains are the same as those derived in Section 2. The flex filters designed in section 1.2 are also included in this analysis with some minor adjustments to improve flexibility attenuation.

3.1 CMG Attitude Control Mode with Flexibility

The CMG/ ACS analysis models that were developed in Section 2.1 will now be modified to include structural flexibility. The simulation model is in file "*Sim_NonLin_CMG.mdl*" and it is shown in Figure 3.1.1. It is similar to Figure 2.1.1 except for the spacecraft dynamics block that now it includes flexibility, as in Fig. 3.1. The spacecraft is initialized in the LVLH frame with negative orbital pitch rate. The command shaper provides smooth commands to the attitude control system by limiting the rate and the acceleration. The simulation model below is used to perform a 3⁰ attitude change maneuver using the CMGs. The command is a simultaneously 3-axis rotation (thecmd=3°) from zero LVLH attitude in an arbitrary direction: com_dir= (1, 1, -1). When the simulation is complete the Matlab script file "pl2.m" is used to plot the results which are shown below.
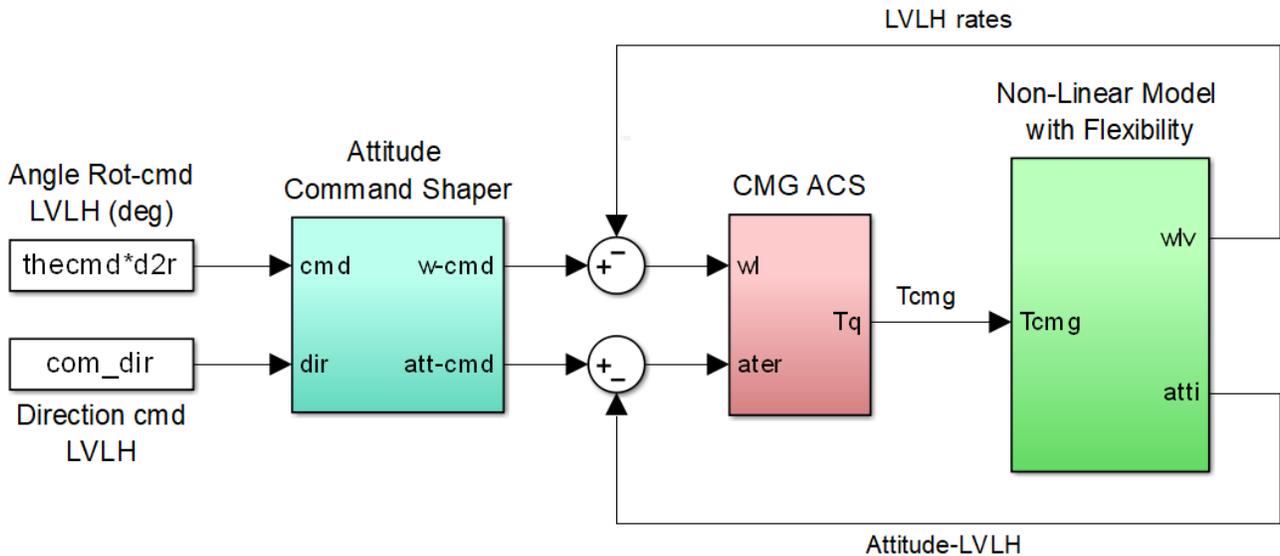
Figure 3.1.1 CMG Attitude Maneuver Simulation Model "Sim_NonLin_CMG.mdl"

Figure 3.1.2a shows the LVLH attitude response in roll, pitch, and yaw that converges to the commanded attitude. When the maneuver is complete the LVLH rate decays to zero. The body rate, however, remains at orbital rate since the Station z-axis is pointing Nadir. Initially the body rate is only in the pitch direction. At the end of the small maneuver the body rate remains mainly in pitch, but it has a small component coupling in the other two directions because the vehicle is now slightly rotated from zero LVLH attitude.

Figure 3.1.2b shows the CMG torque and momentum. The simulation includes a function "Torq_Lim" that limits the torque and prevents it from exceeding its maximum value. It is not zero at steady state because of the external disturbance torque which causes the CMG momentum to diverge with time as it is trying to provide steady control torque to counteract the disturbance.
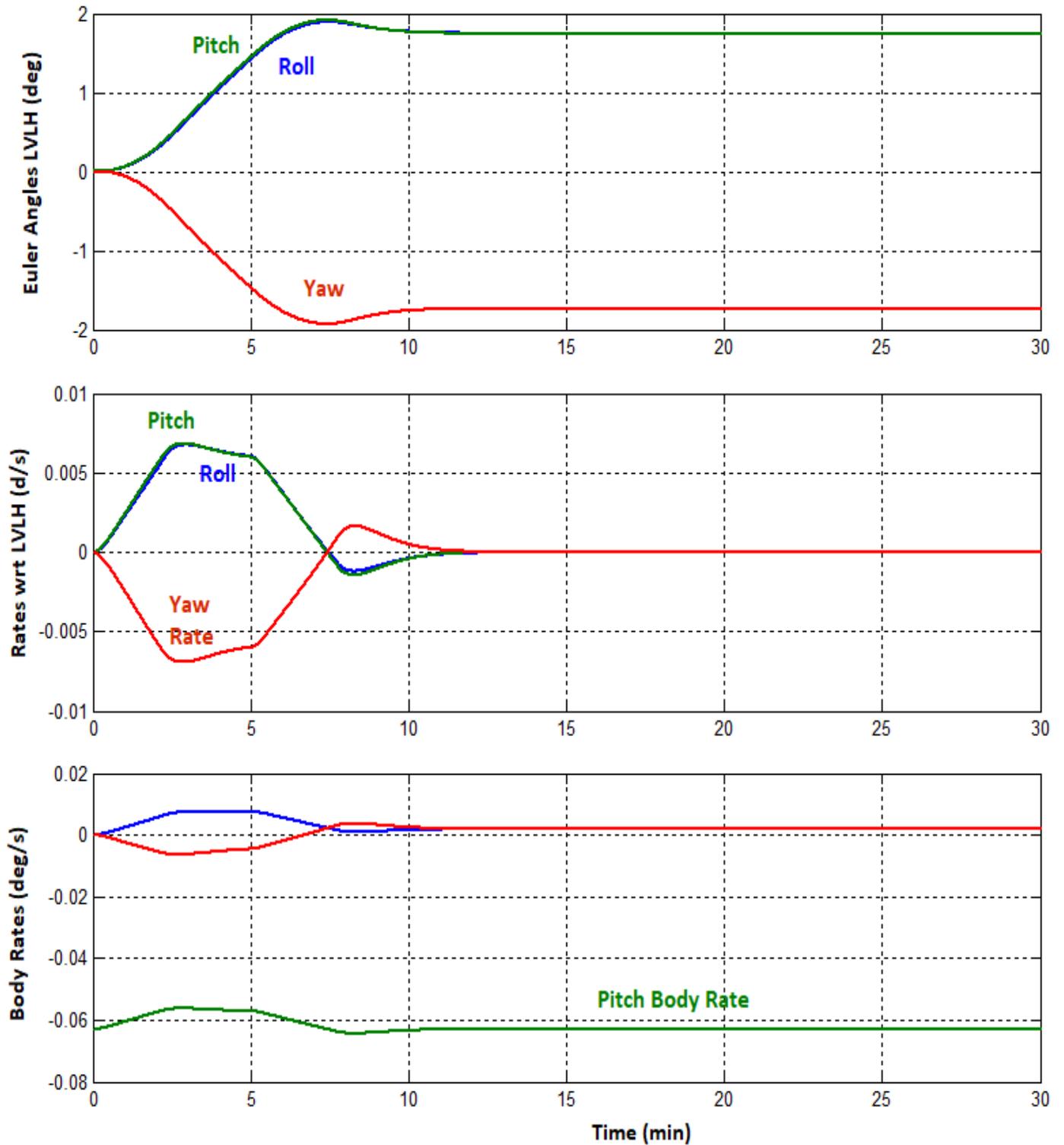
Figure 3.1.2a Space Station Attitude and Rates during a Small 3⁰ Maneuver
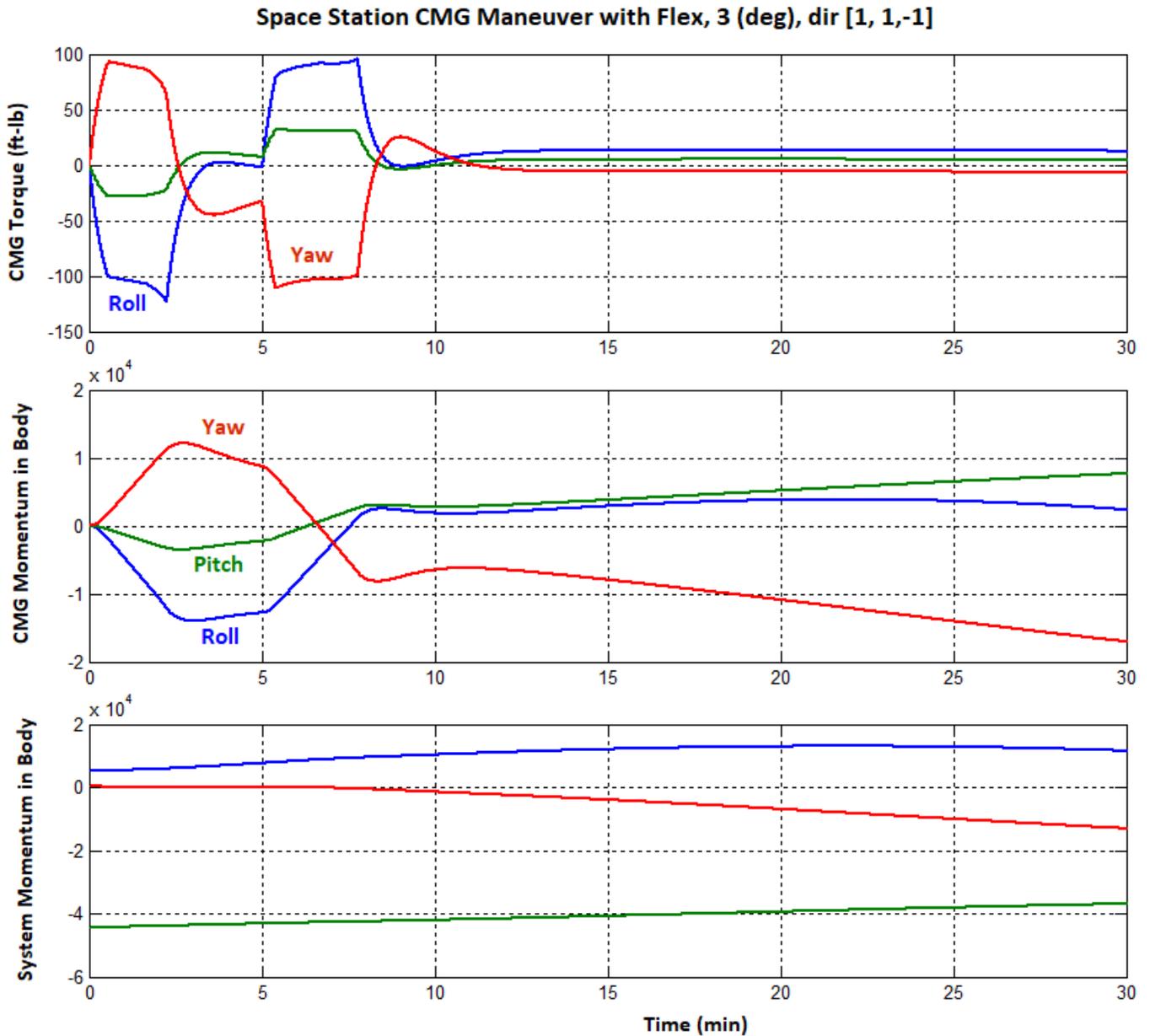
Figure 3.1.2b CMG Torque and Momentum during the Small 3⁰ Maneuver

Stability Analysis of the CMG Attitude Control System

Stability of the CMG/ ACS mode is calculated using the model "*Open_Loop_CMG.mdl*" in folder "*\Large Space Station\(c) Mat NonLin Flex*" and shown in Figure 3.1.3. It is similar to Fig. 3.1.1 but has the control loop broken at the CMG torque. The frequency response for each axis is calculated separately by opening one loop at a time and closing the other two. In the configuration shown, the Simulink model is set up for analyzing pitch stability. The model must be modified to check the other axes. The Matlab file "freq.m" calculates the frequency responses by running it separately for each axis. It linearizes the system using the Matlab function (linmod), calculates the SISO state-space system and plots the Nyquist diagrams. The Nichols plots for all three axes are shown in figure 3.1.4. The results demonstrate that all axes are stable and are very similar to those obtained in Section 1 using the Nastran model with the rigid-body modes.

```
[Ao,Bo,Co,Do]=linmod('Open_Loop_CMG');      % Load the CMG/ACS model for freq analysis
sys=ss(Ao,Bo,Co,Do);                         % frequency response analysis
w=logspace(-3.2,2,32000);
figure(2); bode(sys); grid on
figure(3); nichols(sys,w)
```


Figure 3.1.3 Simulink model "*Open-Loop-CMG.mdl*" used for stability analysis of the CMG Mode
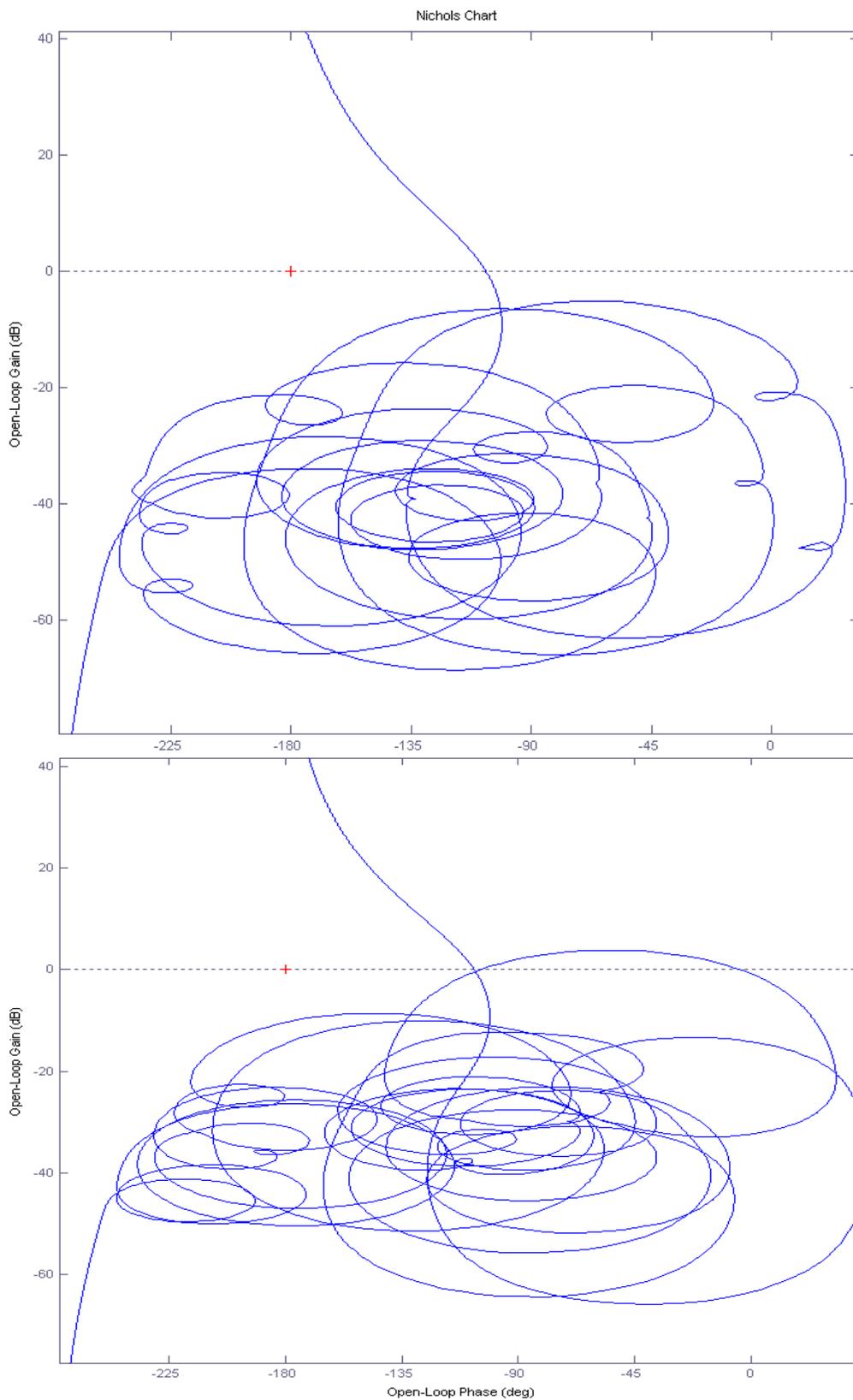
Figure 3.1.4 Pitch, Roll and Yaw Nichols Plots Showing Phase and Gain Margins of the CMG ACS with Flexibility

3.2 RCS Attitude Control Analysis with Flexibility

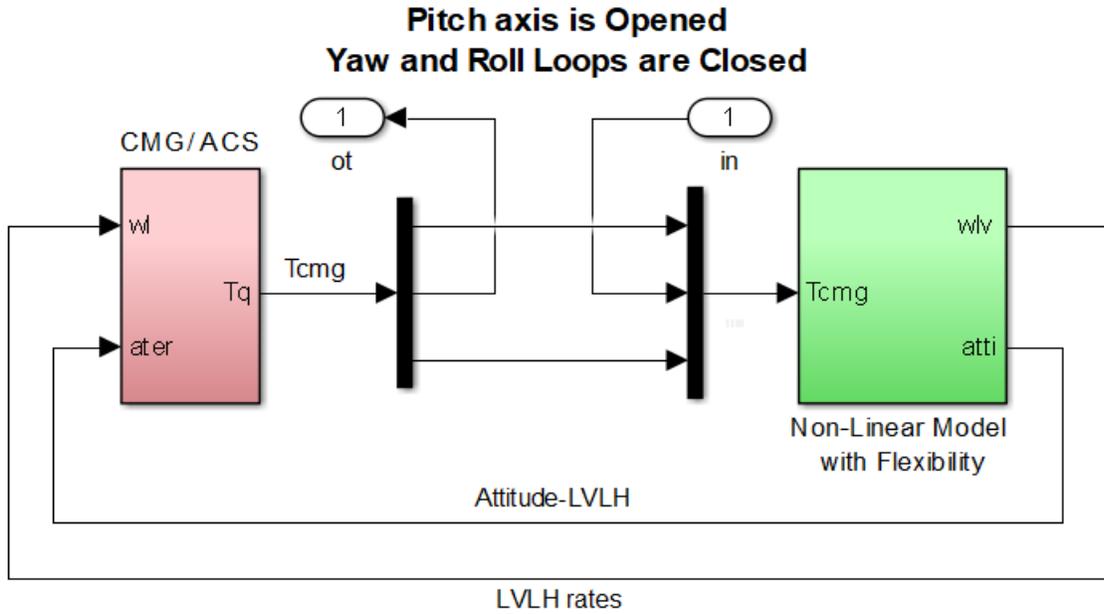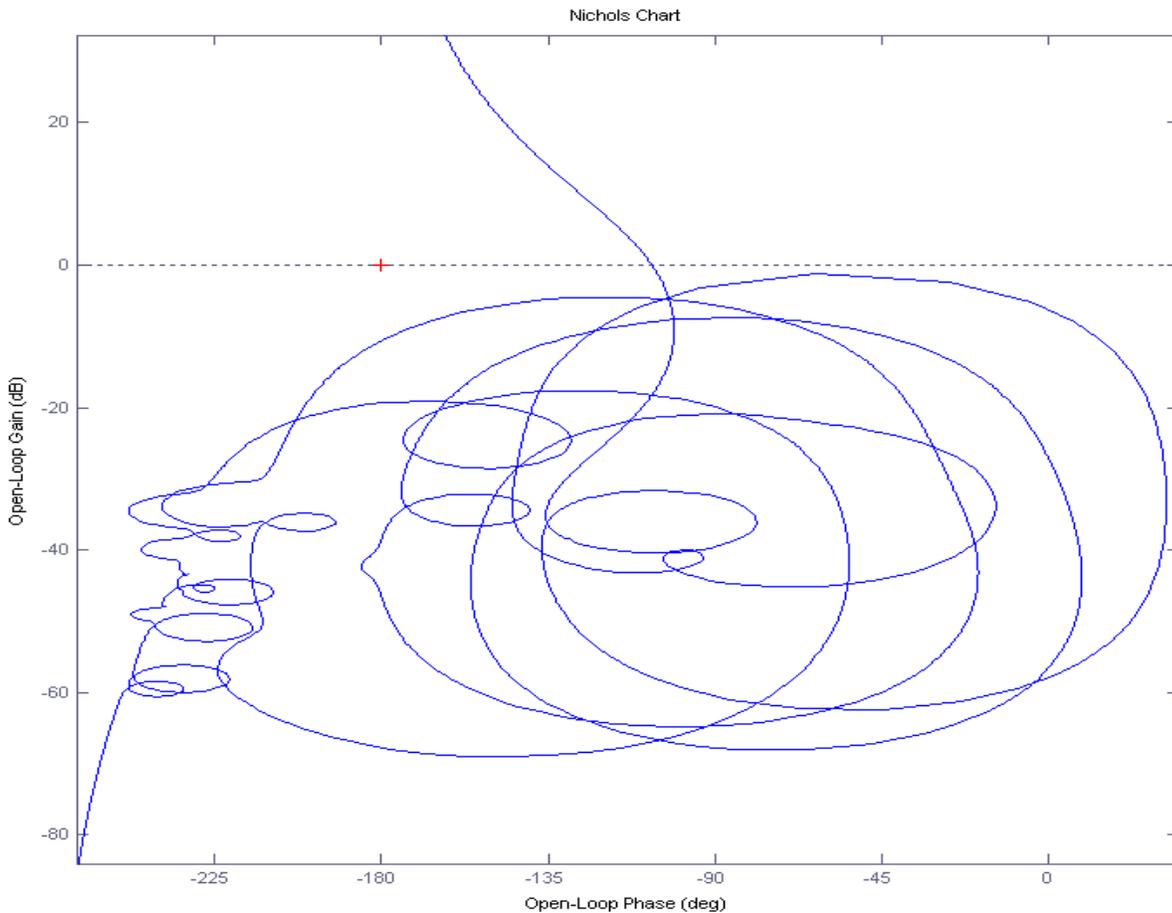The RCS models that were developed in Section 2 are now modified to include structural flexibility. The Simulink model used for RCS attitude control and momentum desaturation simulations is in file "*Sim_NonLin_RCS_Dump.Mdl*" and shown in figure 3.2.1. It is similar to the one used in Section 2.2, except that the spacecraft model includes flexibility and bending filters were introduced to prevent limit-cycling.

This Simulink model is used to perform attitude maneuvers using only the RCS jets. It can also perform momentum desaturation either at steady attitude or while the Station is maneuvering. In the simulation that follows we are commanding the Station to rotate 20° in a direction: (1, 1, -1) and at the same time we are desaturating the CMG momentum from (1, 2, -1)x10^4 (ft-lb-sec) by applying torque at the CMG cluster in the direction that reduces the CMG momentum. The reaction control system being more powerful counteracts the CMG torque while it simultaneously performs the attitude maneuver.
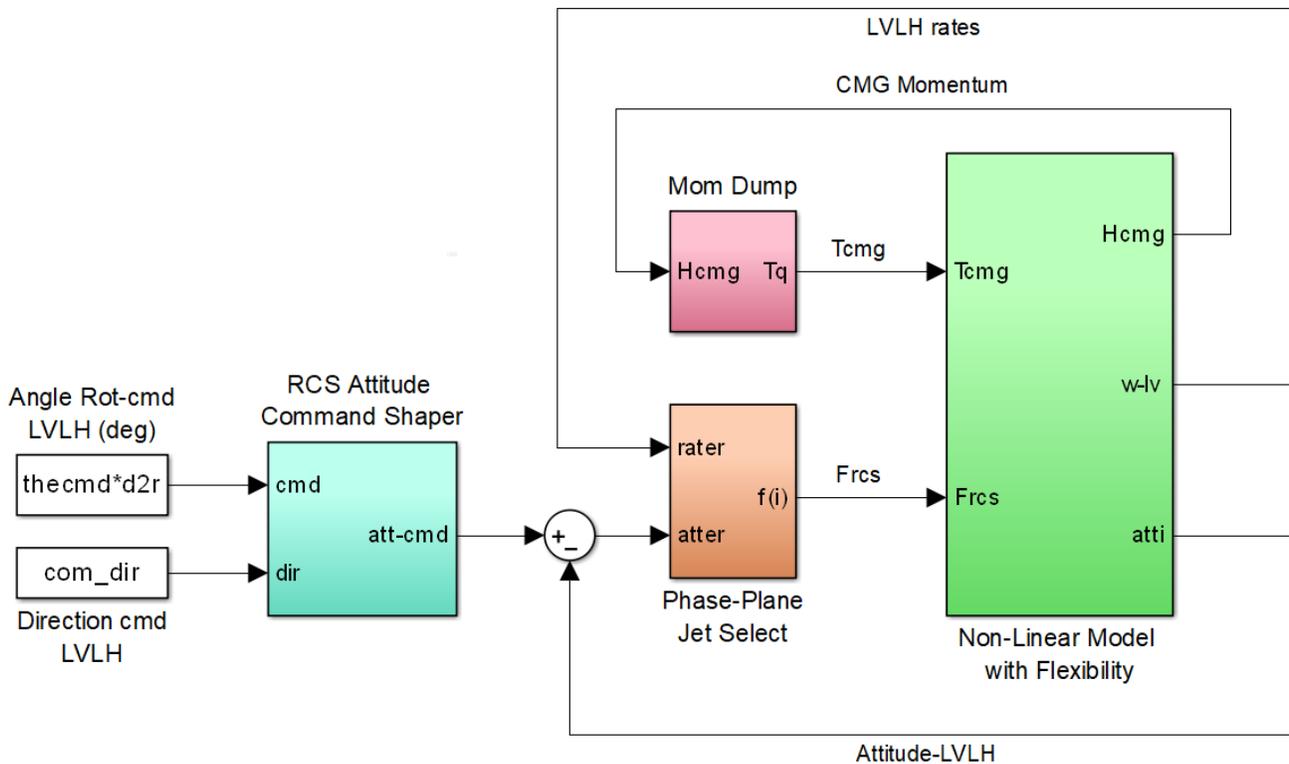
Figure 3.2.1 Simulink Model "Sim_NonLin_RCS_Dump.Mdl" used for RCS ACS and Momentum Dump Simulations

The model is initialized by running the m-file "start2.m" and the file "Pl.m" is used to plot the results which are shown in Figure 3.2.2. The spacecraft is initialized in the LVLH frame with a body rate equal to (0, -ω_o, 0). The spacecraft response is limited in rate and acceleration by the command shaper. The jet firings excite the structure but the flex oscillations do not diverge because flexibility filters are included at the rate-gyro outputs. Figure 3.2.2b shows the CMG torque applied during the momentum dump and the momentum which is reduced in all 3 axes simultaneously. Figure 3.2.2c shows the jets firing in the x and y directions.
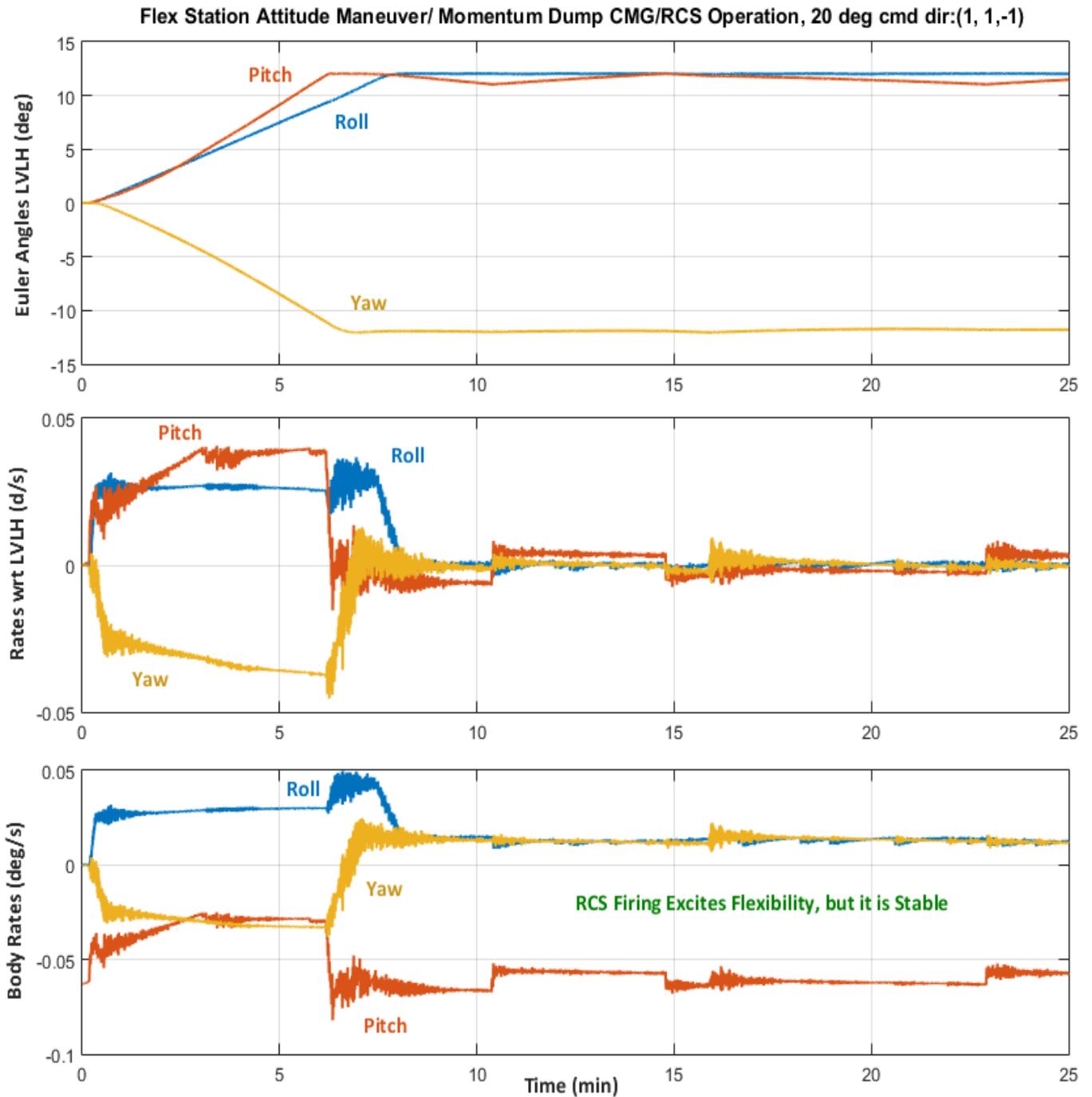
Figure 3.2.2a Flex Space Station Attitude and Rate Response to a 20º Attitude Command using RCS
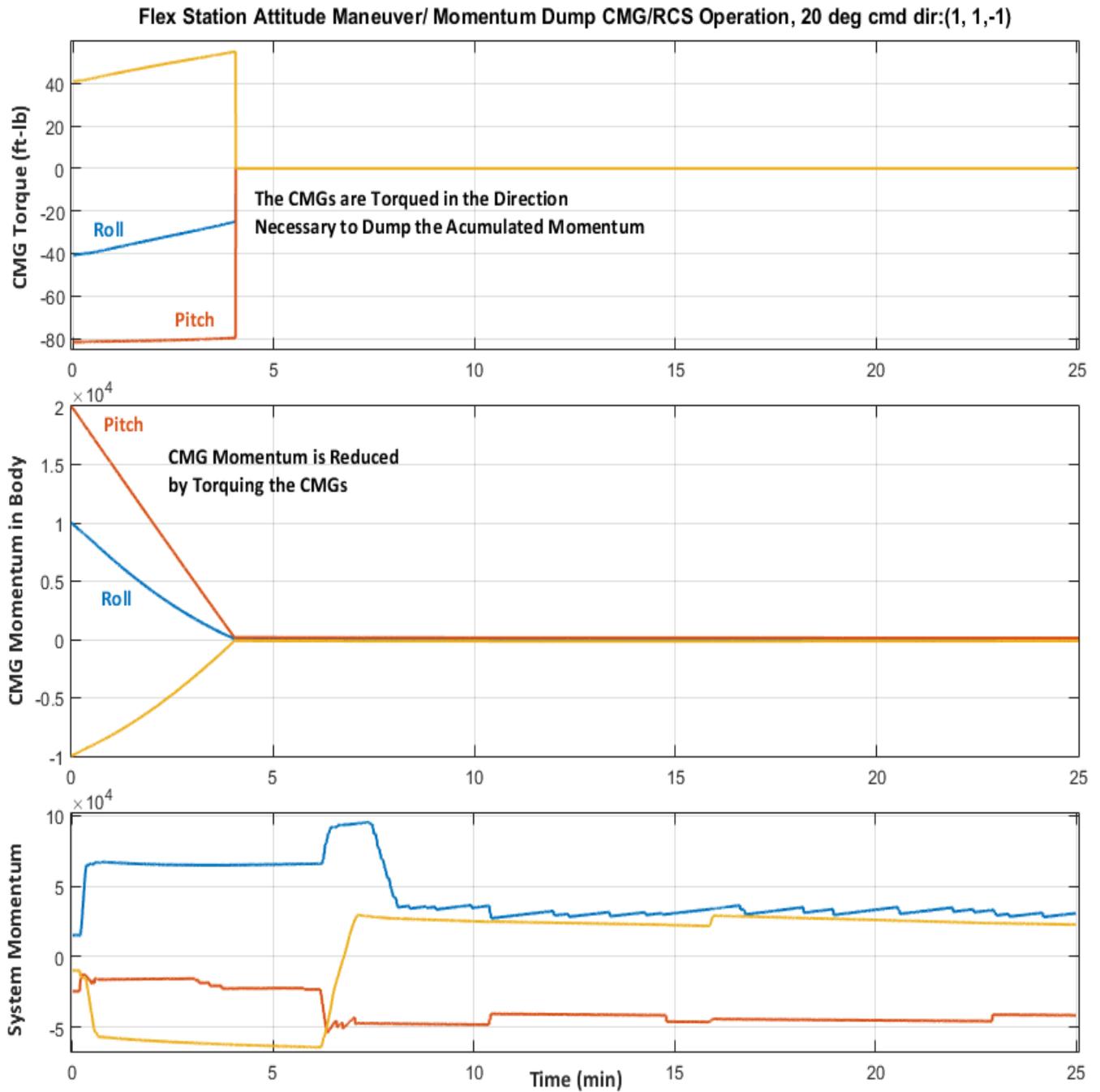
Figure 3.2.2b CMG Torque is applied in the Direction that Reduces the CMG Momentum. The RCS Dumps Momentum and Performs the 20º Maneuver Simultaneously
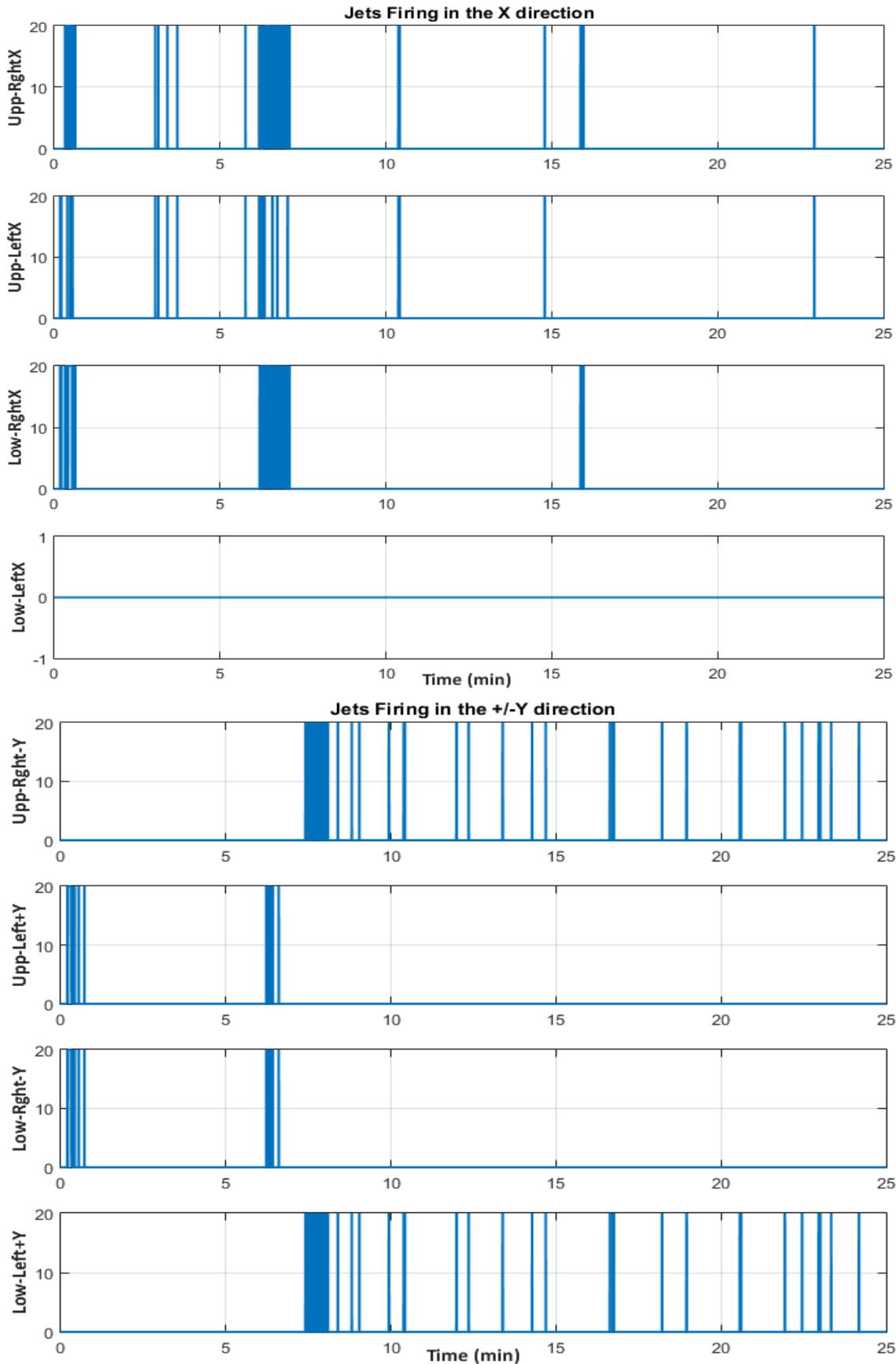
Figure 3.2.2c RCS jet firing during the 20º RCS Attitude Maneuver

Stability Analysis of the RCS Attitude Control System Using Describing Function

We will repeat the Describing Function method in order to analyze the stability of the control system to flex mode excitation and design filters that will attenuate the flex modes and prevent them from limit-cycling. Figure 3.2.3 is a block diagram showing the non-linear system. The linear and the non-linear parts are separated in two SISO subsystems as described in Section 1.3. The continuous system is at the top and the dead-band non-linearity is at the bottom. The continuous system is constrained to rotate about one axis which is defined as input, and stability is analyzed one axis at a time: roll, pitch, yaw, plus other skewed directions can be analyzed separately. The phase-plane logic was simplified to a SISO non-linear dead-zone block that has a known DF representation N(e), where the input (e) is the output of the continuous system G(s) consisting of a linear combination of rate plus attitude error in a fixed direction specified. The linear system G(s) is implemented in a Simulink file: "*Open_Loop-RCS.mdl*" which is in folder "*Large Space Station\(c) Mat NonLin Flex*". This approach allows us to use the same model to analyze stability in all 3 axes, plus an infinite number of skewed directions, by specifying the rotational axis. The direction to be analyzed is specified by an input vector. The input to the non-linearity is a combination of attitude and rate error in a specific direction and the output of the non-linearity drives the jet-select logic that will rotate the vehicle in the specified direction and excite some of the modes. The dead-band non-linearity is theoretically connected across the two open ends of G(s). In the analysis, however, the non-linearity is not physically connected across G(s) but we calculate the frequency response G(jω) across the two open ends and plot it in Nichols or Nyquist diagram. On the same diagram we also plot the inverse of the DF, that is: $-1/N(e)$.
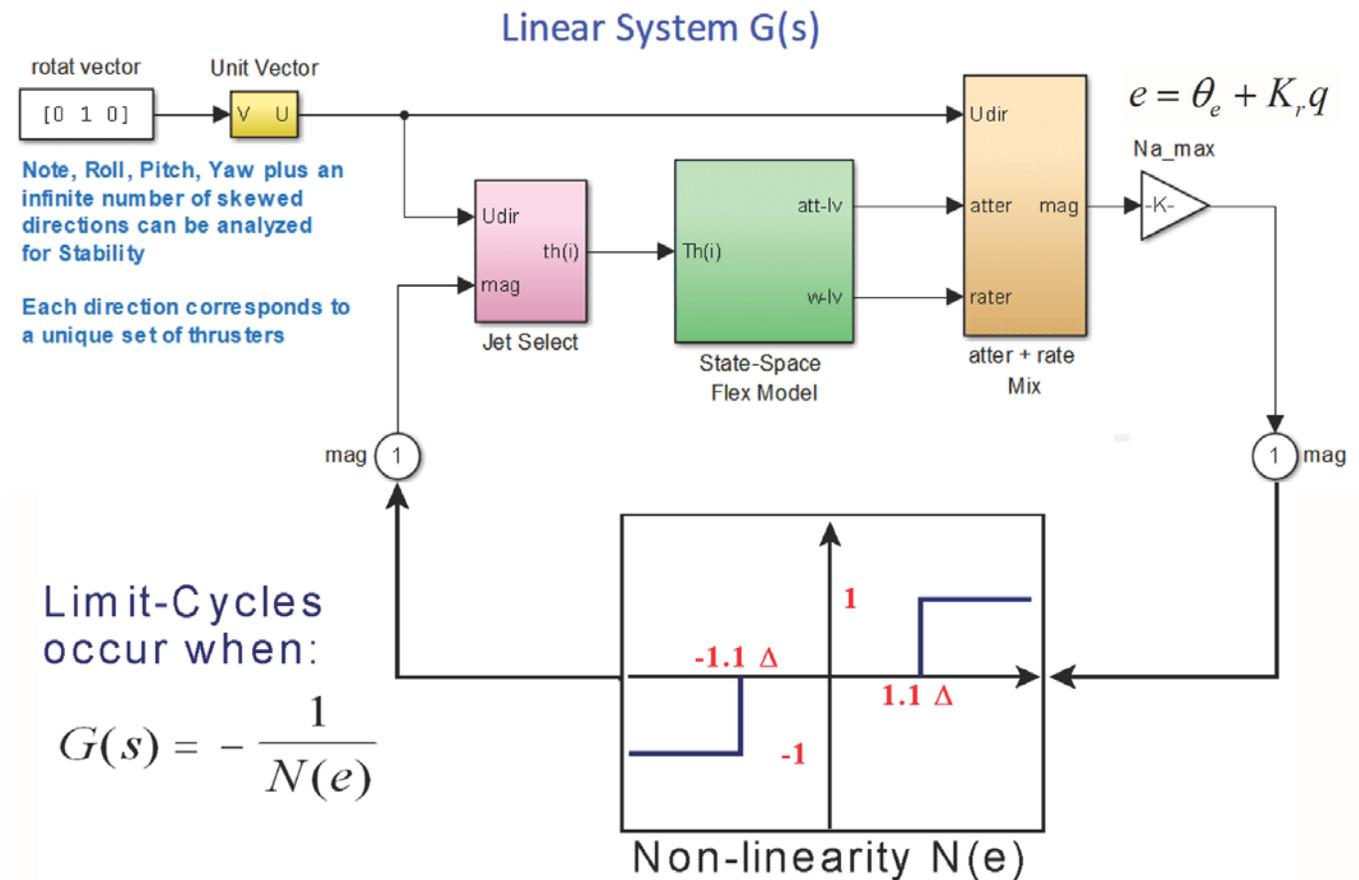
Figure 3.2.3 Simulink Model "Open_Loop_RCS.mdl" used for RCS Describing Function Analysis

74

Limit cycles occur when the DF locus which is a function of the error amplitude (e) intersects the frequency response locus G(jω) on a Nyquist or Nichols chart. The intersection point(s) on the G(jω) locus will predict the frequency of oscillation(s) and on the N(e) locus will approximately predict the limit-cycle amplitude. The linear system G(s) in addition to flex spacecraft dynamics it contains also other component blocks needed for applying the Describing Function method. Since the Describing Function is a SISO method we can only analyze one axis at a time and the direction is specified by a rotational unit vector input in the block diagram. The orange block combines the rate and attitude to approximate the attitude error and rate combination in the phase-plane as it was described in Section 1.3. The (3x1) error signal is resolved (dotted) in the specified rotational direction and normalized by multiplying it with the maximum value of the DF, N(e)$_{max}$. The G(jω) locus is scaled by multiplying it with N(e)$_{max}$. This makes it more convenient when using Matlab. The (+) sign in Nichols and Nyquist plots now represent the minimum point of the -1/N(e) locus. The model uses a linearized jet select logic function "JSel_ln.m" that includes both groups of jets: the ones contributing in the positive axis rotation, and also the jets that contribute in the reverse direction. It applies positive half thrust to the jets in the positive direction and negative half thrust to the jets that rotate the vehicle in the opposite direction. This makes the system more symmetrical than using only the thrusters that contribute in the positive rotation about the specified axis.

The initial analysis showed that a lot of flex modes were getting excited to instability by the RCS control system and bending filters were included in the rate feedback to attenuate the potentially unstable resonances in the G(jω) response. The block diagram in Figure 3.2.3b shows the bending filters that attenuate flexibility from the roll, pitch, and yaw rate gyro measurements and it is included in the spacecraft dynamics block. The Matlab file "freq.m" is used to calculate the frequency response across the open ends of the Simulink file: "*Open_Loop_RCS.mdl*" and calculates the frequency response locus G(jω) on a Nichols plot.
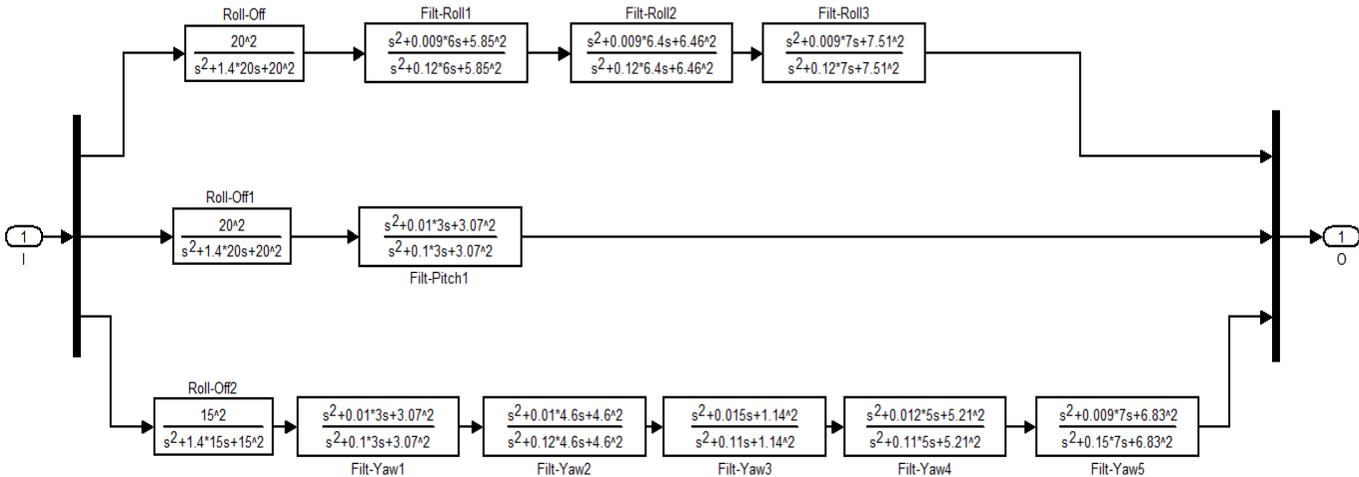
Figure 3.2.3b Structural Flexibility Filters for Roll, Pitch, and Yaw

The Nichols plots in Figures 3.2.4 show the DF analysis results in roll, pitch, and yaw and there are no intersections in those directions that would imply limit-cycles. Some of the resonances spike above the zero (dB) line but they are phase stable. Other skewed directions must also be analyzed for limit-cycle stability by specifying different rotational direction in Figure 3.2.3. This is may be necessary because there is a unique set of jets selected for each direction that excite different modes in all directions, plus the observability of the flex modes differs with direction and some skewed directions may potentially be unstable.

Roll Axis RCS Describing Function Analysis
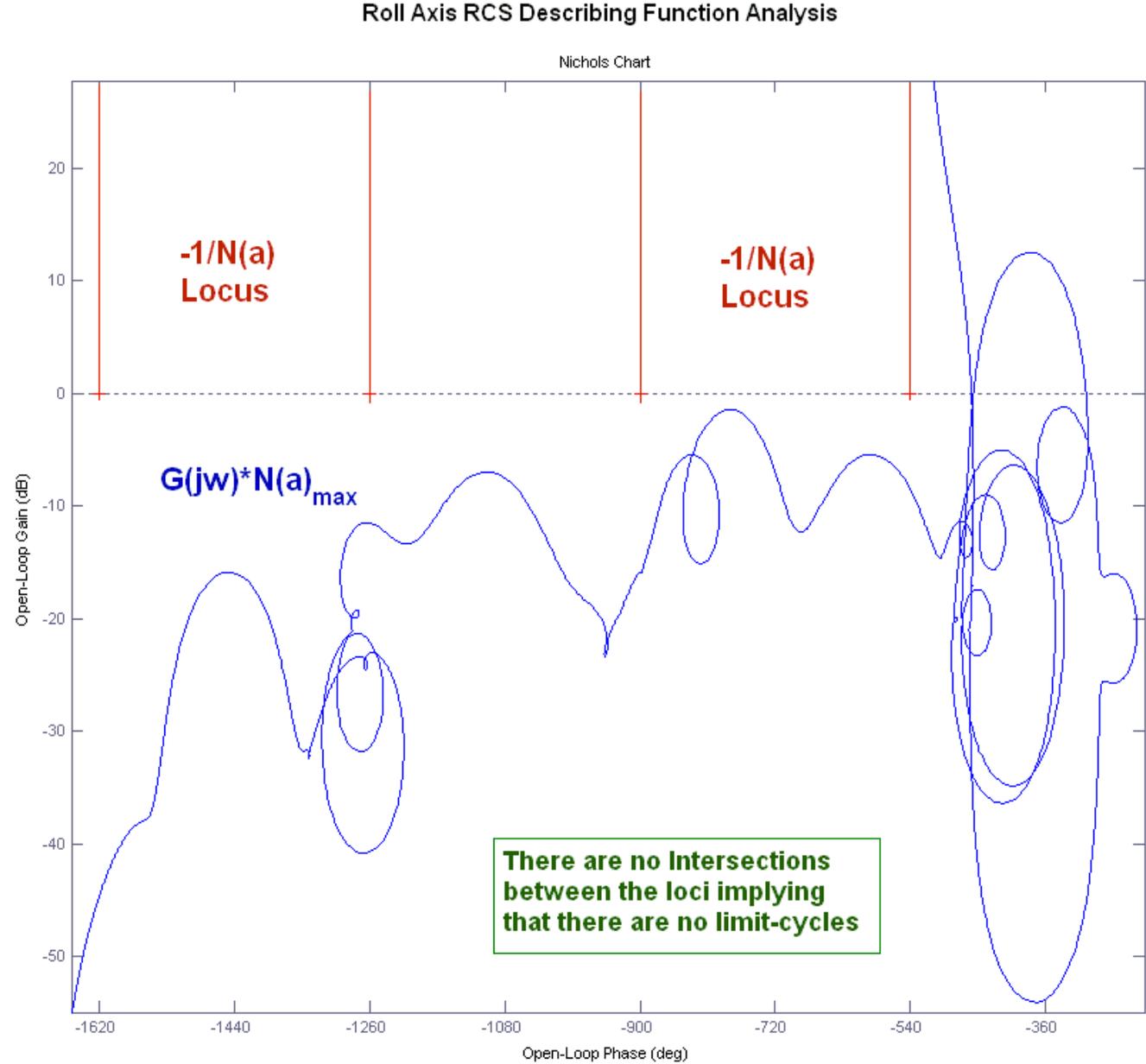
Figure 3.2.4a Nichols plot in Roll direction (1, 0, 0), Showing No Intersections between the two Loci and hence there is No Limit-Cycling
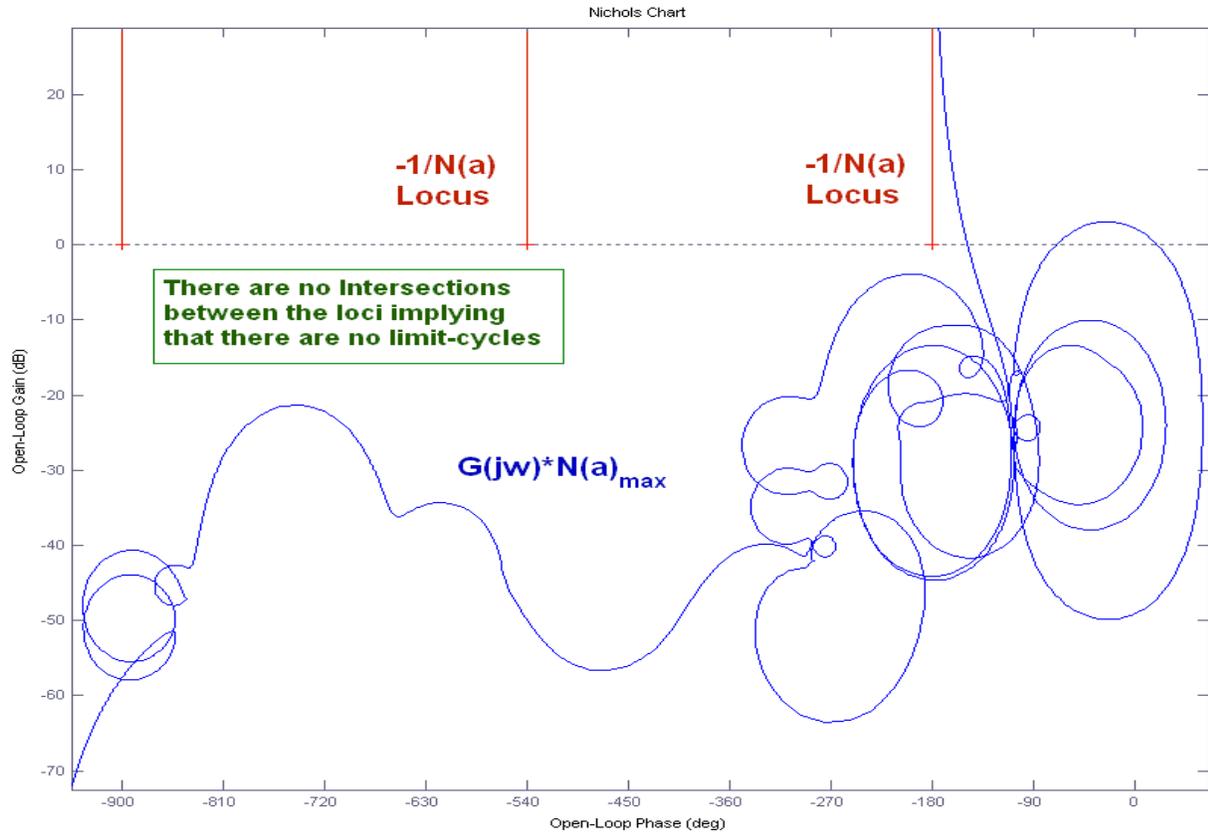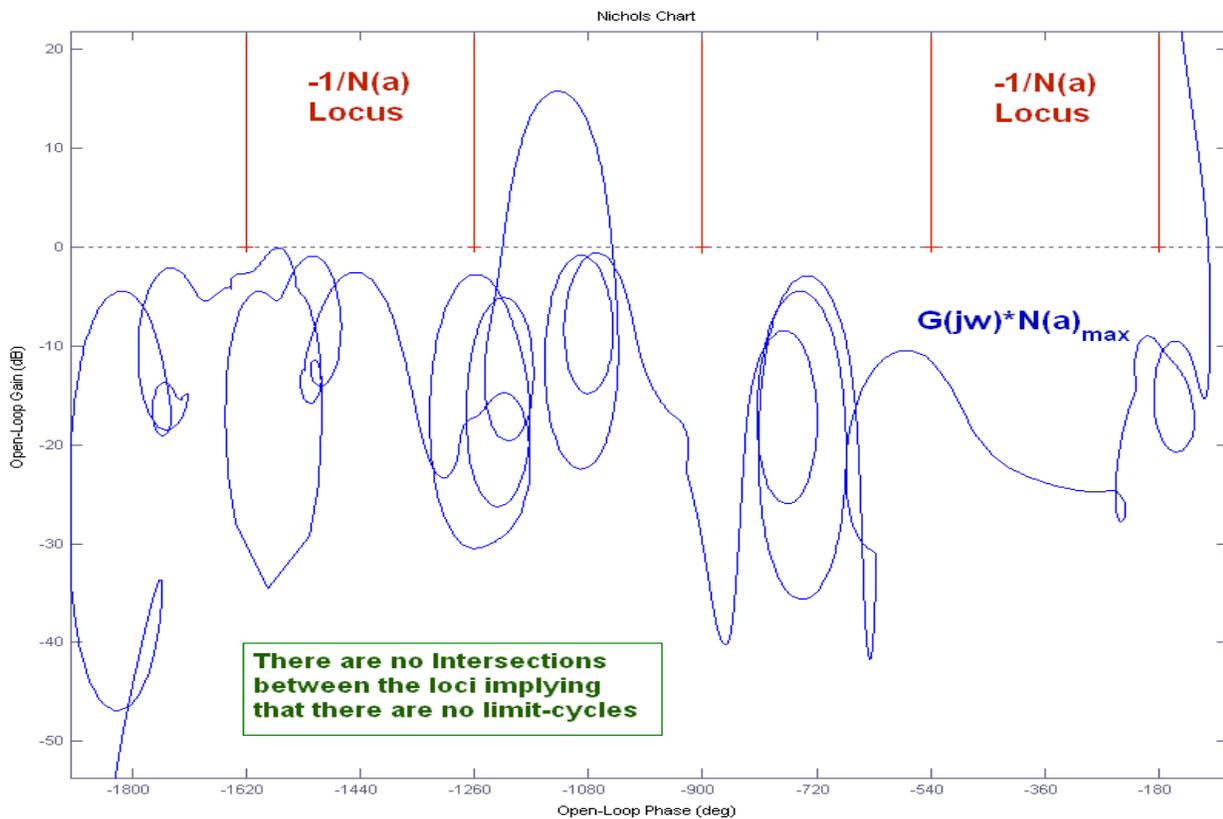
Figure 4.2.4 (b and c) Describing Function Analysis for the RCS Attitude Control System

3.3 Combined CMG and RCS Attitude Control with Flexibility

This mode was described in the rigid-body Section 2.3 and it is repeated here using the flexible spacecraft model. It uses both, the CMG and the RCS attitude controllers operating together. The Simulink model for this mode of operation is shown in Figure 3.3.1, and it is located in file "*Sim_NonLin_CMG_RCS.Mdl*", in directory: "*Large Space Station\ (c) Mat NonLin Flex*".
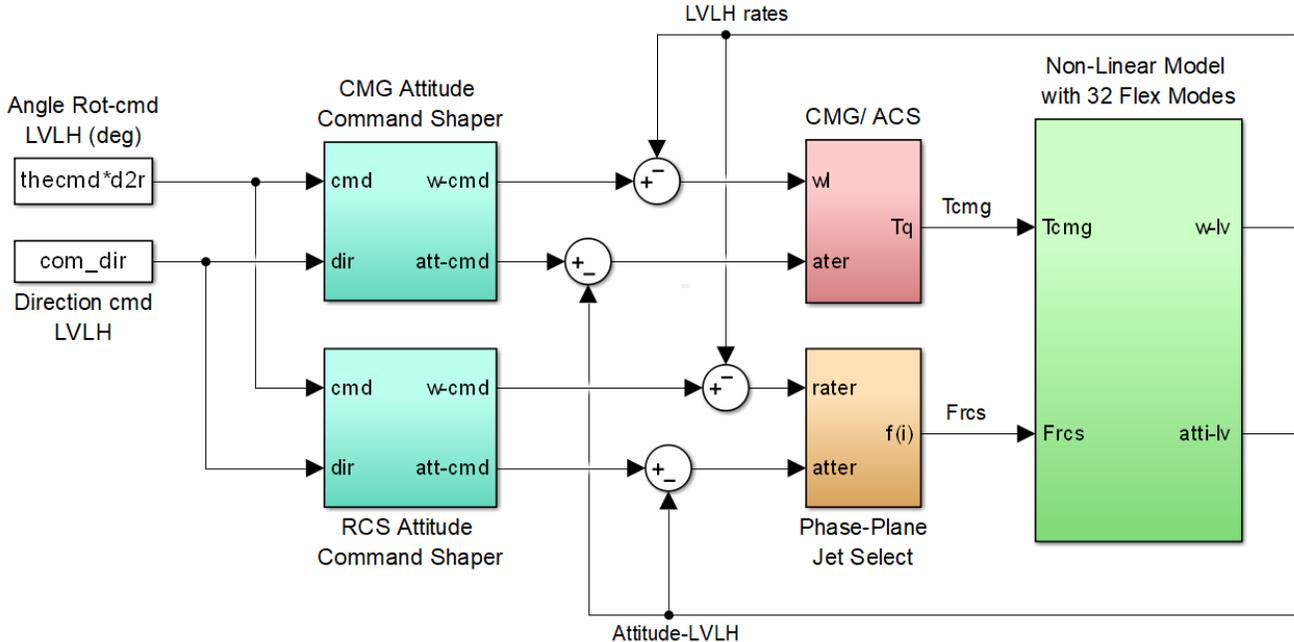
Figure 3.3.1 Combined CMG and RCS Mode of Operation

The CMG attitude control system is shown in Figure 3.3.2. The PD gains are designed for a bandwidth 20 times the orbital rate, that is: 0.022 (radians/sec). They are calculated and loaded into Matlab by file "start3.m" which also initializes the simulation. A switching logic disables the CMG control when the torque demand is large to prevent the CMG torque from limiting. It is similar to the rigid-body version but slightly modified. The logic activates the CMGs when the magnitude of the combined rate and attitude errors become sufficiently small. Figure 3.3.3 shows the system response to a 20° attitude command. The file "Pl.m" is used to plot the simulation results.
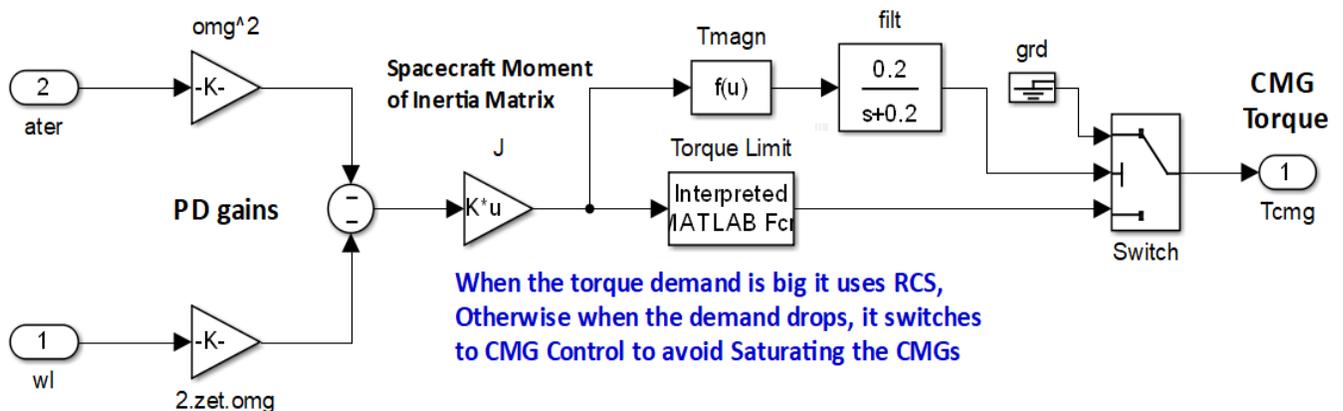
Figure 3.3.2 CMG/ PD Attitude Control System with Switching Logic
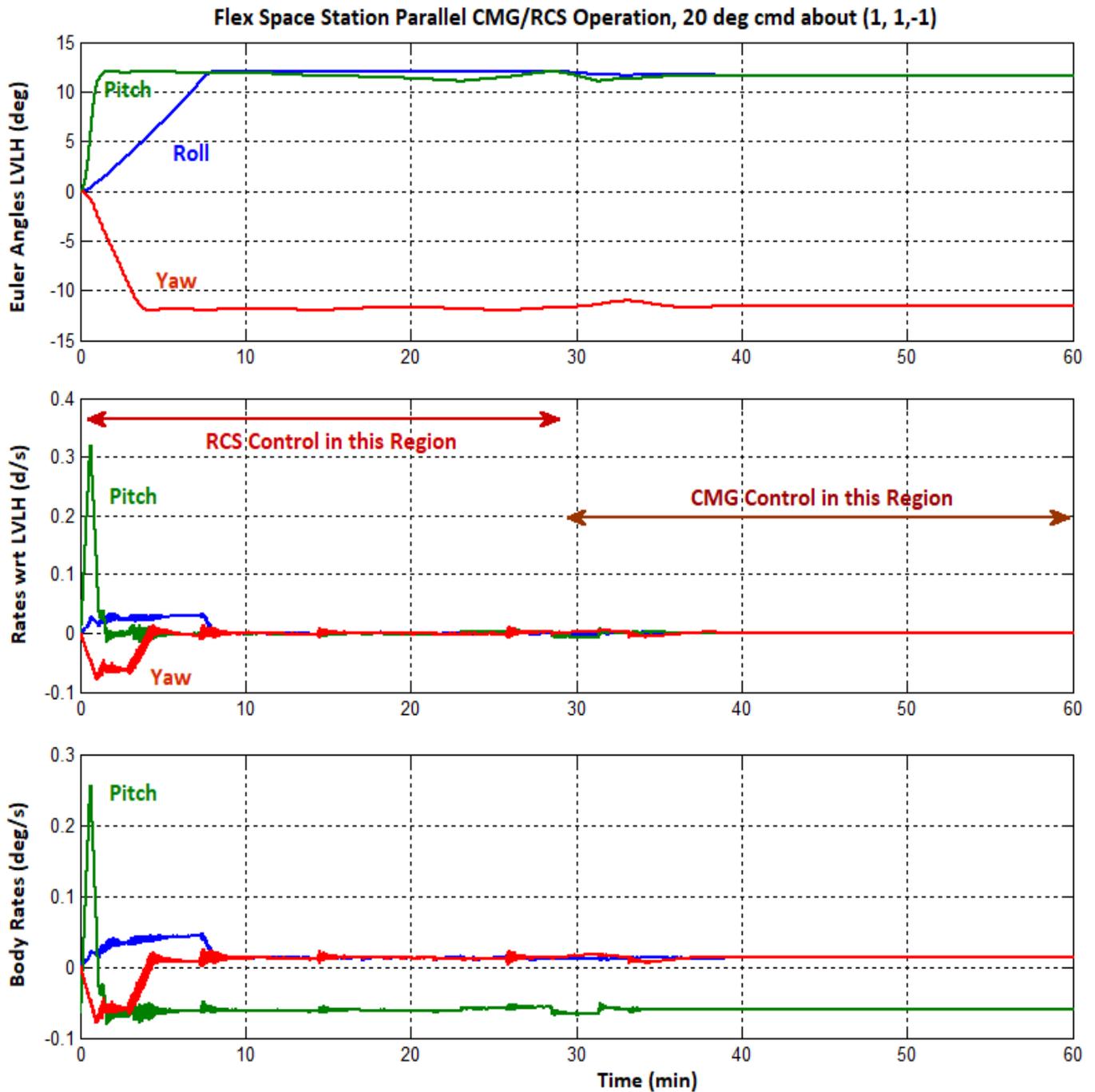
Figure 3.3.3a CMG/ RCS Combined System Attitude Response to a 20° Step Command

The pitch response to the attitude step command is faster because it receives an initial boost by the CMG system before the CMG is turned off at 0.25 (min). The RCS completes the maneuver at t=28 (min) where the CMG is turned back on. The RCS system excites structural vibrations but they decay without sustaining limit-cycles, as it was predicted by the DF analysis. At steady state the CMG control system maintains a smooth attitude with very small attitude errors and it does not excite the structure. The momentum however, is growing due to the steady aero disturbances.
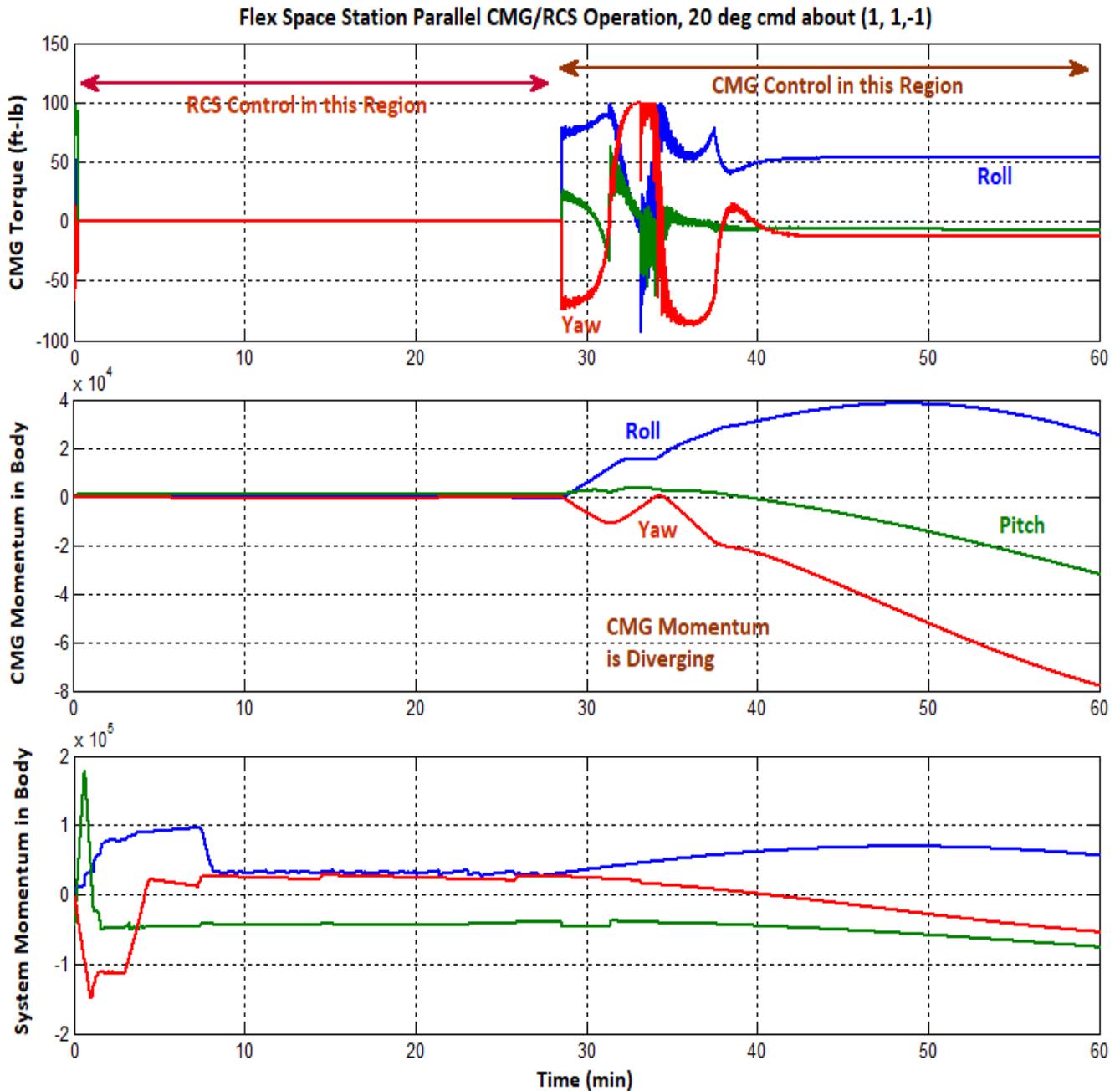
Figure 3.3.3b CMG/ RCS Combined System CMG Torque/ Momentum Response 20° Attitude Command

The CMG torque is turned off during RCS control. A steady CMG torque is necessary to maintain the required attitude because of the external disturbances. This causes building up of the CMG momentum which would eventually saturate (not shown) due to hardware limitations. This leads to the necessity of a continuous momentum management mode of operation that will stabilize the Station attitude without saturating the CMGs which will be described in the next section.
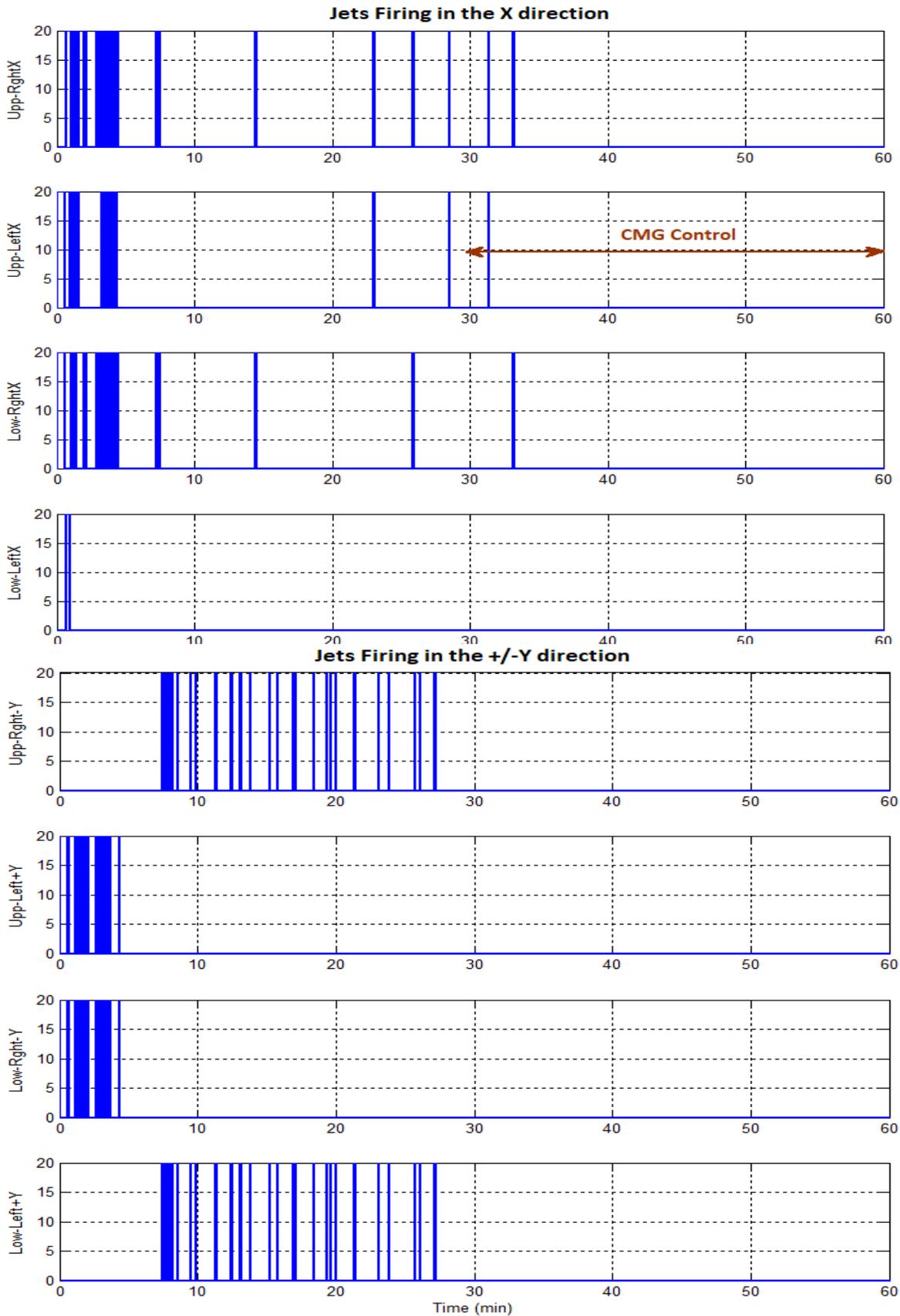
Figure 3.3.3c RCS Activity in Response to the 20° Attitude Command

3.4 TEA Converge/ Momentum Management Mode with Flexibility

The analysis in Section 2.4 will be repeated here with structure flexibility. The Space Station model consists of the non-linear dynamics with the state-space flex model, as in Figure 3.1, and the control loop is closed via the state-feedback gain K_{pqr} which was designed using the LQR method in Section 2.4. The upgraded simulation model is "*Sim_NonLin_TEA.Mdl*" in directory: "*Large Space Station\ (c) Mat NonLin Flex*", shown in figure 3.4.1. The simulation parameters are loaded into Matlab by running the file "start.m", and when the simulation is complete the Matlab file "pl3.m" is used to plot the simulation results. The vehicle is initialized in the LVLH frame and it slowly drifts towards the torque equilibrium attitude as it stabilizes the CMG momentum. The results are shown in Figure 3.4.2 and they are similar to rigid-body results in Figure 2.4.5 because flexibility is not excited by the CMG and aero torques.
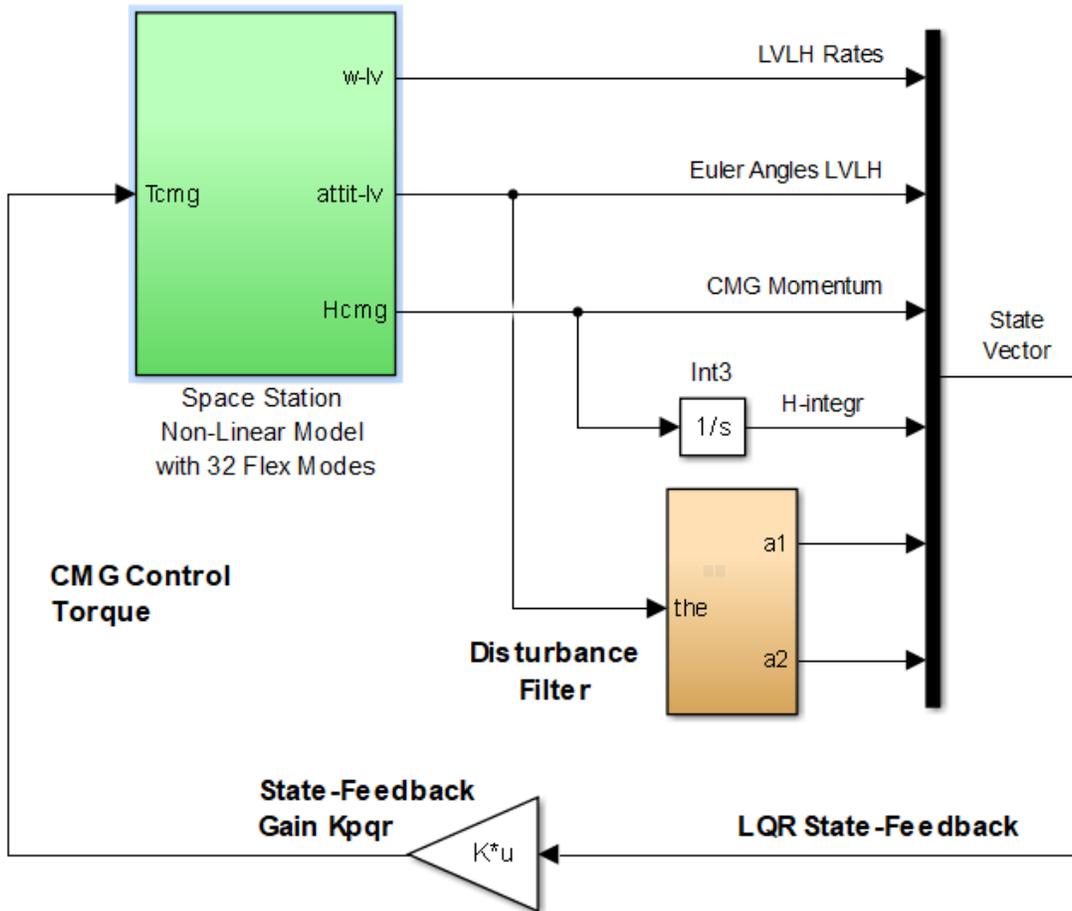
Figure 3.4.1 TEA Converging Mode uses State-Feedback to Control the CMG Momentum

There is no attitude command in the system when the Station is operating in this mode. The vehicle attitude simply drifts under the influence of the aerodynamic torques which are included in the Space Station dynamics (green) block, and the gravity gradient torques which are also included in the equations of motion 2.1. The state-feedback stabilizes not only the attitude but also the CMG momentum and the attitude slowly drifts to the TEA as the CMG momentum cycles around zero. The CMG control also attempts to reduce the attitude oscillations under the influence of cyclic disturbances occurring at (ω_o) and at $(2\omega_o)$. The purpose of the disturbance accommodation filter is to further attenuate the pitch oscillations at orbital rate as already described in Section 2.4.
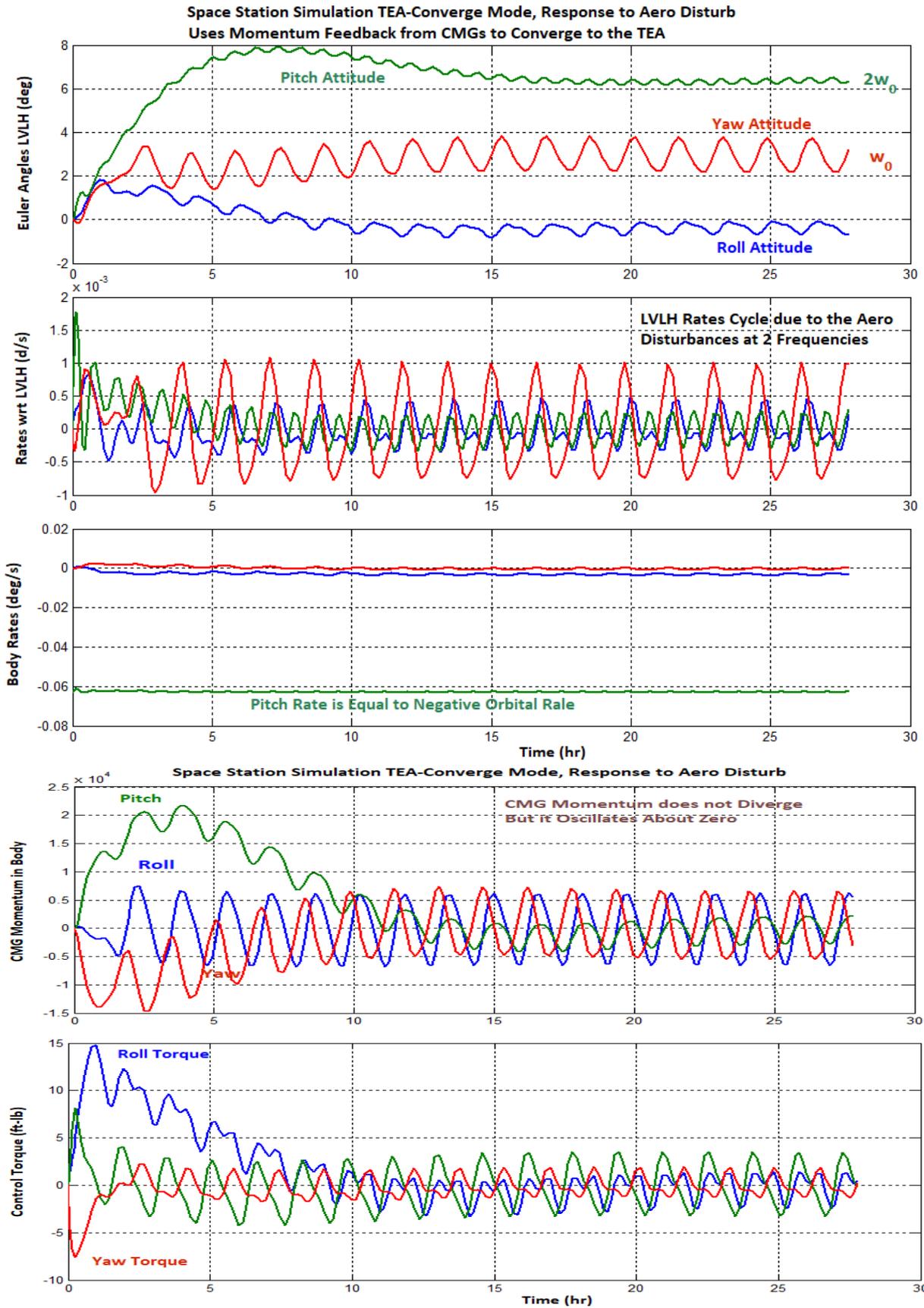
Figure 3.4.2a Attitude Response in TEA-Seek mode under the influence of external torques

3.4.1 Flex Stability of the TEA Converging Mode under CMG Control

The TEA-Seeking mode has a much slower bandwidth than the regular CMG attitude control mode. Control stability is analyzed using the open-loop analysis Simulink model "*Open-Loop-TEA.Mdl*" shown in Figure 3.4.3 with the loop broken at the CMG torque. It includes flexibility and it is an upgraded version of the previous rigid-body simulation model. The frequency response for each axis is calculated separately by opening one loop at a time with the other two loops closed and must be modified for analyzing other axes. In Figure 3.4.3 it is configured for yaw axis analysis. The Matlab file "freq.m" linearizes the system using the Matlab function "Linmod" and calculates the SISO system frequency responses by running it separately for each axis. Figure 3.4.4 shows the Nichols plots for all three axes. The stability margins are plentiful because the control bandwidth is very low.
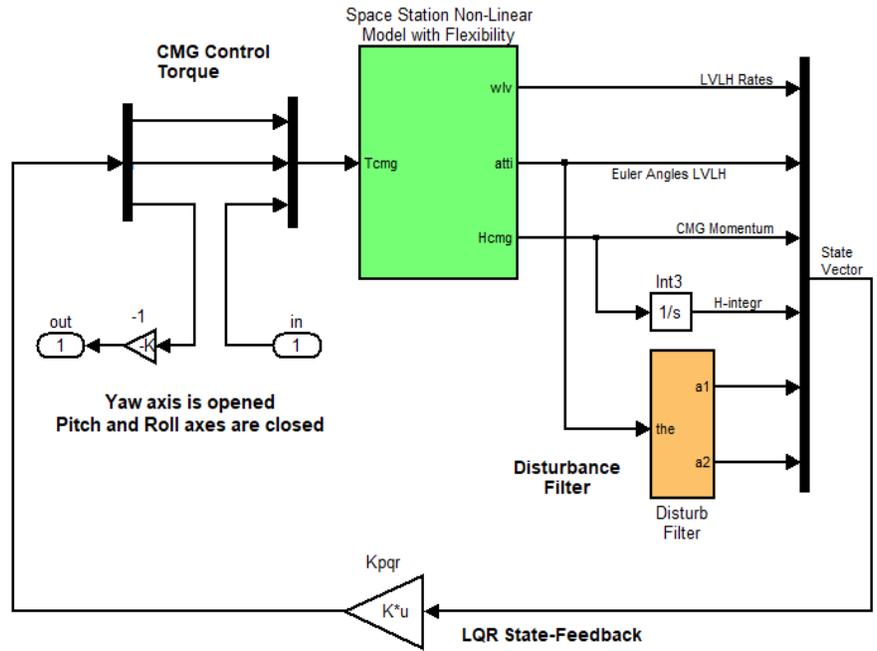
Figure 3.4.3 Open-Loop model for analyzing stability of TEA-Seek mode

Roll Axis Stability in TEA Seek Mode by linearizing the Non-Linear model with Flex

Nichols Chart

0.0013
(r/s)

Phase Margin
65 (deg)

2.2
(r/s)

1.29
(r/s)
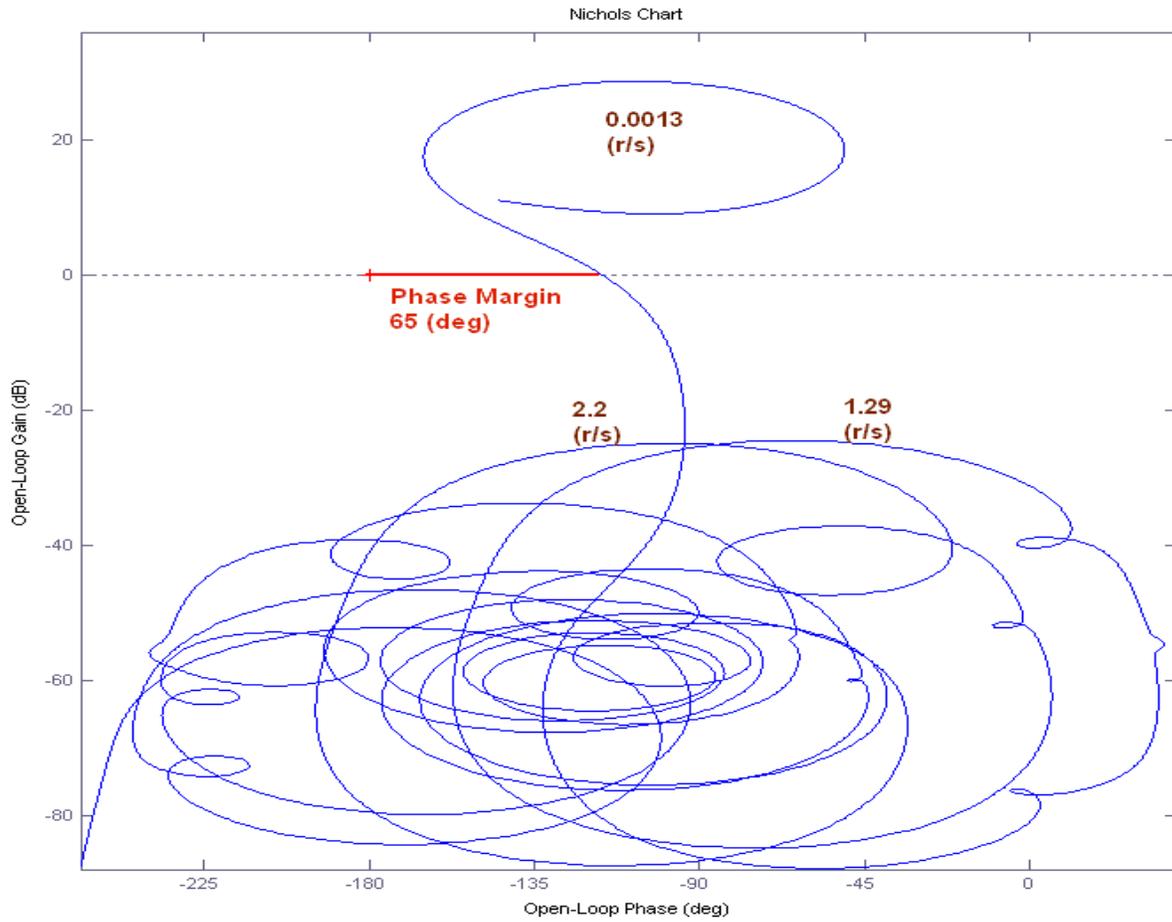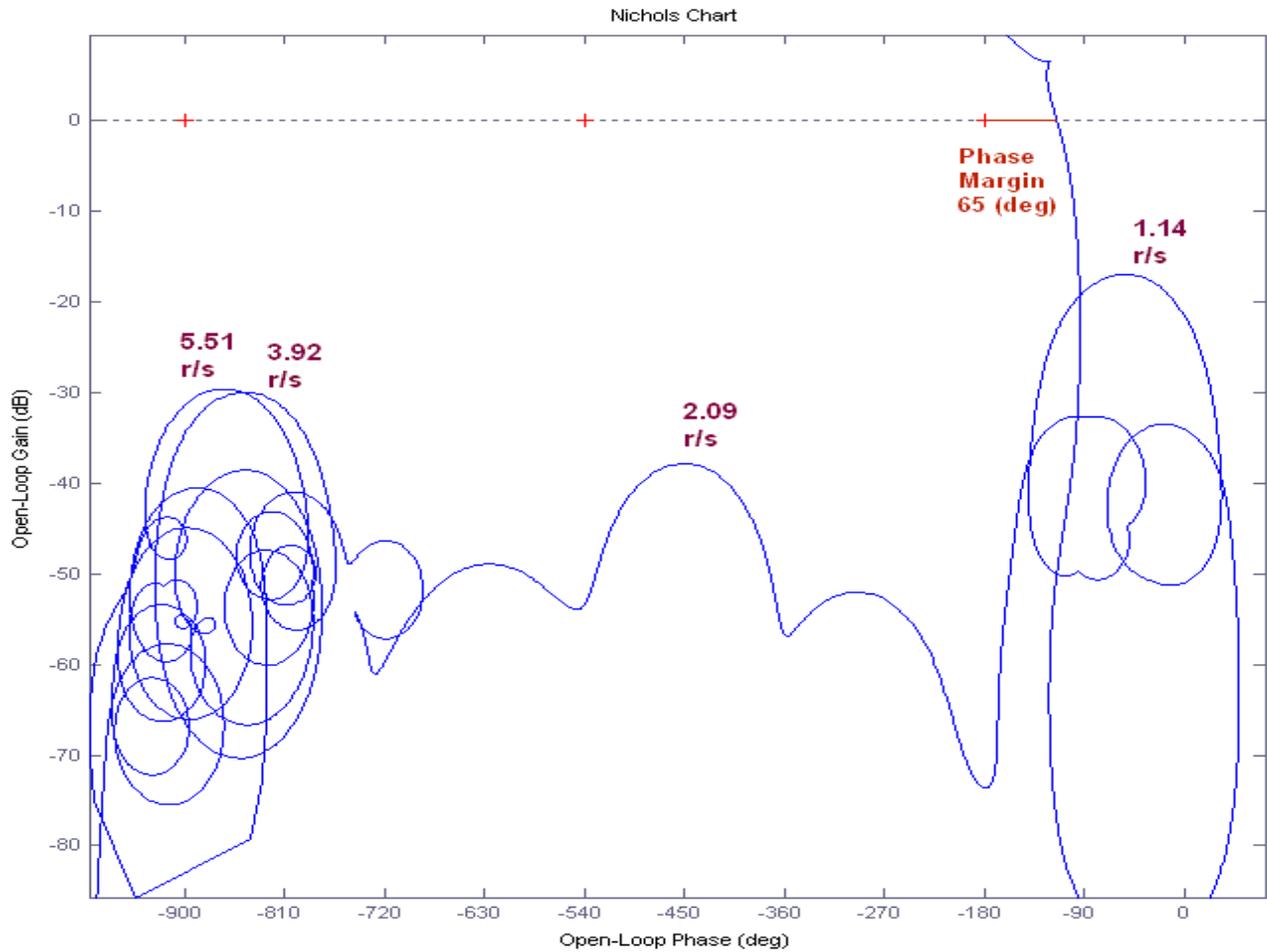
Roll axis stability analysis in TEA Seek mode after linearizing the non-linear dynamic model

Nyquist Diagram
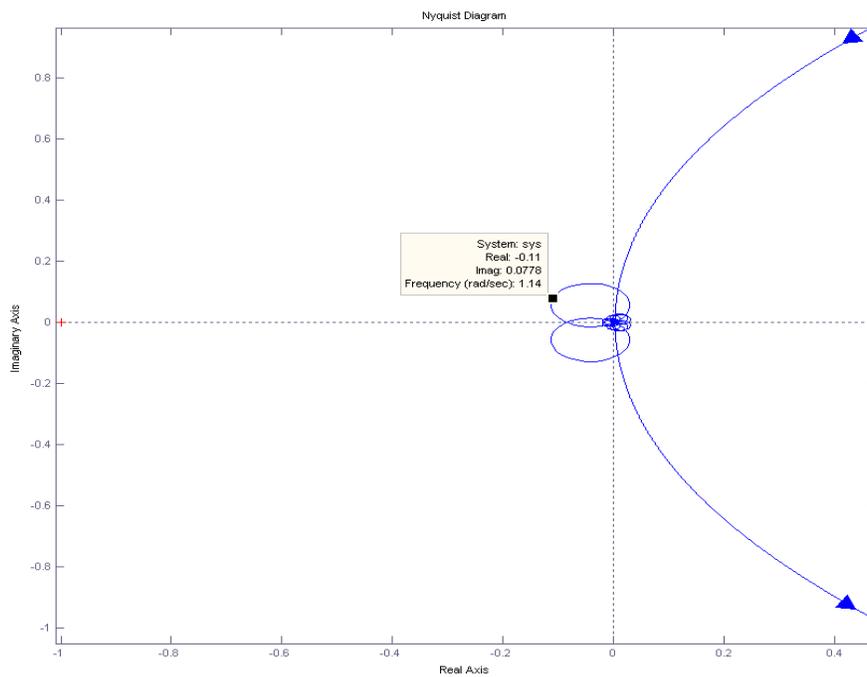
Figure 3.4.4 Stability Analysis of the TEA Converging Mode shown in both Nichols and Nyquist Plots

3.4.2 Sensitivity Response to Aerodynamic Disturbances

It is also necessary to calculate the sensitivity response of the spacecraft attitude to external disturbance torques. This is done by using singular values frequency response of the TEA-seeking system in Figure 3.4.5, which is implemented in the Simulink model "*Sensitivity_TEA.mdl*". This is similar to the simulation model in figure 3.4.1 but it was modified for frequency domain analysis by including an aerodynamic disturbance input and an attitude sensitivity output. The aero disturbance function generator was replaced by a (3x1) torque input, and the output is a (3x1) attitude variation.
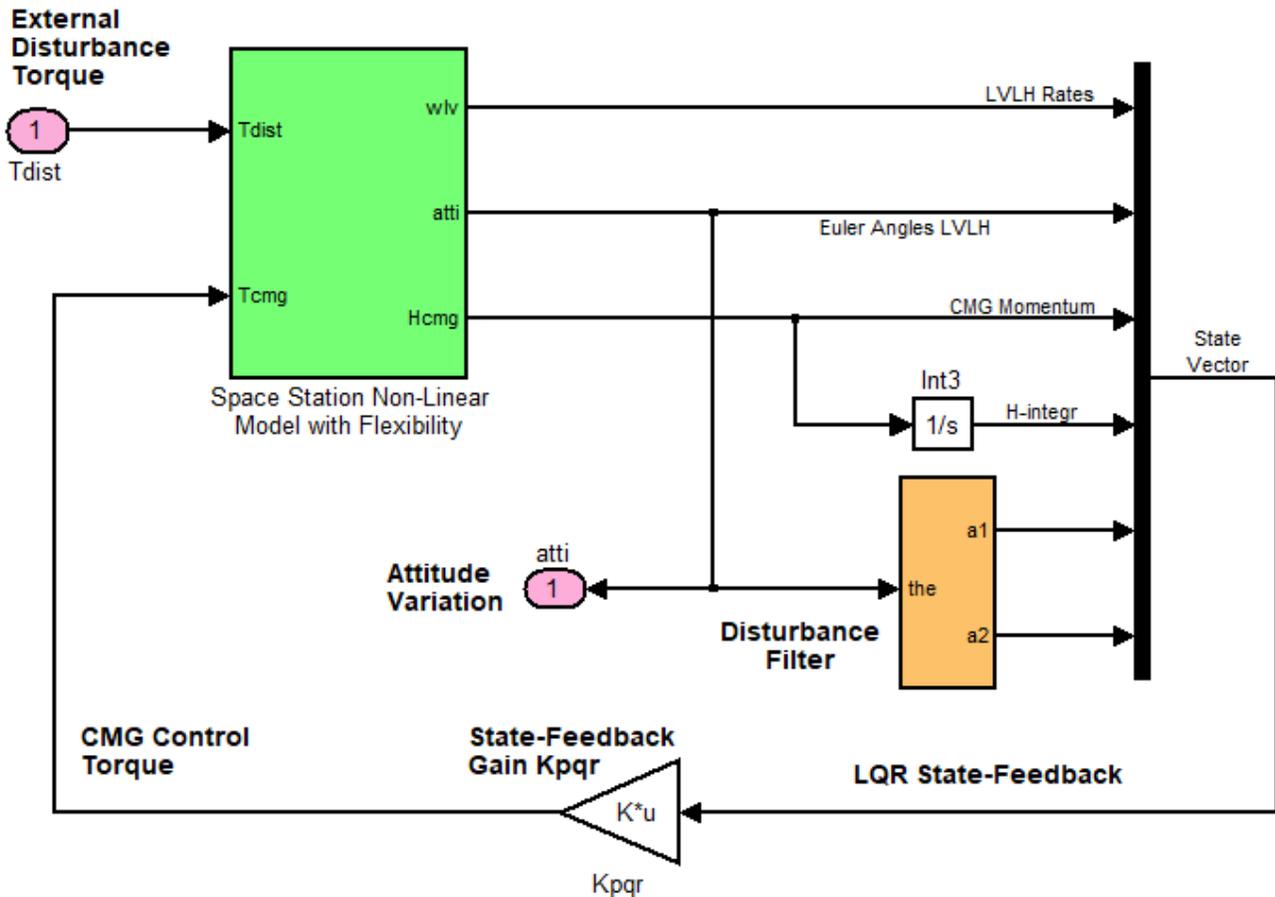
Figure 3.4.5 Disturbance Sensitivity Analysis Model for the TEA-Seek Mode

Flexibility is not excited by the aero disturbance input because aero disturbances occur at very low frequencies and we are analyzing rigid body sensitivity. The m-file "frq.m" is used to linearize the above model and to calculate its singular values frequency response which is shown in Figure 3.4.6. The notch at orbital rate frequency is the result of the disturbance accommodation filter that was designed by the LQR method. It attenuates the effect of the aero disturbances in the pitch attitude. It appears only in the pitch direction because we did not include filters in roll and yaw since the aero disturbance is stronger in pitch.
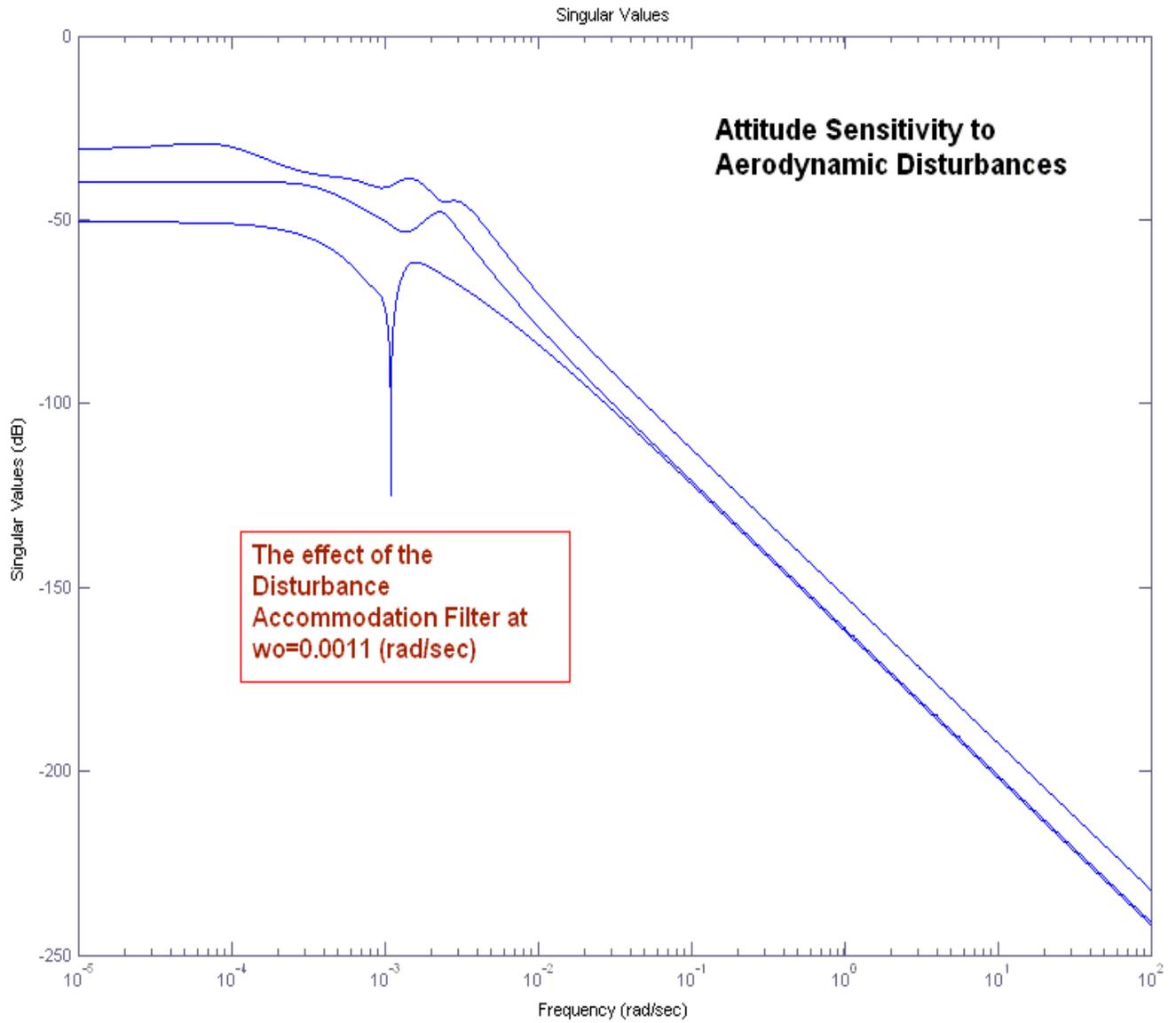
Figure 3.4.6 Attitude Sensitivity to Aerodynamic Disturbance Torque

4. Modeling the Space Station Using the Flight Vehicle Modeling Program

In the previous sections the Space Station models were created using the flexible spacecraft modeling program that creates state-space systems from finite element models (FEM). The state-space models derived from this program often include the rigid-body modes obtained from the FEM together with the flex modes. The rigid-body modes are usually the first 6 modes in the FEM. We also created models consisting only of flex modes that were combined with separate non-linear rigid-body equations implemented in Matlab functions in a Simulink block and connected in parallel with the flex model.

In this section we will perform the Space Station analysis using the flight vehicle modeling program to implement the linearized spacecraft dynamics in orbit around the earth and maintaining a constant LVLH attitude. This program includes the spacecraft rigid-body and CMG dynamics combined with flexibility. The derived model, shown in equations (4a to 4c), assumes that the CMGs are a collocated cluster and not separate units that provides control torque in all 3 axes. The internal CMGs steering dynamics and steering logic are not included in the equations of motion, but the CMG cluster generates control torques in the body axes and the CMG momentum is also calculated in the spacecraft body axes. For small attitude deviations from the LVLH attitude the linearized equations of motion are:

$$
\begin{bmatrix} I_{XX} & I_{XY} & I_{XZ} \\ I_{XY} & I_{YY} & I_{YZ} \\ I_{XZ} & I_{YZ} & I_{ZZ} \end{bmatrix} \begin{pmatrix} \dot{\omega}_X \\ \dot{\omega}_Y \\ \dot{\omega}_Z \end{pmatrix} = \omega_o \begin{bmatrix} I_{XZ} & 2I_{YZ} & I_{ZZ} - I_{YY} \\ -I_{YZ} & 0 & I_{XY} \\ I_{YY} - I_{XX} & -2I_{XY} & -I_{XZ} \end{bmatrix} \begin{pmatrix} \omega_X \\ \omega_Y \\ \omega_Z \end{pmatrix}
$$

$$
+3\omega_o^2 \begin{bmatrix} I_{ZZ} - I_{YY} & I_{XY} & 0 \\ I_{XY} & I_{ZZ} - I_{XX} & 0 \\ -I_{XZ} & -I_{YZ} & 0 \end{bmatrix} \begin{pmatrix} \phi \\ \theta \\ \psi \end{pmatrix} + \omega_o^2 \begin{bmatrix} -2I_{YZ} \\ 3I_{XZ} \\ -I_{XY} \end{bmatrix} + T_C + T_D \qquad \dots (4a)
$$

The torques on the right hand side of Equation 4a consist of gyroscopic terms, gravity gradient torques which are a function of the LVLH attitude, the CMG control torques (T_C), disturbance torques (T_D), and some constant bias torques which are in fixed direction and are function of the vehicle products of inertia. In Equation 4a it is assumed that the pitch rate ω_y is initialized at negative orbital rate $-\omega_0$. Otherwise, if we change its definition and initialize the pitch rate at zero, the bias torque must be changed to: $\omega_0^2 \begin{bmatrix} -4I_{YZ} & 3I_{XZ} & I_{XY} \end{bmatrix}^T$. Equation 4b shows the LVLH attitude kinematics

$$
\begin{pmatrix} \dot{\phi} \\ \dot{\theta} \\ \dot{\psi} \end{pmatrix} = \begin{bmatrix} \omega_o \psi + \omega_X \\ \omega_o + \omega_Y \\ -\omega_o \phi + \omega_Z \end{bmatrix} \qquad \dots (4b)
$$

The rate of change in CMG momentum is calculated in body axes by integrating the following equation

$$\dot{\underline{h}}_c = -\left(\underline{\Omega}_0 \times \underline{h}_c\right) - \left(\underline{\omega} \times \underline{H}_0\right) - \underline{T}_C$$

Where: $\underline{\Omega}_0$ is the spacecraft steady-state rate, and $\underline{H}_0$ is the nominal CMG momentum. Assuming that the steady-state rate is in pitch and equal to the negative orbital rate $(-\omega_0)$, the variation in CMG momentum equations become:

$$\dot{h}_X = \omega_o h_Z + \omega_Z H_{Y0} - \omega_Y H_{Z0} - T_{CX}$$

$$\dot{h}_Y = -\omega_Z H_{X0} + \omega_X H_{Z0} - T_{CY}$$

$$\dot{h}_Z = -\omega_o h_X + \omega_Y H_{X0} - \omega_X H_{Y0} - T_{CZ}$$

(4c)

The flight vehicle input data for the Space station model is in file "*SpaceStation.Inp*" and its title is "*Space Station with RCS and a Double-Gimbal CMG Array*". In the flags line which is below the comments, we must specify "**body axes**" for the rates, and "**LVLH Attitude**" for local vertical, local horizontal attitude. The vehicle is initialized with a constant negative pitch rate -0.063 (deg/sec) which is equal to minus the orbital rate (0.0011 rad/sec) since it maintains a constant LVLH attitude. The aerodynamic coefficients are all set to zero. The aerodynamic disturbances due to the solar array rotations are treated as external torques applied in the x, y, and z directions, similar to our previous analysis. The Space Station has 12 RCS jets which are represented in this model by 8 throttling jets of 20 (lb) thrust each. The reduced number is because the 4 jets in the +x direction and the 4 jets in the –x direction are represented with only 4 throttling jets capable of firing in both: +x and -x directions. The control torque effector represents a cluster of collocated double-gimbal CMGs. The CMG dynamics and steering logic are not included in this model but it is assumed that the cluster can provide the same amount of torque in all three axes. The CMG momentum is calculated by equation 4c and its initial value is set to zero (no momentum bias).

For attitude control the Space Station uses three rate gyros measuring body rates and three (roll, pitch, and yaw) LVLH attitude measurements, Eq. 4b. The model also uses four accelerometers, two on the left boom and two on the right boom that will be used for analyzing sensitivity to disturbances. The input file "*SpaceStation.Inp*" also includes selected sets of modal data already prepared for the Space Station. The modal data set consists of 34 modes selected from all directions and its title is "*Space Station with RCS and a Double-Gimbal CMG Array, 34 Modes*". The set consist of mode shapes at the 8 RCS jets, the location of the CMG cluster, the locations of the 3 external disturbances, the gyros, accelerometers, and at the disturbance point where we shall apply the bias torque. External disturbances are also applied at the crew habitat module for analyzing sensitivity to structural excitations between the habitat module and the boom accelerometers. In the following section we shall describe the modes selection process.

4.1 Generating a Set of Selected Modes

The data files for this analysis are in directory *"Examples\Large Space Station"* and the Matlab analysis is performed in the subdirectory *"(d) Mat Flex Lin (FVP)"*. The file that contains the original finite element structural modes is *"FlexSpaceStruct.Mod"*. It includes mode shapes and slopes for 55 modes, at 28 locations (also known as nodes). The modal data file contains frames of data for every mode frequency. Each frame consists of the mode frequency in (rad/sec), the modal damping coefficient (they are all set to $\zeta=0.005$), the generalized mass (all set to 1). It also includes the mode shapes and slopes at the 28 vehicle locations, that is, generalized translations along x, y, z, and generalized rotations about x, y, z. This file is formatted to be recognizable by the mode selection program which will create a much smaller set of modal data and will save it in the input data file *"SpaceStation.Inp"*. The vehicle data and the modal data set will be processed together by the vehicle modeling program to generate the flexible spacecraft state-space system. The locations which are important for flight control analysis are the 8 RCS jets, the CMG location, the locations of the external torques, and sensors. The map file *"FlexSpaceStruct.Nod"* is a table that lists the locations (nodes) of the modal data file. It contains a short description for each node, the node numbers (in this case 1 to 28), a node identification number (which is a number created by the FEM), and the location of each node in vehicle coordinates (this is only for reference and it is not used by the program).

To run the mode selection program you must first start the Flixan program and select the folder *"Examples\ Large Space Station"*. It is selected from *"Program Functions"*, *"Flight Vehicle/ Spacecraft Modeling Tools"*, and then *"Flex Mode Selection"*. Use the following filenames selection menu to select the modal data file, the nodes file, the flight vehicle input data file, and an output filename "Modsel.Msl" where at the completion of the mode selection the program saves the relative mode strength . The modal data input filenames must have an extension (Mod). The node filenames must have an extension (Nod), the vehicle input data filenames (Inp), and the mode selection output filenames extension is (Msl).
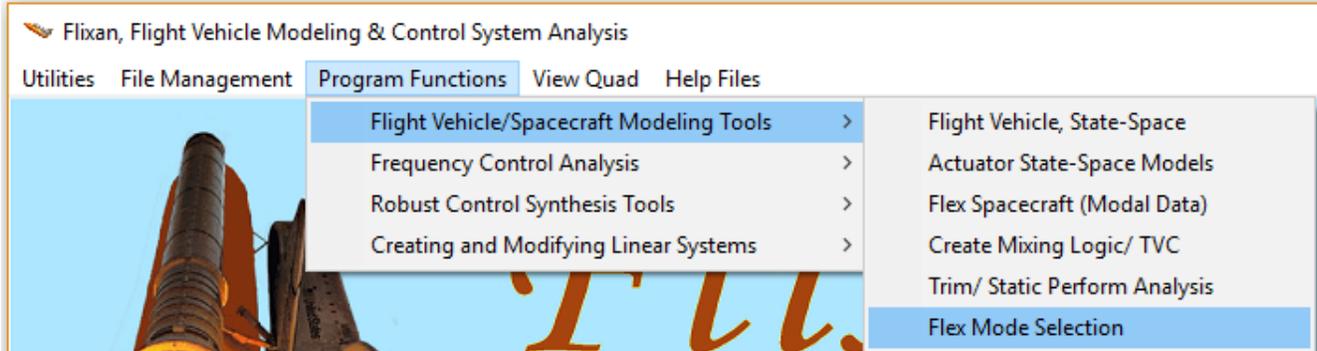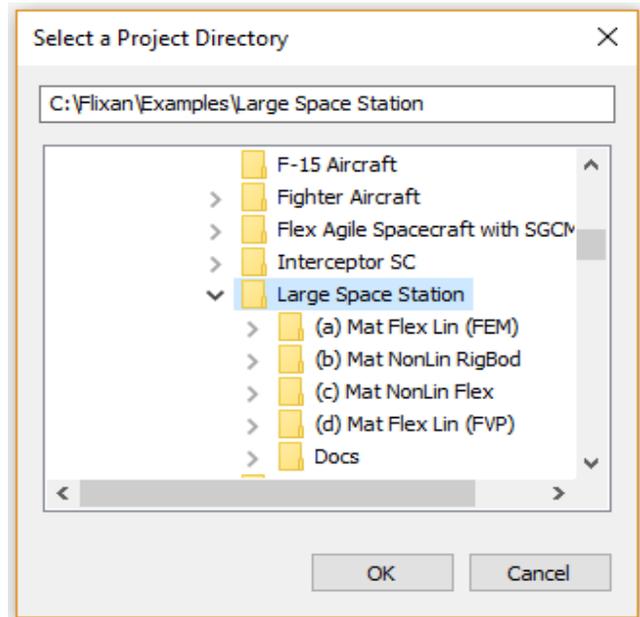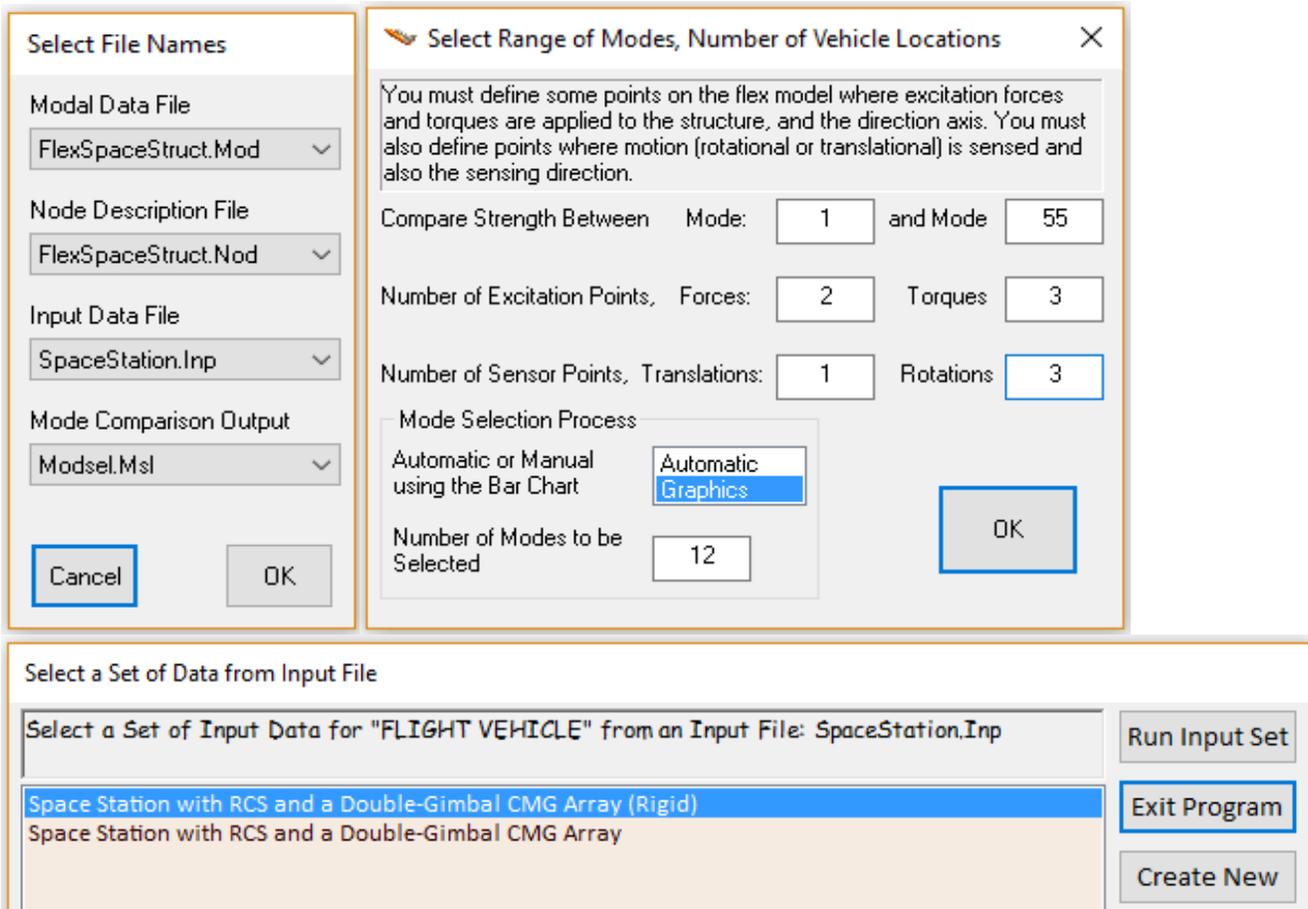
The next step is to locate the flight vehicle input dataset in file "*SpaceStation.Inp*". This data set is normally used to create the vehicle system, but it is also used by the mode selection program because the program needs information regarding the RCS jets, the CMG cluster, the external torques, the gyros and accelerometers which are defined in the vehicle dataset. The menu above shows the flight vehicle titles which are included in file "*SpaceStation.Inp*". Select the title: "*Space Station with RCS and a Double-Gimbal CMG Array*" and click on "*Run Input Set*". The next dialog is used to define the number of excitation points and the number of sensor points used for mode selection. This does not have to be equal to the actual number of vehicle effectors and sensors used in the model. It is only for mode selection purposes. We must also define the range of mode selection (1 to 55 modes in this case). We must remember, however, to exclude the first 6 rigid body modes in the mode selection, and include only flex modes, because the rigid-body dynamics is included in the vehicle model. We must enter the number of excitation forces (2 locations in this case), the number of torque excitations (3 locations in this case), and three rotational sensors for gyros. We will also select the graphic mode selection option where the user selects the modes from a bar-chart using the mouse. The number of modes to be selected does not apply in this case.

The next dialog is used to define unit conversions and axes transformation between the finite elements model and the vehicle model because structures and GN&C groups in general use different units and directions. Answer "Yes" that you want to modify the modal data. In this case the FEM directions are the same as in our vehicle model. Some of the default signs in the dialog are initially set to (-) because the x and z directions are usually opposite in the structural model, but in this example they should be changed to (+) because they are defined in the same directions. The units, however, of the modal data between the two models are not the same and they should be changed. The modal masses in the FEM

92

should be scaled up by a factor of 12 because Nastran uses (snails), while we use (slugs) for mass. The modal rotations (slopes) also need to be scaled up by a factor of 12 because in the FEM they are in (rad/inch) and they should be converted to (rad/feet). The modal displacements do not change because they go from (inches/inch) to (feet/foot). The scaling parameters in the dialog should be changed as shown below.
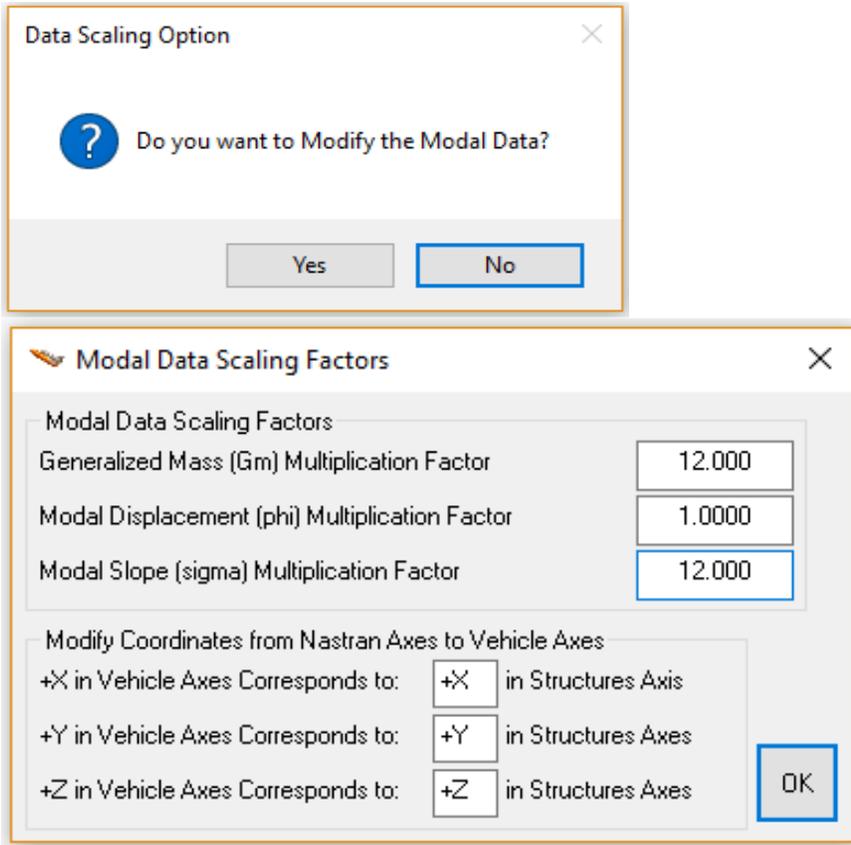
The next step is to specify nodes for the 2 force excitation points (which are two RCS jets) and the three torque excitation points (which are at the CMGs). These locations are only for mode selection purposes and they do not have to be the same as the actual RCS jet locations, the CMG cluster location, or the attitude control sensors. In this case the mode strength is calculated between the 2 upper RCS jets, the CMG torques, and three arbitrary rotational sensors.

The nodes map, which is the file "*FlexSpaceStruct.Nod*" is used by the program to assist the user in identifying the excitation and sensor nodes in the modal data file by using menus and dialogs. The upper left and the upper right RCS locations (nodes #26 and #25) were associated with the two force excitations. The force directions at the two nodes must also be selected as shown. Node #10 is selected three times to represent the torque excitations in roll, pitch, and yaw directions respectively. Nodes #9, #1, and #22 were arbitrarily selected for the three rotational measurements in roll, pitch, and yaw directions respectively. The selection of these nodes is only used for mode comparison and selection purposes.

Table of Vehicle Structure FEM Nodes

In mode selection, in order to calculate the relative mode strength of a number of modes in a specified direction you must define some node points in the Nastran model where the excitation forces or torques will be applied and also the forcing directions.

Similarly, you must also define the sensor points (translations or rotations) and the sensing directions.

OK

Cancel

Select a Location (Node) for Force Excitation : 1

Axis

Along-X
Along-Y
Along-Z

Description	No.	ID	X	Y	Z
Payload boom, (top-right)	1	1060			
Payload boom, (center)	2	3000			
Payload boom, (top-left)	3	2060			
Unknown	4	3100			
Right Solar Array Boom	5	6070	0.0	232.35	18.0
Right Solar Array (Connect)	6	505			
Right SA Boom, Outboard the Hinge	7	6045			
Right SA Boom, Inboard the Hinge Servo	8	6039			
Right Boom (Sensor Assembly)	9	6001			
Right Keel/Boom Intrsect, CMG Location	10	1000			
CG Center of Structure	11	7001			
Left Keel/Boom Intersection	12	7010			
Unknown	13	2000			
Left Boom	14	5001			
Left Boom, Inboard the Hinge Servo	15	5039			
Left SA Boom, Outboard the Hinge Servo	16	5045			
Left Solar Array (Connect)	17	410			
Left SA Boom, Extreme end	18	5070	0.0	-224.63	16.0
Right Habitat Module	19	9017			
Module, (Front Dock)	20	9018			
Center Habitat Module	21	9007			
Bottom Payload Boom (Right)	22	1160			
Bottom Payload Boom (Center)	23	4000			
Bottom Payload Boom (Left) Antenna	24	2160			
Top Right RCS Thruster Assembly	25	1050	0.0	73.7	-185.0
Top Left RCS Thrusters Assembly	26	2050	0.0	-65.58	-185.0
Bottom Right RCS Thruster Assembly	27	1150	0.0	73.7	144.0
Bottom Left RCS Thrusters Assembly	28	2150	0.0	-65.58	144.0

Direction

+ (positive)
- (negative)

Node Description,   Node Number,   Nastran Node ID Number,   Location Coordinates (X, Y, Z)

Table of Vehicle Structure FEM Nodes

In mode selection, in order to calculate the relative mode strength of a number of modes in a specified direction you must define some node points in the Nastran model where the excitation forces or torques will be applied and also the forcing directions.

Similarly, you must also define the sensor points (translations or rotations) and the sensing directions.

OK

Cancel

Select a Location (Node) for Force Excitation : 2

Axis

Along-X
Along-Y
Along-Z

Description	No.	ID	X	Y	Z
Payload boom, (top-right)	1	1060			
Payload boom, (center)	2	3000			
Payload boom, (top-left)	3	2060			
Unknown	4	3100			
Right Solar Array Boom	5	6070	0.0	232.35	18.0
Right Solar Array (Connect)	6	505			
Right SA Boom, Outboard the Hinge	7	6045			
Right SA Boom, Inboard the Hinge Servo	8	6039			
Right Boom (Sensor Assembly)	9	6001			
Right Keel/Boom Intrsect, CMG Location	10	1000			
CG Center of Structure	11	7001			
Left Keel/Boom Intersection	12	7010			
Unknown	13	2000			
Left Boom	14	5001			
Left Boom, Inboard the Hinge Servo	15	5039			
Left SA Boom, Outboard the Hinge Servo	16	5045			
Left Solar Array (Connect)	17	410			
Left SA Boom, Extreme end	18	5070	0.0	-224.63	16.0
Right Habitat Module	19	9017			
Module, (Front Dock)	20	9018			
Center Habitat Module	21	9007			
Bottom Payload Boom (Right)	22	1160			
Bottom Payload Boom (Center)	23	4000			
Bottom Payload Boom (Left) Antenna	24	2160			
Top Right RCS Thruster Assembly	25	1050	0.0	73.7	-185.0
Top Left RCS Thrusters Assembly	26	2050	0.0	-65.58	-185.0
Bottom Right RCS Thruster Assembly	27	1150	0.0	73.7	144.0
Bottom Left RCS Thrusters Assembly	28	2150	0.0	-65.58	144.0

Direction

+ (positive)
- (negative)

Node Description,   Node Number,   Nastran Node ID Number,   Location Coordinates (X, Y, Z)

Table of Vehicle Structure FEM Nodes

In mode selection, in order to calculate the relative mode strength of a number of modes in a specified direction you must define some node points in the Nastran model where the excitation forces or torques will be applied and also the forcing directions.

Similarly, you must also define the sensor points (translations or rotations) and the sensing directions.

OK

Cancel

Select a Location (Node) for Torque Excitation: 1

Node Description	Node Number	Nastran Node ID	X	Y	Z
Payload boom, (top-right)	1	1060			
Payload boom, (center)	2	3000			
Payload boom, (top-left)	3	2060			
Unknown	4	3100			
Right Solar Array Boom	5	6070	0.0	232.35	18.0
Right Solar Array (Connect)	6	505			
Right SA Boom, Outboard the Hinge	7	6045			
Right SA Boom, Inboard the Hinge Servo	8	6039			
Right Boom (Sensor Assembly)	9	6001			
Right Keel/Boom Intrsect, CMG Location	10	1000			
CG Center of Structure	11	7001			
Left Keel/Boom Intersection	12	7010			
Unknown	13	2000			
Left Boom	14	5001			
Left Boom, Inboard the Hinge Servo	15	5039			
Left SA Boom, Outboard the Hinge Servo	16	5045			
Left Solar Array (Connect)	17	410			
Left SA Boom, Extreme end	18	5070	0.0	-224.63	16.0
Right Habitat Module	19	9017			
Module, (Front Dock)	20	9018			
Center Habitat Module	21	9007			
Bottom Payload Boom (Right)	22	1160			
Bottom Payload Boom (Center)	23	4000			
Bottom Payload Boom (Left) Antenna	24	2160			
Top Right RCS Thruster Assembly	25	1050	0.0	73.7	-185.0
Top Left RCS Thrusters Assembly	26	2050	0.0	-65.58	-185.0
Bottom Right RCS Thruster Assembly	27	1150	0.0	73.7	144.0
Bottom Left RCS Thrusters Assembly	28	2150	0.0	-65.58	144.0

Axis

Roll
Pitch
Yaw

Direction

+ (positive)
- (negative)

Node Description,   Node Number,   Nastran Node ID Number,   Location Coordinates (X, Y, Z)

95

Table of Vehicle Structure FEM Nodes

In mode selection, in order to calculate the relative mode strength of a number of modes in a specified direction you must define some node points in the Nastran model where the excitation forces or torques will be applied and also the forcing directions.

Similarly, you must also define the sensor points (translations or rotations) and the sensing directions.

OK

Cancel

Select a Location (Node) for Rotational Sensor: 1

Node Description	Node Number	Nastran Node ID	X	Y	Z
Payload boom, (top-right)	1	1060			
Payload boom, (center)	2	3000			
Payload boom, (top-left)	3	2060			
Unknown	4	3100			
Right Solar Array Boom	5	6070			
Right Solar Array (Connect)	6	505			
Right SA Boom, Outboard the Hinge	7	6045			
Right SA Boom, Inboard the Hinge Servo	8	6039			
Right Boom (Sensor Assembly)	9	6001			
Right Keel/Boom Intrsect, CMG Location	10	1000			
CG Center of Structure	11	7001			
Left Keel/Boom Intersection	12	7010			
Unknown	13	2000			
Left Boom	14	5001			
Left Boom, Inboard the Hinge Servo	15	5039			
Left SA Boom, Outboard the Hinge Servo	16	5045			
Left Solar Array (Connect)	17	410			
Left SA Boom, Extreme end	18	5070			
Right Habitat Module	19	9017			
Module, (Front Dock)	20	9018			
Center Habitat Module	21	9007			
Bottom Payload Boom (Right)	22	1160			
Bottom Payload Boom (Center)	23	4000			
Bottom Payload Boom (Left) Antenna	24	2160			
Top Right RCS Thruster Assembly	25	1050	0.0	73.7	-185.0
Top Left RCS Thrusters Assembly	26	2050	0.0	-65.58	-185.0
Bottom Right RCS Thruster Assembly	27	1150	0.0	73.7	144.0
Bottom Left RCS Thrusters Assembly	28	2150	0.0	-65.58	144.0

Axis
Roll
Pitch
Yaw

Direction
+ (positive)
- (negative)

Node Description,   Node Number,   Nastran Node ID Number,   Location Coordinates (X, Y, Z)

Table of Vehicle Structure FEM Nodes

In mode selection, in order to calculate the relative mode strength of a number of modes in a specified direction you must define some node points in the Nastran model where the excitation forces or torques will be applied and also the forcing directions.

Similarly, you must also define the sensor points (translations or rotations) and the sensing directions.

OK

Cancel

Select a Location (Node) for Rotational Sensor: 3

Node Description	Node Number	Nastran Node ID	X	Y	Z
Payload boom, (top-right)	1	1060			
Payload boom, (center)	2	3000			
Payload boom, (top-left)	3	2060			
Unknown	4	3100			
Right Solar Array Boom	5	6070			
Right Solar Array (Connect)	6	505			
Right SA Boom, Outboard the Hinge	7	6045			
Right SA Boom, Inboard the Hinge Servo	8	6039			
Right Boom (Sensor Assembly)	9	6001			
Right Keel/Boom Intrsect, CMG Location	10	1000			
CG Center of Structure	11	7001			
Left Keel/Boom Intersection	12	7010			
Unknown	13	2000			
Left Boom	14	5001			
Left Boom, Inboard the Hinge Servo	15	5039			
Left SA Boom, Outboard the Hinge Servo	16	5045			
Left Solar Array (Connect)	17	410			
Left SA Boom, Extreme end	18	5070			
Right Habitat Module	19	9017			
Module, (Front Dock)	20	9018			
Center Habitat Module	21	9007			
Bottom Payload Boom (Right)	22	1160			
Bottom Payload Boom (Center)	23	4000			
Bottom Payload Boom (Left) Antenna	24	2160			
Top Right RCS Thruster Assembly	25	1050	0.0	73.7	-185.0
Top Left RCS Thrusters Assembly	26	2050	0.0	-65.58	-185.0
Bottom Right RCS Thruster Assembly	27	1150	0.0	73.7	144.0
Bottom Left RCS Thrusters Assembly	28	2150	0.0	-65.58	144.0

Axis
Roll
Pitch
Yaw

Direction
+ (positive)
- (negative)

Node Description,   Node Number,   Nastran Node ID Number,   Location Coordinates (X, Y, Z)

At this point the excitation and sensor points and directions for the mode selection process have been defined. The modal strength for each mode is determined by the values of the mode shapes at the nodes where the forces and torques are applied, the force direction, and also by the values of the mode shapes at the 3 rotational sensors in the directions measured. High mode shape values at the excitation and sensor points imply strong contributions from those modes. The mode selection program calculates the mode strength for each mode and saves it in file "Modsel.Msl" from where the user can select the dominant modes graphically. The mode selection process, however, is not yet complete because the program needs additional info before allowing the user to select which modes to retain from the big modal data file. The selected modal data set will contain only the selected few dominant modes and modal shapes at a few important locations which are defined in the Space Station input dataset, such as: the RCS jets, the CMG location, the external disturbances, the attitude control sensors, and the disturbance point. The program will display similar menus (different color) that show the nodes map from where the user may select structural nodes for the required spacecraft locations.

To begin, the user must identify 8 nodes (#25, #25, #26, #26, #27, #27, #28, and #28) that correspond to the 8 RCS jet locations. The upper right (in the X and -Y directions), upper left (X and Y directions), bottom right (X and -Y directions), and bottom left jets (X and Y directions) respectively. The user must also select a location for the CMG cluster. The right boom and keel intersection point, node #10 (1000), was selected for the CMGs. Three locations must also be selected for the three external torques to be used for crew disturbance excitations. The "Center Habitat Module", node #21 (9007) is selected three times for roll, pitch, and yaw disturbances respectively.

Table of Vehicle Structure FEM Nodes

You must now identify some points on the finite element model that correspont to the important locations on the vehicle (as specified in the vehicle data) where the forces are being applied and the motion is being sensed. Such as TVC gimbals, gyros, etc.

Select a Location (Node) for Dougle Gimbal CMG: 1   [OK]

Node Description	Node Number	Nastran ID	X	Y	Z
Payload boom, (top-right)	1	1060			
Payload boom, (center)	2	3000			
Payload boom, (top-left)	3	2060			
Unknown	4	3100			
Right Solar Array Boom	5	6070			
Right Solar Array (Connect)	6	505			
Right SA Boom, Outboard the Hinge	7	6045			
Right SA Boom, Inboard the Hinge Servo	8	6039			
Right Boom (Sensor Assembly)	9	6001			
Right Keel/Boom Intrsect, CMG Location	10	1000			
CG Center of Structure	11	7001			
Left Keel/Boom Intersection	12	7010			
Unknown	13	2000			
Left Boom	14	5001			
Left Boom, Inboard the Hinge Servo	15	5039			
Left SA Boom, Outboard the Hinge Servo	16	5045			
Left Solar Array (Connect)	17	410			
Left SA Boom, Extreme end	18	5070			
Right Habitat Module	19	9017			
Module, (Front Dock)	20	9018			
Center Habitat Module	21	9007			
Bottom Payload Boom (Right)	22	1160			
Bottom Payload Boom (Center)	23	4000			
Bottom Payload Boom (Left) Antenna	24	2160			
Top Right RCS Thruster Assembly	25	1050	0.0	73.7	-185.0
Top Left RCS Thrusters Assembly	26	2050	0.0	-65.58	-185.0
Bottom Right RCS Thruster Assembly	27	1150	0.0	73.7	144.0
Bottom Left RCS Thrusters Assembly	28	2150	0.0	-65.58	144.0

Node Description, Node Number, Nastran ID, Location (X, Y, Z)

Table of Vehicle Structure FEM Nodes ✕

You must now identify some points on the finite element model that correspont to the important locations on the vehicle (as specified in the vehicle data) where the forces are being applied and the motion is being sensed. Such as TVC gimbals, gyros, etc.

Select a Location (Node) for Thruster Engine : 1   [OK]

Node Description	Node Number	Nastran ID	Location (X, Y, Z)		
Payload boom, (top-right)	1	1060			
Payload boom, (center)	2	3000			
Payload boom, (top-left)	3	2060			
Unknown	4	3100			
Right Solar Array Boom	5	6070	0.0	232.35	18.0
Right Solar Array (Connect)	6	505			
Right SA Boom, Outboard the Hinge	7	6045			
Right SA Boom, Inboard the Hinge Servo	8	6039			
Right Boom (Sensor Assembly)	9	6001			
Right Keel/Boom Intrsect, CMG Location	10	1000			
CG Center of Structure	11	7001			
Left Keel/Boom Intersection	12	7010			
Unknown	13	2000			
Left Boom	14	5001			
Left Boom, Inboard the Hinge Servo	15	5039			
Left SA Boom, Outboard the Hinge Servo	16	5045			
Left Solar Array (Connect)	17	410			
Left SA Boom, Extreme end	18	5070	0.0	-224.63	16.0
Right Habitat Module	19	9017			
Module, (Front Dock)	20	9018			
Center Habitat Module	21	9007			
Bottom Payload Boom (Right)	22	1160			
Bottom Payload Boom (Center)	23	4000			
Bottom Payload Boom (Left) Antenna	24	2160			
Top Right RCS Thruster Assembly	25	1050	0.0	73.7	-185.0
Top Left RCS Thrusters Assembly	26	2050	0.0	-65.58	-185.0
Bottom Right RCS Thruster Assembly	27	1150	0.0	73.7	144.0
Bottom Left RCS Thrusters Assembly	28	2150	0.0	-65.58	144.0

Node Description,   Node Number,   Nastran ID,   Location (X, Y, Z)

Table of Vehicle Structure FEM Nodes ✕

You must now identify some points on the finite element model that correspont to the important locations on the vehicle (as specified in the vehicle data) where the forces are being applied and the motion is being sensed. Such as TVC gimbals, gyros, etc.

Select a Location (Node) for Thruster Engine : 4   [OK]

Node Description	Node Number	Nastran ID	Location (X, Y, Z)		
Payload boom, (top-right)	1	1060			
Payload boom, (center)	2	3000			
Payload boom, (top-left)	3	2060			
Unknown	4	3100			
Right Solar Array Boom	5	6070	0.0	232.35	18.0
Right Solar Array (Connect)	6	505			
Right SA Boom, Outboard the Hinge	7	6045			
Right SA Boom, Inboard the Hinge Servo	8	6039			
Right Boom (Sensor Assembly)	9	6001			
Right Keel/Boom Intrsect, CMG Location	10	1000			
CG Center of Structure	11	7001			
Left Keel/Boom Intersection	12	7010			
Unknown	13	2000			
Left Boom	14	5001			
Left Boom, Inboard the Hinge Servo	15	5039			
Left SA Boom, Outboard the Hinge Servo	16	5045			
Left Solar Array (Connect)	17	410			
Left SA Boom, Extreme end	18	5070	0.0	-224.63	16.0
Right Habitat Module	19	9017			
Module, (Front Dock)	20	9018			
Center Habitat Module	21	9007			
Bottom Payload Boom (Right)	22	1160			
Bottom Payload Boom (Center)	23	4000			
Bottom Payload Boom (Left) Antenna	24	2160			
Top Right RCS Thruster Assembly	25	1050	0.0	73.7	-185.0
Top Left RCS Thrusters Assembly	26	2050	0.0	-65.58	-185.0
Bottom Right RCS Thruster Assembly	27	1150	0.0	73.7	144.0
Bottom Left RCS Thrusters Assembly	28	2150	0.0	-65.58	144.0

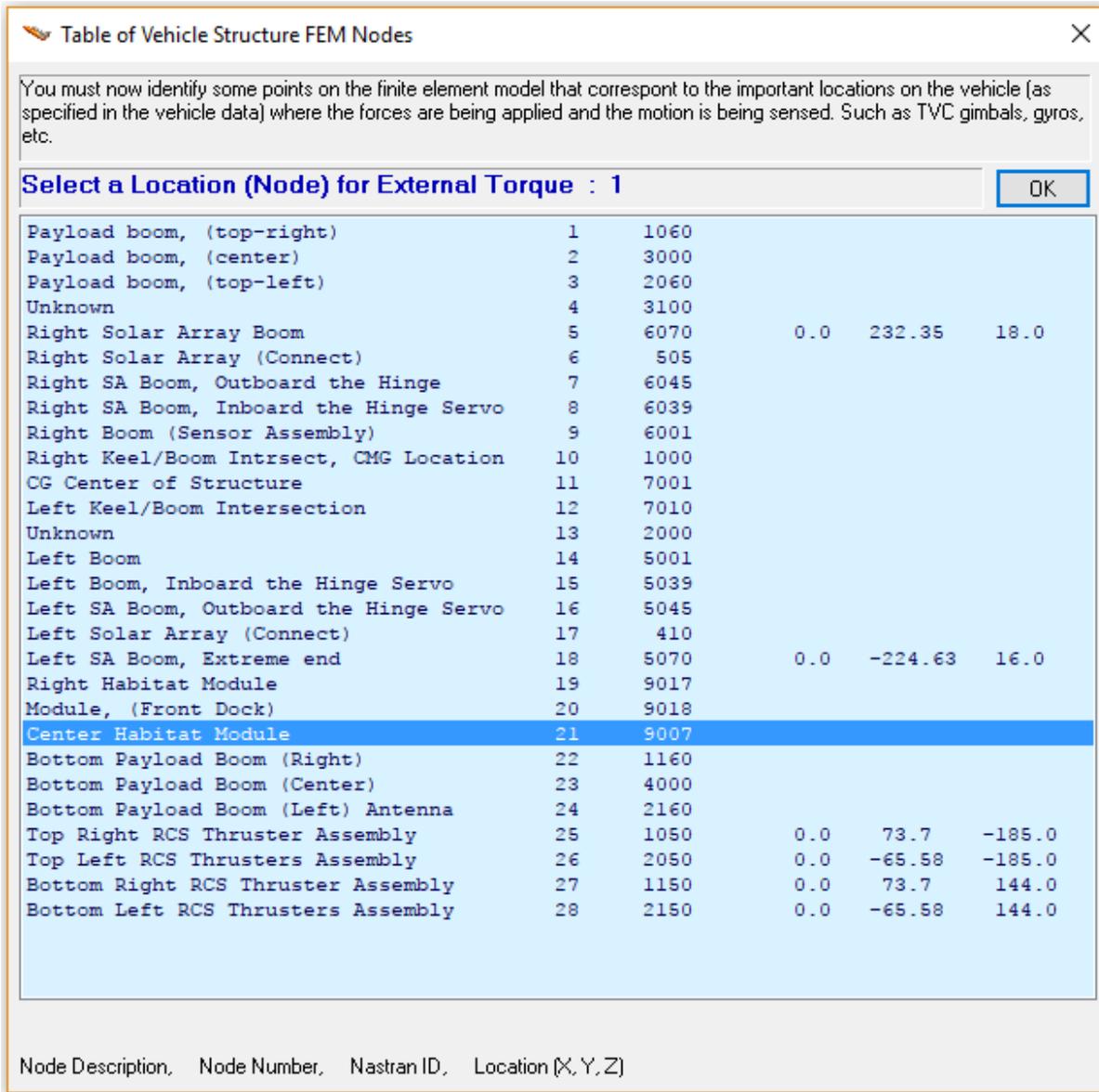Node Description,   Node Number,   Nastran ID,   Location (X, Y, Z)

Table of Vehicle Structure FEM Nodes ✕

You must now identify some points on the finite element model that correspont to the important locations on the vehicle (as specified in the vehicle data) where the forces are being applied and the motion is being sensed. Such as TVC gimbals, gyros, etc.

Select a Location (Node) for External Torque : 1   [OK]

Node Description	Node Number	Nastran ID	X	Y	Z
Payload boom, (top-right)	1	1060			
Payload boom, (center)	2	3000			
Payload boom, (top-left)	3	2060			
Unknown	4	3100			
Right Solar Array Boom	5	6070	0.0	232.35	18.0
Right Solar Array (Connect)	6	505			
Right SA Boom, Outboard the Hinge	7	6045			
Right SA Boom, Inboard the Hinge Servo	8	6039			
Right Boom (Sensor Assembly)	9	6001			
Right Keel/Boom Intrsect, CMG Location	10	1000			
CG Center of Structure	11	7001			
Left Keel/Boom Intersection	12	7010			
Unknown	13	2000			
Left Boom	14	5001			
Left Boom, Inboard the Hinge Servo	15	5039			
Left SA Boom, Outboard the Hinge Servo	16	5045			
Left Solar Array (Connect)	17	410			
Left SA Boom, Extreme end	18	5070	0.0	-224.63	16.0
Right Habitat Module	19	9017			
Module, (Front Dock)	20	9018			
Center Habitat Module	21	9007			
Bottom Payload Boom (Right)	22	1160			
Bottom Payload Boom (Center)	23	4000			
Bottom Payload Boom (Left) Antenna	24	2160			
Top Right RCS Thruster Assembly	25	1050	0.0	73.7	-185.0
Top Left RCS Thrusters Assembly	26	2050	0.0	-65.58	-185.0
Bottom Right RCS Thruster Assembly	27	1150	0.0	73.7	144.0
Bottom Left RCS Thrusters Assembly	28	2150	0.0	-65.58	144.0

Node Description,   Node Number,   Nastran ID,   Location (X, Y, Z)

The right boom sensor assembly, node #9 (6001), is selected 6 times for the 6 rotational measurement. Three times for the 3 rate measurements in roll, pitch, and yaw directions, and three times for the 3 attitude measurements in roll, pitch, and yaw directions.

We must also select locations for the four accelerometers to be used in the sensitivity analysis. The "Right Solar Array Boom", node #5 (6070), is selected twice for the x and z right boom accelerometer measurements, and the "Left Solar Array Boom, Extreme end", node #18 (5070), is selected twice for the x and z left boom accelerometer measurements. We finally select node #20 (9018) for the disturbance torque location, which is not used for flex excitation in this case because the disturbance point is used for applying the constant bias torque.

Table of Vehicle Structure FEM Nodes   ✕

You must now identify some points on the finite element model that correspont to the important locations on the vehicle (as specified in the vehicle data) where the forces are being applied and the motion is being sensed. Such as TVC gimbals, gyros, etc.

Select a Location (Node) for Gyro/Rate Sensor : 1   [OK]

Node Description	Node Number	Nastran ID	X	Y	Z
Payload boom, (top-right)	1	1060			
Payload boom, (center)	2	3000			
Payload boom, (top-left)	3	2060			
Unknown	4	3100			
Right Solar Array Boom	5	6070	0.0	232.35	18.0
Right Solar Array (Connect)	6	505			
Right SA Boom, Outboard the Hinge	7	6045			
Right SA Boom, Inboard the Hinge Servo	8	6039			
Right Boom (Sensor Assembly)	9	6001			
Right Keel/Boom Intrsect, CMG Location	10	1000			
CG Center of Structure	11	7001			
Left Keel/Boom Intersection	12	7010			
Unknown	13	2000			
Left Boom	14	5001			
Left Boom, Inboard the Hinge Servo	15	5039			
Left SA Boom, Outboard the Hinge Servo	16	5045			
Left Solar Array (Connect)	17	410			
Left SA Boom, Extreme end	18	5070	0.0	-224.63	16.0
Right Habitat Module	19	9017			
Module, (Front Dock)	20	9018			
Center Habitat Module	21	9007			
Bottom Payload Boom (Right)	22	1160			
Bottom Payload Boom (Center)	23	4000			
Bottom Payload Boom (Left) Antenna	24	2160			
Top Right RCS Thruster Assembly	25	1050	0.0	73.7	-185.0
Top Left RCS Thrusters Assembly	26	2050	0.0	-65.58	-185.0
Bottom Right RCS Thruster Assembly	27	1150	0.0	73.7	144.0
Bottom Left RCS Thrusters Assembly	28	2150	0.0	-65.58	144.0

Node Description,   Node Number,   Nastran ID,   Location (X, Y, Z)

Table of Vehicle Structure FEM Nodes   ✕

You must now identify some points on the finite element model that correspont to the important locations on the vehicle (as specified in the vehicle data) where the forces are being applied and the motion is being sensed. Such as TVC gimbals, gyros, etc.

Select a Location (Node) for Accelerometer   : 1   [OK]

Node Description	Node Number	Nastran ID	X	Y	Z
Payload boom, (top-right)	1	1060			
Payload boom, (center)	2	3000			
Payload boom, (top-left)	3	2060			
Unknown	4	3100			
Right Solar Array Boom	5	6070	0.0	232.35	18.0
Right Solar Array (Connect)	6	505			
Right SA Boom, Outboard the Hinge	7	6045			
Right SA Boom, Inboard the Hinge Servo	8	6039			
Right Boom (Sensor Assembly)	9	6001			
Right Keel/Boom Intrsect, CMG Location	10	1000			
CG Center of Structure	11	7001			
Left Keel/Boom Intersection	12	7010			
Unknown	13	2000			
Left Boom	14	5001			
Left Boom, Inboard the Hinge Servo	15	5039			
Left SA Boom, Outboard the Hinge Servo	16	5045			
Left Solar Array (Connect)	17	410			
Left SA Boom, Extreme end	18	5070	0.0	-224.63	16.0
Right Habitat Module	19	9017			
Module, (Front Dock)	20	9018			
Center Habitat Module	21	9007			
Bottom Payload Boom (Right)	22	1160			
Bottom Payload Boom (Center)	23	4000			
Bottom Payload Boom (Left) Antenna	24	2160			
Top Right RCS Thruster Assembly	25	1050	0.0	73.7	-185.0
Top Left RCS Thrusters Assembly	26	2050	0.0	-65.58	-185.0
Bottom Right RCS Thruster Assembly	27	1150	0.0	73.7	144.0
Bottom Left RCS Thrusters Assembly	28	2150	0.0	-65.58	144.0

Node Description,   Node Number,   Nastran ID,   Location (X, Y, Z)

Table of Vehicle Structure FEM Nodes   ✕

You must now identify some points on the finite element model that correspont to the important locations on the vehicle (as specified in the vehicle data) where the forces are being applied and the motion is being sensed. Such as TVC gimbals, gyros, etc.

Select a Location (Node) for Accelerometer   : 3   OK

Node Description	Node Number	Nastran ID	X	Y	Z
Payload boom, (top-right)	1	1060			
Payload boom, (center)	2	3000			
Payload boom, (top-left)	3	2060			
Unknown	4	3100			
Right Solar Array Boom	5	6070	0.0	232.35	18.0
Right Solar Array (Connect)	6	505			
Right SA Boom, Outboard the Hinge	7	6045			
Right SA Boom, Inboard the Hinge Servo	8	6039			
Right Boom (Sensor Assembly)	9	6001			
Right Keel/Boom Intrsect, CMG Location	10	1000			
CG Center of Structure	11	7001			
Left Keel/Boom Intersection	12	7010			
Unknown	13	2000			
Left Boom	14	5001			
Left Boom, Inboard the Hinge Servo	15	5039			
Left SA Boom, Outboard the Hinge Servo	16	5045			
Left Solar Array (Connect)	17	410			
Left SA Boom, Extreme end	18	5070	0.0	-224.63	16.0
Right Habitat Module	19	9017			
Module, (Front Dock)	20	9018			
Center Habitat Module	21	9007			
Bottom Payload Boom (Right)	22	1160			
Bottom Payload Boom (Center)	23	4000			
Bottom Payload Boom (Left) Antenna	24	2160			
Top Right RCS Thruster Assembly	25	1050	0.0	73.7	-185.0
Top Left RCS Thrusters Assembly	26	2050	0.0	-65.58	-185.0
Bottom Right RCS Thruster Assembly	27	1150	0.0	73.7	144.0
Bottom Left RCS Thrusters Assembly	28	2150	0.0	-65.58	144.0

Node Description,   Node Number,   Nastran ID,   Location (X, Y, Z)

Table of Vehicle Structure FEM Nodes   ✕

You must now identify some points on the finite element model that correspont to the important locations on the vehicle (as specified in the vehicle data) where the forces are being applied and the motion is being sensed. Such as TVC gimbals, gyros, etc.

Select a Location (Node) for Double Gimbal CMG: 1   OK

Node Description	Node Number	Nastran ID	X	Y	Z
Payload boom, (top-right)	1	1060			
Payload boom, (center)	2	3000			
Payload boom, (top-left)	3	2060			
Unknown	4	3100			
Right Solar Array Boom	5	6070	0.0	232.35	18.0
Right Solar Array (Connect)	6	505			
Right SA Boom, Outboard the Hinge	7	6045			
Right SA Boom, Inboard the Hinge Servo	8	6039			
Right Boom (Sensor Assembly)	9	6001			
Right Keel/Boom Intrsect, CMG Location	10	1000			
CG Center of Structure	11	7001			
Left Keel/Boom Intersection	12	7010			
Unknown	13	2000			
Left Boom	14	5001			
Left Boom, Inboard the Hinge Servo	15	5039			
Left SA Boom, Outboard the Hinge Servo	16	5045			
Left Solar Array (Connect)	17	410			
Left SA Boom, Extreme end	18	5070	0.0	-224.63	16.0
Right Habitat Module	19	9017			
Module, (Front Dock)	20	9018			
Center Habitat Module	21	9007			
Bottom Payload Boom (Right)	22	1160			
Bottom Payload Boom (Center)	23	4000			
Bottom Payload Boom (Left) Antenna	24	2160			
Top Right RCS Thruster Assembly	25	1050	0.0	73.7	-185.0
Top Left RCS Thrusters Assembly	26	2050	0.0	-65.58	-185.0
Bottom Right RCS Thruster Assembly	27	1150	0.0	73.7	144.0
Bottom Left RCS Thrusters Assembly	28	2150	0.0	-65.58	144.0

Node Description,   Node Number,   Nastran ID,   Location (X, Y, Z)

At this point the mode selection program performs a mode strength comparison between the excitation points and directions to the sensor points and directions, and it saves the relative mode strength for each mode in file "Modsel.Dat". It displays also the following bar chart that plots the relative mode strength for each mode versus the mode number. The height of each bar is logarithmically proportional to the relative mode strength. The strong modes are tall and the weak modes are short. The modal strength is not an absolute number but it is adjusted relative to the minimum and maximum modal strengths. All modes are initially red before selection. The user selects some of the strongest modes from the chart by pointing the mouse cursor at the bar and clicking the mouse to select it. The modes change color from red to green when they are selected. Notice that the first six modes, although strong, were not selected because they are rigid-body modes and the rigid-body dynamics are already included in the vehicle model. We select 34 flex modes and press the enter button to complete the mode selection.
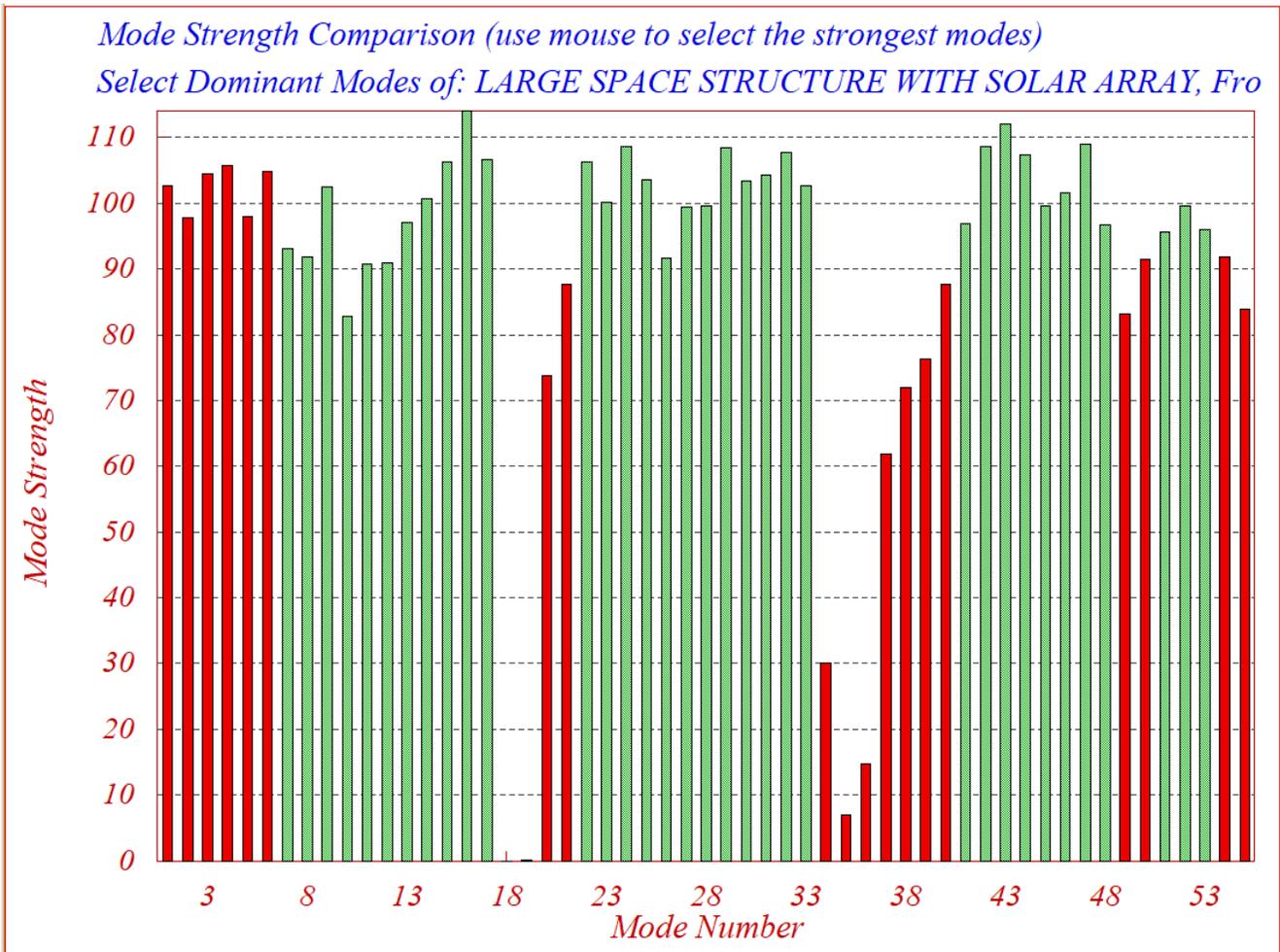
The selected set of modes now contains the frequencies and mode shapes of the strongest modes at important vehicle locations and it is saved in file "*SpaceStation.Inp*". You may also enter a short label that briefly describes the selected set of modal data that will be included in the title, for example:

The final step before finishing the mode selection process is to complete the dialog below where the user enters some notes regarding the mode selection process to be used for future reference. Describing, for example, what type of modes were selected, conditions of mode selection, excitation and measurement points, axes directions, etc. This information will be included as comments below the title in the selected modes set that will be saved in the input data file "*SpaceStation.Inp*". The title of the selected modes set is "*Space Station with RCS and a Double-Gimbal CMG Array, 34 Modes*". The title must also be included at the bottom of the Space Station input dataset (below the number of flex modes) in order for the flight vehicle modeling program to associate the modes with the spacecraft data.

Enter Notes

Enter some notes describing the mode selection criteria, excitation points, directions, etc. To be used for future reference | OK

34 Flex Modes were selected from all directions. Same Modes as in Previous Examples. The 6 Rigid Modes were not included
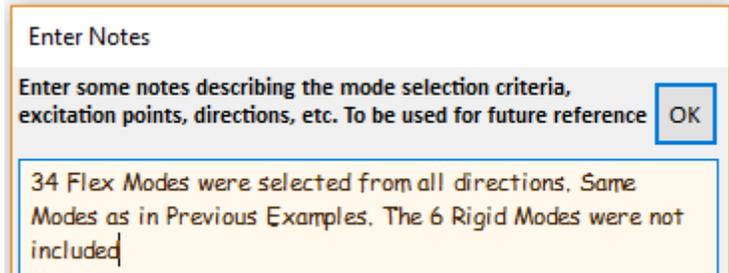
```
SELECTED MODAL DATA AND LOCATIONS FOR: From All 3 Axes
Space Station with RCS and a Double-Gimbal CMG Array, 34 Modes from All 3 Axes
! 34 modes were selected from all directions, the same modes as in Previous Examples.
! The first 6 Rigid-Body Modes were not included

MODE#  1/  7, Frequency (rad/sec), Damping (zeta), Generalized Mass=    1.0097      0.50000E-02    12.000
DEFINITION OF LOCATIONS (NODES)          phi along X   phi along Y   phi along Z   sigm about X  sigm about Y  sigm about Z

                          Node ID#   Modal Data at the  8 Engines, (x,y,z)...
Top Right RCS Thruster Assembl  1050    0.59628D-02  -0.16325D-04   0.96510D-04   0.42971D-06  -0.33256D-04   0.10894D-04
Top Right RCS Thruster Assembl  1050    0.59628D-02  -0.16325D-04   0.96510D-04   0.42971D-06  -0.33256D-04   0.10894D-04
Top Left RCS Thrusters Assembl  2050    0.54261D-02  -0.62395D-05   0.74506D-04  -0.10905D-06  -0.31918D-04  -0.18344D-04
Top Left RCS Thrusters Assembl  2050    0.54261D-02  -0.62395D-05   0.74506D-04  -0.10905D-06  -0.31918D-04  -0.18344D-04
Bottom Right RCS Thruster Asse  1150   -0.35170D-02  -0.59190D-04   0.96566D-04   0.13160D-06  -0.31650D-04   0.15942D-04
Bottom Right RCS Thruster Asse  1150   -0.35170D-02  -0.59190D-04   0.96566D-04   0.13160D-06  -0.31650D-04   0.15942D-04
Bottom Left RCS Thrusters Asse  2150   -0.32580D-02  -0.58408D-04   0.74465D-04   0.21757D-06  -0.30306D-04  -0.12670D-04
Bottom Left RCS Thrusters Asse  2150   -0.32580D-02  -0.58408D-04   0.74465D-04   0.21757D-06  -0.30306D-04  -0.12670D-04


                          Node ID#   Modal Data at the Double Gimbal GMGs Cluster...
Right Keel/Boom Intrsect, CMG   1000    0.11384D-02  -0.58736D-04   0.96470D-04  -0.23552D-06  -0.30827D-04   0.65746D-04


                          Node ID#   Modal Data at the  3 External Torque Points...
Center Habitat Module           9007    0.29012D-02  -0.26348D-04   0.31307D-04   0.30160D-06  -0.43846D-05  -0.97127D-07
Center Habitat Module           9007    0.29012D-02  -0.26348D-04   0.31307D-04   0.30160D-06  -0.43846D-05  -0.97127D-07
Center Habitat Module           9007    0.29012D-02  -0.26348D-04   0.31307D-04   0.30160D-06  -0.43846D-05  -0.97127D-07

                          Node ID#   Modal Data at the  6 Gyros ...
Right Boom (Sensor Assembly)    6001   -0.14682D-03  -0.65626D-04   0.90529D-04  -0.37958D-06  -0.33769D-04   0.86246D-04
Right Boom (Sensor Assembly)    6001   -0.14682D-03  -0.65626D-04   0.90529D-04  -0.37958D-06  -0.33769D-04   0.86246D-04
Right Boom (Sensor Assembly)    6001   -0.14682D-03  -0.65626D-04   0.90529D-04  -0.37958D-06  -0.33769D-04   0.86246D-04
Right Boom (Sensor Assembly)    6001   -0.14682D-03  -0.65626D-04   0.90529D-04  -0.37958D-06  -0.33769D-04   0.86246D-04
Right Boom (Sensor Assembly)    6001   -0.14682D-03  -0.65626D-04   0.90529D-04  -0.37958D-06  -0.33769D-04   0.86246D-04
Right Boom (Sensor Assembly)    6001   -0.14682D-03  -0.65626D-04   0.90529D-04  -0.37958D-06  -0.33769D-04   0.86246D-04

                          Node ID#   Modal Data at the  4 Accelerometers, along (x,y,z)...
Right Solar Array Boom          6070   -0.25921D-01  -0.73995D-04  -0.57584D-04
Right Solar Array Boom          6070   -0.25921D-01  -0.73995D-04  -0.57584D-04
Left SA Boom, Extreme end       5070   -0.26691D-01   0.68332D-05  -0.15103D-03
Left SA Boom, Extreme end       5070   -0.26691D-01   0.68332D-05  -0.15103D-03

                          Node ID#   Modal Data at the Disturbance Point
Module, (Front Dock)            9018    0.28820D-02  -0.73445D-04   0.35876D-03   0.49346D-06  -0.54146D-05  -0.28216D-06
```
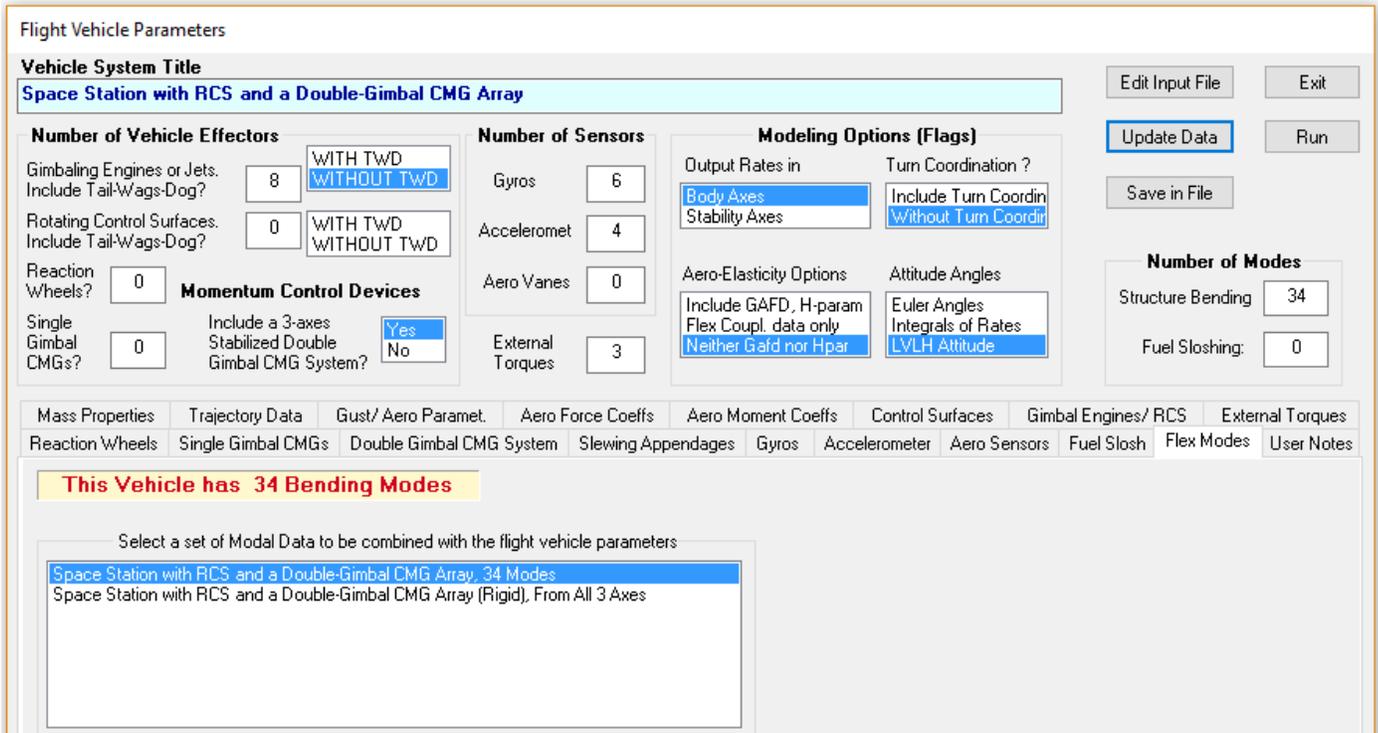
4.2 Creating the Space Station Model

We will now run the flight vehicle modeling program to process interactively the input data from file "*SpaceStation.Inp*" and to create the state-space system of the flexible Space Station. Start the Flixan program and choose the project directory: "*\Flixan\ Examples\ Large Space Station*". From the main menu choose "*Program Functions*", "*Flight Vehicle/ Spacecraft Model Tools*", and "*Flight Vehicle State-Space*". From the filenames selection menu choose the input vehicle data file "*SpaceStation.Inp*", the output systems file "*SpaceStation.Qdr*", and click on "*Process Files*".
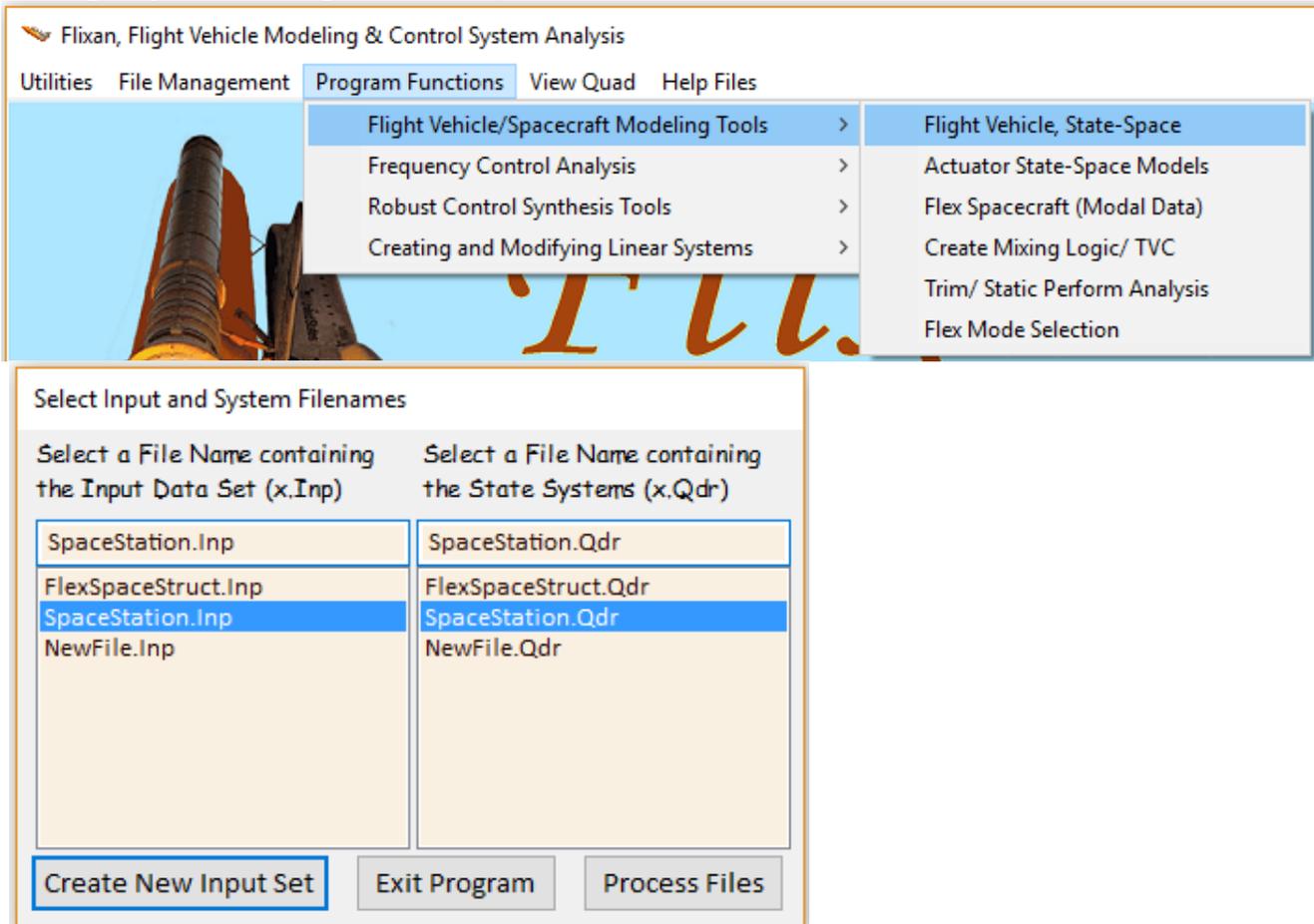
The following menu shows the titles of all vehicle datasets which are included in the input file. Select the vehicle title "*Space Station with RCS and a Double-Gimbal CMG Array*" that includes flexibility and click on "*Run Input Set*".
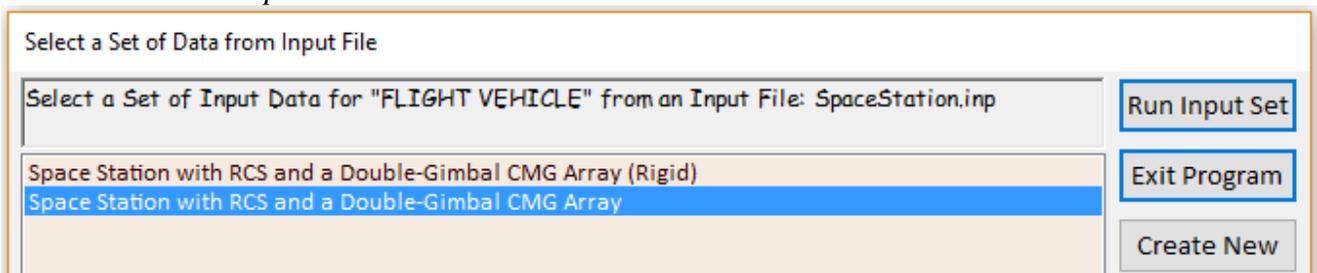
The following dialog is presented by the vehicle modeling program showing the spacecraft parameters. You may click on the various tabs to view the vehicle data in groups. To process it, click on "Run" and the program will combine the Space Station rigid body data with the flexibility dataset that includes the selected 34 structural modes to create the flex model. It will save the state-space model in file "*SpaceStation.Qdr*" using the same title as the input data "*Space Station with RCS and a Double-Gimbal CMG Array*".

4.2.1 Exporting to Matlab Format

The Space Station systems must also be reformatted to Matlab m-file in subdirectory "*Large Space Station\(d) Mat Flex Lin (FVP)*" for further analysis, using the Flixan "Export to Matlab" utility. Start Flixan and select the project directory: "*Large Space Station*". Then go to "*Utilities*" and select "*Matlab Conversions*", and then "*Export to Matlab*". From the systems menu select the systems file "*SpaceStation.Qdr*" that contains the Space Station systems and click OK. You must also select the destination directory "*\Large Space Station\(d) Mat Flex Lin (FVP)*" where the m-file will be placed for Matlab analysis.
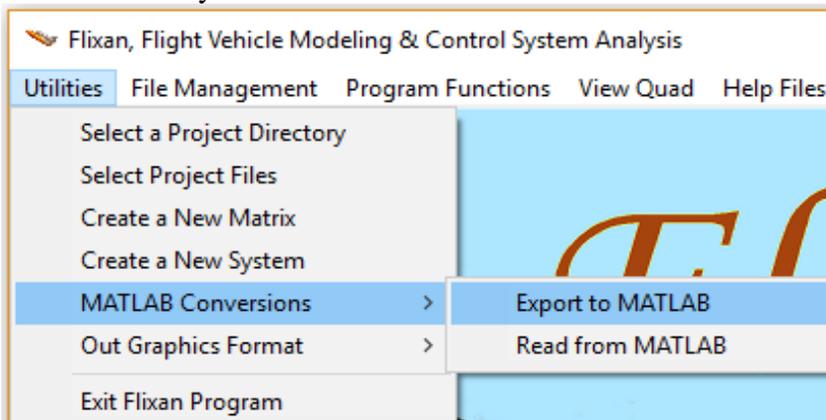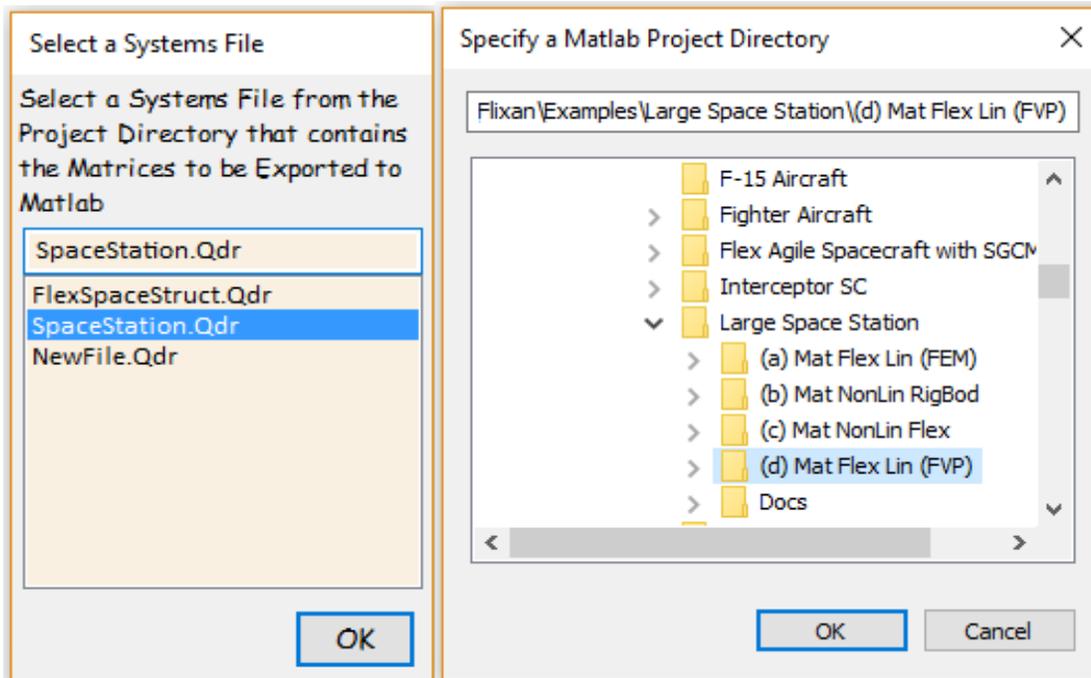
Use the next dialog to specify that the system will be saved as an m-file function of 4 matrices (A, B, C, D). The next menu shows the titles of systems in file "*SpaceStation.Qdr*". Select the first title: "*Space Station with RCS and a Double-Gimbal CMG Array*" and click on "Select".
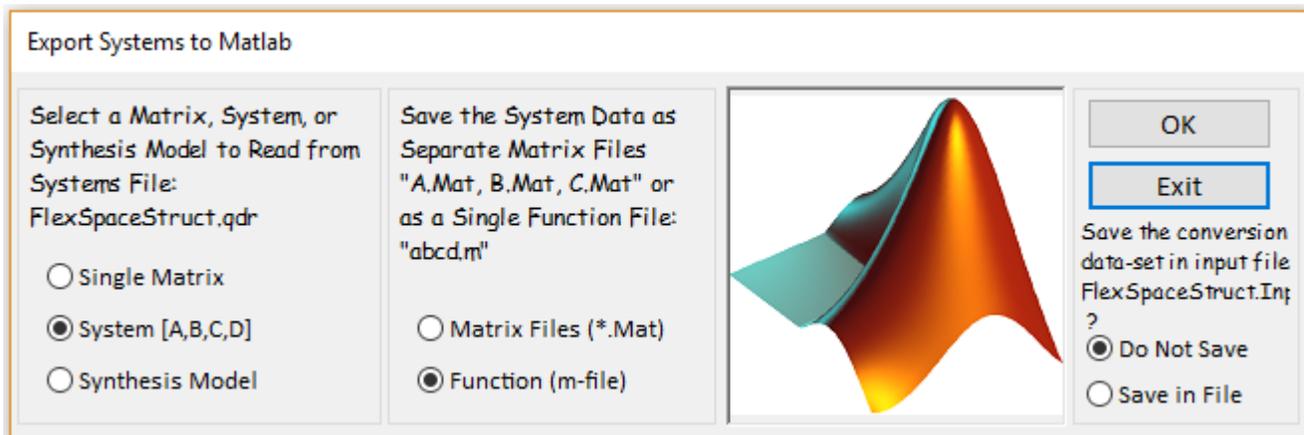
Finally enter the name of the m-file to save the system (without the extension .m), and click OK. The name of the m-file is "*vehicle_flex34.m*". It contains the four state-space matrices of the flexible spacecraft system and it will be loaded into Matlab for control analysis. The flexible Space Station model is now saved in the Matlab project directory "*Examples\ Large Space Station\ (d) Mat Flex Lin (FVP)*" to be analyzed using Matlab/ Simulink.
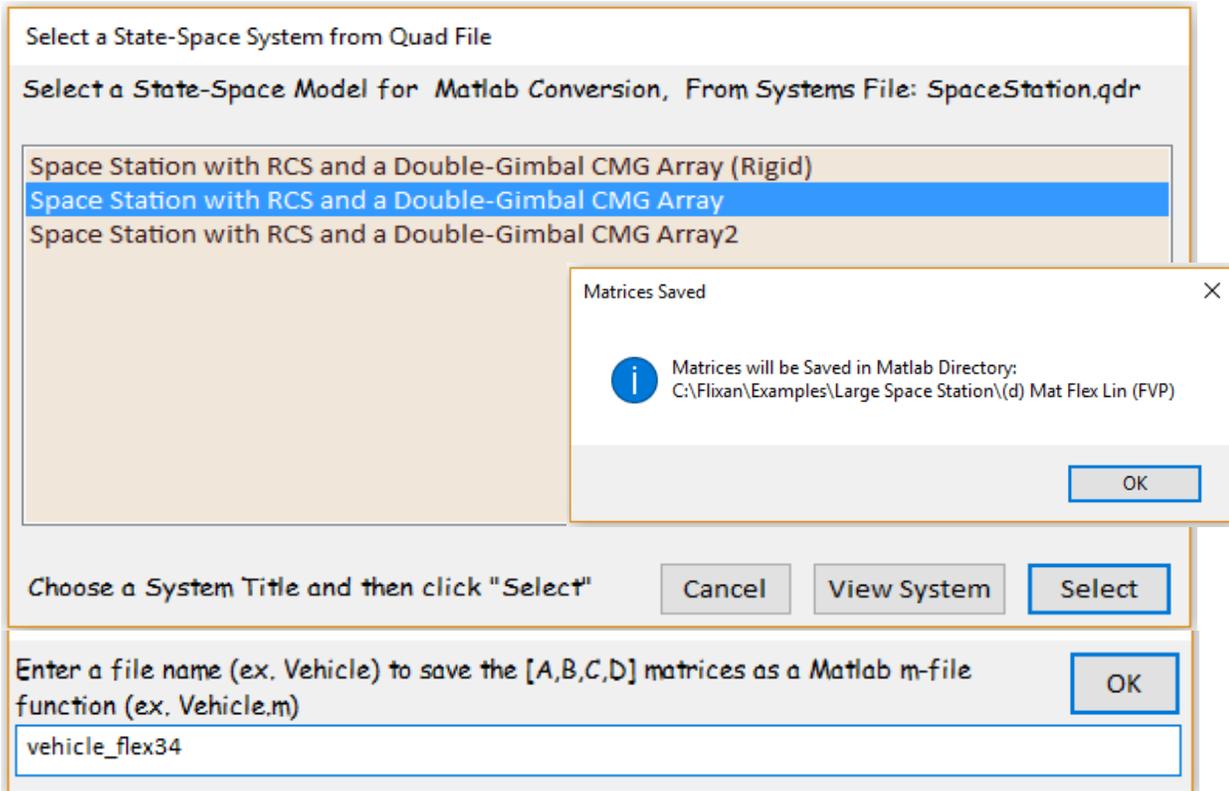
4.2.2 Processing the Input Data in Batch Mode

The input data file also includes a batch set that can process the datasets fast by calling the corresponding programs and saving the data in the systems file. It also converts the vehicle systems to Matlab m-files for analysis. In order to run the batch and process the datasets, go to the Flixan main menu and select "*File Management*", "*Manage Input Files*", and then "*Edit/ Process Input Data*".
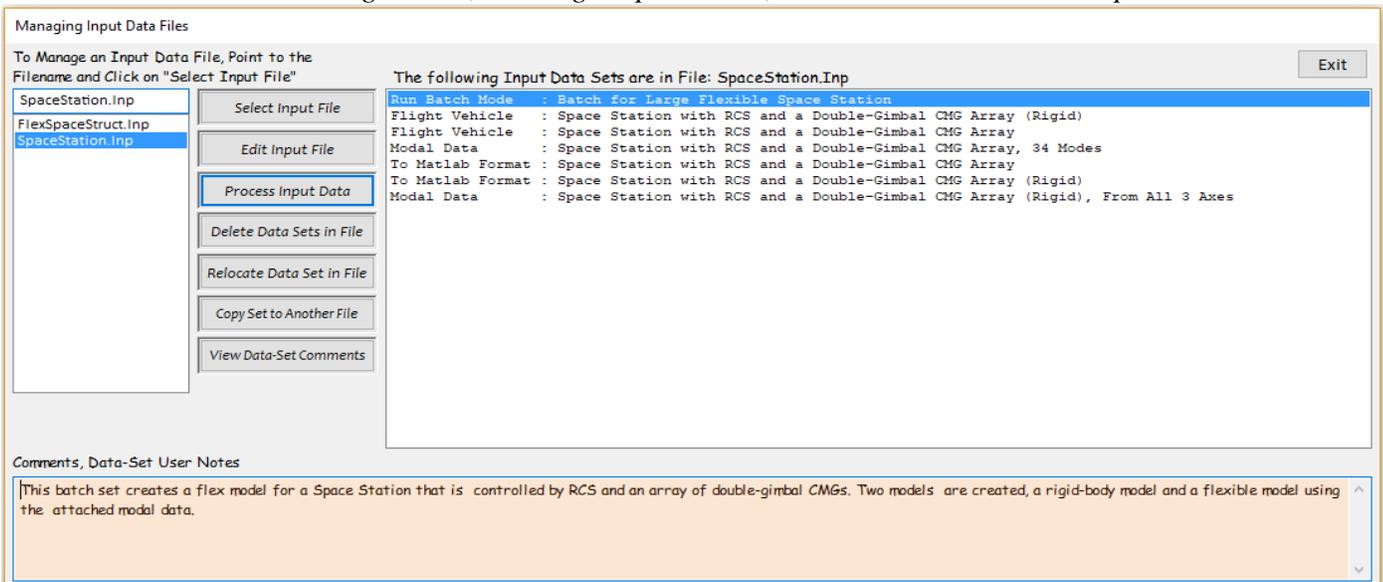
The m-files for the two vehicle models are: "*vehicle_flex34.m*" and "*vehicle_rigid.m*". They are moved to the Matlab project subdirectory "*(d) Mat Flex Lin (FVP)*" to be analyzed in Matlab/ Simulink.

4.3 Simulation of the TEA Converging Attitude Control Mode

The Momentum Management/ TEA Seeking mode of operation was described in Sections 2.4 and 3.4. In this section we will repeat the analysis using the Flixan derived flex state-space system "*Space Station with RCS and a Double-Gimbal CMG Array*" which is loaded into Matlab from file "*vehicle-flex34.m*". The closed-loop Simulink model for this mode is in file: "*Sim_Lin_TEA_Flex.Mdl*" shown in Figure 4.3.1, which is located in folder "*Large Space Station\ (d) Mat Flex Lin (FVP)*". This model is used for linear time-domain simulations of the Space Station near the LVLH attitude. The linear equations of motion in LVLH are defined in equations (4a-4c). The vehicle attitude is initialized in the LVLH frame and it slowly drifts towards the torque equilibrium attitude under the influence of the external torques. The rate in the state vector $\underline{x}(0)$ is initialized at zero. The pitch rate is not initialized at negative orbit rate $(-\omega_0)$ but at zero because it is defined relative to the LVLH frame. The bias torque in equation (4.a) is modified to: $\omega_0^2\begin{bmatrix} -4I_{YZ} & 3I_{XZ} & I_{XY} \end{bmatrix}^T$. This term is introduced in the model as a constant disturbance of amplitude 7.4015 (ft-lb) in the unit vector direction (0.196972, -0.596376, -0.778163). The direction of the bias torque is defined in the vehicle input data and its magnitude is set by constant input in the Simulink model. The aerodynamic disturbances are defined as external torque inputs in the x, y, and z directions in the vehicle input data and the disturbance torques are produced by sinusoidal functions generated in the simulation. The rate-gyro measurements are generated from the vehicle outputs #12, #13, #14 which include flexibility and not using the rigid-body rates, outputs #2, #4, #6. They are body rates and they are converted to LVLH rates by means of the transformation CBL. Notice that, the rigid-body LVLH attitudes are used in the transformation. The Matlab file "start.m" loads the state-space system and other parameters into Matlab to initialize the simulation. It also loads the state-feedback gain K_{pqr} that was designed using the LQR method in Section 2.4.
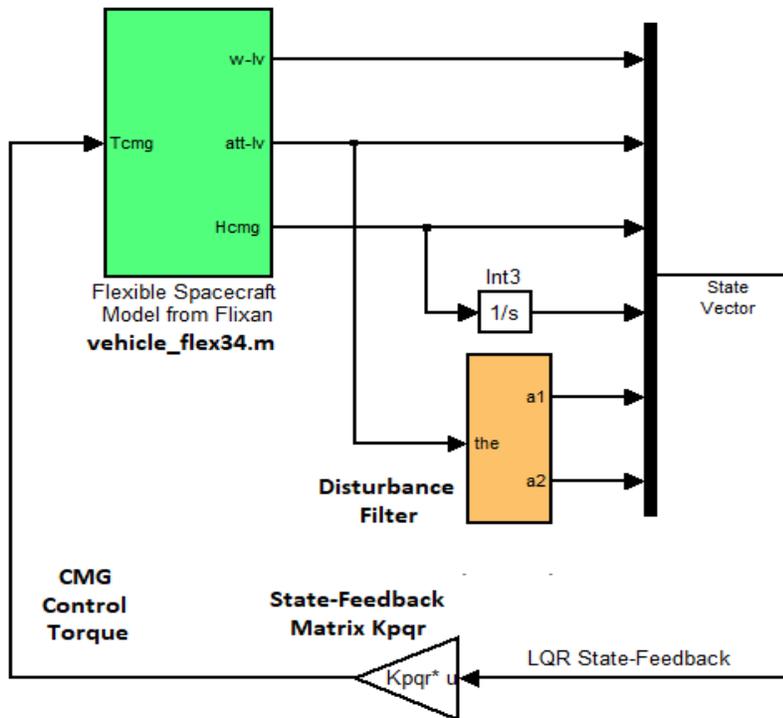
Figure 4.3.1 Linear Simulation Model with Flexibility "*Sim_Lin_TEA_Flex.mdl*" Used for the Momentum Management TEA-Converging Mode

There is no attitude command in the system when the Station is operating in this mode. The vehicle attitude drifts under the influence of the aerodynamic torques which are included in the Space Station dynamics (green block) and the gravity gradient torques which are also included in the equations of motion, Equations 2.1, since the body-rates in Equations 4 are transformed to LVLH rates similar to Eq. 2.1. The state-feedback stabilizes not only the vehicle attitude but it also bounds the CMG momentum. The attitude slowly drifts to the torque equilibrium attitude and the CMG momentum cycles around zero momentum under the influence of the cyclic disturbance torques occurring at (ω_o) and at ($2\omega_o$). The CMG control system is also attenuating the attitude oscillations caused by the cyclic disturbances. The disturbance accommodation filter further attenuates the pitch oscillations that occur at orbital rate ω_o, as it was described in detail in Section 2.4.
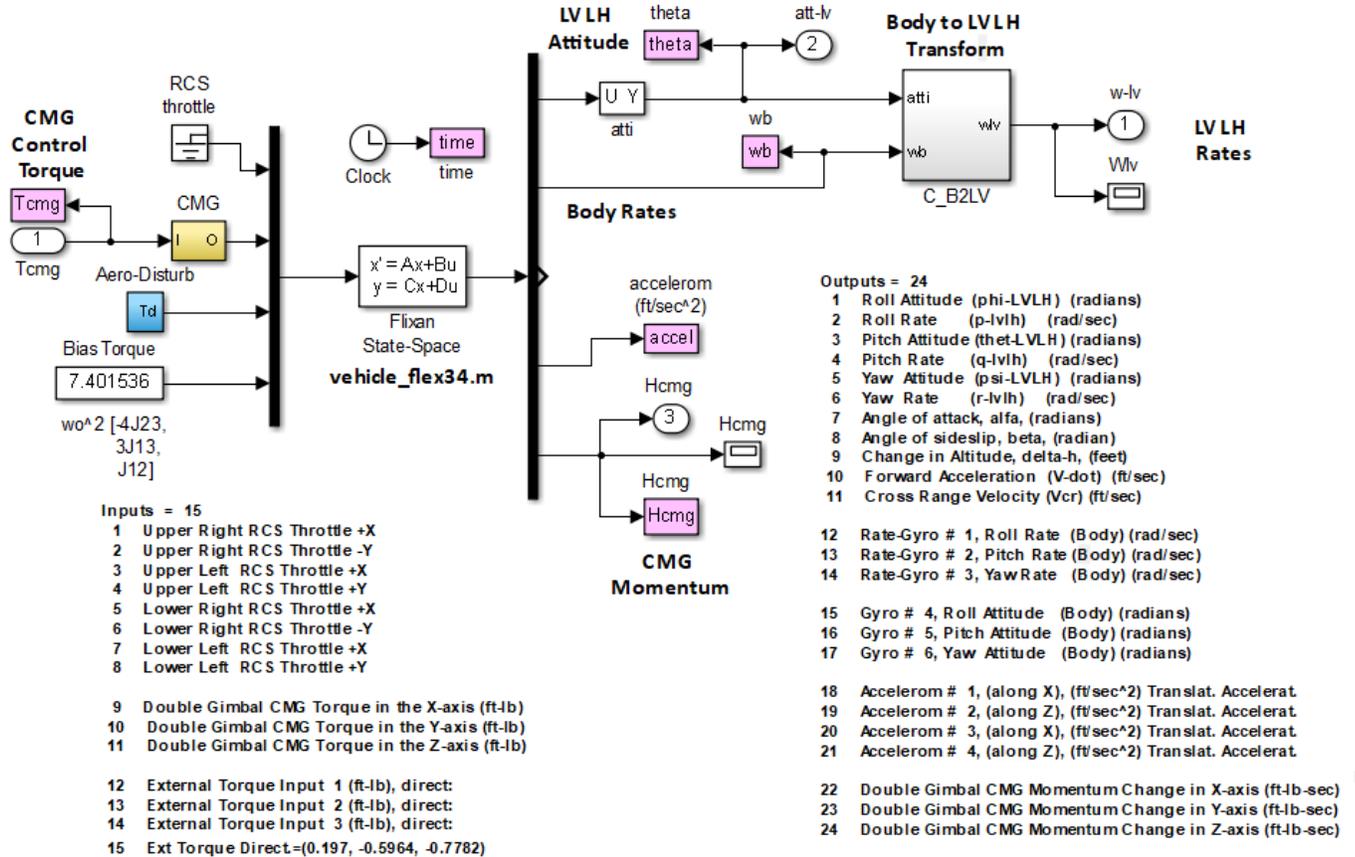
Figure 4.3.2 Space-Station Linear Dynamic Model Subsystem that includes Flexibility

The Matlab file "pl2.m" plots the simulation results which are shown in Figure 4.3.3 and they are similar to the non-linear simulatin results obtained in Figure 3.4.2. The non-linear closed-loop simulation model in Simulink file "*Sim_NonLin-TEA.mdl*" is also included in this folder for comparison, where the spacecraft dynamics is implemented in Matlab file "*Rigbod-Dynam-LVLH.m*" using the non-linear rigid-body equations, as described in Section 2. Some simulation results from the non-linear rigid-body model are also included for comparison in Figure 4.3.4, and they are pretty close to the linear results. Structural flexibility is also visible in the accelerometers.
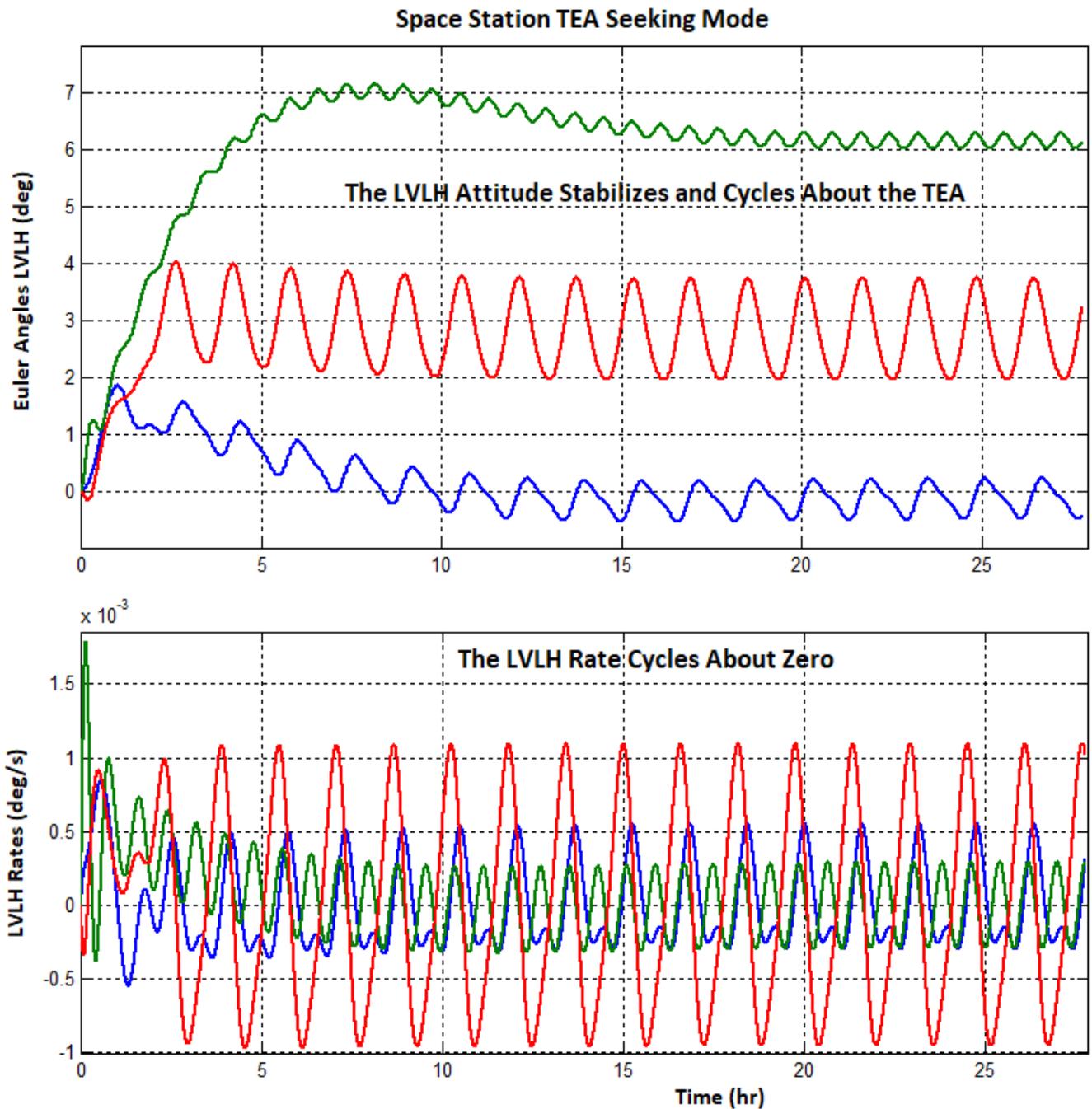
Figure 4.3.3 Space Station LVLH Attitude and Rates during the Momentum Management TEA-Seeking Mode Converging to the TEA under the influence of the Environmental Torques

The pitch and yaw attitudes converge to 6.2 and 3 degrees respectively in order to produce gravity gradient torques that will balance the aero moments. The LVLH rates, the CMG torques, and CMG momentum oscillate at orbital rate about a zero mean. The roll body rate is slightly negative because yaw LVLH attitude is 3⁰.
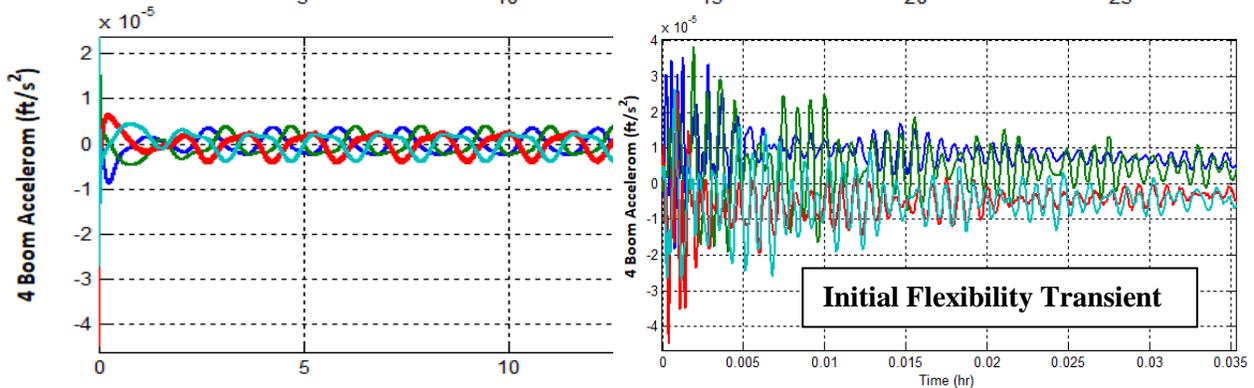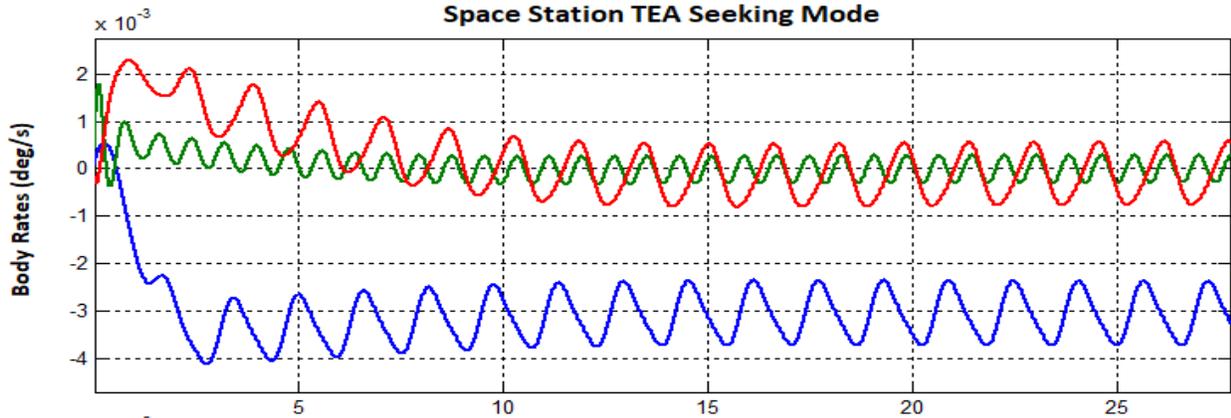
Space Station TEA Seeking Mode
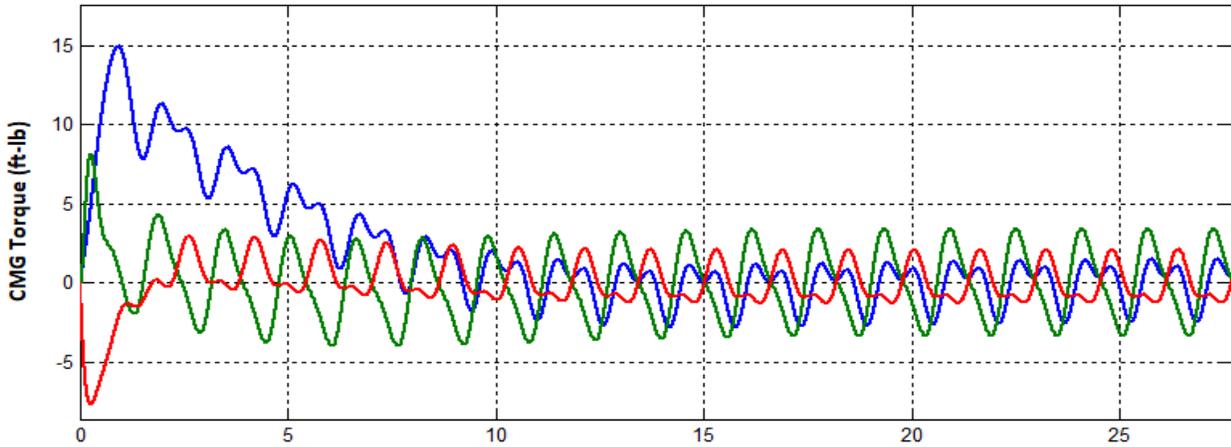
CMG Torque and Momentum are Stable and they Cycle About Zero

Space Station TEA Seeking Mode

Initial Flexibility Transient
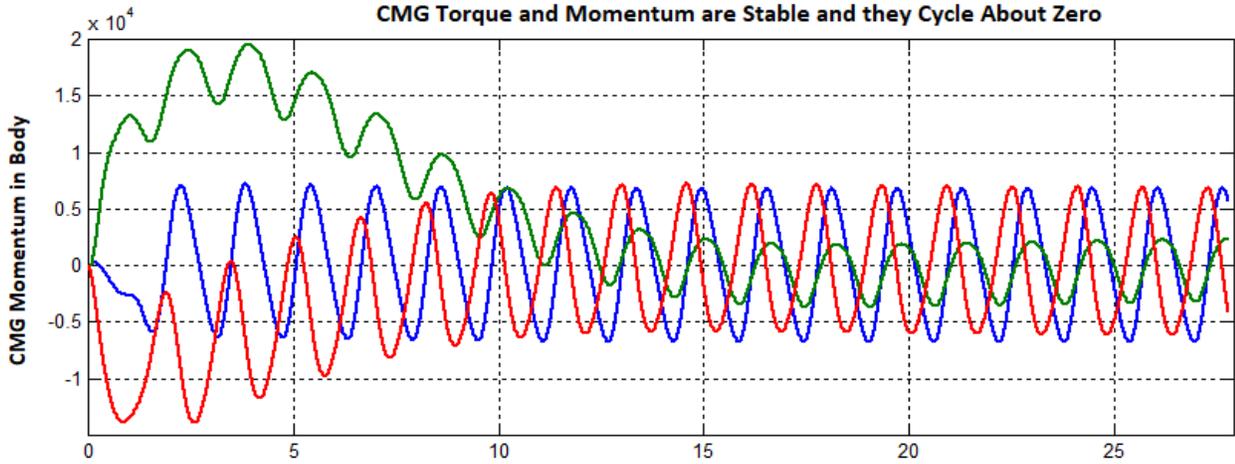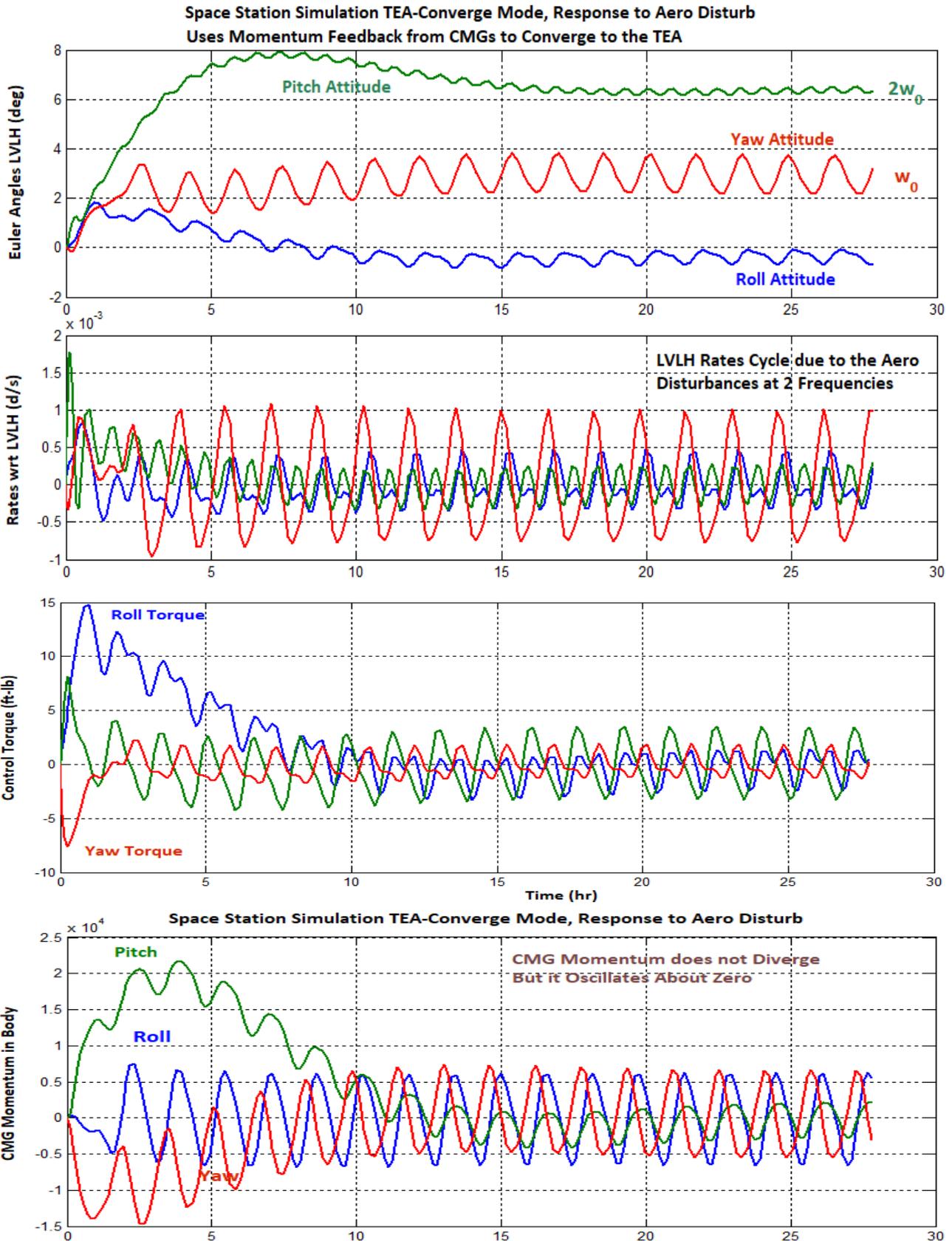
Figure 4.3.4 Simulation Results Obtained from the Non-Linear Simulation Model "Sim_NonLin_TEA.mdl", are Included here for Comparison

4.4 Stability Analysis of the TEA-Converging Mode

Figure 4.4.1 shows the Simulink model "*Open_Lin_TEA_Flex.mdl*" used for calculating the open-loop frequency response of the TEA-Converging Momentum Control mode and analyzing its stability. The spacecraft dynamics block is similar to Fig. 4.3.1 and it includes the flexible spacecraft state-space system "*Space Station with RCS and a Double-Gimbal CMG Array*" that is loaded into Matlab from file "*vehicle_flex34.m*" by the initialization file "start.m". It includes also the state feedback controller which is loaded from a matrix Kpqr.mat. The orange block is the disturbance attenuation filter that was already described. The CMG servo gimbal dynamics block is modelled by 2nd order transfer functions of bandwidth equal to 2 (rad/sec), and it is included in the spacecraft block shown in Figure 4.3.2. Figure 4.4.1 is set for roll axis stability analysis and it must be modified to analyze pitch and yaw.
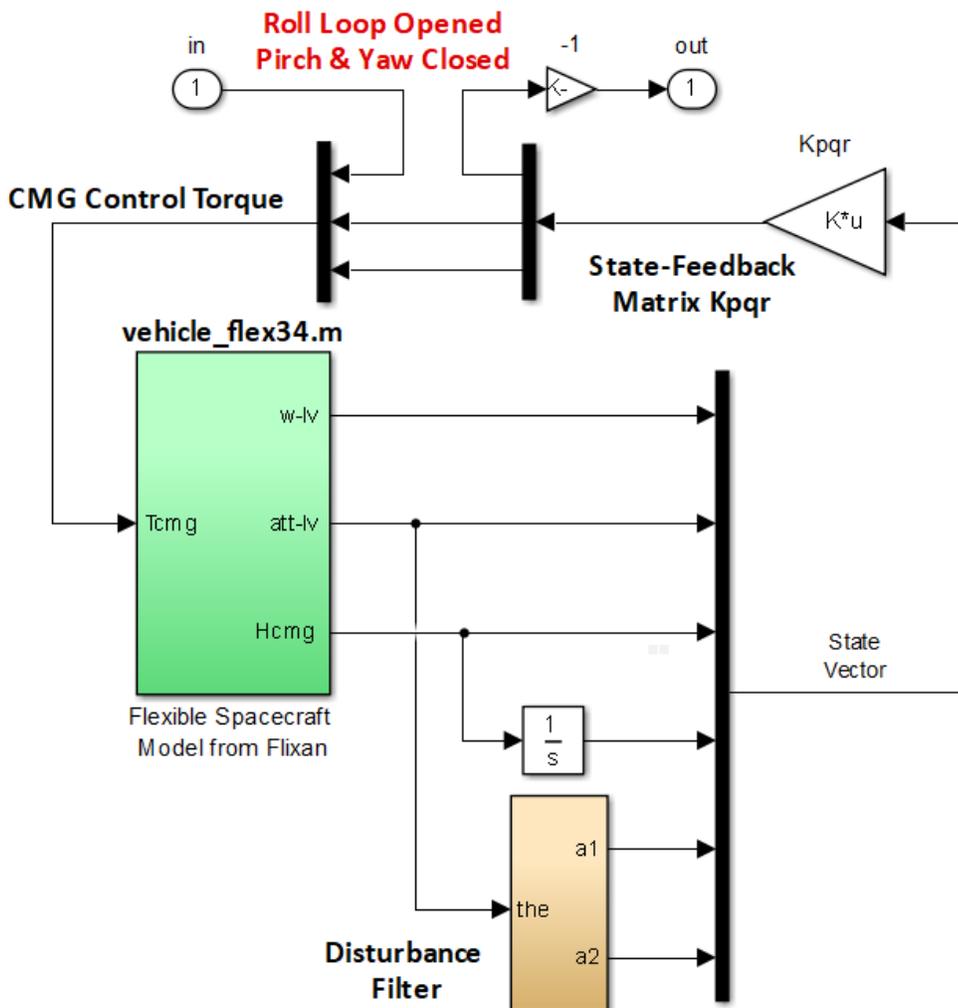
Figure 4.4.1 Model "*Open_Lin_TEA_Flex.mdl*" used for TEA Stability Analysis

The file "freq.m" linearizes this open-loop model, calculates the frequency responses and plots the Bode, Nichols or Nyquist diagrams for roll, pitch, and yaw axes, shown in Figure 4.4.3. Amazingly the results are almost identical to the results obtained from the flex analysis in Section 3.1. The stability margins are plentiful since the attitude control system bandwidth is very low in this mode of operation.
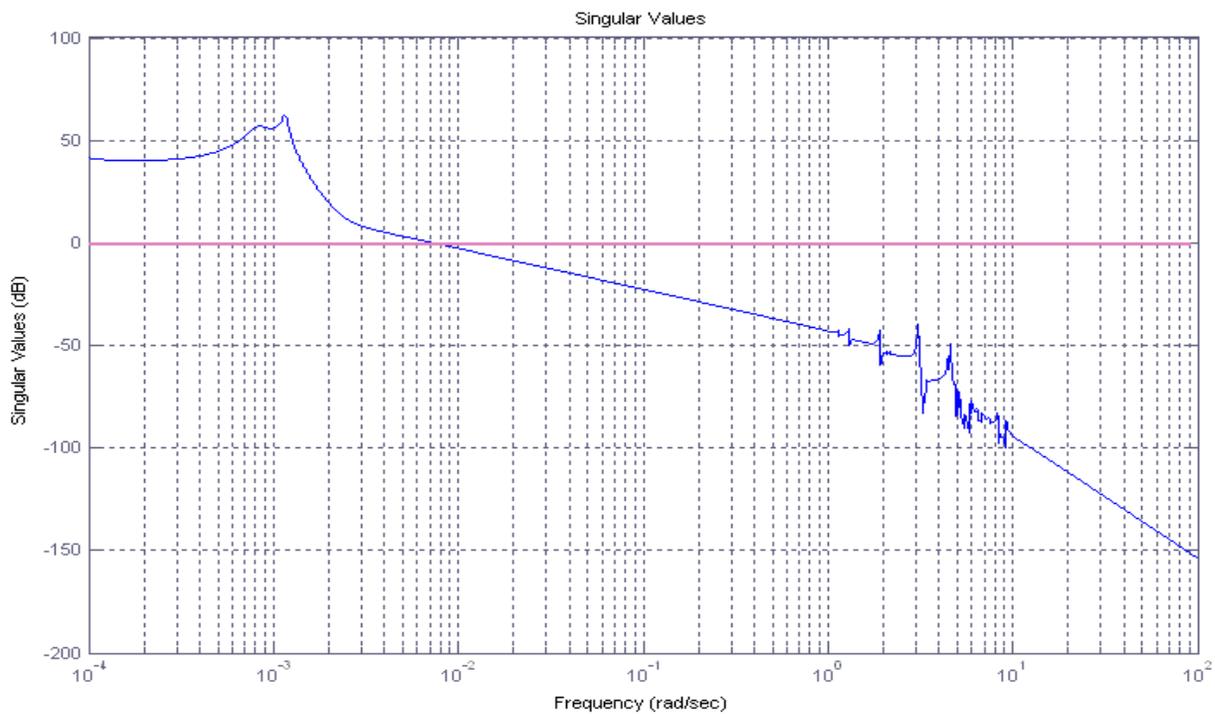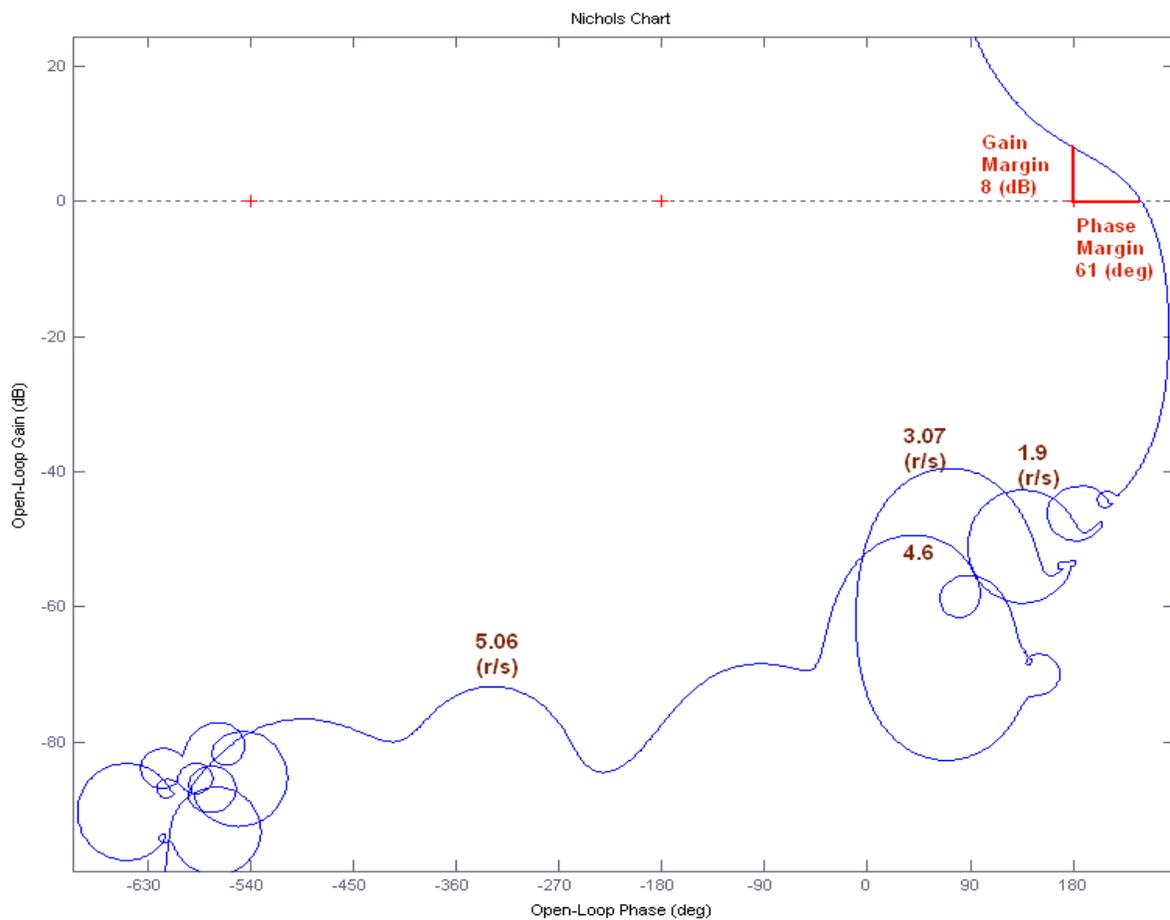
Roll Axis Open-Loop Frequ Response

Singular Values

Roll Axis Stability in TEA Seek Mode using Linear Flex Model

Nichols Chart
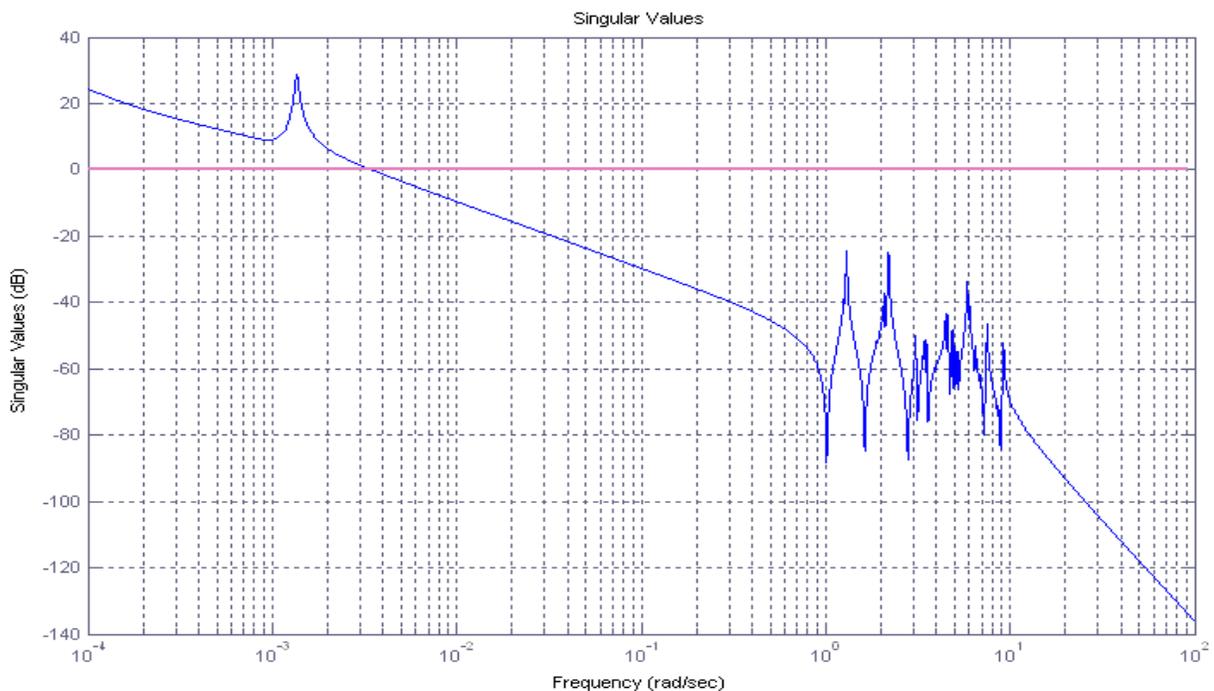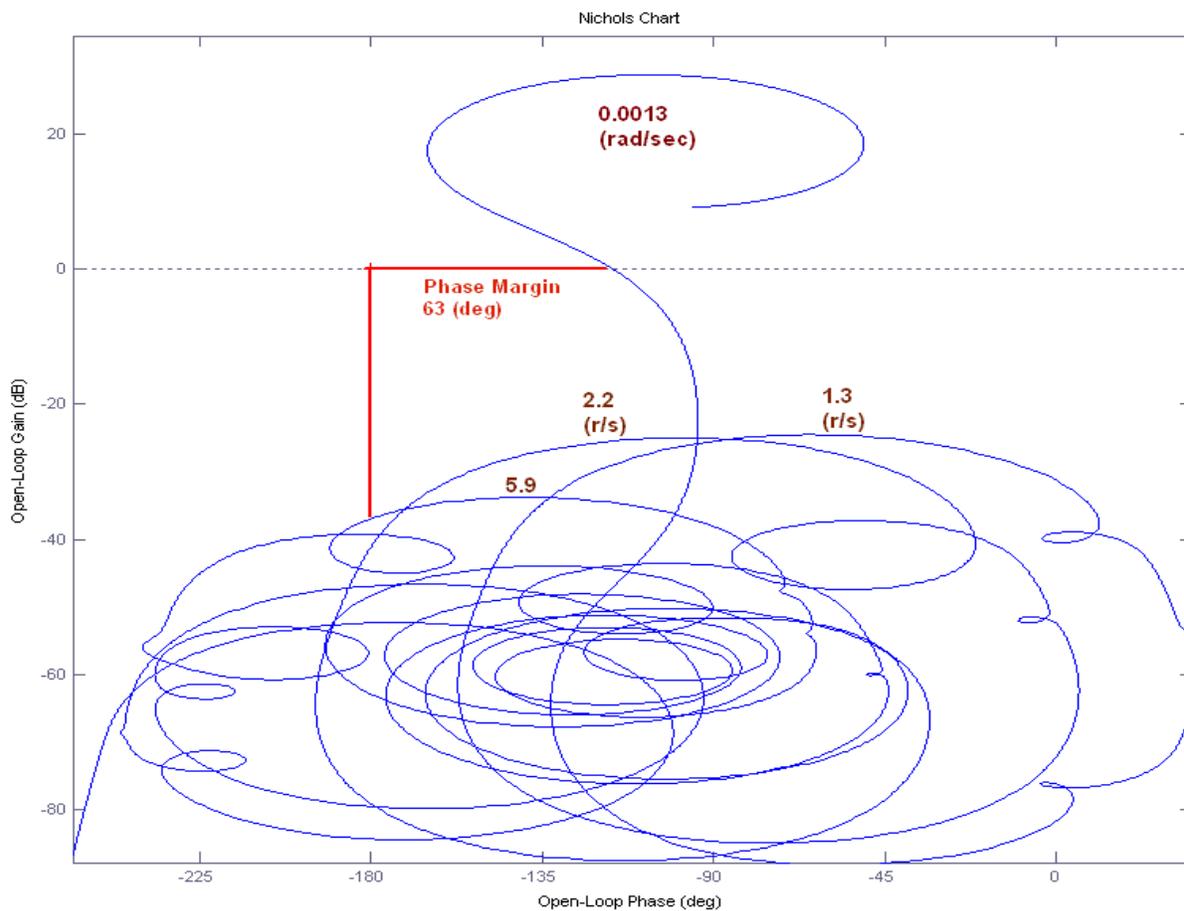
Pitch Axis Open-Loop Frequ Response

Singular Values

Pitch Axis Stability in TEA Seek Mode using Linear Flex Model

Nichols Chart

Yaw Axis Open-Loop Frequ Response

Singular Values
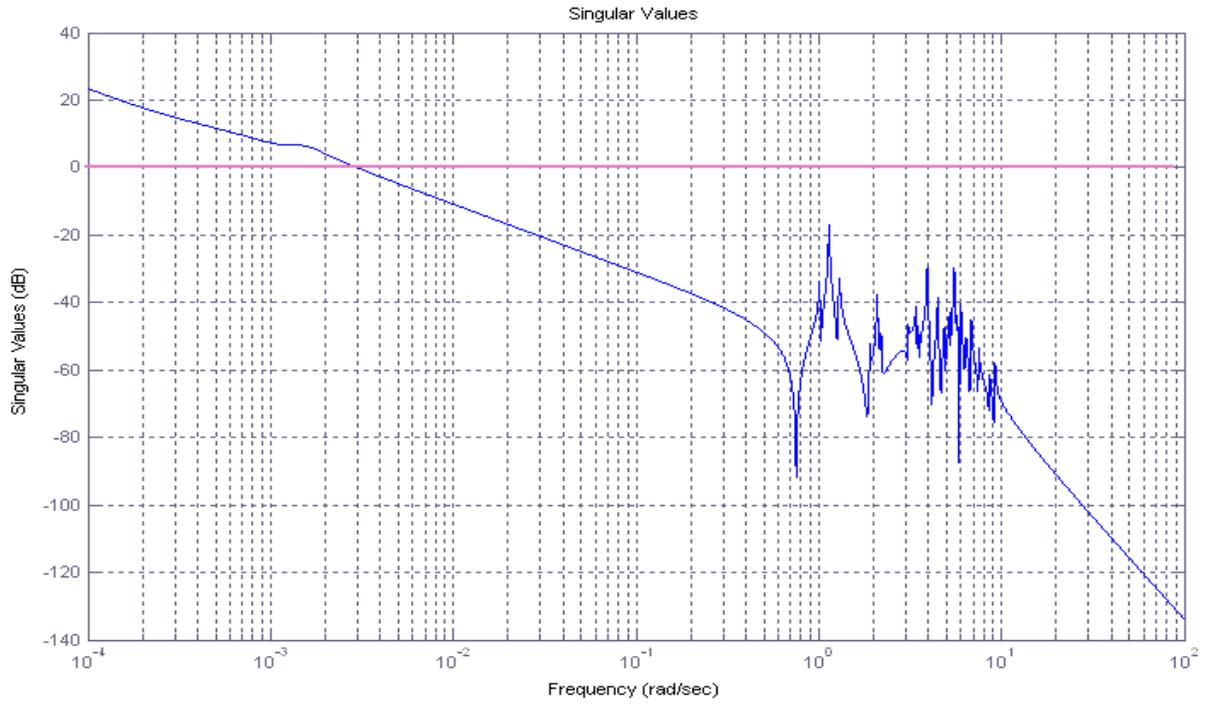
Yaw Axis Stability in TEA Seek Mode using Linear Flex Model

Nichols Chart
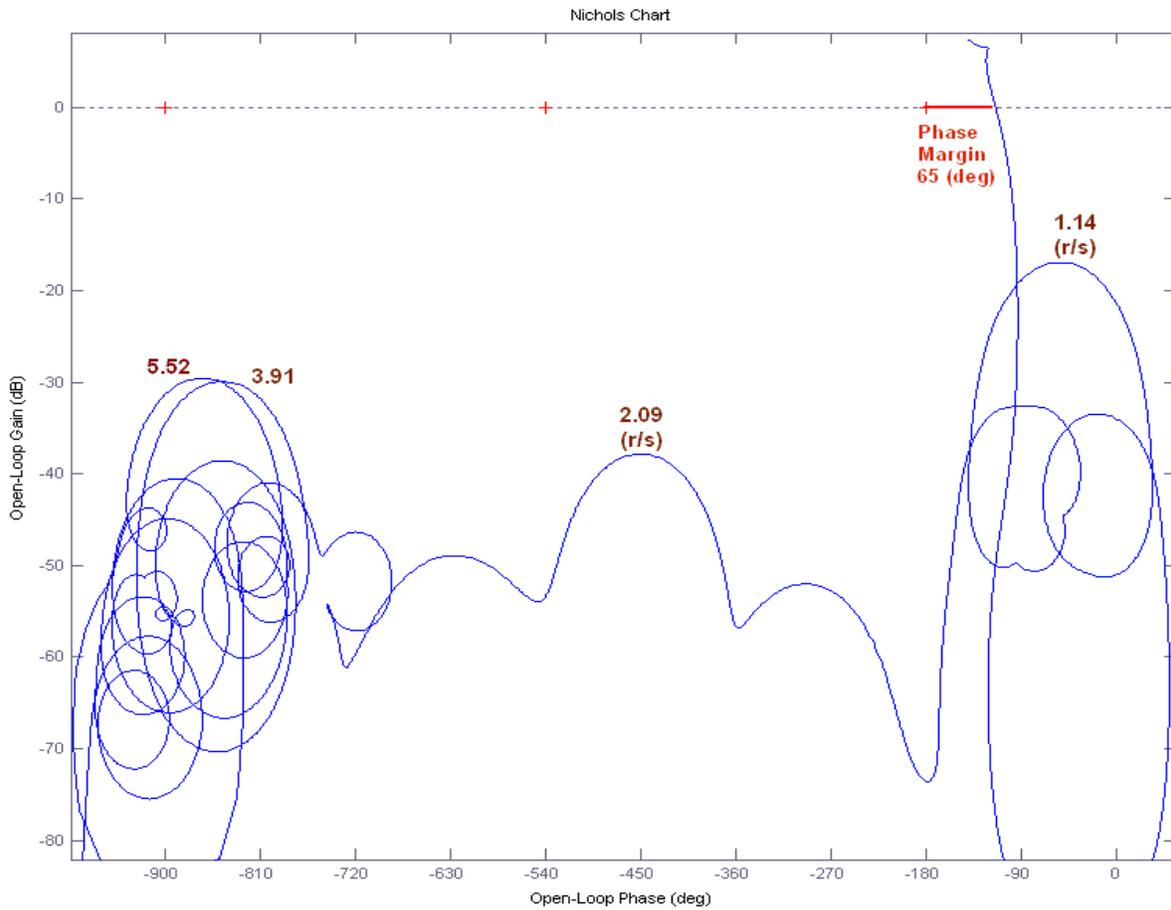
4.4.1 Accelerometer Sensitivity to Crew Disturbances

When operating in the Momentum Management mode, it is also required to analyze the vehicle sensitivity at the 4 accelerometers specified to disturbances occurring in the habitat module. We will use the closed-loop Simulink model: "*Accelerom_Sensitivity.mdl*" shown in figure 4.4.4 to perform the sensitivity analysis using Singular Values. The input is a vector of three torques about x, y, and z axes. That is, input numbers: 12, 13, and 14 in the vehicle system. They are defined as external input torques at the central habitat module which is node #9007 in the finite elements model. The output is a vector of four accelerometers. Two accelerometers at the end of the right solar array boom (node #6070) measuring in the x and z directions, and two accelerometers at the end of the left solar array boom (node #5070) measuring also in the x and z directions. The sensitivity at the accelerometers to crew disturbances is analyzed using Singular Values frequency response (sigma) plots. The Matlab file "freq.m" calculates and plots the sigma response from this Simulink model and it is shown in Figure 4.4.5.
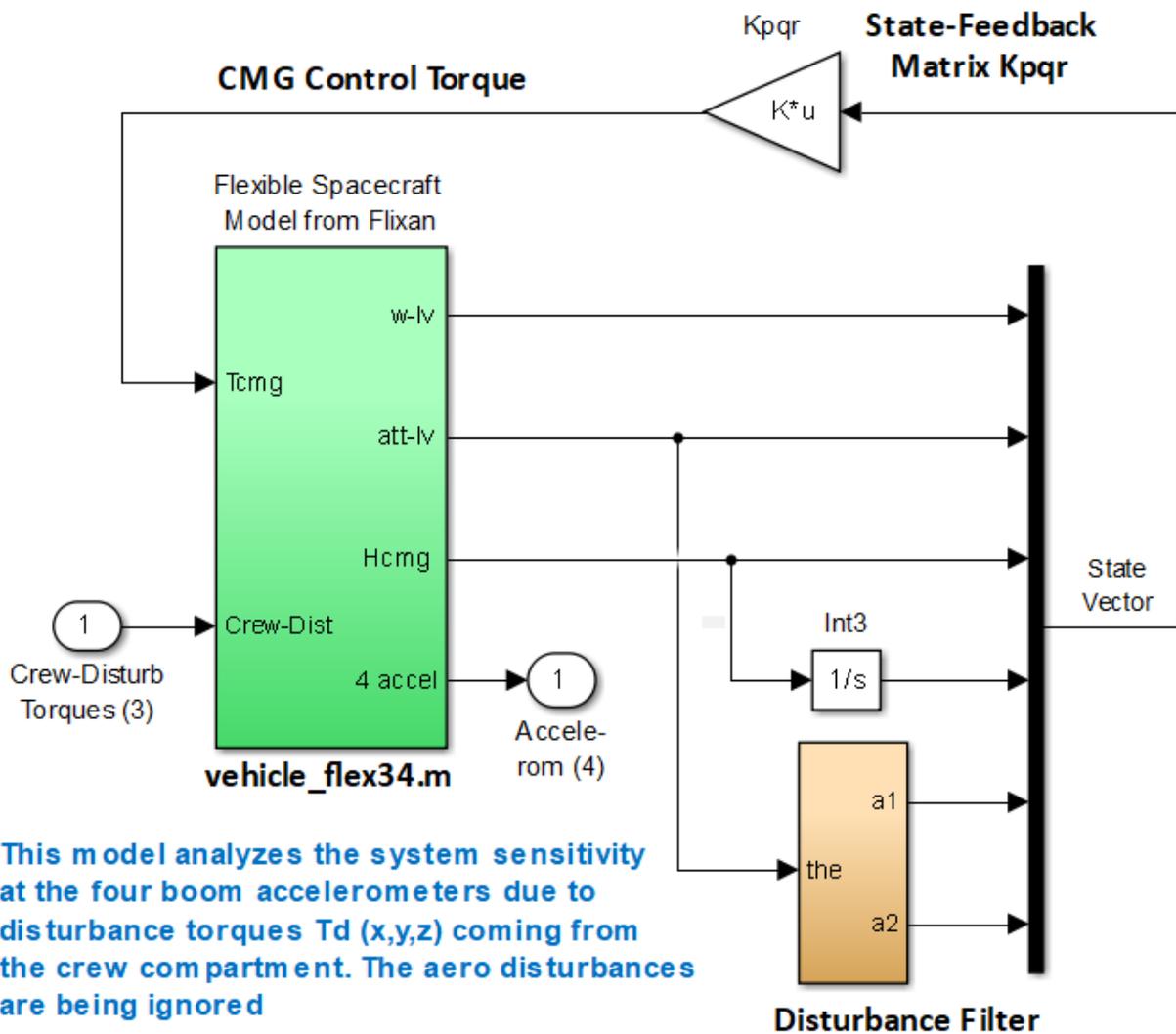

Figure 4.4.4 Simulink Model "Accelerom_Sensitivity.Mdl" used for Calculating Vehicle Sensitivity at the Accelerometers due to Disturbances from the Habitat Module
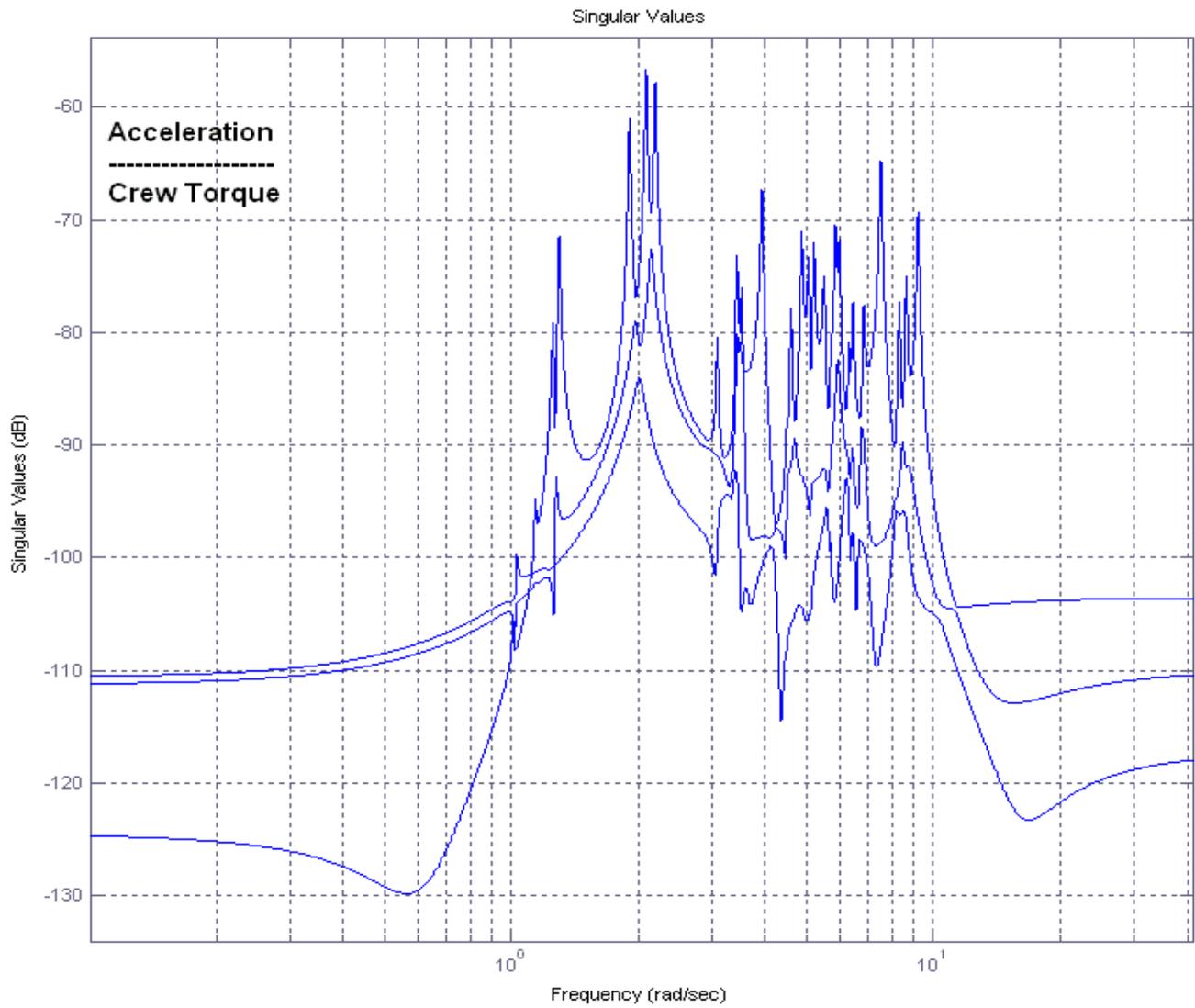
117

Figure 4.4.5 Sensitivity plot showing the Maximum Excitation of the Structure as a function of Frequency

4.5 Combined CMG/ RCS Attitude Control Simulation

The Simulink model in Figure 4.5.1 is in file "*Sim_Lin_CMG_RCS_Flex.Mdl*" in folder: "*Large Space Station\ (d) Mat Flex Lin (FVP)*". It is used to simulate the combined parallel operation of the CMG and RCS control systems. It is similar to the models described in Sections 2.3 and 3.3, except that instead of the non-linear Space Station dynamic model we are now using the Flixan derived state-space system "*Space Station with RCS and a Double-Gimbal CMG Array*" which is loaded into the Matlab workspace from file "*vehicle_flex34.m*".
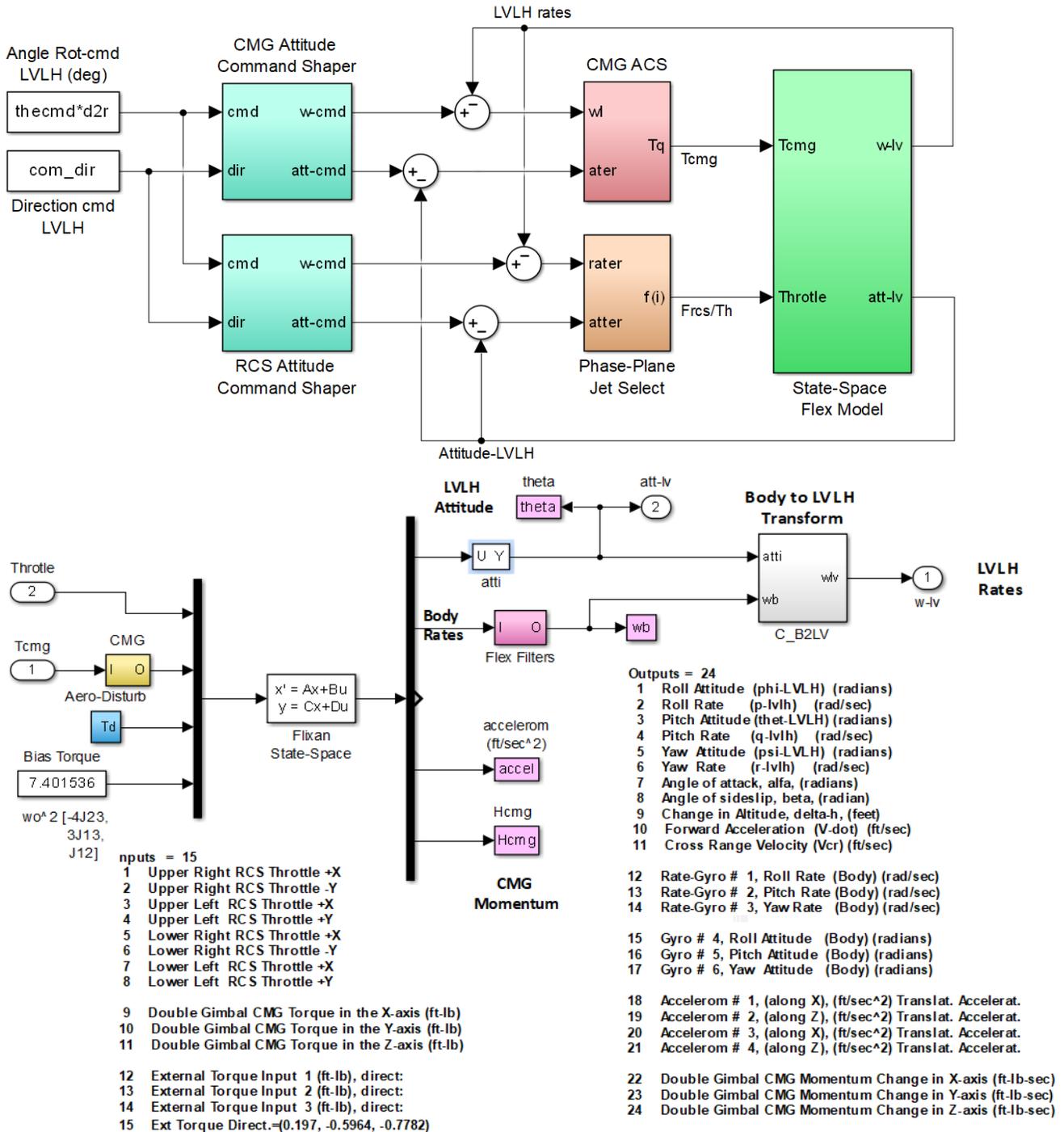
Figure 4.5.1 Parallel RCS/ CMG Simulation Model "*Sim_Lin_CMG_RCS_Flex.mdl*"

The equations of motion of the vehicle state-space system are the same as Equations (4a-4c) but the attitude and rates are transformed to the LVLH frame. The state vector the vehicle pitch rate is not initialized at $-\omega_0$ but it is defined instead with respect to the LVLH frame and it is initialized to zero. The bias torque is: $\omega_0^2 \begin{bmatrix} -4I_{YZ} & 3I_{XZ} & I_{XY} \end{bmatrix}^T$, which is introduced in the model as a constant disturbance of amplitude 7.4015 (ft-lb) in the direction (0.196972, -0.596376, -0.778163). The disturbance direction is defined in the vehicle input dataset and the magnitude of the bias is an input to the Simulink model. The aerodynamic disturbances are introduced in the model as external torques in the x, y, and z directions and they are defined in the vehicle input data. The rate-gyro measurements (outputs #12, #13, #14) are measuring body rates and they include flexibility. They must be converted to LVLH rates by a transformation CBL. The Matlab file "start.m" loads the vehicle state-space system and other parameters into the Matlab workspace.

The CMG attitude control system is shown in Figure 3.3.2. It consists of simple PD gains designed for a bandwidth 20 times the orbital rate which is 0.022 (radians/sec). It includes a switching logic that disables the CMG control when the torque demand is large because the CMGs have torque limitations. The logic turns the CMG system on when the magnitudes of rate and attitude errors become sufficiently small.

The RCS attitude control system is shown in figure 4.5.2. It uses phase-plane and jet selection logic that determines the thruster firing based on the rate and attitude errors. The jet thrust outputs are converted into throttles by dividing them with the jet thrust because the vehicle model is expecting throttle inputs between 0 and ±1, rather than actual thrusts. The 12 jet output vector is also adjusted to match the vehicle throttle inputs. The vehicle model was defined to have 8 throttling engines instead of the actual number 12 because four pairs of jets are defined to fire in both: +x and in–x directions, so they are represented in the vehicle model with 4 single thrusters instead of 8, capable of thrusting in both ±x directions. The m-file "Pl.m" is used to plot the simulation data.
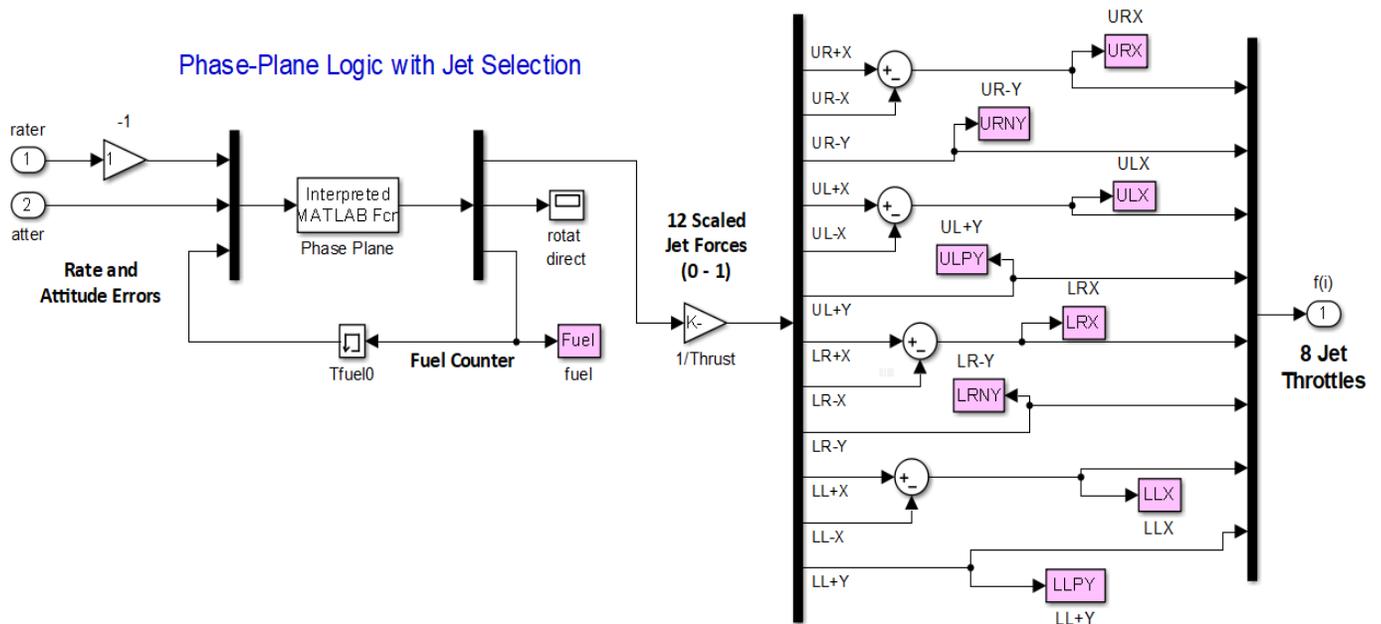

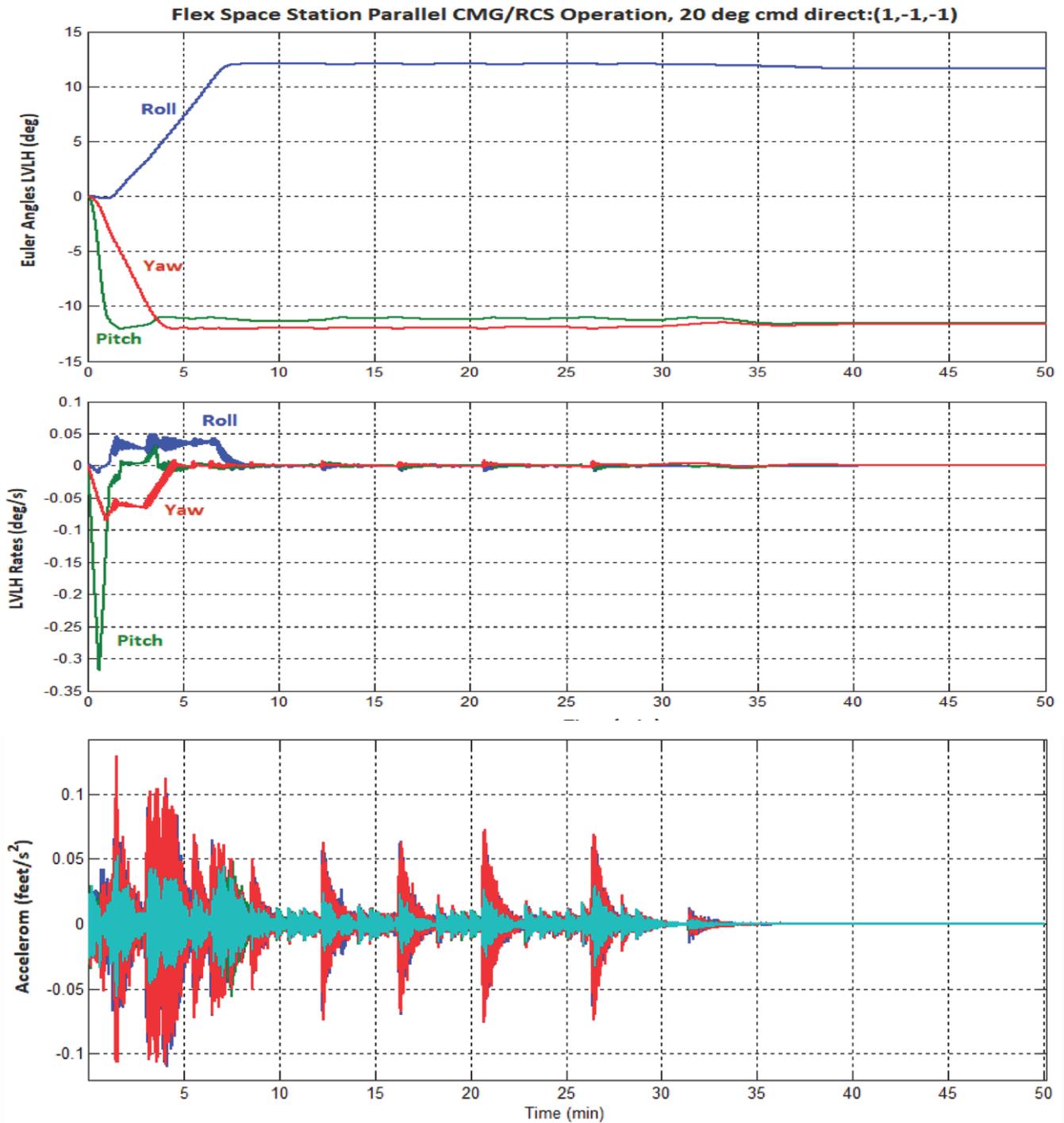**Figure 4.5.2 Phase-Plane and Jet Selection Logic**

Figure 4.5.3 Combined RCS/CMG, 20º Attitude Control Maneuver

Figure 4.5.3 shows the system response to a 20° attitude command in direction (1, -1, -1). The pitch attitude responds faster because it receives an initial boost from the CMG system before the CMG is turned off. The RCS responds fast and the attitude reaches the commanded value in 8 min but the RCS activity stops and the CMGs regain control 28 min later when the errors are very small. The RCS system excites structural vibrations but they decay and do not produce limit-cycles, as predicted by the non-linear analysis. At steady state the CMG control system maintains smooth attitude control, avoids structural excitations, and the attitude errors are very small.
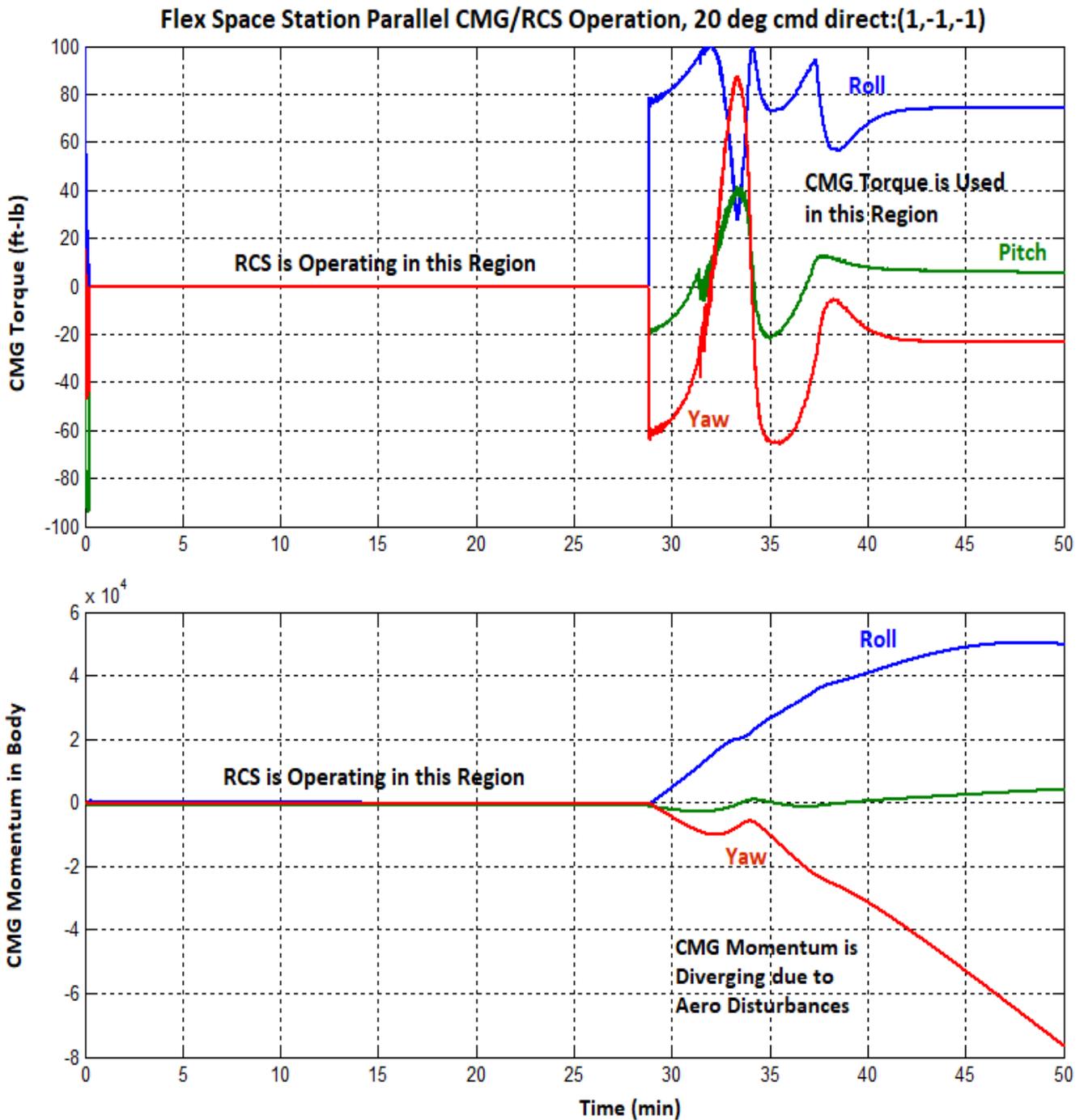
Figure 4.5.4 CMG Torque and Momentum Activity during the Maneuver

The CMG torque is turned off during RCS control. The CMG control system requires a steady CMG torque in order to maintain the desired attitude in the presence of external disturbances. This causes a divergence in the CMG momentum that will eventually saturate due to hardware limitations. This justifies the necessity of the TEA-converging mode that prevents the CMG momentum from saturating and was described in Section 4.3. Figure 4.5.5 shows the RCS thrusters activity. They stop firing during CMG control. Notice that the 4 x-thrusters are defined as bidirectional, each representing a pair of back-to-back firing jets.

Jet Thrusts (lb) Firing in the +/-X direction

CMGs are Used in this Region
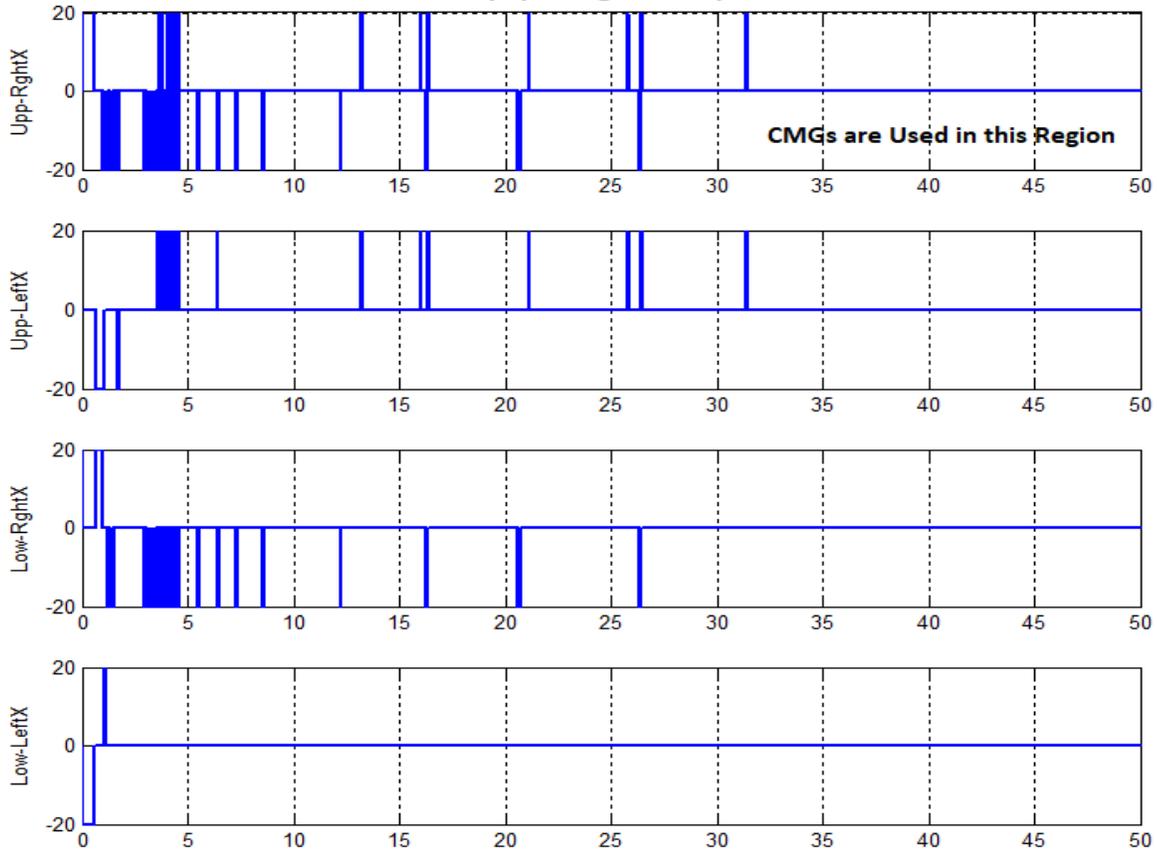
Jet Thrusts (lb) Firing in the +/-Y direction

CMGs are Used in this Region

Time (min)
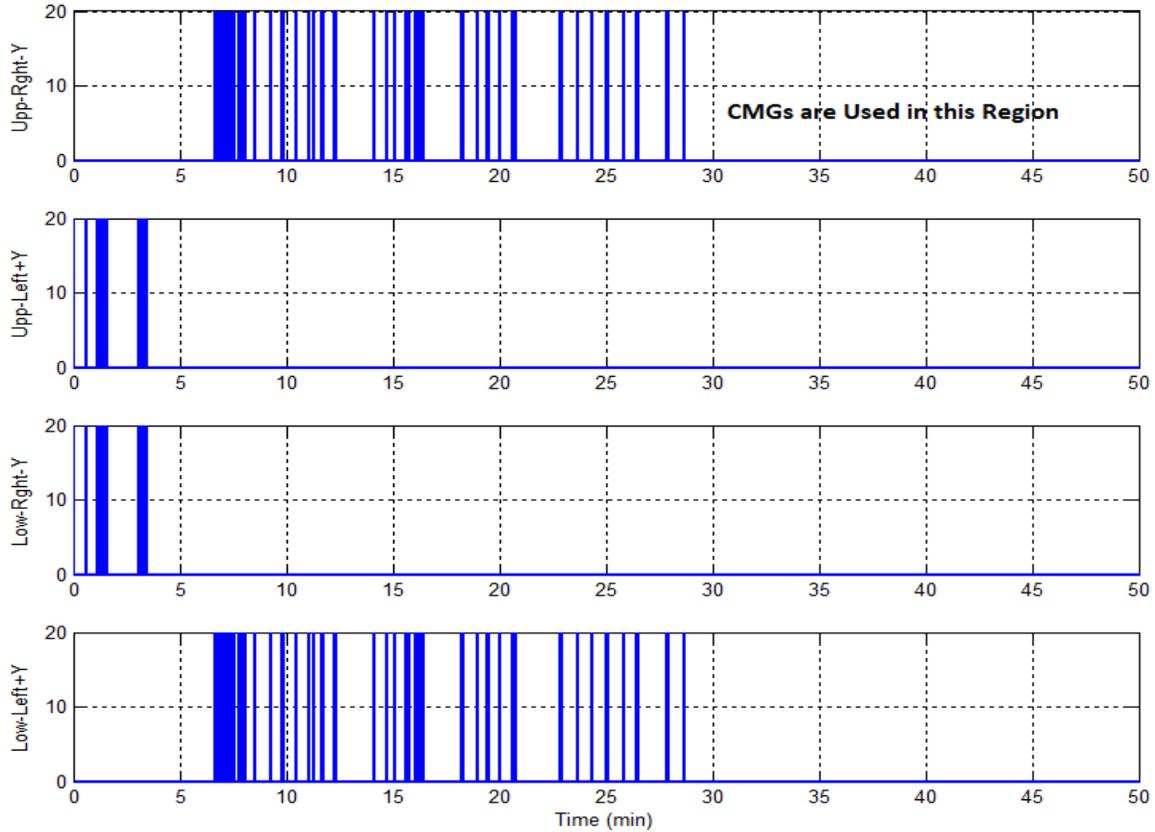
4.6 Stability Analysis of the CMG / PD Attitude Control System

Stability analysis of the CMG attitude control system in the PD mode is performed using the Simulink model "*Open_Loop_CMG.mdl*", shown below. The frequency response for each axis is calculated separately by opening one loop at a time while the other two loops are closed. In this case it is set up for pitch axis analysis. The Matlab file "freq.m" loads the vehicle and ACS parameters and calculates the frequency responses. It linearizes the system, calculates the state-space system from a single input to a single output, and plots the Nichols charts. The stability analysis plots for the roll, pitch, and yaw axes are shown in Figure 4.6.1. The results are identical to those obtained in Section 3.
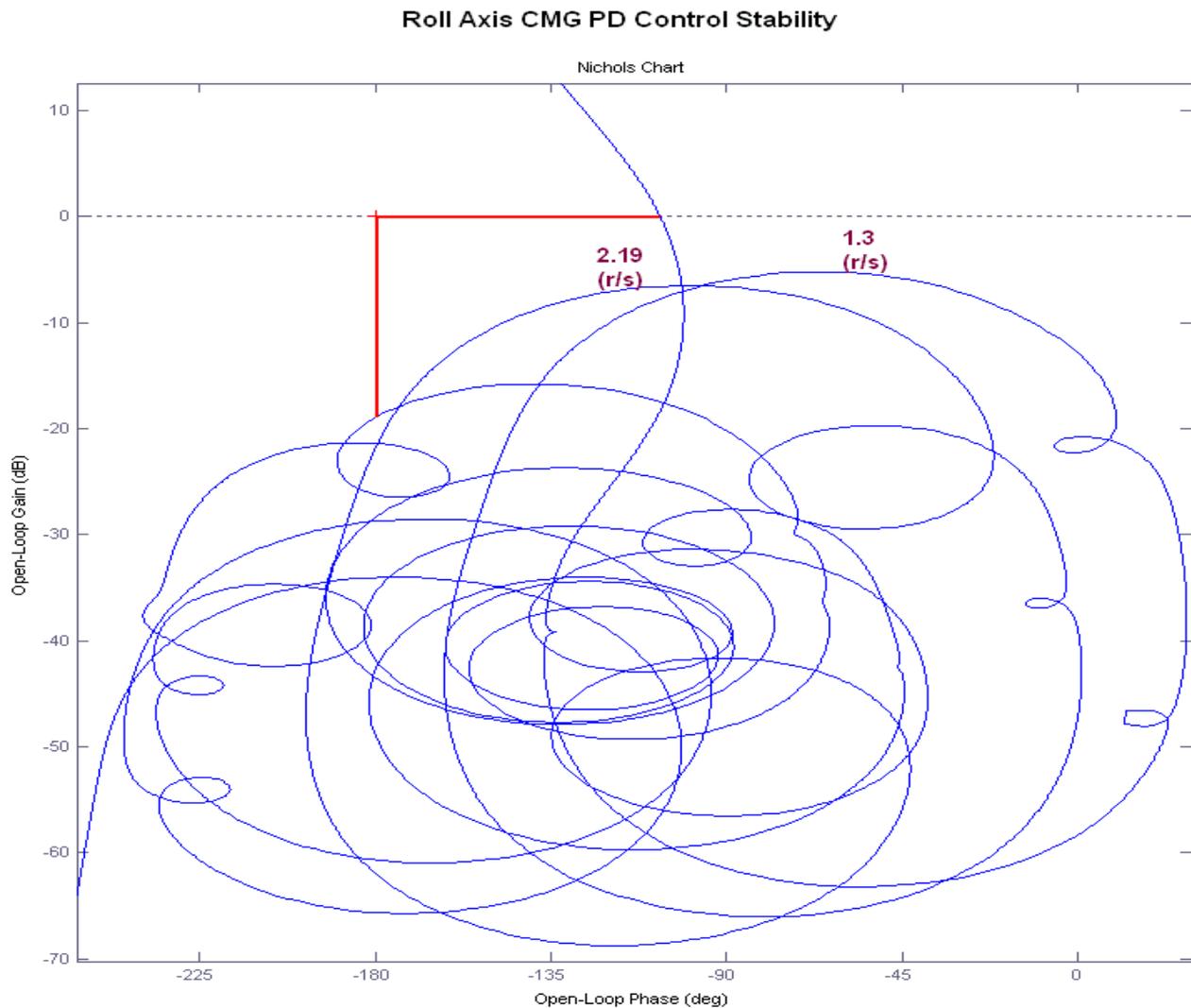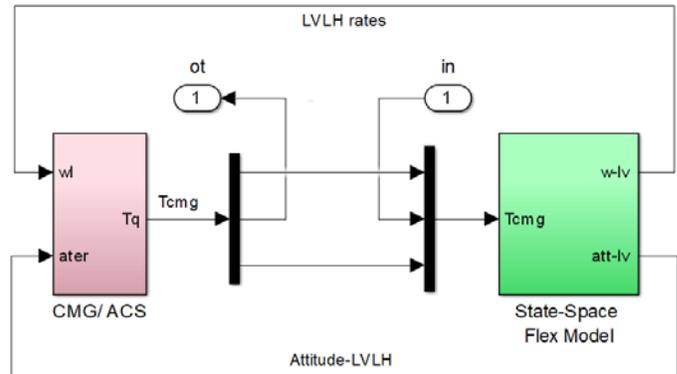

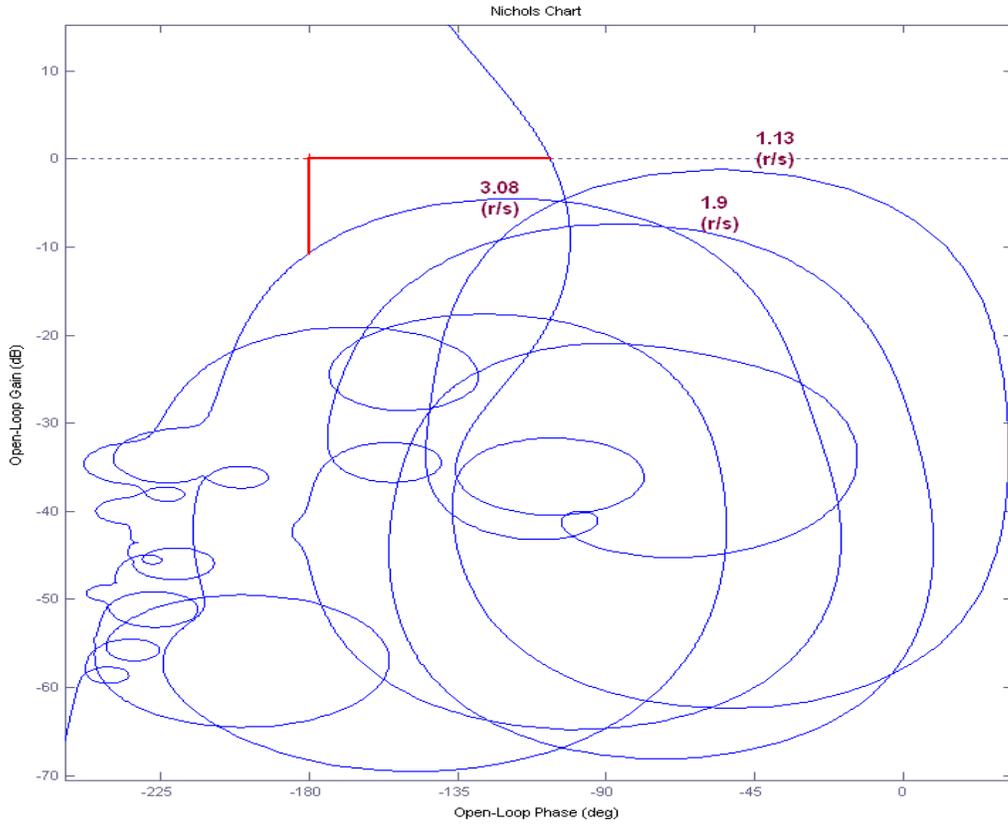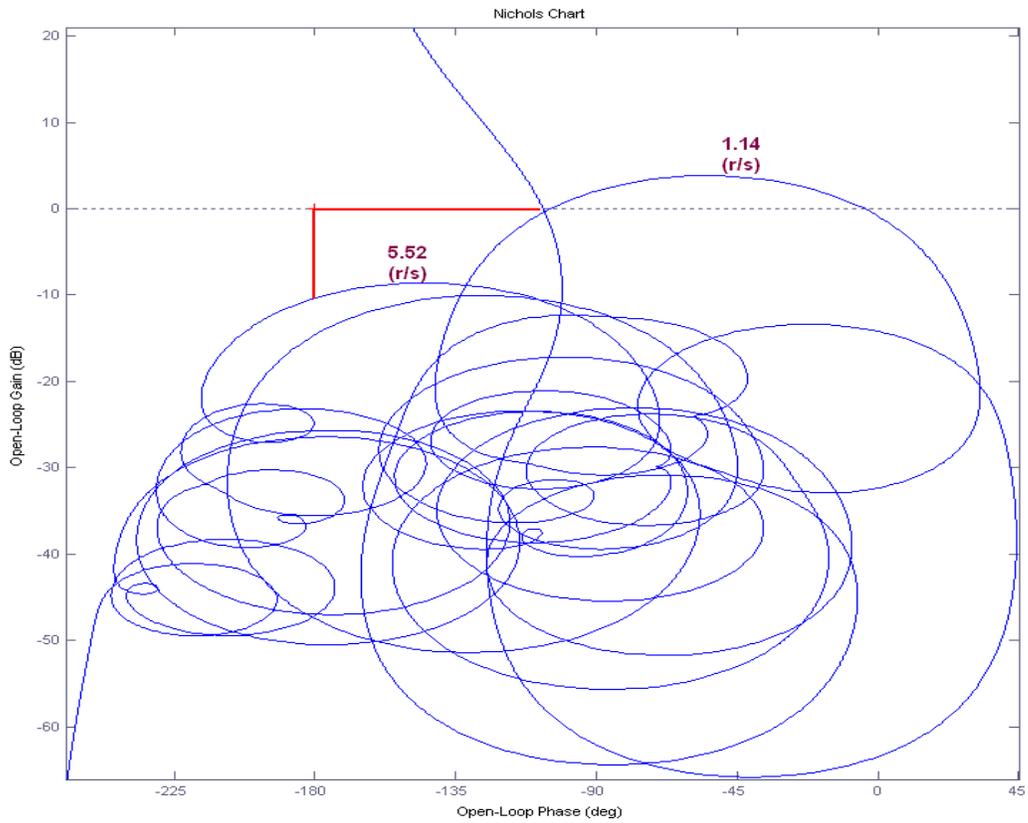**Figure 4.6.1 Stability Analysis Results for the CMG Attitude Control System in the PD Mode using the Simulink model "*Open_Loop_CMG.mdl*"**

Pitch Axis CMG PD Control Stability

Nichols Chart

Yaw Axis CMG PD Control Stability

Nichols Chart

4.7 Stability Analysis of the RCS/ ACS using the Describing Function Method

In Section 3.2 we described the methodology of applying the Describing Function method to analyze the reaction control system stability and the potential for limit cycling as a result of the interaction between the control system and the structural modes. The linear and the non-linear parts of the control loop are separated into two SISO subsystems. The phase-plane logic is simplified to a dead-band non-linearity that has a DF equal to N(e) where the input (e) is a linear combination of rate plus attitude error in a specific direction, that is, either: roll, pitch, yaw, plus many other skewed directions, as shown in Figure 4.7.1.

Each direction is analyzed separately and the control direction is defined by a unit vector. The output of the dead-band non-linearity is input to the jet-select logic that excites the linear SISO system G(s) in the specified direction. The system G(s) which includes rigid dynamics and flexibility is constrained to rotate in a single direction defined by the input vector. The jet select logic is implemented in function "JSel_ln.m". It is a linearized version of the logic used in simulations "Jet_Select_dot.m" that selects jets for a specified rotational direction. The linear logic selects the jets contributing positive accelerations in the selected direction, and also the jets contributing in the opposite direction, but negative thrusts are applied to the jets contributing in the reverse direction. The thrusts are halved in order to produce the same acceleration as if only the positive contributing jets were firing. This creates a more symmetrical system for linear analysis. The output of G(s) is a linear combination of attitude plus rate error which is a vector. This output is resolved (dotted) in the specified direction to produce a scalar output which represents the vehicle response in the specified rotational axis. So the system G(s) is only excited in the specified direction and its response is only measured in the same direction. It is a SISO system and we can, therefore, apply the Describing Function method to analyze for limit-cycles. In addition, the G(s) plant is scaled by multiplying it with the maximum value of N(e). This makes it more convenient when analyzing stability in Matlab using Nichols or Nyquist plots because the (+) sign now represents the minimum point of the -1/N(e) locus and makes it easier to measure the margins.

This method allows us to use the same Simulink model of Fig. 4.7.1 to analyze all directions, including skewed axes. All linear dynamics of the control loop are included in the system G(s) where we can use it to apply the DF method. G(s) is implemented in a Simulink file "*Open_Loop_RCS.mdl*" and used to calculate Nichols plots. It includes the Flixan derived state-space system "*Space Station with RCS and a Double-Gimbal CMG Array*" which is loaded into Matlab from file "*vehicle_flex34.m*". Limit cycles would occur when the DF locus -1/N(e) of the dead-zone non-linearity which approximates the phase-plane, intersects the plant frequency response G(jω) in a Nichols or a Nyquist plot. The intersection point(s) on the G(jω) locus predict the frequency of oscillation(s) when the control loop is closed. The same intersections on the -1/N(e) locus would predict the amplitude of the limit-cycles. Bending filters have been included on the rate signals to attenuate any potentially unstable structural resonances of the G(jω) frequency response. They are located in the vehicle dynamics block.

Figures 4.7.2 show the DF analysis results in roll, pitch, and yaw. However, there are infinite skewed directions to be analyzed for limit-cycle stability by specifying a different rotational direction in figure 4.7.1. This is because there is a unique set of jets involved for each direction that may drive the system at different amplitudes and excite different structural modes. The results are identical to the results obtained in section 3.2.
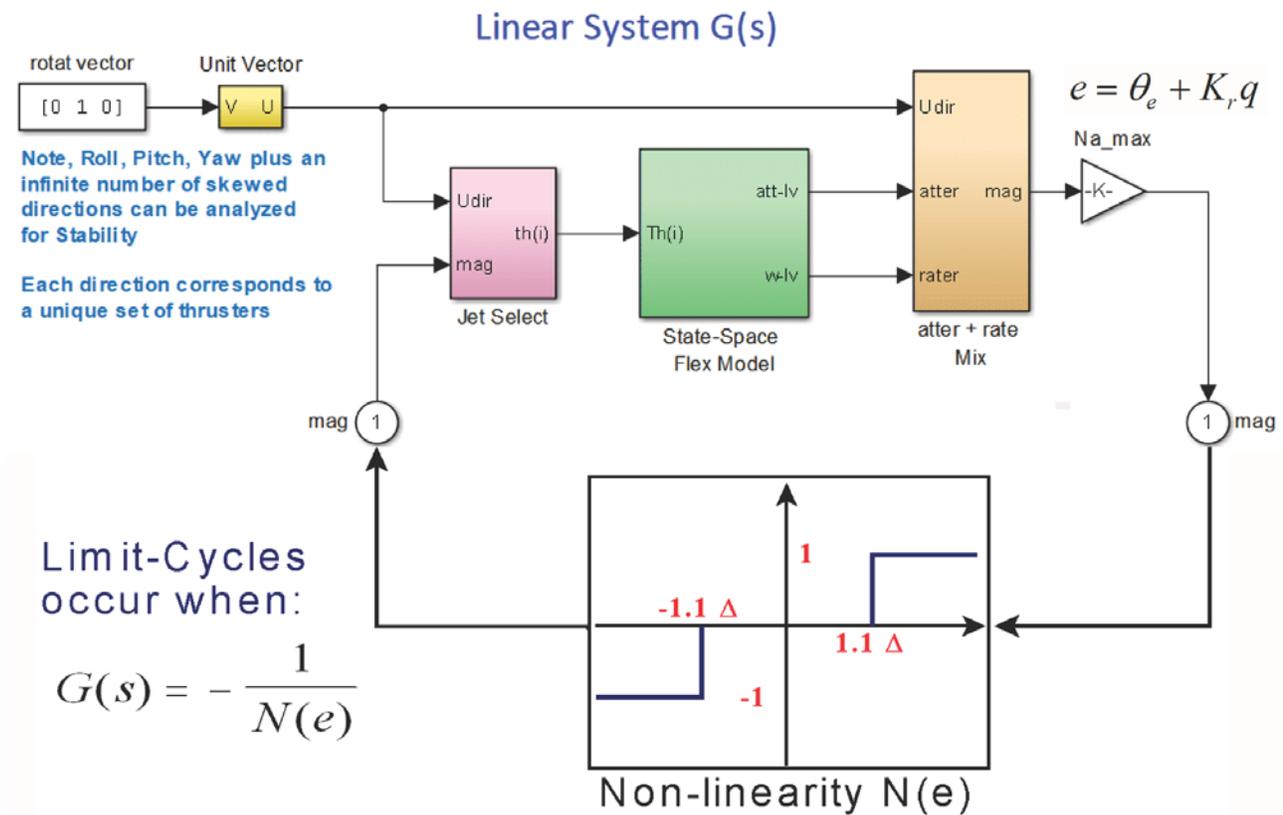
Figure 4.7.1 Simulink Model "Open_Loop_RCS.mdl" used for Describing Function RCS Stability Analysis
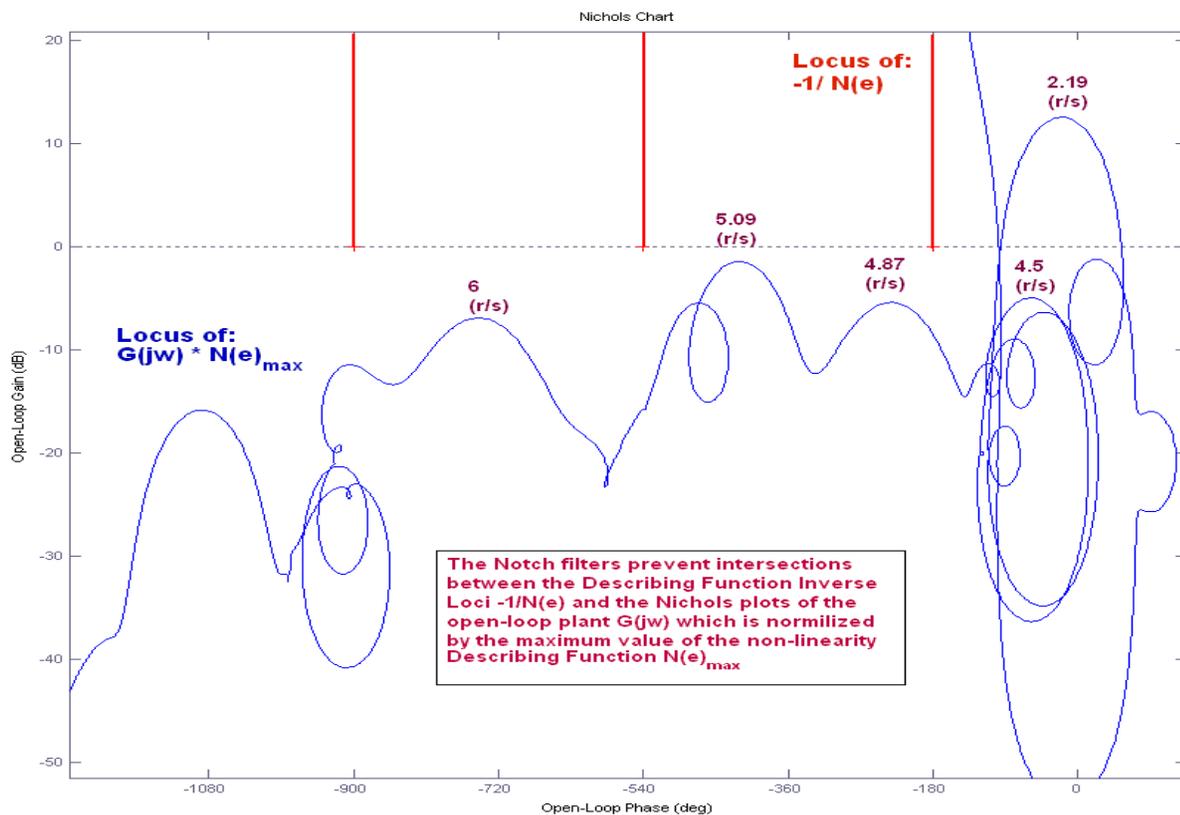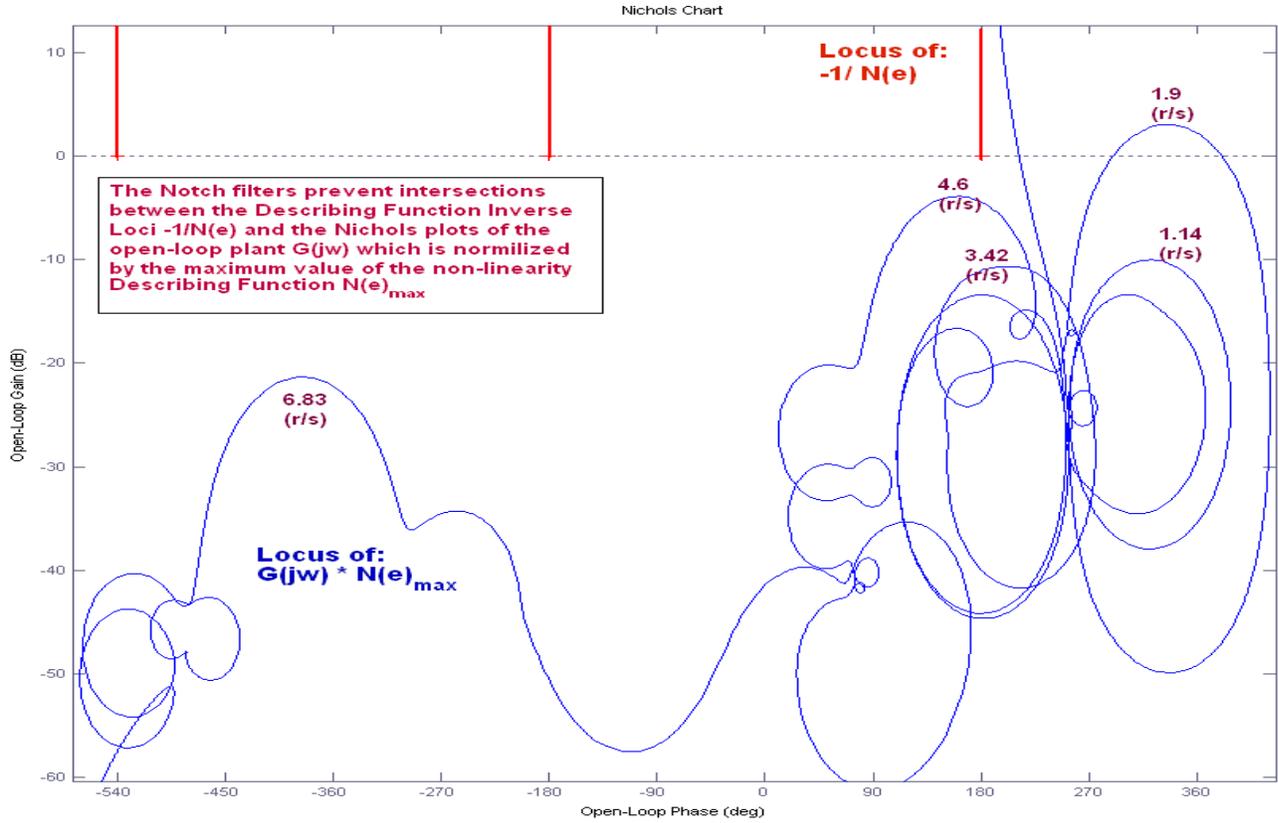

Figure 4.7.2 Describing Function Analysis for the RCS Phase-Plane Attitude Control System using the Simulink Model "Open_Loop_RCS.mdl"

Describing Function Analysis for the Pitch Axis

Nichols Chart

Locus of:
-1/ N(e)

1.9
(r/s)

4.6
(r/s)

1.14
(r/s)

3.42
(r/s)

The Notch filters prevent intersections
between the Describing Function Inverse
Loci -1/N(e) and the Nichols plots of the
open-loop plant G(jw) which is normilized
by the maximum value of the non-linearity
Describing Function N(e)max

6.83
(r/s)

Locus of:
G(jw) * N(e)max

Open-Loop Gain (dB)

Open-Loop Phase (deg)

Describing Function Analysis for the Yaw Axis

Nichols Chart

3.92
(r/s)

This mode is
phase-stable

Locus of:
-1/ N(e)

6.47

6

4.87

3.4

7.5

1.9

2.09

1.29
(r/s)

1.14

Locus of:
G(jw) * N(e)max

The Notch filters prevent intersections
between the Describing Function Inverse
Loci -1/N(e) and the Nichols plots of the
open-loop plant G(jw) which is normilized
by the maximum value of the non-linearity
Describing Function N(e)max

Open-Loop Gain (dB)

Open-Loop Phase (deg)